

**DEVELOPMENT OF HYBRID MEMBRANES FOR
APPLICATION IN DIRECT METHANOL FUEL CELLS
(DMFC)**

A THESIS

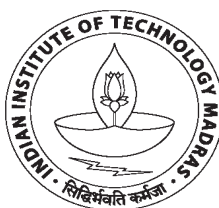
submitted by

M. HELEN

for the award of the degree

of

DOCTOR OF PHILOSOPHY



**DEPARTMENT OF CHEMISTRY
INDIAN INSTITUTE OF TECHNOLOGY MADRAS
CHENNAI – 600 036**

APRIL 2009

**To Almighty
&
My Family**

THESIS CERTIFICATE

This is to certify that the thesis entitled “**DEVELOPMENT OF HYBRID MEMBRANES FOR APPLICATION IN DIRECT METHANOL FUEL CELLS (DMFC)**” submitted by Ms. **M. HELEN** to the Indian Institute of Technology, Madras, for the award of degree of **Doctor of Philosophy** is a bonafide record of research work carried out by her under our supervision. The contents of this thesis, in full or in parts, have not been submitted to any other Institute or University for the award of any degree or diploma.

Research Guides

Prof. B. Viswanathan

Prof. S. Srinivasa Murthy

Date:

Place: Chennai - 600 036.

ACKNOWLEDGEMENTS

With reverence and regards, hence with my bliss, I set to place on record my deep, sincere gratitude to my mentor **Prof. B. Viswanathan**, a shepherd in science, for his inspirations, guidance, constant encouragements, and for steering me in the fields of untrodden paths throughout the period of my research. His uncompromising and unequivocal demands for logistics, persuasive criticisms in arguments and presentations have benefited every page. Gratefully, and with bountiful joy I recall the day one I entered his laboratory as a tender person, carrying only my hopes and dreams and nothing else. He accepted me with all my emptiness, nucleated in me the thirst for science, set within me the courage and daringness to face any challenge in science and piloted me step by step, with all his meticulous care carving me out by remaining as a guiding star leading me in right directions. You mean to me what an architect means to a piece of stone. By the two little words *Thank You*, I can never sufficiently express my gratitude for you in its completeness, and I wish to state that you have played a most wonderful and remarkable role in what I am today and what I would be in the life yet to come.

Pleasure screens my mind and gladness encamp my heart while I place my deep gratitude to **Prof. S. Srinivasa Murthy**, for all his supports, helps and for cheering me up at every stages of this research work. I am delighted for having him as my co-guide. He was always accessible and available showing kindness, offering suggestions with his gentle care.

I wish to thank most sincerely the Doctoral Committee members, **Prof. T.K. Varadarajan**, **Prof. U.V. Varadaraju**, **Prof. A. Subrahmanyam**, and **Prof. S.**

Ramaprabhu for their limitless kindness, supports, fruitful discussions and suggestions during the doctoral committee meetings.

As I walk in the corridors of department of chemistry, memories flash across my mind and hence irresistibly the gratitude gushes in my heart to recall the greatness and gracefulness of the former Heads of the Department, right from **Prof. B. Viswanathan, Late Prof. S. Vanchesan, Prof. M.N. Sudheendra Rao** to **Late Prof. G. Sundararajan** and the present Head of the Department, **Prof. R. Dhamodharan** for their kind helps and for providing the necessary infrastructures to carry out the research work.

I wish to express my sincere gratitude to **Prof. P. Selvam**, for all his suggestions, discussions, constructive criticisms and the interests shown towards my research work and developments. I am thankful to **Prof. S. Sivasanker, Prof. A.V. Ramaswamy** and all the faculty members of National Center for Catalysis Research and Department of Chemistry for their constant encouragements and supports.

I wish to acknowledge **Columbian Chemical Company, U.S.A** for a graduate fellowship, **Council of Scientific and Industrial Research (CSIR-India)** for awarding me a Senior Research Fellowship (SRF) and **Department of Science and Technology (DST-India)** for the grants for the creation of National Centre for Catalysis Research (NCCR), where most of my research works has been carried out. I wish to thank **Indian Institute of Technology, Madras (IITM)** for providing me the opportunity to pursue my PhD program and for extending the facilities to carry out my research.

I thank all the non-teaching staff members of the Department of Chemistry, and the supporting staffs of this institute for their technical and timely helps. Specially, I

thank **Mr. Narayanan** for TGA, **Mrs. Kanchanamala** for TEM, **Mrs. Shanthi** and **Mr. T. Ragavaiya** for SEM.

I thank my seniors and friends **Dr. V. Raghuvier, Dr. B. Rajesh, Dr. V. Chidambaram, Dr. M. Sankaran, Dr. M. Sathish, Dr. S. Shanmugam, Dr. T. Maiyalagan, Dr. Ch. Venkateswara Rao, Dr. L. Hima Kumar, Mr. P. Indra Neel, Dr. J. Rajeswari, Dr. Satyananda Kishore, Dr. C.M. Janet, Dr. S. Navaladian, Mr. G. Magesh, Dr. Joseph Anthoy Raj, Dr. P. George, Dr. P. Anuradha, Dr. S. Thirunavukarasu, Dr. S. Srimurugan, Dr. P. Suresh, Dr. Vidhya Krishna, Dr. Joyce, Dr. Radhika, Dr. Mahalakshmy, Mrs. S. Chandravathanam, Mr. B. Kuppan, Mr. P. Ramana Murthy, Mr. Vamsi Krishna, Mr. Suthakar, Mr. T.M. Sankaranarayanan, Ms. M. Banu, Ms. R. Sumathi, Ms. Nithya, Mr. Poli Raju, Mr. R. Jude Vimal, Mr. Mahendran, Mr. Anil Kumar, Ms. A. Kiruba, Mr. R. Kumaravel and Mr. P.R.Venkatesan** for their kindness, supports and encouragements and **Ms. S. Indumathi** for her kind assistance in lab. I also thank all the research scholars of department of chemistry for their cherishable companionships and friendliness.

Limitless joy lingering in my heart to recall my dear friend **Dr. Anji Reddy**, for his motivation, support, timely helps and constant encouragements throughout my research period.

A place where I can be myself - truly and trustfully, resting, relaxing and refreshing, amidst the people - who set me with a smile on my face, no matter what the burdens - the hours of the days bring into my life, my dearest friends **Dr. Navaratna Vajpai, Mr. Atul Kumar, Ms. Samanwita Pal, Ms. N. Nithiya, Ms. P. Biji, Mr. Manoj Kumar, Dr. A. Saieswari Amaran, Ms. S. Susithra, Ms. Tanuja, Dr. Vijayanthi**

and Mrs. Nimmy. I thank them all for their companionship, loving presence, supports, kindness and helps through which each one of them constantly supplying me with joy, pleasantness, fulfillment, spreading fragrances in the life's garden.

I thank **Almighty** for keeping me in His mind while He planned His creations and for all His countless blessings. I thank my grandparents who are the spirits moving me from within, setting me to soar higher, my parents, who are the wind behind my wings, my sisters and my brothers, who are the rainbows remaining colorful and vibrant in the galaxy of my life. I gratefully recall all my teachers, in the past and present for they are the sunshines of my life.

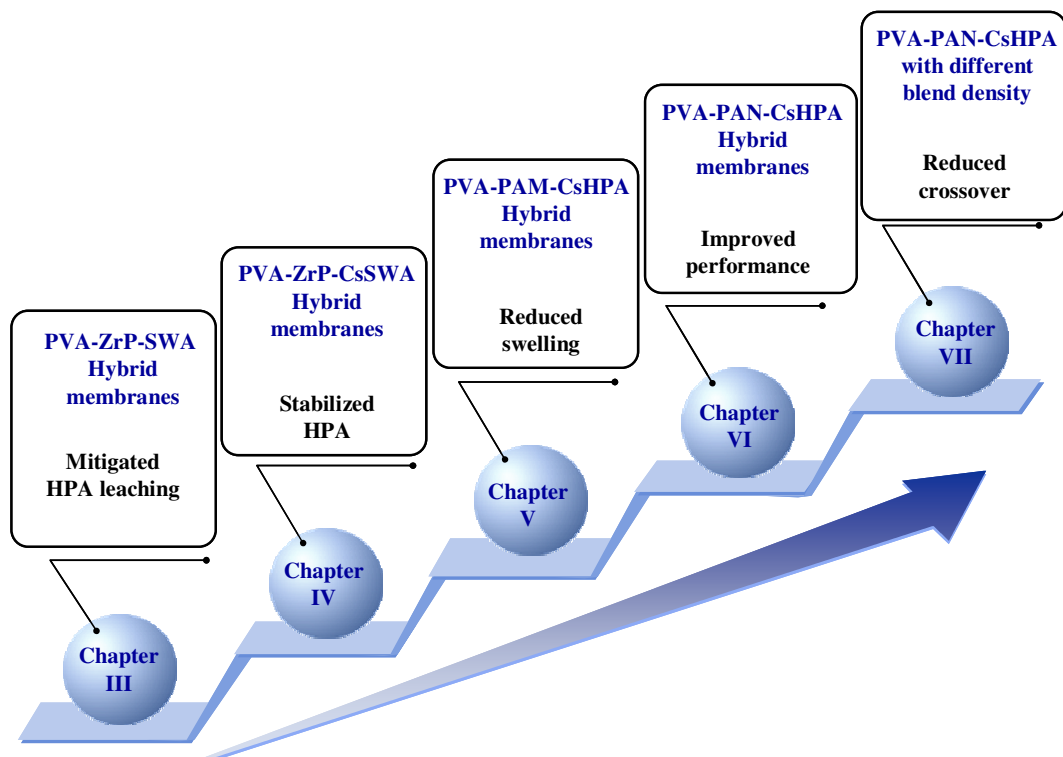
Forever I am indebted and hence I salute my **Nation** and all the **Stewards** of science and knowledge who walked before me and prepared the path for me to sail further. This world where I live and the modern advancements which I enjoy in all sectors and at all settings are the fruits of their toil and their infinite love for the humanity.

M. HELEN

ABSTRACT

KEYWORDS: Direct methanol fuel cell (DMFC), hybrid proton conducting membrane, hybrid membrane, poly(vinyl alcohol), heteropoly acid, salt of heteropoly acids, zirconium phosphate, methanol cross-over, proton conductivity, polymer blends.

Fuel cells are emerging as an alternate energy conversion source for both mobile and stationary applications. Among low temperature fuel cells, direct methanol fuel cell (DMFC) is attractive due to its system simplicity and adaptability for a liquid fuel, methanol. One of the challenges awaiting commercialization of DMFC technology is to develop alternate membranes to state of the art Nafion[®] possessing high proton conductivity, low swelling and low diffusion for methanol by a simple and environmentally benign fabrication method. As Nafion[®] holds the utmost electronegative environment possible in a chemical system it is nearly impossible to design a membrane that will have better ionic conductivity compared to Nafion[®]. Realizing this limitation, it was considered worthwhile to design a membrane which may possess ionic conductivity less than that of Nafion[®], but should have at least one property (for fuel cell applications) better than that of Nafion[®]. Since the fuel crossover from anode to the cathode drastically reduces the performance of the DMFC, it was considered that the membrane development must mainly focus to this aspect of fuel crossover. This investigation therefore focuses on the following aspects of this development by formulating organic-inorganic hybrid membranes based on poly(vinyl alcohol) (PVA) as organic matrix and heteropoly acids (HPA) as proton conducting moiety.



Bird's eye view of the investigations reported in the thesis

The scope of the initial part of the study is to investigate hybrid membranes made of poly(vinyl alcohol) (PVA) and α -zirconium phosphate (ZrP) with silicotungstic acid (SWA) as an active moiety. SWA was fixed in a stable matrix by forming composites with PVA and ZrP, while maintaining their high proton conductivity. Through this attempt, the leaching of SWA is mitigated. Following this, heteropoly acids (HPA) were stabilized in the membrane matrix, by combining both approaches of composite formation, with salts of HPA for the first time. Hybrid membranes based on cesium salt of SWA, ZrP and PVA were fabricated and characterized for their applicability in DMFC.

PVA membranes incorporated with heteropoly acids by forming composites are swelling too strongly to be used. In order to improve the dimensional stability of PVA based membranes, blending of poly(vinyl alcohol) (PVA) with polyacrylamide (PAM) and polyacrylonitrile (PAN) followed by cross-linking with glutaraldehyde (Glu) was investigated. Cesium salts of different heteropoly acids such as phosphomolybdic acid (PMA), phosphotungstic acid (PWA) and silicotungstic acid (SWA) were incorporated into the polymer network to form corresponding hybrid membrane materials and were characterized for their applicability in DMFC. Blending PVA with PAM and PAN reduced swelling and methanol crossover. Finally, the effects of blend density on water uptake, swelling, proton conductivity and methanol crossover were investigated.

TABLE OF CONTENTS

Title	Page No.
ACKNOWLEDGEMENTS	i
ABSTRACT.....	v
LIST OF TABLES	xiii
LIST OF FIGURES	xv
ABBREVIATIONS	xx
NOTATIONS.....	xxii
 CHAPTER 1 INTRODUCTION	
1.1 Membrane technology and membrane processes	1
1.2 Fuel cells	3
1.2.1 Classification of fuel cells	3
1.3 Direct methanol fuel cell (DMFC)	6
1.3.1 Working principle of DMFC	6
1.3.2 Thermodynamic consideration	7
1.3.3 Polymer electrolyte membrane for DMFC applications	9
1.3.4 Factors affecting performance of membranes	10
1.3.4.1 Water uptake or Hydration	10
1.3.4.2 Thickness	11
1.4 Literature Background	12
1.4.1 Perfluorosulfonic acid (PFSA) membranes	12
1.4.2 Limitations with PFSA membranes	15
1.4.3 Modified PFSA membranes	16
1.4.3.1 Composite formation	16
1.4.3.2 Swelling with low volatile and non-aqueous solvents.....	16
1.4.3.3 Reinforced PFSA membranes.....	17
1.5 Alternative sulfonated polymer membranes	18
1.5.1 Partially fluorinated membranes.....	19
1.5.2 Aromatic hydrocarbon membranes.....	21
1.5.3 Limitations of sulfonated polymers	25

Table of contents (contd.)

1.6	Acid base polymers.....	26
1.6.1	Doping with acids	26
1.6.2	Doping with bases.....	28
1.7	Organic-inorganic composite membranes	30
1.7.1	Heteropoly acids	34
1.7.2	Zirconium phosphates.....	46
1.8	Composite Membranes <i>vs</i> Nafion [®] – Rationale	47
1.9	Motivation and objective of the present investigation.....	50

CHAPTER 2 EXPERIMENTAL METHODOLOGY

2.1	Chemicals and materials used.....	52
2.2	Characterization of membranes	52
2.2.1	Fourier transformed infrared (FT-IR) study	52
2.2.2	X-ray diffraction study	52
2.2.3	Thermogravimetric analysis (TGA)	52
2.2.4	Differential scanning calorimetry (DSC).....	53
2.2.5	Electron Microscopy study	53
2.2.5.1	Scanning electron microscope (SEM)	53
2.2.5.2	Transmission electron microscope (TEM)	53
2.2.6	X-ray fluorescence (XRF) analysis.....	53
2.2.7	Water/methanol uptake	54
2.2.8	Swelling	54
2.2.9	Ion-exchange capacity (IEC)	54
2.2.10	Oxidative stability.....	55
2.2.11	Additive stability in membrane matrix	55
2.2.12	Proton conductivity by Electrochemical Impedance Spectroscopy (EIS)....	56
2.2.13	Methanol crossover study	57

CHAPTER 3 SYNTHESIS AND CHARACTERIZATION OF HYBRID MEMBRANES BASED ON α -ZIRCONIUM PHOSPHATE AND SILICOTUNGSTIC ACID

3.1	Introduction.....	59
3.2	Experimental.....	61

Table of contents (contd.)

3.2.1	Preparation of α -zirconium phosphate.....	61
3.2.2	Fabrication of PVA-ZrP-SWA hybrid membranes	62
3.3	Membrane characterization	62
3.3.1	Fourier transform infrared spectroscopic analysis.....	62
3.3.2	X-ray diffraction analysis	64
3.3.3	Thermal analysis	65
3.3.4	Scanning electron microscopy analysis	67
3.3.5	Water uptake, swelling and ion exchange capacity (IEC)	69
3.3.6	Test for SWA leaching	69
3.3.7	Proton conductivity study	70
3.3.8	Methanol crossover study	72
3.4	Conclusions.....	74

CHAPTER 4 FABRICATION AND PROPERTIES OF HYBRID MEMBRANES BASED ON SALTS OF HETEROPOLY ACID, ZIRCONIUM PHOSPHATE AND POLY(VINYL ALCOHOL)

4.1	Introduction.....	76
4.2	Experimental.....	77
4.2.1	Preparation of salts of silicotungstic acid	77
4.2.2	Fabrication of PVA-ZrP-CsSWA hybrid membranes	78
4.3	Membrane characterization	78
4.3.1	Fourier transform infrared spectroscopic analysis.....	78
4.3.2	X-ray diffraction analysis	80
4.3.3	Thermal analysis	81
4.3.4	Scanning electron microscopy analysis	83
4.3.5	Water uptake, swelling and ion exchange capacity (IEC)	84
4.3.6	Proton conductivity study	84
4.3.7	Methanol crossover study	85
4.3.8	Full cell testing	87
4.3.8.1	Membrane electrode assembly (MEA) fabrication.....	87
4.3.8.2	Single cell performance in DMFC.....	89
4.4	Conclusions.....	91

Table of contents (contd.)

CHAPTER 5 CESIUM SALTS OF HETEROPOLY ACID EMBEDDED POLY(VINYL ALCOHOL) (PVA) - POLYACRYLAMIDE (PAM) ORGANIC INORGANIC HYBRIDS AS POSSIBLE ELECTROLYTE FOR DMFC APPLICATION

5.1	Introduction.....	92
5.2	Experimental.....	93
5.2.1	Preparation of salts of heteropoly acid	93
5.2.2	Fabrication of hybrid membranes	94
5.3	Membrane characterization	95
5.3.1	Fourier transform infrared (FT-IR) spectral studies	95
5.3.2	X-ray diffraction (XRD) analysis	98
5.3.3	Thermogravimetric (TGA) studies	99
5.3.4	Scanning electron microscopy interfaced with EDXA.....	100
5.3.5	Water uptake, swelling and ion-exchange capacity (IEC).....	102
5.3.6	Oxidative stability.....	103
5.3.7	Additive stability	105
5.3.8	Proton conductivity study	107
5.3.9	Methanol crossover study	108
5.4	Conclusions.....	112

CHAPTER 6 DEVELOPMENT OF HYBRID MEMBRANE MATERIALS WITH CESIUM SALTS OF VARIOUS HETEROPOLY ACIDS IN POLY(VINYL ALCOHOL) (PVA) - POLYACRYLONITRILE (PAN) MATRIX FOR DMFC APPLICATION

6.1	Introduction.....	114
6.2	Experimental.....	116
6.2.1	Fabrication of hybrid membranes	116
6.3	Membrane characterization	119
6.3.1	Fourier transform infrared (FT-IR) spectral studies	120
6.3.2	X-ray diffraction (XRD) analysis	121
6.3.3	Thermogravimetric (TGA) studies	123
6.3.4	Scanning electron microscopy interfaced with EDXA.....	124
6.3.5	Water uptake, swelling and ion-exchange capacity (IEC).....	126
6.3.6	Oxidative stability.....	127

Table of contents (contd.)

6.3.7	Additive stability	129
6.3.8	Proton conductivity study	131
6.3.9	Methanol crossover study	132
6.4	Conclusions.....	136

**CHAPTER 7 EFFECT OF BLEND DENSITY ON THE PROPERTIES OF
POLY(VINYL ALCOHOL) (PVA) - POLYACRYLONITRILE
(PAN) MATRIX WITH CESIUM SALTS OF HETEROPOLY
ACIDS INVESTIGATED AS ELECTROLYTES FOR DMFC
APPLICATION**

7.1	Introduction.....	137
7.2	Experimental.....	138
7.2.1	Fabrication of hybrid membranes	138
7.3	Membrane characterization	139
7.3.1	Fourier transform infrared (FT-IR) spectral studies	139
7.3.2	X-ray diffraction (XRD) analysis	142
7.3.3	Thermogravimetric (TGA) studies	145
7.3.4	Scanning electron microscopy interfaced with EDXA.....	147
7.3.5	Water uptake, methanol uptake, swelling and ion-exchange capacity (IEC)	151
7.3.6	Oxidative stability.....	152
7.3.7	Additive stability	156
7.3.8	Proton conductivity study	160
7.3.9	Methanol crossover study	162
7.3.10	Selectivity	166
7.4	Conclusions.....	167

CHAPTER 8 SUMMARY AND CONCLUSIONS.....169

REFERENCES.....175

LIST OF PUBLICATIONS204

LIST OF TABLES

Table	Title	Page No.
1.1	Possible variables of fuel cells	4
1.2	Characteristics of commercial polymer membranes	13
1.3	Conductivity (100 % RH) of benzyisulfonate grafted PBI after dehydration and immersion in basic aqueous solutions (1 M, 15 min, 25 °C).....	28
1.4	Summary of inorganic-organic composite membranes	35
3.1	Assignments of main absorption bands for hybrid membranes and its components.....	63
3.2	Water uptake, swelling and IEC values for PVA-ZrP-SWA hybrid membranes of different composition with a thickness of 250 μm	69
3.3	Proton conductivity (σ) and activation energy (E_a) for hybrid membranes and its components	72
4.1	Cesium content in salts of silicotungstic acid	78
4.2	Assignments of main absorption bands for PVA-ZrP-C ₅ SWA and PVA-ZrP-C ₅ SWA hybrid membranes	80
4.3	Water uptake, swelling and IEC values for PVA-ZrP-C ₅ SWA and PVA-ZrP-C ₅ SWA hybrid membranes with a 180 μm thickness compared with that of Nafion [®] 115	84
4.4	Comparison of conductivity and permeability of various membranes.....	87
5.1	Assignments of main absorption bands of fabricated hybrid membranes.....	97
5.2	Water uptake, swelling and ion-exchange capacity (IEC) values for different hybrid membranes compared with that of Nafion [®] 115	103
5.3	Comparison of proton conductivity and permeability of various membranes.....	111
6.1	Water uptake at different cross-linking time for PVA-PAN-C ₅ PMA-Glu hybrid membrane.....	118
6.2	Water uptake, swelling and ion-exchange capacity (IEC) values for different hybrid membranes	127
6.3	Comparison of proton conductivity and methanol permeability values for various membranes.....	135

List of tables (contd.)

7.1	Assignments of main absorption bands of fabricated hybrid membranes with different blend density	142
7.2	Water uptake, methanol uptake, swelling and ion-exchange capacity (IEC) values for different hybrid membranes compared with that of Nafion [®] 115	152

LIST OF FIGURES

Figure	Title	Page No.
1.1	Schematic representation of membrane and processes therein.....	2
1.2	Schematic of the operating principal of a direct methanol fuel cell	7
1.3	A typical polarization curve of DMFC	9
1.4	General structure of perfluorosulfonic acid membrane	14
1.5	Chemical structure of polymers	22
1.6	Proton transport in hybrid membranes.....	32
2.1	Typical impedance spectra of a hybrid membrane	57
2.2	Schematic view of proton conductivity cell.....	57
2.3	Schematic view of two compartment cell for the determination of methanol diffusion coefficients	58
3.1	FT-IR spectra of hybrid membranes and its components for comparison.....	63
3.2	Cu K _α XRD patterns of hybrid membranes and its components for comparison.....	64
3.3	TGA traces of hybrid membranes in a temperature range from 50 to 800 °C.....	65
3.4	DSC thermograms of hybrid membranes with different contents of silicotungstic acid.....	66
3.5	Scanning electron micrographs of PVA-ZrP-SWA hybrid membranes	68
3.6	UV-visible spectra of pure SWA in water and for the water immersed with PVA-ZrP-SWA(30%) hybrid membrane at different time intervals	70
3.7	Proton conductivity at 60 % RH as a function of temperature for PVA-ZrP-SWA(10%), PVA-ZrP-SWA(20%), PVA-ZrP-SWA(30%) and Nafion [®] 115 (at 100 % RH)	71
3.8	Concentration of crossed over methanol as a function of crossover time	73
3.9	Methanol permeability of hybrid membranes compared with that of Nafion [®] 115	74

List of figures (contd.)

4.1	FT-IR spectra of PVA-ZrP-Cs ₁ SWA and PVA-ZrP-Cs ₂ SWA hybrid membranes	79
4.2	Cu K _α XRD patterns of PVA-ZrP-Cs ₁ SWA and PVA-ZrP-Cs ₂ SWA hybrid membranes	81
4.3	TGA analysis of PVA-ZrP-Cs ₁ SWA and PVA-ZrP-Cs ₂ SWA hybrid membranes in a temperature range from 50 to 800 °C	82
4.4	Scanning electron micrographs of hybrid membranes.....	83
4.5	Proton conductivity at 50 % RH as a function of temperature for PVA-ZrP-Cs ₁ SWA and PVA-ZrP-Cs ₂ SWA membranes compared with that of Nafion [®] 115 at 100 % RH.....	85
4.6	Concentration of crossed methanol as a function of crossover time.....	86
4.7	Methanol permeability of PVA-ZrP-Cs ₁ SWA and PVA-ZrP-Cs ₂ SWA hybrid membranes compared with that of Nafion [®] 115	86
4.8	Photograph of a fabricated membrane electrode assembly.....	88
4.9	Schematic view of cathode cell fixture and anode cell fixture with built in fuel reservoir	89
4.10	Polarization and power density curves for passive DMFC cell with Nafion [®] 115, PVA-ZrP-Cs ₁ SWA and PVA-ZrP-Cs ₂ SWA hybrid membranes as proton conducting electrolyte at 25 °C and at atmospheric pressure	90
5.1.	FT-IR spectra of hybrid membrane materials: Cross-linked PVA-PAM blends by glutaraldehyde with cesium salts of different heteropoly acid along with that of pristine PAM and PVA.....	96
5.2	XRD patterns of the PVA-PAM hybrid membranes with different heteropoly acids.	98
5.3	Thermogravimetric analysis (TGA) traces of hybrid membranes in the temperature region 40 to 800 °C.....	100
5.4	Scanning electron micrographs (SEM) of the surfaces of hybrid membranes incorporated with different heteropoly acids. (a) PVA-PAM-CsPMA-Glu (b) PVA-PAM-CsPWA-Glu (c) PVA-PAM-CsSWA-Glu. The insert spectra represent the corresponding energy-dispersive X-ray analysis (EDXA) traces	101
5.5	Oxidative stabilities of fabricated membranes immersed in Fenton's reagent at room temperature at various time intervals.....	104

List of figures (contd.)

5.6	FT-IR spectra of hybrid membranes (a) PVA-PAM-CsPMA-Glu (b) PVA-PAM-CsPWA-Glu (c) PVA-PAM-CsSWA-Glu placed in water for different durations	106
5.7	Proton conductivities of the fabricated hybrid membranes and Nafion [®] 115 membrane at different temperatures.....	108
5.8	Concentration of crossed over methanol as a function of crossover time	109
5.9	Methanol permeability of fabricated hybrid membranes compared with that of Nafion [®] 115	110
6.1.	The process of cross-linking hydroxyl group of PVA with Glu	119
6.2	FT-IR spectra of hybrid membrane materials: Cross-linked PVA-PAN blends by glutaraldehyde with cesium salts of different heteropoly acid (a) phosphomolybdic acid (PMA) (b) phosphotungstic acid (PWA) or (c) silicotungstic acid (SWA).....	121
6.3	XRD patterns of the PVA-PAN hybrid membranes with different heteropoly acids and pristine PVA and PAN	122
6.4	Traces of thermogravimetric analysis (TGA) traces of hybrid membranes in the temperature region 40 to 800 °C.....	124
6.5	Scanning electron micrographs (SEM) of the surfaces of hybrid membranes incorporated with different heteropoly acids. (a) PVA-PAN-CsPMA-Glu (b) PVA-PAN-CsPWA-Glu (c) PVA-PAN-CsSWA-Glu. The insert spectra represent the corresponding energy-dispersive X-ray analysis (EDXA) traces confirming the presence of finely dispersed heteropoly acids.....	125
6.6	Oxidative stability of fabricated membranes immersed in Fenton's reagent at room temperature at various time intervals.....	128
6.7	FT-IR spectra of hybrid membranes (a) PVA-PAN-CsPMA-Glu (b) PVA-PAN-CsPWA-Glu (c) PVA-PAN-CsSWA-Glu placed in water at different time intervals	130
6.8	Proton conductivities of the fabricated hybrid membranes and Nafion [®] 115 membrane at different temperatures.....	131
6.9	Concentration of crossed over methanol as a function of crossover time	133
6.10	Methanol permeability of fabricated hybrid membranes compared with that of Nafion [®] 115	133
7.1a	FT-IR spectra of hybrid membranes fabricated with different blend density: Cross-linked PVA-PAN blends by glutaraldehyde with cesium salt of phosphomolybdic acid (PMA).....	140

List of figures (contd.)

7.1b	FT-IR spectra of hybrid membranes fabricated with different blend density: Cross-linked PVA-PAN blends by glutaraldehyde with cesium salt of phosphotungstic acid (PWA)	140
7.1c	FT-IR spectra of hybrid membranes fabricated with different blend density: Cross-linked PVA-PAN blends by glutaraldehyde with cesium salt of silicotungstic acid (SWA)	141
7.1d	FT-IR spectra of the individual components constituting the hybrid membranes.....	141
7.2a	XRD patterns of the PVA-PAN hybrid membranes of different blend density with cesium salt of phosphomolybdic acid (PMA) and its components	143
7.2b	XRD patterns of the PVA-PAN hybrid membranes of different blend density with cesium salt of phosphotungstic acid (PWA) and its components	144
7.2c	XRD patterns of the PVA-PAN hybrid membranes of different blend density with cesium salt of silicotungstic acid (SWA) and its components ..	144
7.3a	Thermogravimetric analysis (TGA) traces of (a) PVA-PAN-CsPMA-Glu with different blend density in the temperature region 40 to 800 °C	146
7.3b	Thermogravimetric analysis (TGA) traces of (a) PVA-PAN-CsPWA-Glu with different blend density in the temperature region 40 to 800 °C	146
7.3c	Thermogravimetric analysis (TGA) traces of (a) PVA-PAN-CsSWA-Glu with different blend density in the temperature region 40 to 800 °C	147
7.4a	Scanning electron micrographs (SEM) of the surfaces of the PVA-PAN hybrid membranes made of different blend density with cesium salt of phosphomolybdic acid (PMA). The insert spectra represent the corresponding energy-dispersive X-ray analysis (EDXA) traces confirming the presence of phosphomolybdic acid (PMA).....	148
7.4b	Scanning electron micrographs (SEM) of the surfaces of the PVA-PAN hybrid membranes made of different blend density with cesium salt of phosphotungstic acid (PWA). The insert spectra represent the corresponding energy-dispersive X-ray analysis (EDXA) traces confirming the presence of phosphotungstic acid (PWA).....	149
7.4c	Scanning electron micrographs (SEM) of the surfaces of the PVA-PAN hybrid membranes made of different blend density with cesium salt of silicotungstic acid (SWA). The insert spectra represent the corresponding energy-dispersive X-ray analysis (EDXA) traces confirming the presence of silicotungstic acid (SWA)	150

List of figures (contd.)

7.5a	Oxidative stability of fabricated membranes with different blend density immersed in Fenton's reagent at 70 °C for various time intervals (a) PVA-PAN-CsPMA-Glu (b) PVA-PAN-CsPWA-Glu (c) PVA-PAN-CsSWA-Glu	154
7.5b	Oxidative stability of fabricated membranes with different blend density immersed in Fenton's reagent at room temperature for various time intervals (a) PVA-PAN-CsPMA-Glu (b) PVA-PAN-CsPWA-Glu (c) PVA-PAN-CsSWA-Glu	155
7.6a	FT-IR spectra of PVA-PAN-CsPMA-Glu membrane with different blend density placed in water for different time intervals	157
7.6b	FT-IR spectra of PVA-PAN-CsPWA-Glu membrane with different blend density placed in water for different time intervals	158
7.6c	FT-IR spectra of PVA-PAN-CsSWA-Glu membrane with different blend density placed in water for different time intervals	159
7.7	Temperature dependence conductivity of hybrid membranes with different blend density	161
7.8a	Concentration of crossed methanol as a function of crossover time for PVA-PAN-CsPMA-Glu hybrid membrane with different blend density	164
7.8b	Concentration of crossed methanol as a function of crossover time for PVA-PAN-CsPWA-Glu hybrid membrane with different blend density	164
7.8c	Concentration of crossed methanol as a function of crossover time for PVA-PAN-CsSWA-Glu hybrid membrane with different blend density	165
7.9	Methanol permeability of hybrid membranes with different blend density compared with that of Nafion [®] 115.....	165
7.10	Selectivity of hybrid membranes compared with that of Nafion [®] 115	166

ABBREVIATIONS

C.E	Counter electrode
Cs ₁ SWA	Monosubstituted SWA, Cs ₁ H ₃ SiW ₁₂ O ₄₀
Cs ₂ SWA	Disubstituted SWA, Cs ₂ H ₂ SiW ₁₂ O ₄₀
CsPMA	Disubstituted PMA, Cs ₂ HPMo ₁₂ O ₄₀
CsPWA	Disubstituted PWA, Cs ₂ HPW ₁₂ O ₄₀
CsSWA	Disubstituted SWA, Cs ₂ H ₂ SiW ₁₂ O ₄₀
DI	Deionized
DMF	<i>N,N</i> -dimethyl formamide
DMFC	Direct Methanol Fuel Cell
DSC	Differential Scanning Calorimetry
EDXA	Energy-Dispersive X-ray analysis
EIS	Electrochemical Impedance Spectroscopy
FT-IR	Fourier transformed Infrared
Glu	Gluteraldehyde
HPA	Heteropoly acids
IEC	Ion-exchange capacity
OCV	Open circuit voltage
PAN	Polyacrylonitrile
PEG	Polyethylene glycol
PFSA	Perfluorosulfonic acid
PMA	Phosphomolybdic acid
PTFE	Polytetrafluoroethylene
PVA	Poly(vinyl alcohol)
PWA	Phosphotungstic acid
R.E	Reference electrode
RH	Relative Humidity
RT	Room Temperature
SEM	Scanning Electron Microscope
SPEEK	Sulfonated poly(ether ether ketone)
SWA	Silicotungstic acid
TEM	Transmission electron microscope

TGA	Thermo gravimetric analysis
W.E	Working electrode
XRD	X-ray Diffraction
XRF	X-ray Fluorescence
ZrP	Zirconium Phosphate

NOTATIONS

%	Percent
μm	micrometer
a.u.	Arbitrary unit
A_{dry}	Area of dry membrane sample
A_{wet}	Area of wet membrane sample
cm	centimeter
E_a	Activation energy
h	Hour
J g^{-1}	Joule per gram
K	Degree Kelvin
kJ	kilo Joules
M	Molar
mA	milli Ampere
meq g^{-1}	Milli-equivalent per gram
MHz	MegaHertz
Min	Minute
ml	Milliliter
mol	Mole
mV	Milli Volts
mW	Milli Watts
nm	nanometer
$^{\circ}\text{C}$	Degree Celsius
S	Siemens
s	second
T	Temperature
T_g	Glass transition temperature
T_m	Melting temperature
V	Volume
W_{dry}	Dry membrane weight
Wt	Weight
W_{wet}	Wet membrane weight

ΔH_f	Heat of fusion
θ	Angle
σ	Proton conductivity

CHAPTER 1

INTRODUCTION

1.1 MEMBRANE TECHNOLOGY AND PROCESSES

Membrane based technologies witness triumphal R & D efforts in recent years and they have a potential to impact multi million dollar industries in various sectors. The reach of advanced membrane spans from food/drug production, separation of pollutants, water purification, textile, biotechnology and to fuel cell markets. Membrane science constitutes a diverse collection of applications involving technologies such as reverse osmosis, ultrafiltration, microfiltration, gas separation, electrodialysis, hemodialysis, pervaporation, and other business trends.

In a simplest term, a membrane can be defined as an interface between two adjacent phases functioning as a selective barrier, and simultaneously organizing a system into compartments and regulating the transport between the two compartments (Ulbricht, 2004). The main advantage of membrane technology stems from its unique separation principle, i.e. the transport selectivity of the membrane. A schematic representation of a membrane and various processes driven by it are given in Fig. 1.1. Membranes often respond to a few gradients that they experience between either sides of the membrane. If concentration is a gradient, the process dialysis results; if pressure is a gradient then reverse osmosis, ultra filtration, micro filtration or nano filtration result. All these processes differ from each other depending on the pore diameter of the membrane. If potential is a gradient then, it drives processes such as electro dialysis or electrophoresis.

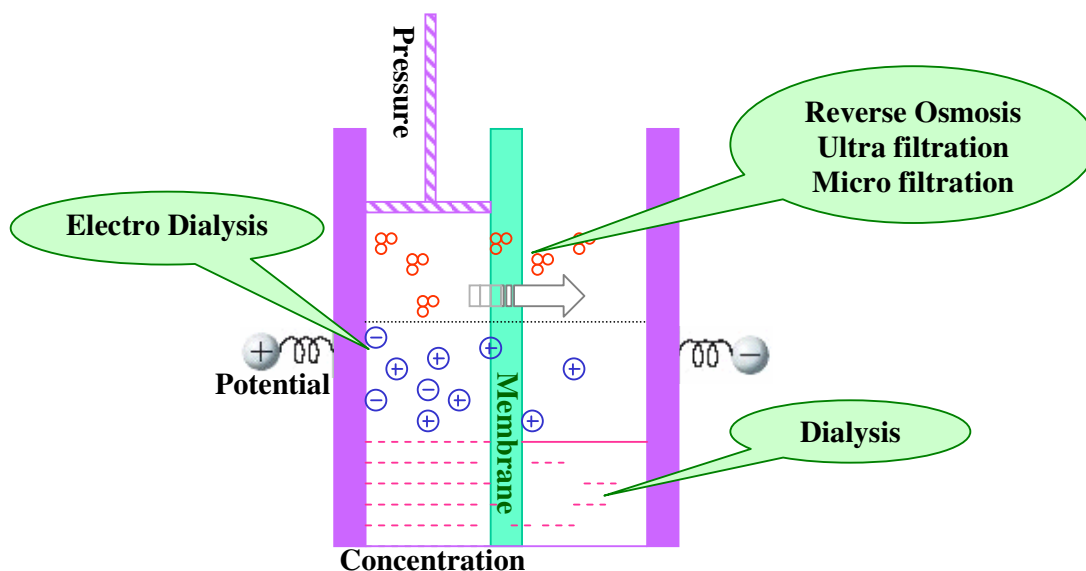


Fig. 1.1 Schematic representation of membrane and processes therein.

It is possible to exploit various parameters in the development of membranes and among them the electrical conductivity of the developed membrane has received a maximum attention. However, in specific applications, the species transfer across the membrane can also be another factor of consideration in the development of membrane for electrochemical device applications such as fuel cells, batteries and water electrolysis. The role of membrane in electrochemical devices is crucial compared to all other processes. In the case of reverse osmosis, ultra filtration, micro filtration or nano filtration the role of membrane is to act as a molecular sieve. Whereas in case of electrochemical devices in spite of acting as a molecular sieve, membrane perform certain other key roles like it separates anode and cathode, it prevents mixing of fuel and oxidant and it also provides a conductive pathway. In case of electric field gradient, the membranes have to face some unusual challenges. Membranes have to withstand pressure gradients (mechanical stability) as well as to exhibit stability under the rigorous chemical environments (chemical stability). Hence, the membranes employed in electrochemical devices need to exhibit electrochemical

stability under the operating conditions of the electrochemical devices in addition to promoting preferential migration of ions in vectorial mode.

1.2 FUEL CELLS

The anxiety for alternate sources of energy has hastened the development of fuel cells. Fuel cells are energy conversion devices that convert chemical energy of fuel and oxidant to electric energy directly. They generate electricity and water from hydrogen and oxygen through an inverse reaction of water electrolysis. The fuel hydrogen gets oxidized at the anode. The protons flow towards the cathode through an electrolyte layer, where, the electrons cannot penetrate. The electrons are attracted to the anode, and then fed through an external circuit to generate electricity. The electrons and protons are then combined with oxygen in another catalyst (cathode) to create heat and water. The operation does not depend on flow of heat between sources and sinks as in heat engine and is not therefore controlled by Carnot limitations (Appleby and Foulkes, 1989). The efficiency reaches about a maximum of 70 % when waste thermal energy in the system is used.

1.2.1 Classification of fuel cells

Fuel cells can be classified on the basis of various parameters, which include the nature and type of fuel used, whether the fuel is processed outside (external reforming) or directly used (without reforming step), oxidant, electrolytes and the temperature of operation. A typical set of variables of fuel cells is given in Table 1.1.

Table 1.1 Possible variables of fuel cells.

Fuel		Oxidant	Electrolyte	Temperature
Direct	Indirect			
Hydrogen	Methanol	Oxygen (pure)	Solid polymer electrolyte	Low (RT-120 °C)
Methanol	Ethanol	Air (oxygen)	Aqueous sulfuric acid	Intermediate (120-250 °C)
Ammonia	Hydrocarbon	Hydrogen peroxide	Aqueous phosphoric acid	High (250-750 °C)
Hydrazine	Ammonia		Aqueous alkaline	Very high (>750 °C)
Formic acid	Hydride		Aqueous carbonate	
Ethanol	Coal		Molten carbonate	
Coal gas			Solid oxide	
Coal				

Among different types of fuel cells, proton exchange membrane fuel cells (PEMFCs) are in forefront of commercialization (Costamagna and Srinivasan, 2001). The PEMFC (originally referred to as the solid polymer electrolyte fuel cell) was the first type of fuel cell to find an application in American spacecraft in 1960 (Simon and Nored, 1987).

The PEMFC is mainly divided into hydrogen fuel cell (PEMFC) and the direct methanol fuel cell (DMFC) based on the fuel employed though there are other fuels used like formic acid, ethanol etc., (Viswanathan and Aulice Scibioh, 2006). The PEMFC and DMFC have their own advantages and disadvantages. When hydrogen is used as fuel fast reaction kinetics can be realized and consequently high energy density can be achieved. But, the handling, storage and transportation of hydrogen are critical issues. On the other hand, methanol being a liquid at room temperature,

storage and handling is relatively easy. Hence there has been considerable interest in the development of direct methanol fuel cell technology. Though DMFC has certain advantages like higher energy density and system simplicity they exhibit shortcomings such as:

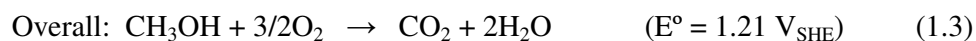
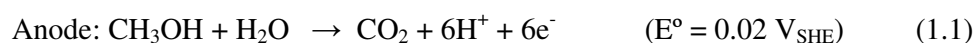
- i) *Slow reaction kinetics of electro-oxidation below 100 °C* (Arico *et al.* 2001): The electro-oxidation of methanol generates six protons and six electrons with one molecule of carbon dioxide at the same time and hence slower reaction kinetics compared to oxidation of hydrogen. Whereas, hydrogen electro-oxidation kinetics at PEMFC is faster as one proton and one electron is generated per molecule exhibiting higher cell performance.
- ii) *Anode poisoning*: In DMFC, poisoning of anode catalyst occurs due to the presence of carbon monoxide as reaction intermediate.
- iii) *Methanol crossover*: Permeation of methanol (fuel) through polymer electrolyte membrane from the anode to the cathode results in fuel loss as well as a fall in efficiency (Hoogers, 2002). The permeated methanol gets oxidized at the cathode in the presence of oxygen (combustion reaction) leading to mixed potential and reduces the number of active sites available at the cathode for oxygen reduction reaction leading to lowering of cathode activity.

Though DMFC technology is known for several decades, the commercial viability of these devices has not been realized for want of technological developments concerning appropriate electrodes and also of cost effective membranes.

1.3 DIRECT METHANOL FUEL CELL (DMFC)

1.3.1 Working principle of DMFC

The basic operating principle of DMFC is the electro-oxidation of methanol at the anode and reduction of oxygen at the cathode. The protons released during the oxidation of methanol are conducted through the proton exchange membrane to the cathode. Since the membrane is not electrically conductive, the electrons released from the methanol travel along the external circuit to the cathode and generate electricity. At the cathode the oxygen combines with the electrons and protons to produce water. The electrodes, active layers are thin layers of carbon supported platinum (Pt) catalyst particulates; the carbon is in the form of porous paper or cloth. The membrane is sandwiched between the electrodes to form a membrane electrode assembly (MEA), and placed in a fuel cell fixture constituting current collector, reservoir for methanol at the anode side and gas flow channel at the cathode side. The reactions and pathways in a DMFC are shown schematically in Fig. 1.2. The typical chemical reaction takes place at each electrode is represented below.



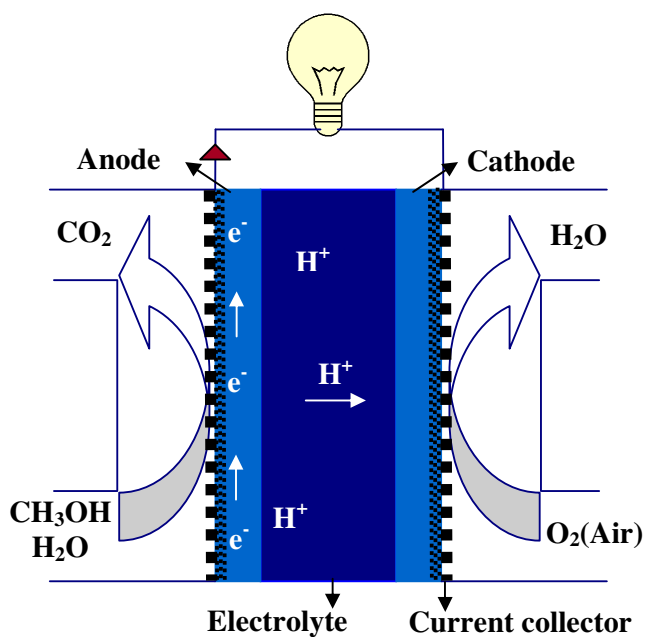


Fig. 1.2 Schematic of the operating principal of a direct methanol fuel cell.

1.3.2 Thermodynamic consideration

The electromotive force (E°) or open circuit voltage (OCV) is defined as the difference between the standard reduction potentials of the cathode and anode reactions.

The open circuit voltage (OCV) can be calculated from equation 1.4.

$$\text{OCV} = \frac{-\Delta G^\circ}{nF} \quad (1.4)$$

where, ΔG° , is the standard free energy of the overall reaction ($-698.2 \text{ kJ mol}^{-1}$), n is the number of electrons produced per molecule of methanol (fuel) and F , Faraday's constant.

As n , F , and E° are positive numbers, the standard free energy change of the overall reaction is negative, indicating a spontaneous reaction.

The theoretical OCV value for DMFC is 1.21 V and it is similar to that of hydrogen based PEMFC. In real fuel cell operation the OCV value is lowered due to several over potentials (voltage loss) as follows (Schultz *et al.* 2001):

Fuel crossover and internal currents: The energy loss occurs due to fuel loss at the anode as methanol permeates through the polymer electrolyte to the cathode side and to a smaller extent due to the electron conduction in the electrolyte. The electrolyte must hence be electrically insulating and should transport only protons. However, a certain amount of fuel loss due to diffusion and electron flow will always be possible. Fuel loss has a marked effect on OCV of the DMFC.

Activation overpotential: It is caused due to the slow reaction kinetics at the electrode surface. A portion of the voltage is lost in driving the chemical reaction that transfers the electrons to or from the electrode. This phenomenon dominates at low current region.

Ohmic overpotential: The voltage drop due to the hindrance to the flow of electrons, ions through electrodes and various components and through electrolyte. This voltage loss is proportional to current density.

Concentration or Mass transport overpotential: It originates due to change in concentration of reactants at the electrode surface as the reactant is consumed. The reduction in concentration is due to insufficient transport of reactant to the electrode surface. It is dominant at high current density.

Among these overpotentials, the OCV of the DMFC is highly affected by the methanol crossover and the ohmic resistance of the polymer electrolyte membrane. Consequently, the OCV of the DMFC is very low compared to theoretical value.

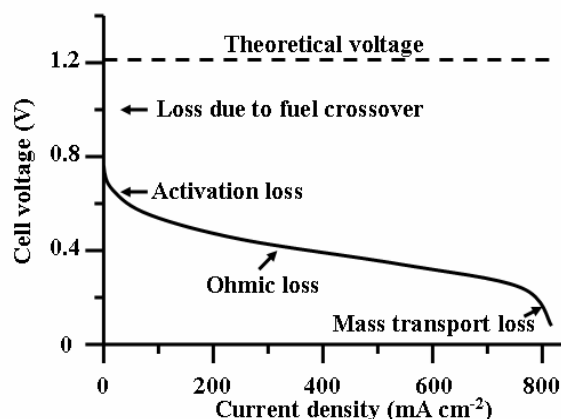


Fig. 1.3 A typical polarization curve of DMFC (Larminie and Dicks, 2000).

A typical polarization curve for a DMFC is shown in Fig. 1.3. In an ideal fuel cell, the cell voltage is independent of the current drawn. Practically, the reversible cell voltage is not realized even under open-circuit (zero current) conditions as a result of countless irreversibilities arising during fuel cell operation. As the current density (current per unit active electrode area) increases the cell potential is lowered quickly due to activation loss. At intermediate current densities, stable potential loss exists due to contact resistance including resistance of polymer electrolyte membrane termed as Ohmic loss. Lastly mass transport resistance arises due to limited supply of reactants at the electrode surface and it is pronounced at high current densities.

1.3.3 Polymer electrolyte membrane for DMFC applications

The successful performance of a fuel cell depends critically on the role played by the membrane. The role of membrane in a fuel cell is the same as in other

electrochemical systems (refer to section 1.1). The desirable properties of a material to be chosen as membrane for fuel cell application are as follows:

- High proton conductivity and zero electronic conductivity
- Electrochemical and chemical stability at elevated temperatures in both oxidizing and reducing environments
- Adequate mechanical strength, preferably resistance to solvent swelling
- Adequate barrier to oxidant and fuel cross-over
- Cost effective and readily available

1.3.4 Factors affecting performance of membranes

1.3.4.1 Water uptake or Hydration

The proton conductivity of the membrane is dependent on the extent of water uptake (Zawodzinski *et al.* 1993). Increased water uptake increases proton conductivity. As water is absorbed in the membrane, there is an enhancement in the hydrophilic domain size resulting in the membrane swelling. As more water is absorbed in the membrane (perfluorosulfonic acid membranes), the cluster size increases and these clusters are connected to form water channels. This phenomenon is called percolation (Gebel, 2000). These water channels provide the passage of protons, in addition, water and hydrophilic solvents to penetrate. There is a possibility of the cathode being flooded due to electro-osmotic drag which reduces the oxidation reaction kinetics. This is one of the problems with Nafion[®] that has been studied by Zadowzinski *et al.* (1995). The electro-osmotic drag coefficient [EODC], is a quantitative measure of hydration, and can be defined as the number of water molecules transported per proton. The studies of Zadowzinski *et al.* (1995) indicate that for Nafion[®] 117 equilibrated with water vapor the EODC is about 1, while for

that immersed in water is about 2.5. They also showed that the drag is mainly a function of water content and is independent of the type of Nafion[®] membrane used. In DMFC, the permeation of methanol (fuel) through the membrane from the anode to the cathode is pronounced which is considered to be a major technical barrier of this technology. Methanol crossover can occur in two modes, namely, molecular diffusion and electro-osmotic drag (Verbrugge, 1989). Increased water uptake increases the diffusion of methanol through the membrane. Hence optimum water uptake contributes for proton conductivity without facilitating electro-osmotic drag or fuel crossover.

1.3.4.2 Thickness

Advantages of reduced thickness include lower membrane resistance (and therefore an enhancement in membrane conductivity), lower cost and rapid hydration. However, there is a limit to the extent to which membrane thickness can be reduced because of difficulties with durability and fuel crossover. The methanol crossover rate decreases with an increase in the thickness of the membrane thereby enabling an improvement in the fuel cell performance (Doyle and Rajendran 2003). Though methanol crossover depends on various other factors like the concentration of methanol in the fuel feed, the operating temperature and the performance of the anode, the membrane thickness has direct impact on the cell performance as studied by Liu *et al.* (2006). They employed various Nafion[®] membranes, including Nafion[®] 117, 115 and 112 with respective thicknesses of 175 μm , 125 μm and 50 μm , in a passive direct methanol fuel cell (DMFC). The passive DMFC operated with a lower methanol concentration (2.0 M), a thicker membrane led to better performance at lower current densities, but exhibited lower performance at higher current densities. When the methanol concentration was increased to 4.0 M, however, all three membranes exhibited similar cell voltages over a wide range of current densities. The test of fuel

utilization indicated that the passive DMFC with a thicker membrane exhibited higher efficiency.

To balance between membrane thickness and membrane resistance, spatial control of acidic regions can be done by surface modification or by increasing the charge density in the microstructure of the proton exchange membrane to obtain highly conductive materials. One promising strategy to enhance the charge density and to minimize methanol crossover is the development of composite membranes, for example, the Nafion[®] composites with SiO₂, zirconium phosphate, heteropoly acids, organically modified silicates and zeolites (Mauritz, 1998; Alberti and Casciola, 2003; Honma *et al.* 2003; Li *et al.* 2006). The non-perfluorinated composite membranes include poly ether ether ketone (PEEK) composite membranes (Robertson *et al.* 2003), PBI composite membranes, (Jorissen *et al.* 2002) or poly(vinyl alcohol) (PVA) composite membranes (Shanmugam *et al.* 2006).

1.4 LITERATURE BACKGROUND

Proton conducting membrane was first employed as electrolyte for fuel cell application by General Electric (GE) in 1959. Phenolic membranes were tested and the membrane exhibited low mechanical strength and a short lifetime of 300–1000 h (Magnet, 1968). The first application of proton conducting membranes was in NASA's Gemini flights. Partially sulfonated polystyrene sulfonic acid membranes developed by GE with better performance was employed however, this membrane exhibited brittleness in the dry state (Bockris and Srinivasan, 1969).

1.4.1 Perfluorosulfonic acid (PFSA) membranes

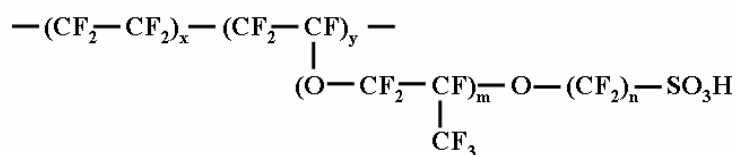
In late 1960s, Dr. Walther Grot of Du Pont developed a perfluorosulfonic acid (PFSA) membrane called “Nafion[®]” for chlor-alkali processes. Later in 1970s it was

employed for fuel cells and exhibited improved performance and durability. Since then, it became a standard for PEMFC applications. Other PFSA membranes include Gore Select (Gore), Aciplex[®] (Asahi Chemicals), and Flemion[®] (Asahi Glass) (Ho and Sirkar, 1992; Nguyen and Vanderborgh, 1998). Table 1.2 provides a comparison of properties of a few commercial membranes (Penner and Martin, 1985; Bahar *et al.* 1996; Küver and Kamloth, 1998; Slade *et al.* 2002; David, 2004; Yoshitake *et al.* 2005; Lobato *et al.* 2006).

Table 1.2 Characteristics of commercial polymer membranes.

Membrane	Membrane type	Dry thickness (µm)	Equivalent weight (gmol ⁻¹ SO ₃ ⁻¹)	Water content (wt %)	Conductivity (S cm ⁻¹)	Manufacturer
Aciplex-S	Perfluorosulfonic acid	120	1000	43	0.108	Asahi Chemical
BAM 3G		140 (wet)	375-920	87	-	Ballard
Dow		125	800	54	0.114	Dow Chemical
Flemion		50	1000	38	0.14	Asahi Glass
Gore Select		5-20	900-1100	32-43	0.028-0.096	Gore
Nafion [®] 105		125	1000	-	-	Du Pont
Nafion [®] 112		50	1100	20.7 ± 0.5	0.065	
Nafion [®] 1135		89	1100	21.1 ± 0.6	0.11	
Nafion [®] 115		127	1100	21.9 ± 0.6	0.09	
Nafion [®] 117		183	1100	23.2 ± 0.4	0.08	
Nafion [®] 1110		254	1100	38	-	
NRE-211	Perfluorosulfonic acid/PTFE copolymer	25.4	-	5.0 ± 3.0	0.1	David Fuel Cell Components
NRE-212		50.8	-	5.0 ± 3.0	0.1	
Sterion [®] L180	Perfluorosulfonic acid	180	-	-	-	David Fuel Cell Components
IonClad [®] R 1010	Tetra-fluoroethylene grafted poly(styrene sulfonic acid)	40	-	-	0.07	Pall Gelman Sciences
IonClad [®] R 4010	Tetrafluoroethylene/perfluoropropylene copolymer	20	-	-	0.08	
CRA	Polyethylene-Tetrafluoroethylene grafted sulphonyls	160	-	-	0.045	Solvay
CRS	Tetra-fluoroethylene with poly(styrene sulfonic acid)	160	-	-	0.05	

General structure of PFSA membrane is given in Fig. 1.4. PFSA consists of three regions: (1) a polytetrafluoroethylene (PTFE, Du Pont's Teflon™)-like backbone, (2) side chains of $\text{---O---CF}_2\text{---CF---O---CF}_2\text{---CF}_2\text{---}$ which connect the molecular backbone to the third region, and (3) ion clusters consisting of sulfonic acid ions. When the membrane becomes hydrated, the hydrogen ions in the third region become mobile by bonding to the water molecules and moving between sulfonic acid sites (Fig. 1.4). There are two advantages in the use of PFSA membranes in fuel cells. First, because the structure is based on PTFE backbone, PFSA membranes are relatively strong and stable in both oxidative and reductive environments. In fact, durability of 60,000 h has been reported (Wakizoe *et al.* 1995). Second, the protonic conductivities achieved in a well-humidified PFSA membrane can be as high as 0.2 S cm^{-1} at PEM fuel cell operating temperatures. The high electronegativity (i.e. electron affinity) of the fluorine atom, bonded to the same carbon atom as the SO_3H group makes the sulfonic acid a superacid (e.g. like the trifluoromethane sulfonic acid)



Nafion 117	$m > 1, n = 2, x = 5 - 13.5, y = 1000$
Flemion	$m = 0, 1; n = 1 - 5$
Aciplex	$m = 0, 3; n = 2 - 5, x = 1.5 - 14$
Dow membrane	$m = 0, n = 2, x = 3.6 - 10$

Fig. 1.4 General structure of perfluorosulfonic acid membrane (Li *et al.* 2003).

The most significant feature of PFSA membrane is its high proton conductivity. In dry state, the PFSA membrane does not contain any ion conductive site. The combination of the perfluorocarbon polymer backbone and the sulfonic acid group provides

excellent electrochemical and mechanical properties. The hydrophilic sulfonic acid group makes the water passage, and the strong matrix originating from the perfluorocarbon backbone prohibits the polymer from dissolution in water. The structure was investigated by Gierke *et al.*, (Gierke *et al.* 1981; Hsu and Gierke, 1982) and reported that the size of the percolation was 4 nm and that of the water passage was 1 nm from the small angle X-ray scattering (SAXS) experiment.

1.4.2 Limitations with PFSA membranes

A PFSA membrane exhibits poor ionic conductivity at low humidity and/or elevated temperature. For example, the conductivity of Nafion[®] reaches up to 10^{-2} S cm⁻¹ in its fully hydrated state but dramatically decreases with temperature above the boiling temperature of water because of the loss of absorbed water in the membranes (Yang *et al.* 2001; Atkins *et al.* 2003; Casciola *et al.* 2006). Its high preparation cost, lack of safety during its manufacturing and use due to fluorine based technology and methanol permeability are also major limitations of PFSA membranes (Surampudi *et al.* 1994; Babir and Gomez, 1996; Curtin *et al.* 2004). The high methanol permeability is related to the structure of the PFSA membrane as already mentioned. Strong sulfonic acid group of PFSA membrane induces considerable phase separation and thus results in large size of the hydrated cluster leading to water and methanol passage. In order to solve these problems numerous approaches have been tried to develop new solid polymer electrolytes, which are cost effective materials with desirable electrochemical properties (Karthikeyan *et al.* 2000; Kreuer, 2001; Smitha *et al.* 2005; Neburchilov *et al.* 2007)

1.4.3 Modified PFSA membranes

1.4.3.1 Composite formation

Considerable efforts have been made to modify the PFSA membranes to ascertain water retention at elevated temperatures and to reduce its methanol permeability (Baradie *et al.* 1998; Antonucci *et al.* 1999; Alberti and Casciola, 2003; Kumar and Fellner, 2003; Savadogo, 2004; Karthikeyan *et al.* 2005). Composite formation with hygroscopic oxides and with solid inorganic proton conductors in order to achieve low-humidity and high-temperature operation PFSA membranes is considered elsewhere in detail (refer to section 1.7).

1.4.3.2 Swelling with low volatile and non-aqueous solvents

Attempts to replace water, which is acting as a host for proton transport, with non-aqueous, and low-volatile solvents leads to membrane stability for their high temperature operation. A very first attempt was made by Savinell *et al.* (1994) by incorporating phosphoric acid in Nafion[®] moiety and they reported the conductivity of 0.05 S cm⁻¹ at 150 °C with lower crossover of methanol compared to bare Nafion[®] membrane. The low volatile phosphoric acid acts as a Bronsted base and solvates the proton from the strong sulfonic acid group in the same way as water does (Wasmus *et al.* 1995). Phosphoric acid (B.P: 158 °C) has low volatility and therefore increases the operational temperature up to 200 °C. However, it should be noted that the conductivity obtained for the phosphoric-acid-swollen Nafion[®] is lower than that of pure phosphoric acid. This may indicate that phosphoric acid in pure form is in fact the intrinsic proton conductor.

Another interesting group of solvents with potential to replace water is the heterocycles (e.g., imidazole, pyrazole, or benzimidazole), containing both proton

donor (NH) and acceptor (N). Kreuer *et al.* (1998) reported an increasing conductivity for sulfuric acid mixed with the heterocycles, though no increase in conductivity was observed for a mixture of phosphoric acid with the heterocycles (Schechter and Savinell, 2002). Sun *et al.* (2001) prepared water-free Nafion[®] 117 membranes by swelling them in imidazole and imidazolium salt (e.g., trifluoroacetate and trifluoromethane sulfonate) solutions. They reported the conductivities of about 10^{-3} S cm⁻¹ at around 100 °C. Sen *et al.* (2008) investigated Nafion[®] 115 and Nafion[®] 112 membranes swelled in the concentrated solution of azoles such as 1H-1,2,4-triazole (Tri), 3-amino-1,2,4-triazole (ATri) and 5-aminotetrazole (ATet) as heterocyclic protogenic solvents and obtained better conductivity at 180 °C, exceeding 10^{-3} S cm⁻¹ compared to other Nafion[®]/heterocycle systems under anhydrous conditions. These membranes exhibited lower methanol permeability compared to Nafion[®] 112. However, it has to be noted that no fuel cell test has been reported with PFSA membranes swollen in these ionic or heterocyclic media. It can be rationalized that the difficulties may arise from (1) the immobilization of the liquids, especially in the presence of water (an attempt has been made to immobilize imidazole as proton solvent (Schuster *et al.* 2001), (2) adsorption of the solvent on the catalyst surface and (3) imidazole groups are not as water in solvating acid groups of the membrane.

1.4.3.3 Reinforced PFSA membranes

In order to reduce the internal resistance and cost of the membrane, thinner membranes are preferred. The challenge in developing thinner membranes is in maintaining the required mechanical strength especially under swelling and/at elevated temperatures. This has lead to the development of reinforcing PFSA with other polymers. Reinforced composite membrane has been developed by the Gore

(Gore-Select[®]), where the micropores of stretched PTFE membrane are filled with perfluorinated ionomer (Bahar *et al.* 1996) and thus a reduced membrane thickness of 5 μm could be achieved. Gore-Select[®] membrane exhibited improved mechanical stability and ten times higher proton conductivity compared to Nafion[®] membranes. Other substrates such as, porous polypropylene (Bae *et al.* 2002), expanded PTFE (Shim *et al.* 2002), and polysulfone and microglass fiber fleece (Haufe and Stimming, 2001), impregnated with Nafion[®] has also been investigated. By means of reinforcement, the thickness of PFSA membranes has been successfully reduced down to 5-30 μm with good conducting and mechanical properties (Nouel and Fedkiw, 1998; Liu *et al.* 2001). But, it has to be mentioned that the thinner membranes are generally employed to hydrogen/air applications to minimize ohmic losses, while thicker membranes are employed for direct methanol fuel cells (DMFCs) to reduce methanol crossover (Kerres, 2001; Doyle and Rajendran, 2003).

1.5 ALTERNATIVE SULFONATED POLYMER MEMBRANES

Significant efforts have been channeled to develop alternative proton exchange membranes for DMFC in order to overcome the disadvantages associated with the PFSA membranes enumerated in section 1.4.2. The developments in alternative proton conducting polymers have been extensively reviewed (Savadogo, 1998; Kreuer, 2001; Kerres, 2001; Jones and Rozie're, 2001; Hickner *et al.* 2004). The main requisite in choosing polymers for fuel cell application is that it should possess high stability in both oxidizing and reducing environment, including thermo-hydrolytic stability. Our rationalization (refer to section 1.9) in addition to the suggestion by Rikukawa and Sanui, (2000) leads to the fact that in order to produce materials that are less expensive than Nafion[®], some sacrifice in material lifetime and mechanical

properties may be acceptable, provided the cost factors are commercially realistic. The main features of hydrocarbon polymers that have made them particularly attractive are their improved water uptake properties over a wide temperature range, since the absorbed water is restricted to the polar groups of hydrocarbon polymer chains, their stability can be improved by proper molecular design, in addition to the fact that they can be recycled by conventional methods and above all they are cost effective. Hence the use of hydrocarbon polymers, even though they had been previously abandoned due to low thermal and chemical stability, presently attracts renewed interest.

1.5.1 Partially fluorinated membranes

Partially fluorinated polymers can be considered as alternative materials for fuel cell applications. This is because, a compromise between the advantages and disadvantages of hydrocarbon-based polymers and perfluoro polymers can be attained with partially fluorinated polymer based membrane materials; in addition, realization of reduced cost with high conductivity and good resistance against hydrolytic and oxidative degradation can also be attained. Thus, such partially fluorinated membranes exhibit good proton conductivity and low methanol permeability (Shena *et al.* 2005). These membranes can be prepared by grafting or blending. Ballard Power Systems Inc. has developed a novel family of partially fluorinated proton-conducting membranes based on sulfonated poly(trifluorostyrene) homopolymers and copolymer membranes by radiation grafting. These membranes have been reported to exhibit long-term stability as well as appreciable proton conductivity (Wei *et al.* 1995; Basura *et al.* 1999).

Disadvantages associated with these membrane material are that a complicated preparation procedure of the monomer α,β,β -trifluorostyrene (Livingston *et al.* 1956) and the difficult sulfonation (Wei *et al.* 1995) procedures for poly(α,β,β -trifluorostyrene)-homopolymers and copolymers.

Poly(ethylene-*alt*-tetrafluoroethylene) (ETFE) films were made proton conductive by means of irradiation treatment followed by sulfonation process. These membranes have exceptionally low water uptake capacities and excellent dimensional stabilities. The membranes were tested in DMFC between 30 °C - 95 °C and exhibited comparable performances to that of Nafion[®] 115 (Saarinen *et al.* 2005). Chemical and mechanical stability of the ETFE-based membrane appeared to be promising since it was tested over 2000 h in the DMFC without any performance loss.

Scott *et al.* (2000), reported the performance data for the direct methanol fuel cell (DMFC) using a series of radiation-grafted proton exchange membranes based on polyethylene and poly(ethylene-*alt*-tetrafluoroethylene) ETFE. Polystyrene sulphuric acid grafted polyethylene and ETFE based membranes were reported to exhibit low methanol diffusion coefficients. The cell voltage performance of the DMFC, for a duration of <100 h testing, with these low cost membranes is as good as, or superior to, that of cells based on Nafion[®] under identical operating conditions. However, the stability of contact between the membrane and the catalyst layer requires improvement before these membranes become real alternatives to materials such as Nafion[®], for the DMFC applications.

Other fluorinated polymers with octafluorobiphenylene or hexafluorobisphenol groups also exhibited good resistance against hydrolytic and oxidative degradation (Chen *et al.* 2005; Wang *et al.* 2005; Kim *et al.* 2006). Based on these, Chang *et al.*

(2008) proposed a new class of sulfonated poly(fluorine-*co*-sulfone)ethers with perfluorocyclobutane (PFCB) groups for DMFC application. Under the state of high sulfonation the membranes showed higher proton conductivity than Nafion[®] 115 at various temperatures and considerably lower methanol permeability.

Polymer blending has been shown to improve the properties of two different polymers including dimensional and thermal stability, and alters surface character (Noshay and McGrath, 1977). Polymeric blends based on sulfonated poly(ether ether ketone) (SPEEK)/poly(vinylidene fluoride) (PVdF) were prepared for direct methanol fuel cell (Jung and Park, 2007) application. The dimensional stability of the hydrocarbon polymer was enhanced by introducing PVdF. The blend membrane containing 2.5 wt % PVdF exhibited proton conductivity close to that of Nafion[®] with lower methanol permeability.

1.5.2 Aromatic hydrocarbon membranes

Aromatic hydrocarbons represent a group of polymers consisting entirely of linked benzene rings, e.g., poly-*p*-phenylene (PP) (structure 1, Fig. 1.5). They exhibit good oxidation stability and hence are considered as rigid polymers. For fuel cell application the polymers employed will have a structure 2 as shown in Fig. 1.5 where X is an atom or group of atoms giving the polymer chains a certain degree of flexibility. More commonly, X can be -C-O-C- ether links, -SO₂- in polysulfone, -NHCO- in polyamides, -COO- in polyesters, and -CO- in polyketones. Well studied hydrocarbon polymers include poly(ether ether ketones) (Victrex PEEK, structure 3, Fig. 1.5) (Mikhailenko *et al.* 2000; Gil *et al.* 2004), poly arylene ether sulfone (PES, structure 4, Fig. 1.5) (Wang *et al.* 2002; Yu *et al.* 2004) and poly benzimidazole (PBI, structure 5, Fig. 1.5) (Wang *et al.* 1996; Samms *et al.* 1996; Wang *et al.* 1996).

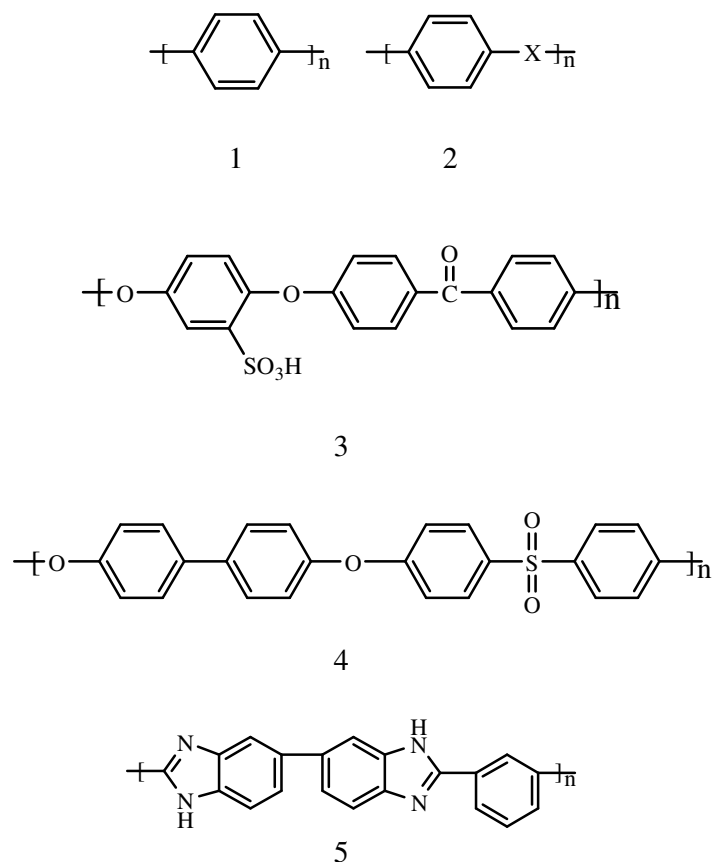


Fig. 1.5 Chemical structure of polymers.

In order to create proton conductivity, hydrocarbon polymers are sulfonated by one of the following ways:

- By direct sulfonation in concentrated sulfuric acid, chlorosulfonic acid or sulfur trioxide (Jin *et al.* 1985; Lee and Marvel, 1984; Bailly *et al.* 1987; Nolte *et al.* 1993)
- By lithiation-sulfonation-oxidation (Kerres *et al.* 1996)
- By chemically grafting a group containing a sulfonic acid onto a polymer (Glipa *et al.* 1997)

- By radiation grafting followed by sulfonation of the aromatic component (Gupta *et al.* 1994), or
- By synthesis from monomers bearing sulfonic acid groups (Genies *et al.* 2001)

The attached sulfonic groups *i.e.*, the hydrophilic region facilitates the transport of proton and the hydrophobic region offers good mechanical strength (Bumsuk *et al.* 2004).

Non-perfluorinated hydrocarbon based membranes are promising candidates for the DMFC because of their low cost and reduced methanol permeability characteristics (Büchi, 1995; Lee *et al.* 1996). The first hydrocarbon based proton conducting polymer membranes have been developed by General Electric. Sulfonated phenol-formaldehyde resins were developed by Adams and Holmes, (1935) followed by sulfonated divinylbenzene-cross-linked polystyrene by D'Alelio (1944). Under fuel cell test, these membranes showed insufficient chemical stability.

Among aromatic membranes, PEEK has been extensively studied owing to its advantages like low cost, high thermal and mechanical stability. The direct methanol fuel cell (DMFC) performance of the sulfonated poly(ether ether ketone) (SPEEK) membranes with various degrees of sulfonation (DS) was better than that of Nafion[®] 115 membrane at 80 °C (Li *et al.* 2003). However, the mechanical properties of SPEEK in aqueous environments at relatively high temperatures may not be suitable for long-term application in fuel cells (Deb *et al.* 2007). Sulfonation increases hydrophilicity, proton conductivity and exhibits higher water uptake there by decreasing the dimensional stability. Various attempts are being made to improve the mechanical properties by adopting routes such as crosslinking (Zhong *et al.* 2007;

Zhong *et al.* 2009), blending membranes with other polymers (Manea and Mulder, 2002; Zhao *et al.* 2007; Cai *et al.* 2007; Yang, 2008; Norddin *et al.* 2008), forming composite membranes with inorganic materials (Chang *et al.* 2003; Silva *et al.* 2005; Zhang *et al.* 2008), and surface modifications (Choi *et al.* 2001; Ren *et al.* 2005) were carried out by various methods like plasma treatment, grafting reaction or surface coating or by combining the above said methods.

Sulfonated polyarylene ether (SPAEE) derivatives are presently under investigations for DMFC applications (Wang *et al.* 2002; Gil *et al.* 2004; Park *et al.* 2005; Shang *et al.* 2006; Ghassemi *et al.* 2006); Wang *et al.* 2006; Gao *et al.* 2006; Li *et al.* 2006; Kim *et al.* 2006; Kim *et al.* 2006; Liu *et al.* 2008; Honga *et al.* 2008; Lufrano *et al.* 2008; Lee *et al.* 2009) [5-14]. These polymers include sulfonated polysulfone (Park *et al.* 2005; Lufrano *et al.* 2008), sulfonated poly(arylene ether ketone) (Gil *et al.* 2004; Shang *et al.* 2006; Wang *et al.* 2006; Gao *et al.* 2006; Liu *et al.* 2008) and sulfonated poly(arylene ether sulfone) (Wang *et al.* 2002; Li *et al.* 2006; Kim *et al.* 2006; Kim *et al.* 2006; Honga *et al.* 2008; Lee *et al.* 2009). High thermal and mechanical stability with strong resistance to decomposition in acidic medium made these membranes as possible alternatives to Nafion[®] membranes.

However, these sulfonated membranes generally suffer from high water swelling and poor hydrolytic stability while increasing the degree of sulfonation (Miyatake and Hay, 2001; Hickner *et al.* 2004). The hydration of the sulfonated membranes leads to microscopic phase separation between the hydrophilic clusters and the hydrophobic domains that are responsible for proton conduction and morphological stability respectively.

Crosslinking or blending can be a solution to overcome the limitations of the intrinsic properties of sulfonated aromatic polymers. Kerres *et al.* (2002), investigated the covalently or ionically crosslinked membranes for DMFC applications. These non-fluorinated membranes exhibited performance in DMFC comparable to that of perfluorinated ionomer membranes, with peak power densities of around 0.25 W cm^{-2} at 110°C .

In the blended system, each of the components was crosslinked *via* ionic or covalent interaction, resulting in a significant enhancement of membrane stability and methanol-barrier property, even under thermally and chemically harsh conditions.

Polybenzimidazoles (structure 5, Fig. 1.5) are another family of high performance polymers. Polybenzimidazole (PBI) doped with phosphoric acid or sulphuric acid show excellent proton conductivities, especially at temperatures greater than 130°C and they are employed as proton-conducting electrolyte (Wainright *et al.* 1995). Such membranes are cheaper than perfluorinated polymer membranes and are suitable for applications at high operating temperature ($>100^\circ\text{C}$) that is for DMFC with vaporized methanol feed.

1.5.3 Limitations of sulfonated polymers

Sulfonated polymers are highly deliquescent (Bailly *et al.* 1987); this limitation has been circumvented by preparing mixed derivatives, where the sulfonated groups are replaced by non-sulfonated groups (Rikukawa *et al.* 2005). It is also of importance to realize that sulfonated materials are likely to have a temperature limit at 200°C (Elamathi *et al.* 2008) where in some instances decaying of the proton conductivity has been attributed to the decomposition of the SO_3H groups. Particularly, aggressive environment in a DMFC can initiate different types of degradation mechanisms and

aging processes that result in either chemical or morphological/textural alteration. Such modification might arise from desulfonation, chain scission caused thermohydrolytically, or by free radicals generated at the electrodes or loss of mechanical properties owing to excessive swelling (Rozière and Jones, 2003; Hogarth *et al.* 2005). Species such as HO· and HOO· could arise from oxygen diffusion through the membrane and incomplete reduction at the anode, and possible degradation mechanisms involving oxidizing species and hydroxy radicals occurs.

1.6 ACID BASE POLYMERS

Acid–base membrane is one of the viable alternatives for Nafion[®] membranes that can maintain high conductivity at elevated temperatures without suffering from dehydration effects. In general, the acid–base complexes considered for fuel cell membranes involve incorporation of a strong or medium acid into an alkaline polymer base (polymers bearing basic sites like ether, alcohol, imine, amide, or imide groups) to promote proton conduction or incorporation of excess base in to an acidic polymer (sulfonated polymer with absorbed imidazole, benzimidazole or another appropriate proton acceptor)

1.6.1 Doping with acids

The basic polymer unit acts as a proton acceptor establishing hydrogen bonds with the acid group by forming an ion pair. A number of basic polymers have been investigated for preparing acid-base electrolytes (Lasségues, 1992), such as polyethyleneoxide (PEO) (Donoso *et al.* 1988), poly(vinylalcohol) (PVA) (Weeks *et al.* 1988), polyacrylamide (PAM) (Weeks *et al.* 1988; Wieczorek and Stevens, 1988), polyethylenimine (PEI) (Tanaka *et al.* 2000), Nylon (Grondin *et al.* 1995), polybenzimidazole (PBI) (Wainright *et al.* 1995), and

poly(diallyldimethylammonium-dihydrogen phosphate, $\text{PAMA}^+-\text{H}_2\text{PO}_4^-$) (Bozkurt *et al.* 1995). The earlier acid-polymer membranes exhibited proton conductivity less than $10^{-3} \text{ S cm}^{-1}$ at room temperature. At higher acid content, the acid-polymer complex leads to formation of a soft paste there by restricting the membrane processing termed as plastifying effect. Wainright *et al.* (1995) first proposed phosphoric acid doped polybenzimidazole (PBI) membranes which was then successfully developed and studied extensively by Savinell's group (Wasmus *et al.* 1995; Savinell and Litt, 1996; Samm *et al.* 1996; Wang *et al.* 1996; Wang *et al.* 1996; Weng *et al.* 1996; Lin *et al.* 1997; Fontanella *et al.* 1998). The nature of the acid influences the conductivity of doped PBI, and after the contact with acid of high concentration (11 M) the conductivity follows the order $\text{H}_2\text{SO}_4 > \text{H}_3\text{PO}_4 > \text{HNO}_3 > \text{HClO}_4 > \text{HCl}$ (Xing and Savadogo, 1999). Among these PBI doped with different acids, H_3PO_4 and H_2SO_4 are well investigated because of their unique proton conduction mechanism through self-ionization and self-dehydration (Gillespie and Robinson, 1965). H_3PO_4 and H_2SO_4 exhibit effective proton conductivity even in an anhydrous (100 %) form. Other important features of phosphoric acid are the excellent thermal stability and low vapour pressure at elevated temperatures. Another remarkable characteristic of acid doped PBI is its electro-osmotic drag co-efficient. For acid doped PBI, the electro-osmotic drag co-efficient was zero (Weng *et al.* 1996), while Nafion[®] 117 showed an electro-osmotic drag co-efficient of 3.2 (Xie and Okada, 1995). From the data on electroosmotic drag and the dependence of ionic conductivity on extent of doping, Grotthus mechanism was suggested to be responsible for proton transport in doped PBI (Bouchet *et al.* 2001). As the doping level increases, the distance between the clusters of acid sites decreases and the anion moieties support the proton hopping between imidazole sites.

1.6.2 Doping with bases

Immersion of pristine PBI in aqueous inorganic bases has been reported to increase its conductivity by almost an order of magnitude (Xing and Savadogo, 2000). However, the kinetics of this reaction is slow (immersion for 10 days), and the concentration of base is (8 M NaOH) high compared with the conditions required to complex PBI with acids. Uptake of base is faster by benzyisulfonate-grafted PBI (PBI-S) (Roziere *et al.* 2001) it has been observed that after a short contact time (15–60 min) with an aqueous solution of an organic or inorganic base, shrunken benzyisulfonate grafted PBI membranes achieve satisfactory textural and proton transport properties. In each case, the conductivity is close to $10^{-2} \text{ S cm}^{-1}$ at 25 °C and 100 % RH. In addition, if such base-treated membranes are exposed to a dry atmosphere, they will dry and wrinkle but recover their flexibility after a few seconds of immersion in water. The conductivity values of sulfonated PBI after dehydration, and after immersion in basic solution are summarized in Table.1.3.

Table 1.3 Conductivity (100 % RH) of benzyisulfonate grafted PBI after dehydration and immersion in basic aqueous solutions (1 M, 15 min, 25 °C) (Adapted from (Roziere *et al.* 2001).

Membrane	Conductivity (S cm^{-1})
PBI-S	4.2×10^{-4}
PBI-S/ NH_4OH	1.5×10^{-2}
PBI-S/imidazole	7.9×10^{-3}
PBI-S/DABCO	1.2×10^{-2}
PBI-S/LiOH	1.2×10^{-2}
PBI-S/NaOH	1.2×10^{-2}
PBI-S/KOH	1.7×10^{-2}
PBI-S/CsOH	1.7×10^{-2}

Though the conductivity of PBI generally increases with increasing acid doping level the mechanical strength decreases. The optimum doping level is thus a compromise between these two effects. Different methods are being explored to improve the proton conductivity without sacrificing mechanical strength or vice versa. The methods involve ionic and covalent cross-linking of the polymer (Kerres, 2005) as well as preparation of composite membranes (Staiti and Minutoli, 2001; He *et al.* 2003; Zaidi, 2005). The extensive studies on syntheses, properties, modifications and applications of proton exchange membranes based on PBI is recently reviewed by (Li *et al.* 2008).

It has been suggested that materials with a low electro-osmotic drag may offer the potential for improved selectivity in DMFCs (Pivovar *et al.* 1999). For PBI membranes, the electro-osmotic drag coefficient of methanol was found to be essentially zero (Weng *et al.* 1999). The methanol permeability of PBI complexed by H_3PO_4 is considerably lower than that of Nafion[®], due to the dense, nonporous characteristics of PBI films (Wainright *et al.* 1999). A direct methanol fuel cell using such a phosphoric acid doped membrane and operating on a 50/50 methanol/water feed to the anode at 150 °C would have a methanol crossover equivalent to less than 10 mA cm⁻², (Wainright *et al.* 1999) which can be compared with crossover rates in excess of 100 mA cm⁻² when Nafion[®] is employed. Gubler *et al.* (2007) investigated Celtec-V membranes based on PBI and PVPA for methanol crossover by a real-time measurement spectrometric analysis. According to their studies there is 10 times higher methanol crossover rate for a liquid fed 1 M methanol solution at 90 °C. These results provide an indication of methanol permeability of the base polymer, but are not relevant to fuel cell operation since doping with phosphoric acid is necessary to achieve conductivity, and thus are not compatible with liquid fed methanol solution.

PBI membranes doped with acids exhibited high conductivity (Bouchet and Siebert, 1999; He *et al.* 2003; Ma *et al.* 2004) good mechanical properties (Litt *et al.* 2004) and excellent thermal stability (Samms *et al.* 1996) up to 200 °C under ambient pressure. The hydrogen bonding and amphoteric properties of the phosphonic acids facilitates the proton transport in such membranes through structure diffusion, under lower-humidity, or through the dynamics of water, at high water contents (Lafitte and Jannasch, 2007). Furthermore, due to the strength of the carbon–phosphorus bond, these compounds are highly stable under hydrolytic conditions and/or high temperatures (Lafitte and Jannasch, 2007). Despite these advantages, PBI composites have some disadvantages, like the long-term stability of doped PBI membranes is yet to be proven despite their excellent attributes for fuel cell applications (Steiner, R. Sandor, 1991; Qinfeng *et al.* 2001). The diffusion of unassociated H₃PO₄ out of the PBI, degradation of membrane due to the attack of H₂O₂ and its radical, •OH or •OOH limits cell performances. PBI–phosphoric acid has been studied for almost a decade for high temperature PEFC applications. Other PBI–acid systems are emerging in literature for fuel-cell applications (Xing and Savadogo, 1999), however many aspects related to the development of PBI–acid systems for this application remain unclear: like the proton conduction mechanism at high temperatures with acid doping levels and relative humidity. PBI material is quite difficult to prepare and exhibits poor solubility hence its applicability appears to be rather limited.

1.7 ORGANIC INORGANIC COMPOSITE MEMBRANES

An effective way to achieve low humidity and high-temperature operation is to recast polymers with fillers like silica (Honma *et al.* 1999; Jung *et al.* 2001; Dimitrova *et al.* 2002; Chang and Lin, 2003; Baglio *et al.* 2006; Lufrano *et al.* 2006; Reichman *et al.*

2006; Huang *et al.* 2006; Duvdevani *et al.* 2006; Croce *et al.* 2006; Martinelli *et al.* 2006; Gosalawit *et al.* 2006; Liang *et al.* 2006; Li *et al.* 2006; Ren *et al.* 2006; Zeng *et al.* 2007; Chen *et al.* 2007; Lee *et al.* 2007; Shahi, 2007; Wang *et al.* 2007; Tay *et al.* 2008; Fu *et al.* 2008), alumina (Martinelli *et al.* 2005; Shen *et al.* 2006; Martinelli *et al.* 2007), zirconia (Nunes *et al.* 2002; Zhai *et al.* 2006; Saccà *et al.* 2006), titania (Saccà *et al.* 2005; Rhee *et al.* 2006; Yang, 2007), tungsten trioxide (Nakajima and Honma, 2002; Shao *et al.* 2006), aluminum oxy hydroxide (Kumar *et al.* 2008) and tin oxide (Mecheri *et al.* 2007) which are hygroscopic in nature. This concept was suggested by Watanabe *et al.* (1995 and 1996) forming a basement for the development of self-humidifying composite membranes.

Hygroscopic oxides were incorporated into various polymers like, Nafion[®] (Dimitrova *et al.* 2002; Saccà *et al.* 2005; Baglio *et al.* 2006; Liang *et al.* 2006; Li *et al.* 2006; Ren *et al.* 2006; Saccà *et al.* 2006; Zhai *et al.* 2006; Rhee *et al.* 2006; Shao *et al.* 2006), polytetrafluoroethylene (PTFE) (Reichman *et al.* 2006; Zeng *et al.* 2007), Nafion[®] NRE-212 membrane (Wang *et al.* 2007), Nafion[®]/polyaniline (Chen *et al.* 2007), sulfonated polysulfone (Lufrano *et al.* 2006), sulfonated poly(ether sulfone) (Shahi, 2007), poly(vinylidene) fluoride (PVDF) (Duvdevani *et al.* 2006; Martinelli *et al.* 2007), Nafion[®]/PTFE (Huang *et al.* 2006), Nafion[®]/Krytox (Gosalawit *et al.* 2006), Poly(vinylidene) fluoride-chloro tetrafluoro ethylene, (PVDFCTFE) copolymer (Croce *et al.* 2006), poly(ethyleneglycol)/(4-dodecylbenzene sulfonic acid (PEG)/(DBSA) (Chang and Lin *et al.* 2003), Sulfonated styrene-(ethylene-butylene)-sulfonated styrene (SEBSS) (Jung *et al.* 2001), poly-(ethylene oxide)s (PEO) (Honma *et al.* 1999; Nakajima and Honma, 2002), Poly(vinyl alcohol) (PVA) (Martinelli *et al.* 2006; Yang, 2007), poly-vinylidene fluoride/poly-acrylonitrile (PVDF/PAN) (Martinelli *et al.* 2007), PVDF-g-PSSA (poly(styrene sulfonic acid) (Shen *et al.* 2006)

and sulfonated poly(ether ether ketone) (SPEEK) (Nunes *et al.* 2002). It has been shown that the water uptake by the oxide containing membrane is higher than that of the pristine polymer. Composite membranes with hygroscopic oxide exhibited improved thermal and mechanical stability than the parent polymer. They all, in common, exhibited reduced methanol permeability. Reduction in fuel crossover can be achieved either by physical or chemical means. The addition of hygroscopic oxide results in a change in structure of the membrane, where the particles block part of the hydrophilic polymer channels through which protons migrate (Fig. 1.6). At the same time narrowing of water channels allow low solvent permeation and electroosmotic drag coefficient. Other problems such as reduction in mechanical stability (becomes brittle) when the inorganic component loading reached a critical level, and decreased fuel cell performances were encountered.

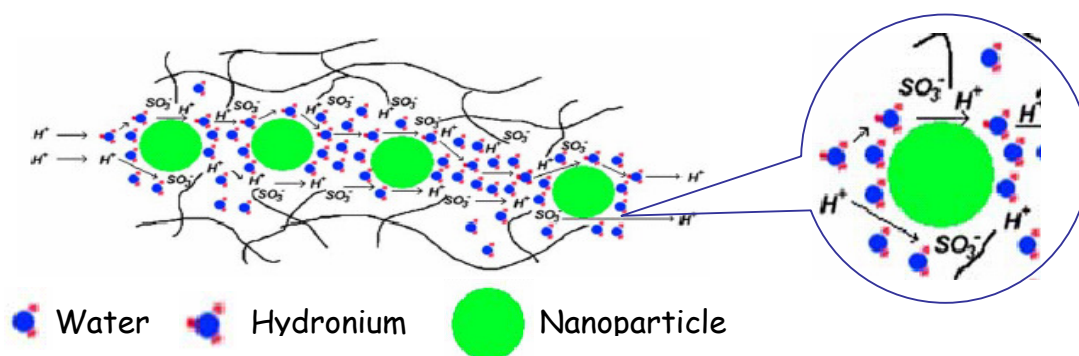


Fig. 1.6 Proton transport in hybrid membranes (Hogarth *et al.* 2005).

In order to improve the conductivity at low humidity and high-temperature operating conditions, *fast proton conductors* like heteropoly acids (Zaidi *et al.* 2000; Staiti *et al.* 2000; Kim *et al.* 2003; Ramani *et al.* 2004; Xu *et al.* 2004; Ponce *et al.* 2004; Lin *et al.* 2005; Sauk *et al.* 2005; Vernon *et al.* 2005; Feng *et al.* 2005; Zaidi and Ahmad, 2006; Shanmugam *et al.* 2006; Kim *et al.* 2006; Li and Wang, 2006; Ramani *et al.* 2006;

Shao *et al.* 2006; Ahmad *et al.* 2006; Cui *et al.* 2007; Kim and Chang, 2007; Cui *et al.* 2008; Kim *et al.* 2008; Colicchio *et al.* 2009), zirconium phosphates (Yang *et al.* 2001; Ruffmann *et al.* 2003; Vaivars *et al.* 2004; Silva *et al.* 2005; Casciola *et al.* 2005; Kim *et al.* 2005; Jang and Yamazaki, 2005; Hill *et al.* 2006; Jiang *et al.* 2006; Chen *et al.* 2007; Søggaard *et al.* 2007; Kim *et al.* 2006; Woo *et al.* 2006; Regina *et al.* 2006; Krishnan *et al.* 2006; Tripathi *et al.* 2009) having a potential to play a dual characteristics of being both hydrophilic and proton conducting have been incorporated into various polymer matrix. Fast proton conductors are the ones, which exhibit conductivity greater than $10^{-5} \text{ S cm}^{-1}$ at 27 °C with activation energy $E_a < 0.4 \text{ eV}$ (Nakamura *et al.* 1979). Polymer matrices like Nafion[®] (Ramani *et al.* 2004; Bauer and Porada, 2005; Kim *et al.* 2006; Shao *et al.* 2006; Kim *et al.* 2006; Ramani *et al.* 2006), sulfonated polyether ether ketone (SPEEK) (Zaidi *et al.* 2000; Ruffmann *et al.* 2003; Ponce *et al.* 2004; Ahmad *et al.* 2006; Zaidi and Ahmad, 2006; Krishnan *et al.* 2006), polyethylene glycol (PEG) (Vernon *et al.* 2005; Lin *et al.* 2005), sulfonated polyethersulfone Cardo (Regina *et al.* 2006), sulfonated poly(arylene ether sulfone) (Kim *et al.* 2003), disulfonated poly(arylene ether sulfone) (Hill *et al.* 2006), Nafion[®]/Teflon[®] (Jiang *et al.* 2006; Chen *et al.* 2007), Nafion[®]/polyphenylene oxide (PPO) (Sauk *et al.* 2005), sulfonated polyether ether ketone (SPEEK)/polybenzimidazole (Silva *et al.* 2005), polybenzimidazole (PBI) (Staiti *et al.* 2000; Jang and Yamazaki, 2005), poly(vinyl alcohol) (PVA) (Xu *et al.* 2004; Lin *et al.* 2005; Shanmugam *et al.* 2006), polyethyleneimine (PEI) (Karthikeyan *et al.* 2005), polystyrene grafted poly(ethylene-alt-tetrafluoroethylene) (Søggaard *et al.* 2007), polyvinylidene fluoride (PVDF) (Casciola *et al.* 2005) and poly (fluorinated arylene ether)s (Woo *et al.* 2006) have been employed.

1.7.1 Heteropoly acids

Among the active components employed, the heteropoly acids (HPA) exhibited exceptionally high conductivities at room temperature, approximately 0.17 S cm^{-1} , when 29 water molecules are presented as hydrated water in the molecule ($n=29$) (England *et al.* 1980). Owing to these characteristics, a series of composite membranes have been prepared by incorporating HPA into polymer matrices (refer to Table. 1.4). Even though these solid acids can be providing high proton conductivity like mineral acids, their conductivity drops drastically once they are heated and dehydrated. The hydration sphere is connected to their conducting behavior and it is essential that some how the hydrated state of HPA has to be maintained in the polymer matrices. This is one of the necessary conditions for these materials to be exploited for the transport of protons through the membrane in fuel cell applications. Moreover, HPAs are in general readily soluble in water. As such, use of these materials in fuel cells implies the impossible requirements of retaining hydration to ensure high conductivity and removing the by-product water to prevent dissolution. However it should be emphasized again that the proton conductivity is not linked to the polymer back bone and hence it is always possible that the stability and durability have to be ensured by proper protection within the polymer matrices but still maintaining the conductivity chain. The fabrication of membranes in this model can be difficult and hence repeatability of the membrane manufacture can become one of the issues.

Table 1.4 Summary of inorganic-organic composite membranes.

Membranes	(Water uptake in %) [Swelling %] {IEC}	Conductivity σ (S cm^{-1}) (Temp in $^{\circ}\text{C}$) [RH %]	Diffusion coefficient/ permeability	Fuel cell performance	References
Silica as filler					
Nafion [®] -SiO ₂			$10^{-5} \text{ cm}^2 \text{ s}^{-1}$	DMFC - current density of 0.6 A cm^{-2} at 0.4 V at 130°C	Baglio <i>et al.</i> 2006
Nafion [®] /Aerosil (SiO ₂)	(30-40)	$0.1 - 0.4$ (90)	$0.1 \text{ mol m}^{-2} \text{ s}^{-1}$		Dimitrova <i>et al.</i> 2002
Nafion [®] /P(SPA)-SiO ₂ 3-sulfopropyl acrylate grafted silica core (<10 nm)	(9.66)	0.04 (80)	$8.45 \times 10^{-7} \text{ cm}^2 \text{ s}^{-1}$	DMFC – maximum power output (W cm^{-2}) of the composite membrane is about 1.8 times > Nafion [®] at 50°C	Tay <i>et al.</i> 2008
Sulfonated poly(arylene ether sulfone)-SiO ₂	(25-40)	$1.3-1.5 \times 10^{-1}$	$10^{-6} \text{ cm}^2 \text{ s}^{-1}$	DMFC - maximum power density = 114.4 mW cm^{-2} at 380 mA cm^{-2} and current density at $0.4 \text{ V} = 234.8 \text{ mA cm}^{-2}$	Lee <i>et al.</i> 2007
Styrene (St)- <i>p</i> -vinylbenzyl chloride (VBC)-divinylbenzene (DVB)-polyvinyl chloride (PVC) copolymer/3-(methylamine)propyl-SiO ₂	(30-50) {1.71 to 2.45 meq g^{-1} }	$2-6 \times 10^{-2}$ (RT)	$1.85 \times 10^{-7} \text{ cm}^2 \text{ s}^{-1}$		Fu <i>et al.</i> 2008
Sulfonated poly(ether sulfone)-SiO ₂ (phosphoric acid functionalized)	(28.7) {0.961 meq g^{-1} }	6.36×10^{-2} (RT)	$4.89 \times 10^{-7} \text{ cm}^2 \text{ s}^{-1}$	DMFC - comparable to the Nafion [®] 117 membrane	Shahi, 2007
Sulfonated polysulfone/ SiO ₂		5×10^{-2} (25-90)		DMFC - power density 0.18 W cm^{-2} (120°C , 2M)	Lufrano <i>et al.</i> 2006
PEO/SiO ₂		10^{-3} (80)			Honma <i>et al.</i> 1999
PTFE/amorphous fumed SiO ₂		0.22		DMFC - (OCV= 0.56 and 0.65 V) 50 and 130 mW cm^{-2} at 80 and 130°C , respectively	Reichman <i>et al.</i> 2006

Table 1.4 (Contd.)

PTFE/SiO ₂ (commercial SiO ₂ sol)		0.1 (RT)			Zeng <i>et al.</i> 2007
Nafion [®] /polyaniline/ SiO ₂	(20)	9.1 x 10 ⁻³ (50) [100]		DMFC - 8 mW cm ⁻² (40 °C, 2 M) two-fold lower than Nafion [®]	Chen <i>et al.</i> 2007
Nafion [®] /PTFE/SiO ₂		3.25 x 10 ⁻³		DMFC – (OCV = 0.564 V) maximum power density = 70 mA cm ⁻² (70 °C, 2 M)	Huang <i>et al.</i> 2006
Poly(vinylidene) fluoride-chloro tetrafluoro ethylene, (PVdF- CTFE) copolymer/SiO ₂		10 ⁻² (RT)		DMFC- power density = 1.4 mW cm ⁻² and current density = 10–20 mA cm ⁻²	Croce <i>et al.</i> 2006
PEG/DBSA(4-dodecylbenzene sulfonic acid) /SiO ₂	(30-60) {0.5 -1 m mol g ⁻¹ }	4 – 7 x 10 ⁻³ (RT) [100]	(0.78 - 2.1) x 10 ⁻⁸ cm ² s ⁻¹		Chang and Lin, 2003
Sulfonated styrene-(ethylene- butylene)-sulfonated styrene (SEBSS)/SiO ₂			8-14 μ mol cm ² s ⁻¹	DMFC- maximum current densities are 74, 229, and 442 mA cm ⁻² at 30, 60, and 90°C at 0.3 V	Jung <i>et al.</i> 2001
PVA/functionalized SiO ₂ / Glutaraldehyde		10 ⁻¹			Martinelli <i>et al.</i> 2006
Krytox-SiO ₂ -Nafion [®]	(42)	10 ⁻⁴ (130)			Gosalawit <i>et al.</i> 2006
Nafion [®] /diphenylsilicate		2.39 x 10 ⁻²		DMFC - OCV = 0.65 V (1 M)	Liang <i>et al.</i> 2006
Nafion [®] / diphenyldimethoxysilicate	[30]	10 ⁻² (RT)		DMFC- comparable to Nafion [®]	Li <i>et al.</i> 2006
Nafion [®] /Organic SiO ₂ with thiol group		1.57 x 10 ⁻² (RT) [100]		DMFC – (75°C, 0.2 MPa O ₂ & 1M) Nafion [®] 117 > Nafion [®] /Organic silica with thiol group>Nafion [®] / silica (unmodified)	Ren <i>et al.</i> 2006
Sulfonation of poly(ether sulfone)/SiO ₂ with phosphonic acid functionality	(28.73) {0.961meq. g ⁻¹ }	6.36 x 10 ⁻²	4.89 x 10 ⁻⁷ cm ² s ⁻¹	DMFC - 30W/cm ² (70 °C, air at 10 psi)	Shahi, 2007
PVDF/SiO ₂ with surface- anchored sulfonic acid		3.6 x 10 ⁻³ (75)		DMFC- (OCV = 0.66 V) power density 32 mW cm ⁻² (70 °C)	Duvdevani <i>et al.</i> 2006

Table 1.4 (Contd.)

Cs _{2.5} H _{0.5} PWO ₄₀ /SiO ₂ /Nafion [®] NRE-212				H ₂ /O ₂ - better performance than Nafion [®] NRE-212 (60 °C and 80 °C)	Wang <i>et al.</i> 2007
Alumina as filler					
Nafion [®] /Al ₂ O ₃				DMFC - current density of 0.4 A/cm ² at 0.4 V (130 °C)	Baglio <i>et al.</i> 2006
PVDF-g-PSSA/Al ₂ O ₃	(68)	4.5×10^{-2}	6.6×10^{-8} cm ² s ⁻¹	DMFC - maximum peak power density = 12 mW cm ⁻² (2.5 M)	Shen <i>et al.</i> 2006
PVDF/PAN/Al ₂ O ₃		0.10			Martinelli <i>et al.</i> 2005
PVDF/Al ₂ O ₃ /PWA		10^{-3} (< 50)			Martinelli <i>et al.</i> 2007
Zirconia as filler					
Nafion [®] /ZrO ₂	(24) {0.85 meq g ⁻¹ }			H ₂ /air - Power density 604 mW cm ⁻² and of 387 mW cm ⁻² at 0.6 V (T = 110 °C (100% RH) and T = 130 °C (85 % RH)	Saccà <i>et al.</i> 2006
Sulfonated poly(ether ether ketone)(SPEEK)/ZrO ₂		34×10^{-3} (25)	60-fold reduction of the methanol flux		Nunes <i>et al.</i> 2002
Nafion [®] /sulfated ZrO ₂	(27) {0.9-1.1 meq g ⁻¹ }			H ₂ /O ₂ - 1.35 W cm ⁻² (80 °C) and 0.99 W cm ⁻² (120 °C) better than Nafion [®] under same condition (e.g. 1.28 W cm ⁻² at 80 °C, 0.75 W cm ⁻² at 120 °C)	Zhai <i>et al.</i> 2006
Titania as filler					
Nafion [®] /TiO ₂	(29) {0.93 meq g ⁻¹ }	0.15–0.18 (85) [100]		PEMFC- Power density = 0.514 and 0.256 W cm ⁻² at 0.56 V at 110 and 130 °C	Saccà <i>et al.</i> 2005
PVA/TiO ₂	(89)	10^{-2} (30)		Alkaline DMFC - maximum peak power density = 7.54 mW cm ⁻² at 60 °C	Yang, 2007

Table 1.4 (Contd.)

Nafion [®] /sulfonated titanate		0.16 (75)	Permeability of methanol reduced by 38 %, relative to Nafion [®] 115	DMFC-57% higher power density (73.0 mW cm ⁻²) than Nafion [®]	Rhee <i>et al.</i> 2006
Tungsten trioxide as filler					
Nafion [®] /WO ₃	(37)	10 ⁻² (100)		PEMFC-)-current densities of 300 and 540 mA cm ⁻² at 0.4 V (110 °C)	Shao <i>et al.</i> 2006
PEO/WO ₃ ·2H ₂ O		10 ⁻² –10 ⁻³ (RT to 120)			Nakajima and Honma, 2002
Aluminum oxy hydroxide as filler					
PVdF-HFP/Nafion [®] /AlO[OH] _n	(34)	1 × 10 ⁻³ (100)	1.4 × 10 ⁻⁶ cm ² min ⁻¹		Kumar <i>et al.</i> 2008
Tin oxide as filler					
Sulfonated polyether ether ketone (SPEEK)/hydrated tin oxide (SnO ₂ ·nH ₂ O)	(15)	0.016 (25)		DMFC - OCV, composite (0.70 V) > unfilled SPEEK (0.65 V) and Nafion [®] (0.59 V) current density = 350 mA cm ⁻² power density = 80 mW cm ⁻² (100 °C, oxygen feed, 2 M)	Mecheri <i>et al.</i> 2007
Heteropoly acids as filler					
Nafion [®] /PWA, PMA, SWA, SMA	(8)	0.06-0.08 (70) [100]		H ₂ /air- current density of 0.1-0.9 A cm ⁻² at 0.6 V (80 °C, 75 % RH)	Ramani <i>et al.</i> 2004
Sulfonated poly(arylene ether sulfone)/PWA	(15-40) {1.4 meq g ⁻¹ }	0.09 - 0.15 (30-100) [100]			Kim <i>et al.</i> 2003
Poly(vinyl alcohol)/PWA	(157) {0.794 m mol g ⁻¹ }	10 ⁻⁴	6.16 × 10 ⁻⁷ to 8.31 × 10 ⁻¹⁰ cm ² s ⁻¹	H ₂ /O ₂ - current density = 46 mA cm ⁻² DMFC - current density = 80 mA cm ⁻² at 80 °C	Lin <i>et al.</i> 2005

Table 1.4 (Contd.)

Chitosan(CS)/HPA CS/PMA, CS/PWA and CS/SWA	(18.6, 17.0 & 17.4) {0.46, 0.38 & 0.41 mmol g ⁻¹ }	0.01 (25)	$2.7 \times 10^{-7} \text{ cm}^2 \text{ s}^{-1}$		Cui <i>et al.</i> 2008
SPEEK/PWA, PMA and disodium salt of PWA, Na ₂ HPW ₁₂ O ₄₀ (Na-PWA)	sPEEK -PWA (600) sPEEK – PMA (320) sPEEK - Na-PWA (400)	sPEEK -PWA 9.5×10^{-3} sPEEK - PMA 3.0×10^{-3} sPEEK - Na- PWA 5.8×10^{-3} (100)			Zaidi <i>et al.</i> 2000
Sulfonated polyethersulfone Cardo/PWA	(52)	6.7×10^{-2} (110)			Li and Wang, 2006
Nafion [®] /chitosan/PWA		0.078 (RT)	$6.5 \times 10^{-7} \text{ cm}^2 \text{ s}^{-1}$	DMFC- (OCV = 0.73 V) maximum power density = 58 mW cm ⁻²	Cui <i>et al.</i> 2007
Nafion [®] /polyphenylene oxide (PPO)/phosphomolybdic acid (PMA)		0.03	$2.01 \times 10^{-6} \text{ cm}^2 \text{ s}^{-1}$	DMFC – (OCV = 0.75 V) current density 160 mA cm ⁻² at 0.35 V	Sauk <i>et al.</i> 2005
Polyethylene glycol/silica/lacunary heteropolyacid (H ₈ SiW ₁₁ O ₃₉)	{2–2.5 meq g ⁻¹ }		$1.2 \times 10^{-6} \text{ cm}^2 \text{ s}^{-1}$	Poor performance compared to a Nafion [®] 117	Vernon <i>et al.</i> 2005
Nafion [®] /Sulfonic-functionalized heteropolyacid/silica nanoparticles				DMFC- power density = 33 mW cm ⁻² (80 °C), 39 mW cm ⁻² (160 °C) and 44 mW cm ⁻² (200 °C)	Kim <i>et al.</i> 2006
SPEEK/silica/divacant tungstosilicate [γ -SiW ₁₀ O ₃₆] ⁸⁻		13×10^{-3} (110) [100]	$0.8 \times 10^{-16} \text{ m}^2 \text{ s}^{-1} \text{ Pa}^{-1}$		Ponce <i>et al.</i> 2004
Nafion [®] /SiO ₂ /PWA			$1.7 \times 10^{-6} \text{ cm}^2 \text{ s}^{-1}$ 50–80 % lower methanol cross- over than Nafion [®]	DMFC - power density = 15 mW cm ⁻² , two times higher in the fuel efficiency than Nafion [®] in 10 M methanol	Kim and Chang, 2007

Table 1.4 (Contd.)

PBI/PWA/SiO ₂		3.0×10^{-3} (100) [100]			Staiti <i>et al.</i> 2000
PVA/PWA/SiO ₂	[10-30]	0.017 (RT)	10^{-7} to 10^{-8} cm ² s ⁻¹		Xu <i>et al.</i> 2004
PVA/SiO ₂ /SWA		$(4.1-8.3) \times 10^{-3}$ (80 - 100) [100]			Shanmugam <i>et al.</i> 2006
PEG/SiO ₂ /PWA	(44.7)	10^{-3}	1.05×10^{-7} cm ² s ⁻¹	DMFC – OCV = 650 mV	Lin <i>et al.</i> 2005
Nafion [®] /PTA /SiO ₂ , ZrO ₂ and TiO ₂			low crossover compared to recast Nafion [®]		Ramani <i>et al.</i> 2006
Nafion [®] /PTA/MCM-41		10^{-2} (RT)	10^{-6} cm ² s ⁻¹	DMFC -current density = 0.0572 A cm ⁻² with maximum power density = 18 W cm ⁻²	Kim <i>et al.</i> 2008
SPEEK/PTA/MCM-41	(74-83)	$6.7-8.1 \times 10^{-3}$ (140)	5.7×10^{-9} cm ² s ⁻¹		Zaidi and Ahmad, 2006
SPEEK/SiO ₂ /PTA		6×10^{-3} (90) [90] 1.2×10^{-3} (90) [60]		DMFC - composite membrane shows better performance than Nafion [®] 112 at all temperatures (60, 80 & 90 °C)	Colicchio <i>et al.</i> 2009
Polyethyleneimine (PEI)/Tungstosilicate mesoporous materials (Si-MCM-41)		6.1×10^{-2} (100) [100]		H ₂ /O ₂ - OCV= 0.93 V (100 °C & 100 % RH) current density= 42.9 mA cm ⁻² power density=18.3 mW cm ⁻²	Feng <i>et al.</i> 2005
SPEEK/heteropoly acid-loaded Y-zeolite	(70-98)	7.8×10^{-3} (140)			Ahmad <i>et al.</i> 2006
Zirconium phosphate (ZrP) or Zirconium sulphophenyl phosphate (ZrSPP) as filler					
Nafion [®] /ZrP		10^{-2} (RT) [100%]		DMFC - OCV = 0.86 V and 0.87V at 120 and 150 °C with oxygen or air	Yang <i>et al.</i> 2001 Vaivars <i>et al.</i> 2004
SPEEK/zeolite/ZrP	{ 1.2-1.4 meq g ⁻¹ }	$2.91-3.35 \times 10^{-2}$ (30)	$3-4 \times 10^{-7}$ cm ² s ⁻¹	DMFC - current densities = 68.75 mA cm ⁻² at 0.36 V, peak power density = 30 mW cm ⁻² (70°C)	Tripathi <i>et al.</i> 2009

Table 1.4 (Contd.)

Disulfonated poly(arylene ether sulfone)/ZrP	(40-60)	0.027 (80) [100]	7.5×10^{-7}		Hill <i>et al.</i> 2006
Nafion [®] /Teflon [®] /ZrP				H ₂ /O ₂ - current density = 400 mA cm ⁻² at 0.73 and 0.59 V (80 and 120 °C) under ambient pressure	Jiang <i>et al.</i> 2006
ZrP/divinylbenzene (DVB) crosslinked, sulfonated, polystyrene grafted poly(ethylene-alt-tetrafluoroethylene) /poly(vinyl difluoride)	{ 1.8–2 meq g ⁻¹ }	40 x10 ⁻³ (130) [90]			Søgaard <i>et al.</i> 2007
Nafion [®] /ZrSPP		10 ⁻¹ (110) [98]		H ₂ /O ₂ -current density = 700 mA cm ⁻² at 0.4 V, four times higher than Nafion [®] (100 °C)	Kim <i>et al.</i> 2006
Polybenzimidazole/zirconium tricarboxybutylphosphonate		3.82 x 10 ⁻³ (200)			Jang and Yamazaki, 2005
PVDF/zirconium sulfophenylphosphonate, Zr(SPP), Zr(HPO ₄) _{1.0} (O ₃ PC ₆ H ₄ SO ₃ H) _{1.0})	(46)	2 x10 ⁻³ (120) [90]			Casciola <i>et al.</i> 2005
SPEEK cardo/zirconium phosphate sulfophenylphosphonate	(10-40)	10 ⁻² (22) [100]	45 x 10 ⁻⁸ cm ² s ⁻¹ an order less than Nafion [®]		Regina <i>et al.</i> 2006
Poly(fluorinated arylene ether)s/ Zirconium phosphate sulfonated	(85.6)	1.63 x 10 ⁻² (RT)		PEMFC- maximum power densities= 481 mW cm ⁻² and 300 mW cm ⁻² at 960 mA cm ⁻² and 640 mA/cm ² (120 °C and 130 °C) respectively. Higher voltage and maximum power density than Nafion [®]	Woo <i>et al.</i> 2006
SPEEK/ZrP/PBI	[0.6]	11.5 x10 ⁻³ (25)		DMFC – power density 14.7 mW cm ⁻² for 58.8 mA cm ⁻² (110 °C and 138 % RH	Silva <i>et al.</i> 2005

Table 1.4 (Contd.)

SPEEK/ZrP/ZrO ₂	(21.5) [100]	0.8 (25)		DMFC- exhibits lower performance compared to Nafion®	Ruffmann <i>et al.</i> 2003
Layered silicate nanoparticles (e.g., montmorillonite (MMT), laponite, and modified montmorillonite) or clay as fillers					
Nafion® 115/sulfonated montmorillonite(MMT)	(93)	0.93	$1.14 \times 10^{-6} \text{ cm}^2 \text{ s}^{-1}$	DMFC - 30 mW cm ⁻² for composite and for Nafion® 25 mW cm ⁻¹ at 0.35 V	Kim <i>et al.</i> 2007
Nafion®/MMT		0.08 (RT)	$1.6 \times 10^{-7} \text{ cm}^2 \text{ s}^{-1}$	DMFC- higher power density than unmodified Nafion® at concentrated methanol feed (10 M)	Song <i>et al.</i> 2004
PVA/MMT		0.0368 (30)	$3\text{-}4 \times 10^{-6} \text{ cm}^2 \text{ s}^{-1}$	DMFC - maximum power density 6.77 mW cm ⁻² at ambient pressure and temperature	Yang <i>et al.</i> 2009
Poly (2,6-Dimethyl-1,4-Phenylene oxide)/MMT	(20) {2.5 meq g ⁻¹ }	1.08×10^{-2}	$4.5 \times 10^{-8} \text{ cm}^2 \text{ s}^{-1}$	DMFC – Higher OCV (0.71 V) than Nafion® (0.69 V) for 1M methanol	Sadrabadi <i>et al.</i> 2008
SPEEK/MCM-41		$8\text{-}16 \times 10^{-3}$	$3 \times 10^{-17} (\text{m}^2 \text{ s}^{-1} \text{ Pa}^{-1})$		Karthikeyan <i>et al.</i> 2005
SPEEK/laponite		$3\text{-}10 \times 10^{-3}$ (90)	$3 \times 10^{-17} (\text{m}^2 \text{ s}^{-1} \text{ Pa}^{-1})$		
SPEEK/organic-montmorillonite (OMMT)	(150)	1.2×10^{-2} (90) [100]	$10^{-8} \text{ cm}^2 \text{ s}^{-1}$		Gaowen and Zhentao, 2005
Nafion®/poly(oxyproplene)/MMT	(32) {0.89 mmol g ⁻¹ }	$60\text{-}90 \times 10^{-3}$	$0.4 \times 10^{-8} \text{ cm}^2 \text{ s}^{-1}$	DMFC –current densities = 56 mA cm ⁻² at 0.2 V with maximum power density of 13.3 mW cm ⁻²	Lin <i>et al.</i> 2007
Nafion®/organic sultones and perfluorinated sultone grafted MMT	{0.8-1.1 mmol g ⁻¹ }	0.13 (50) [98]	Reduced by 40% compared to Nafion®	DMFC – current densities 140 mA cm ⁻² , at 0.3 V	Kim <i>et al.</i> 2006

Table 1.4 (Contd.)

Polyimide (PI), polyamideimide (PAI), polyvinylidene fluoride PVDF/styrene–ethylene–butylenes–styrene elastomer (SEBS)/phosphosilicate (P_2O_5 – SiO_2)		<p>PI/(P_2O_5–SiO_2) - 1.6×10^{-2} (150) [18]</p> <p>PAI/(P_2O_5–SiO_2) - 1.5×10^{-3} (150) [18]</p> <p>PVdF/(P_2O_5–SiO_2) - 8.1×10^{-4} (130) [25]</p> <p>SEBS/(P_2O_5–SiO_2) - 6.9×10^{-3} (130) [25]</p>		<p>PI/(P_2O_5–SiO_2) OCV = 0.9 V, power density = 20 mW cm^{-2} (150 °C, 4 % RH)</p> <p>PAI /(P_2O_5–SiO_2) OCV = 0.95 V, power density = 52 mW cm^{-2} (30 °C, 60 % RH)</p> <p>PVdF/(P_2O_5–SiO_2) OCV = 0.79 V, Power density = 29 mW cm^{-2} (130 °C, 25 % RH)</p> <p>SEBS/ (P_2O_5–SiO_2) OCV = 0.72 V, Power density = 34 mW cm^{-2} (110 °C, 30 % RH)</p>	Matsuda <i>et al.</i> 2006
poly(vinyl alcohol)-poly(styrene sulfonic acid-co-maleic acid) /Clay-15A	{0.79 x 1.65 meq g ⁻¹ }	0.023	$2.19 \times 10^{-7} \text{ cm}^2 \text{ s}^{-1}$		Kim <i>et al.</i> 2009
Noble metals (Pt, Ru, Pd, Ag)					
(Pt– SiO_2)/Nafion [®] coated /SPEEK/PTFE				H ₂ /O ₂ - (OCV = 0.98 V) and maximum power density = 0.8 W cm^{-2} than SPEEK/PTFE	Zhang <i>et al.</i> 2007
Pt/ SiO_2 / Nafion [®] /PTFE	(54) [6.7]		$10^{-3} \text{ cm}^2 \text{ s}^{-1}$	PEMFC - 1.65 W cm^{-2} (80 °C), performance with the Pt– SiO_2 /Nafion [®] /PTFE- was better than NRE-212	Wang <i>et al.</i> 2006
Pt–ZrP/Nafion [®]		0.06 [RT]		PEMFC performance – 275 mA cm ⁻² at 0.620 V	Lee <i>et al.</i> 2004
PtRu/Nafion [®]		0.18 (90) [100]		DMFC – 28 % and 31 % > Nafion [®] membrane (30 and 45 °C)	Jung <i>et al.</i> 2007

Table 1.4 (Contd.)

Pd/Nafion [®]	(25)		$1.598 \times 10^{-6} \text{ cm}^2 \text{ s}^{-1}$	DMFC- improved OCVs and current-voltage performance	Choi <i>et al.</i> 2001
Ag-SiO ₂ /sulfonated poly(biphenyl ether sulfone	(60-100)			H ₂ /O ₂ - improved performance than parent polymer	Xing <i>et al.</i> 2007
Zeolite					
Nafion [®] /Zeolite(ZSM-5)	(30)	0.14 (RT)	$1.4 \times 10^{-6} \text{ cm}^2 \text{ s}^{-1}$		Byun <i>et al.</i> 2006
Chitosan(CS)/zeolite (3A, 4A, 5A, 13X, mordenite and HZSM-5)	(50-68) [10-45]	10^{-2}	$10^{-5} \text{ cm}^2 \text{ s}^{-1}$		Wang <i>et al.</i> 2008
Chitosan/surface-modified Y-zeolite	(60-100) [55] {0.098- 0.168 mmol g ⁻¹ }	2.58×10^{-2}	$3.90\text{-} 9.04 \times 10^{-7} \text{ cm}^2 \text{ s}^{-1}$		Wu <i>et al.</i> 2007
PVDF/NaA zeolite (LTA), mordenite (MOR), ETS-10 and Sn-Umbite silicates	(27.1, 27.8, 17.8, 19.3)	2.3, 0.06, 0.17, 14.4×10^{-3} (40) [100]	18.5, 9.7 $9.6, 7.3 \times 10^{-5} \text{ cm}^2 \text{ s}^{-1}$		Sancho <i>et al.</i> 2008
Nafion [®] /chabazite and clinoptilolite				DMFC- Maximum power densities = $350\text{--}370 \text{ mW cm}^{-2}$ and $200\text{--}210 \text{ mW cm}^{-2}$ (140 °C)	Baglio <i>et al.</i> 2005
PTFE/zeolite	(60-80)	0.01 (RT)		DMFC – highest current and power densities = 50 mA cm^{-2} and 4 mW cm^{-2} (70°C)	Połtarzewski <i>et al.</i> 1999
Pt/zeolite/Nafion [®]	(38.6)			H ₂ /O ₂ –(50 °C) membrane with 0.65 wt % of Pt/zeolite shows 75 % of the performance at 0.6 V	Son <i>et al.</i> 2007
Nafion [®] /mordenite		0.01 (70) [100]		H ₂ /O ₂ - current densities 400 mA cm^{-2} (0.5 V, 100°C)	Kwak <i>et al.</i> 2004
Acrylic acid/Tin mordenite		1×10^{-2} (RT) [100]	11% methanol uptake compared to 54 % methanol uptake for Nafion [®]		Rao <i>et al.</i> 1994

Table 1.4 (Contd.)

Phosphates					
Nafion [®] /calcium phosphate			$1.8 \times 10^{-6} \text{ cm}^2 \text{ s}^{-1}$		Park and Yamazaki, 2005
Nafion [®] /CHP(calcium hydroxyphosphate)	(34)		$0.6 \times 10^{-7} \text{ cm}^2 \text{ s}^{-1}$		Park and Yamazaki, 2006
PVA/hydroxyapatite	(45-60)	10^{-2} (RT)	methanol uptake 15-16 %	Air-breathing DMFC- maximum peak power density 11.48 mW cm ⁻²	Yang <i>et al.</i> 2008
SPEEK/boron phosphate	(50-130) {2.18 meq g ⁻¹ }	0.065 (70) [100]	$2.42 \times 10^{-6} \text{ cm}^2 \text{ s}^{-1}$		Choa <i>et al.</i> 2008 Othman <i>et al.</i> 2007
SPEEK/PBI/boron phosphate	(25)	5.9×10^{-3}			Zaidi, 2005
Layered Double Hydroxides (LDH)					
Acrylonitrile (AN)-sodium styrene sulfonate (SSS) copolymer/4-Vinylbenzenesulfonate intercalated layered double hydroxides (MgAl-VBS LDHs)		2.60×10^{-3}	$5-9 \times 10^{-9} \text{ cm}^2 \text{ s}^{-1}$		Angran <i>et al.</i> 2008
Nafion [®] /LDH		0.0187	$1.51 \times 10^{-7} \text{ cm}^2 \text{ s}^{-1}$	DMFC - Increased OCV (5 & 7 M CH ₃ OH)	Lee and Nam, 2006

1.7.2 Zirconium phosphates

Zirconium phosphates are water-insoluble, and it is known that layered compounds containing intercalated hydronium ions exhibit reasonable conductivity at room temperature (10^{-3} at 90 % RH) (Casciola and Constantino, 1986). However, the proton transport properties are highly dependent on the humidity level and thus for fuel cell applications, water management remains still a challenge. Attempts were made to improve the conductivity of layered compounds by intercalating Brønsted bases or functionalized organic radicals to replace the hydroxyl moieties of the phosphate group (Alberti *et al.* 1996). When the organic moieties contain a proton generating function such as $-\text{COOH}$, $-\text{PO}_3\text{H}$, $-\text{SO}_3\text{H}$, or NH_3^+ , these compounds can be used as proton conductors. For example, zirconium alkyl sulfophenylphosphonates have been investigated for their conductivity under different temperatures and relative humidity regimes for possible use in fuel cell applications (Alberti *et al.* 1992). As can be seen from Table 1.4, some of these composite membranes exhibit promising conductivities at temperatures above 100 °C.

Although many other stable inorganic systems like layered silicates (e.g., montmorillonite (Lin *et al.* 1992), modified montmorillonite (Song *et al.* 2004; Gaowen and Zhentao, 2005; Kim *et al.* 2006; Kim *et al.* 2007; Sadrabadi *et al.* 2008; Yang *et al.* 2009) and laponite (Karthikeyan *et al.* 2005), zeolites (Połtarzewski *et al.* 1999; Kwak *et al.* 2004; Baglio *et al.* 2005; Byun *et al.* 2006; Son *et al.* 2007), calcium phosphate (Park and Yamazaki, 2005 and 2006) and boron phosphate (Zaidi, 2005 ;Krishnan *et al.* 2006), have been dispersed in a variety of polymeric matrices and have been considered for membrane applications, the structure, degree of crystallinity, shape and dimensions of the particles, as well as their distribution in the

various domains of the hydrated polymers, are not thoroughly investigated. Hence it is not possible to explicitly predict their possible behaviour in membranes useful for fuel cells. An overall observation, when reviewing research in this field is that a tremendous effort has been invested in polymer electrolyte membrane development, but little effort has been expended in developing a clear understanding of the mechanisms that lead to polymer electrolyte membranes with improved proton transport properties. The goal of preparing economical membranes, the attention should be directed to low-cost polymers filled with optimum amount of particles exhibiting desired properties. Both inorganic and organic components must be chosen depending on the swelling index and water of hydration of the components.

1.8 COMPOSITE MEMBRANES vs NAFION[®] – RATIONALE

This section will address several key issues of relevance such as why one looks for composite materials as alternative membrane materials for DMFC applications, what are the components that are used in the formulation of composite membranes, and a comparative as well as parallel understanding of perfluorosulfonic acid membrane materials which are commercially known as Nafion[®] by Du pont with the composite membranes in terms of *bondings, chemical and structural compositions and mechanisms* involved in proton conduction.

Composite membranes have attracted attention, because they exhibit controllable physical properties, such as thermal and mechanical behavior, by combining the properties of both organic polymers and inorganic compounds (hygroscopic oxides, solid inorganic proton conductors). In composite membranes, inorganic fillers of micrometer to nanometer size are uniformly distributed in the polymer matrix either by dispersing the preformed inorganic particles or by forming inorganic particles in

situ into the polymer matrix. A number of impermeable fillers (e.g. oxides, clay) or proton conductive fillers (e.g. heteropoly acids, ZrP, metal hydrogen sulfates) have been employed. The driving force in these developments appear to be to formulate a geometrical shape (in the form of a formable film architecture) with proton conductivity induced in them by appropriate proton conducting materials. In this sense, this is a multi-component system unlike the Nafion[®] membrane where in the proton conducting moiety is directly linked to the film forming polymer architecture. Though multi-component systems can give rise to cumulative effects, there are other disadvantages associated with them. Since the bonding characteristics are not well defined, they are susceptible for easy removal (dissolution, leaching and other degradation processes in the presence of other constituents and possible chemical reaction with them) and hence they have not been successful for the fuel cell application.

Conceptual developments are required if one were to employ composite membranes as substitutes for Nafion[®], especially in terms of the bonding of the proton conducting substances with the film forming polymers. This is one aspect wherein some new concepts have to emerge to make composite membranes viable. The simple dispersion of the proton conducting species like heteropoly acids, zirconium phosphate and other substances though can give rise to proton conduction, since they are not directly linked to the polymer and hence susceptible for degradation with respect to time. Secondly, since the proton conducting species are present as individual entity, it is not possible to enhance the conductivity like the Nafion[®] wherein the highly electronegative backbone environment makes the proton (very similar to bare proton) and hence give rise to exclusive Grotthus type conduction. This aspect is discussed in more detail below (Viswanathan and Helen, 2007).

In Nafion[®], the proton transport is due to the classical ion exchange mechanism (Grotthus hopping mechanism (Agmon, 1995) and hence conductivity will be approximately four times higher compared to other mechanism (vehicle mechanism (Kreuer *et al.* 1982). Fully hydrated membrane contains a water phase similar to bulk water (as assessed by its dielectric properties). The phase separation is caused due to the extreme hydrophobicity of the perfluorinated polymer with the extreme hydrophilicity of the terminal sulfonic acid group of the Nafion[®] (Kreuer, 2001). In the presence of water, the hydrophilic part is hydrated and helps in further phase separation. The hydrophobic part provides good mechanical stability even in presence of water, while the hydrated hydrophilic domains provide the high proton conductivity. Proton transport in water is generally a result of protonic defects and occurs through the breaking and reformation of hydrogen bonds. This is caused because the protonic defect weakens the intermolecular interaction which causes large variations in bond length combined with rapid breaking and forming of bonds. Like Nafion[®], the extent of separation of hydrophobic and hydrophilic domain may not be possible in other system (e.g. SPEEK (Kreuer, 2001)). In composite membranes, one meets with hybrid transport mechanism because the inorganic component can also exhibit vehicular proton transport mechanism. Hence, conduction may not reach the magnitude that one observes in Nafion[®] (Grotthus mechanism). In essence, it appears that one may not be able to formulate at present a material that can have equivalent conductivity as that of Nafion[®]. This is particularly true that one can not create an electronegative environment more than that already available in Nafion[®] (Viswanathan and Helen, 2007).

Grounded on these logistics, one can see that for stepping away from Nafion[®] for a membrane material choice, it requires in particular hydration stability at high

temperatures, low fuel crossover, mechanical, thermal, and oxidative stability as well as appreciable proton conductivity. And, of course, all of these objectives must be achieved while maintaining low cost and by a simple and controllable fabrication method. *This is a challenge in front of us!*

1.9 MOTIVATION AND OBJECTIVE OF THE PRESENT INVESTIGATION

The driving force for this investigation is to design newer class of membranes, which may not demand the exacting experimental conditions and critical management of chemical environments that are necessary for the synthesis of membranes like Nafion[®] and other sulfonated polymers. In literature, there have been various attempts to develop alternate membranes to Nafion[®] (a monopoly product of Du pont), as indicated earlier. However, these attempts have not been successful due to the fact that it may be nearly impossible to design a membrane that will have better ionic conductivity compared to Nafion[®], due to its inherent chemical composition; namely, Nafion[®] holds the utmost electronegative environment possible in a chemical system (Viswanathan and Helen, 2007). Realizing this limitation, it was considered worthwhile to design a membrane which may possess ionic conductivity less than that of Nafion[®], but should have at least one property (for fuel cell applications) better than that of Nafion[®]. Since the fuel crossover from anode to the cathode in a DMFC causes mixed potential at the cathode and hence affects the normally slow reaction of oxygen reduction, it was considered that the membrane development must mainly focus to this aspect of fuel crossover. To focus the issue more precisely the crossover of methanol in case of DMFC is considered as the property of concern.

This investigation therefore focuses on the following aspects of this development:

1. Having realized that membrane development for fuel cell applications is still a challenging proposition, what is current feasible technology available as an alternative to the monopolistic Nafion[®]?
2. Having chosen hybrid membranes as possible appropriate ones, how does one incorporate the active components in the membrane?
3. What is the relative performance of the developed membrane compared to Nafion[®] with respect to methanol crossover?

It is realized that the problem on hand is the most challenging, the solutions sought may not readily yield the final answers but it is believed that they have at least provided some possible (if not appropriate) alternatives to carry the research forward in this field.

CHAPTER 2

EXPERIMENTAL METHODOLOGY

2.1 CHEMICALS AND MATERIALS USED

Poly(vinyl alcohol) (PVA; MW: 125,000, 90 % hydrolyzed), *N,N*-dimethyl formamide (DMF), phosphomolybdic acid (PMA), phosphotungstic acid (PWA) and silicotungstic acid (SWA) were obtained from Sisco Research Laboratory, India, orthophosphoric acid (H_3PO_4) was obtained from E-Merck and zirconium oxychloride ($\text{ZrOCl}_2 \cdot 8\text{H}_2\text{O}$) was obtained from Loba Chemie and were used as received. All aqueous solutions were made with deionized (DI) water, which was further purified with a Milli-Q system (Millipore water, 18.2 $\text{M}\Omega \text{ cm}$).

2.2 CHARACTERIZATION OF MEMBRANES

2.2.1 Fourier transformed infrared (FT-IR) study

The FT-IR spectra for the samples were recorded by using Perkin Elmer spectrometer in the range 400 to 4000 cm^{-1} at room temperature.

2.2.2 X-ray diffraction study

X-ray diffraction patterns were collected with a Rigaku D/max 2400 powder diffractometer using Ni filtered $\text{Cu-K}\alpha$ monochromatic radiation. The angle (2θ) was measured in steps of 0.02° with a dwell time of 1 s, between 5° and 80° .

2.2.3 Thermogravimetric analysis (TGA)

The thermal stability of the samples were examined by thermogravimetric analysis using Perkin Elmer TGA (Delta Series TGA 7) instrument at a heating rate of $20^\circ \text{C min}^{-1}$ under a flow of air from 40 to 800°C .

2.2.4 Differential scanning calorimetry (DSC)

The differential scanning calorimetric (DSC) measurements were performed on the dried samples, in the temperature range between 50 °C and 550 °C using a Perkin-Elmer DSC-7 instrument.

2.2.5 Electron Microscopy study

2.2.5.1 Scanning electron microscope (SEM)

Scanning electron microscope (FEI, Model: Quanta 200) equipped with an Energy Dispersive Spectroscopy (EDS) detector was used to observe the microstructures and composition of the dried membranes. The membrane sample was attached on the carbon tape (Adhesive tape, normally used in SEM measurements for conduction purpose) and mounted on the SEM sample holder and imaged.

2.2.5.2 Transmission electron microscope (TEM)

Transmission electron microscope (TEM) analysis of the sample was performed on a JEOL JEM 2010 electron microscope operated at 200 KeV with a point-to-point resolution of 2.3 Å. TEM samples were prepared by dispersion of the material in alcohol and drops of dispersed material were placed on copper TEM grids and dried for TEM analysis.

2.2.6 X-ray fluorescence (XRF) analysis

Elemental analysis of salts of heteropolyacid was performed by means of X-ray fluorescence analysis (XRF, Model S4 PIONEER BRUKER aXS) for Cs, Mo and W.

2.2.7 Water/methanol uptake

The water/methanol uptake of the hybrid membranes were determined by measuring the change in the weight before and after the immersion in water or in methanol. The membranes were first immersed in deionized water or methanol for 24 h. Then membranes were weighed quickly after wiping off the surface water to determine the wetted membrane weight (W_{wet}). The dry membrane weight (W_{dry}) was determined after complete drying. The water or methanol uptake was calculated by using the following equation:

$$\text{Water or methanol uptake (\%)} = \frac{W_{\text{wet}} - W_{\text{dry}}}{W_{\text{dry}}} \times 100 \quad (2.1)$$

2.2.8 Swelling

The surface swelling characteristics were determined by measuring the change in the membrane geometrical area upon equilibrating the membranes in water at room temperature for 2 h. The swelling ratio was calculated by the following equation:

$$\text{Swelling (\%)} = \frac{A_{\text{wet}} - A_{\text{dry}}}{A_{\text{dry}}} \times 100 \quad (2.2)$$

Where, A_{dry} and A_{wet} are the area of dry and wet samples, respectively.

2.2.9 Ion-exchange capacity (IEC)

The ion-exchange capacity, or *IEC*, is defined as the moles of exchangeable acidic protons per gram of dry polymer and the *IEC* of membranes can be experimentally determined through an acid–base titration. The dry composite membrane was immersed in 50 ml of 1 M sodium chloride aqueous solution for 24 h in order to extract all protons from the membrane. After taking out the membrane, electrolyte

solution was titrated with 5 millimolar sodium hydroxide solution using phenolphthalein as an indicator. The ion exchange capacity (IEC) was calculated using the following equation:

$$IEC = \frac{V \times M}{W_{\text{dry}}} \quad (2.3)$$

where, IEC is the ion exchange capacity (meq g⁻¹); V is the added titrant volume at the equivalent point (ml); M is the molar concentration of the titrant; W_{dry} is the dry mass of the sample (g).

2.2.10 Oxidative stability

Oxidative stability of the membranes was tested by immersing the membrane sample (90-100 mg) into 50 ml of Fenton's reagent (3 % H₂O₂ containing 2 ppm FeSO₄) at room temperature and at 70 °C. The membrane samples were intermittently taken out of the oxidative solution and weighed after removing the surface bounded water. Oxidative stability of the fabricated hybrid membranes was evaluated from the weight change of the membrane sample.

2.2.11 Additive stability in membrane matrix

The stability of salts of heteropolyacid in the membrane matrix is studied by placing the membrane samples (50-60 mg) in 50 ml of water under constant stirring at 30 °C. The membrane samples were intermittently taken out of the aqueous solution and examined by using FT-IR spectroscopy after removing the surface attached water. The FT-IR technique was used to confirm the stability of the additive in the membrane matrix.

2.2.12 Proton conductivity by Electrochemical Impedance Spectroscopy (EIS)

Proton conductivity studies of the fabricated membranes were done by employing an alternate current (ac) impedance technique (PARSTAT 2263) using four electrode probe method, in which the ac frequency was scanned from 1 MHz to 1 Hz at voltage of 5 mV. The proton conductivity (σ) of the samples in the longitudinal direction was calculated from the impedance data, using the relationship $\sigma = d/Rtl$, where d is the distance between the electrodes, t and l the thickness and length of the membrane along the electrode, respectively, and R was derived from the low intersect of the high frequency semi-circle (Fig. 2.1) on a complex impedance plane with the $\text{Re}(Z)$ axis, where Re refers to 'Real' in the complex impedance plane. Prior to the proton conductivity measurements, membranes were immersed in deionised water for 24 h to attain hydration equilibrium. Fully hydrated membranes were sandwiched in a Teflon[®] conductivity cell (Fig. 2.2) equipped with Pt foil contacts and the impedance was measured by placing the cell in a temperature-controlled chamber under a temperature range of 30 °C–100 °C. Constant relative humidity (RH) was maintained at 50 % RH and at 60 % RH by using saturated magnesium nitrate [$\text{Mg}(\text{NO}_3)_2$] and saturated sodium nitrite [NaNO_2] respectively and it was sensed by a hygrometer which was calibrated prior to the experiments. The experiments were repeated three times to check the reproducibility.

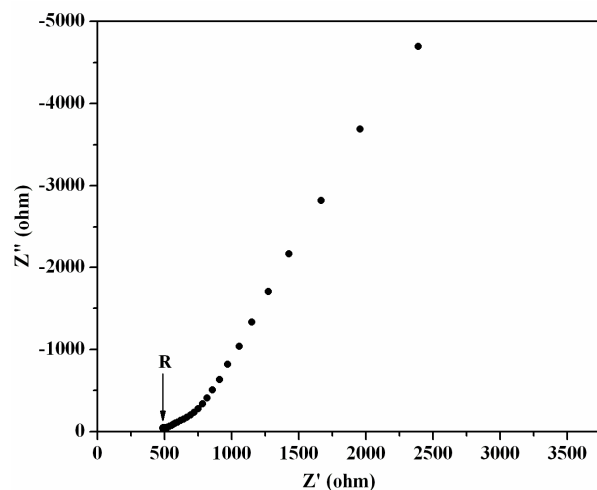


Fig. 2.1 Typical impedance spectra of a hybrid membrane.

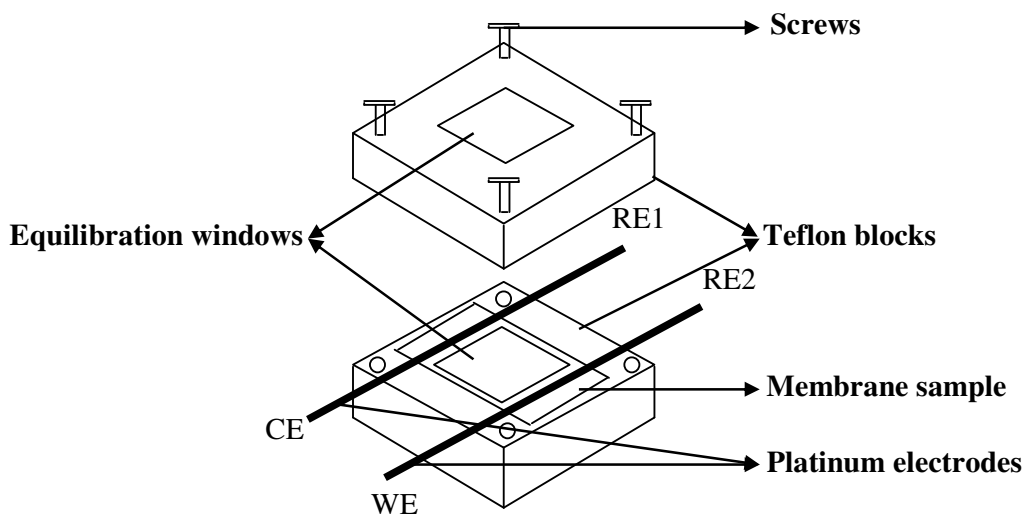


Fig. 2.2 Schematic view of proton conductivity cell.

2.2.13 Methanol crossover study

Cyclic voltammetric technique was used to estimate the amount of crossed over methanol. For the experiment, a two-compartment glass cell with the membrane separating the two compartments was used (Fig. 2.3). Prior to the measurements, membranes were immersed in deionised water for 24 h to attain hydration equilibrium. Platinum foil with a geometric surface area of 2 cm^2 and smooth platinum electrode were used as working (WE) and counter (CE) electrode, and Ag/AgCl (saturated KCl)

electrode as the reference (RE). The working electrode was immersed in one compartment considered as cathode and counter and reference electrode was immersed in the second compartment considered as anode. The cell was connected to BAS Epsilon potentiostat. A blank electrolyte of 50 ml of 0.5 M H_2SO_4 was first taken in either compartment of the cell and CV scanning was performed prior to the permeability test. The permeability was studied by introducing methanol of known concentration in 0.5 M H_2SO_4 to one compartment of the cell and analyzing the other compartment for its permeability. The permeability test was performed at room temperature for 1 M initial methanol concentration at the anode compartment and cyclic voltomograms were recorded between 0.2 to 1 V and from the response the concentration of methanol in the cathode side was determined. The concentration of crossed methanol was determined from the calibration curve which was obtained as described by Ling and Savadogo, (2004). These experiments were repeated three times to confirm the reproducibility of the results obtained.

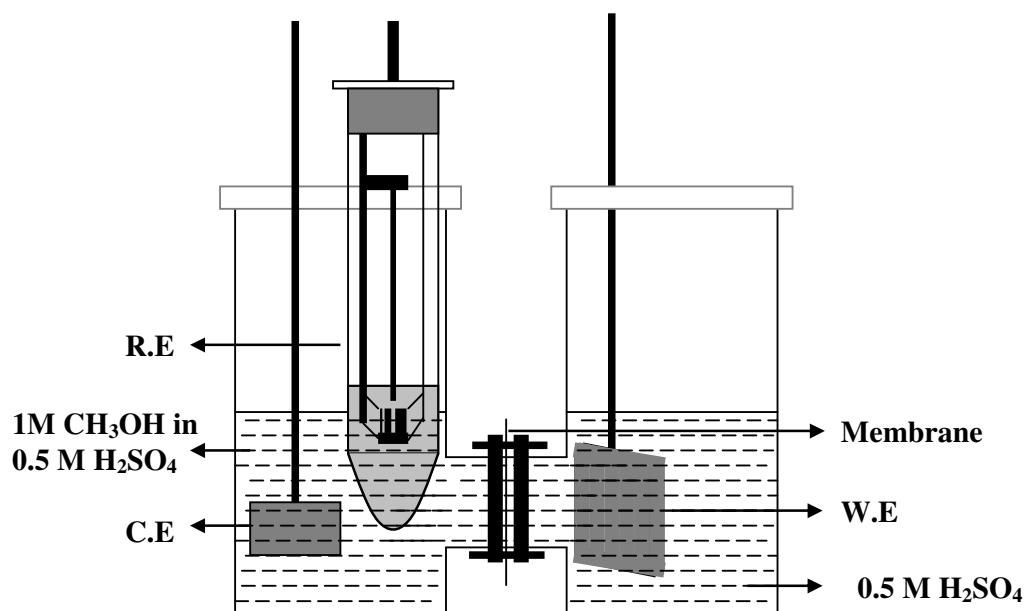


Fig. 2.3 Schematic view of two compartment cell used for the determination of methanol diffusion coefficients.

CHAPTER 3

FABRICATION AND PROPERTIES OF HYBRID MEMBRANES BASED ON SILICOTUNGSTIC ACID, α -ZIRCONIUM PHOSPHATE AND POLY(VINYL ALCOHOL)

3.1 INTRODUCTION

Fuel cells are emerging as an alternate energy source for mobile and stationary applications. Membranes play a critical role in attaining a successful performance of a fuel cell. Though Nafion[®] (a perfluorosulphonated polymer marketed by Ms. Du Pont) has been identified as the preferred membrane for PEM fuel cells, various attempts have been made to develop alternate, adaptable and acceptable class of membranes. Nafion[®] membranes currently employed in hydrogen oxygen fuel cells are not highly suitable for use in DMFC, since Nafion[®] exhibits reduced conductivity at low humidity condition and/or at elevated temperatures (Yang *et al.* 2001; Casciola *et al.* 2006). In addition, considerable fuel crossover takes place (Surampudi *et al.* 1994) from anode to cathode compartment. Nafion[®] based membranes are unstable at temperatures higher than 80 °C. These limitations have prompted the search for alternative membranes. In this direction, various approaches have been attempted like: (i) modifying perfluorosulfonic acid (PFSA) membranes to improve their water retention properties at temperatures above 100 °C by crosslinking (Bae *et al.* 2002; Shim *et al.* 2002; Haufe and Stimming, 2001; Nouel and Fedkiw, 1998; Liu *et al.* 2001) or by forming hybrids with hygroscopic oxides, MO₂ (M = Zr, Si, Ti) (Apichatachutapan *et al.* 1996; Shao *et al.* 1995) or with inorganic proton conductors (Yang *et al.* 2001; Staiti *et al.* 2001; Bauer and Porada, 2004; Kim *et al.* 2004; Ramani *et al.* 2005; Shao *et al.* 2006), (ii) by selecting other non-fluorinated polymer electrolytes such as sulfonated poly(ether ketones) (Bailly *et al.* 1987), and sulfonated

poly(ether ether ketones) (Robertson *et al.* 2003; Kaliaguine *et al.* 2003), sulfonated poly(arylene ether sulfone) (PES) (Nolte *et al.* 1993), basic polymers such as, poly(4-vinylpyridine) (Jorissen *et al.* 2002), and polybenzimidazole (Jorissen *et al.* 2002). However, sulfonation of these polymers is not simple, and will demand exacting experimental conditions (Yoshikawa *et al.* 1999), (iii) designing inorganic organic hybrid membranes (Ruffmann *et al.* 2003; Xu *et al.* 2004; Kim *et al.* 2004; Tezuka *et al.* 2005; Romero *et al.* 2005; Vernon *et al.* 2005; Panero *et al.* 2005; Li *et al.* 2006; Shanmugam *et al.* 2006). The later has attracted attention, because such hybrids may show controllable physical properties, such as thermal, electrical and mechanical behavior, by combining the properties of both organic polymers and inorganic compounds (solid inorganic proton conductors). Solid inorganic proton conductors like zirconium phosphates, heteropoly acids (HPAs), and metal hydrogen sulfates play a dual role of being both hydrophilic and proton conducting. Although heteropoly acids have been known for more than a century (Berzelius, 1826), it was not found until 1979 that these heteropoly acid hydrates exhibited exceptional high proton conductivities (Nakamura *et al.* 1979). The conductivity of a single crystal of silicotungstic acid, STA (28H₂O) was reported to be $2.7 \times 10^{-2} \text{ S cm}^{-1}$ at room temperature (Kreuer *et al.* 1988) indicating the potential applicability of heteropoly acid as a solid electrolyte for use in fuel cells at ambient temperatures. The use of solid heteropoly acids as fuel cell electrolytes was first investigated by Nakamura *et al.* in 1979, and subsequently by Staiti *et al.* (1997), and they found that at room temperature the fuel cell performance was similar to that of Nafion[®] electrolyte employed fuel cell. The solid heteropoly acid electrolyte was unstable and dissolved in water that is formed during cell operation. Alternatively aqueous solution of heteropoly acids (60 wt %) was used as fuel cell electrolytes and it was found to

promote fuel cell electrochemical reactions while maintaining high proton conductivity (Giordano et al. 1996). However, earlier efforts of using HPAs failed due to its high solubility in water and strong influence of humidity on proton conductivity (Katsoulis, 1998). Consequently, a major research objective is to fix the HPAs in a stable structure by forming hybrids (Tazi and Savadogo 2000; Zaidi *et al.* 2000; Lin *et al.* 2005) which can maintain their high proton conductivity. In addition, hybrid matrix reduces the leaching of HPA. The scope of the present study is to investigate a hybrid membrane made of poly(vinyl alcohol) (PVA) and α -zirconium phosphate (ZrP) with silicotungstic acid (SWA) as an active moiety. Water insoluble zirconium phosphate was added to suppress the crack formation which might arise due to shrinkage during drying. It also contributes to protonic conduction through the proton of phosphate moiety and crystalline water thereby reducing the humidity dependence on conductivity (Park and Nagai, 2001). The driving force for this attempt is to design newer class of membranes, which may not demand the exacting experimental conditions and critical management of chemical environments that are necessary for the synthesis of membranes like Nafion[®] and other sulfonated polymers.

3.2 EXPERIMENTAL

3.2.1 Preparation of α -zirconium phosphate

α -Zirconium phosphate (ZrP) is prepared by taking 1 M aqueous solution of $\text{ZrOCl}_2 \cdot 8 \text{H}_2\text{O}$ and it is slowly added to a 10 times excess of 1 M H_3PO_4 (Bauer and Porada, 2005). The precipitate was washed several times with de-ionized water, dried for 2 h at 95 °C and stored at 100 % RH and room temperature.

3.2.2 Fabrication of PVA-ZrP-SWA hybrid membranes

The hybrid membranes were prepared by sol-gel process. A 10 % solution of PVA in water was made with constant stirring at 70 °C and to that zirconium phosphate (10 wt %) and silicotungstic acid (10, 20 and 30 wt %) were added and the resultant mixture was refluxed at 70 °C for 8 h, to obtain a clear viscous solution. The resulting viscous solution was gelled for 2 days. The film was cast on a clean glass plate with the desired thickness and dried at room temperature.

3.3 MEMBRANE CHARACTERIZATION

3.3.1 Fourier transform infrared spectroscopic analysis

The FT-IR spectra obtained for the membrane are given in Fig. 3.1. The spectrum of a typical membrane reveals the characteristic bands of PVA, α -ZrP and SWA. The FT-IR spectrum of hybrid membranes showed bands at 972, 917, 850 and 780 cm^{-1} , which agree with those reported in literature (Deltcheff *et al.* 1976; Okuhara *et al.* 1996) for silicotungstic acid. The bands around 3275 cm^{-1} and 2940 cm^{-1} represent O-H stretching and $-\text{CH}_2$ stretching; the band around 1440 cm^{-1} is for $-\text{CH}_3$ bending, all these bands are characteristics of PVA. The bands around 506 cm^{-1} and 1080 cm^{-1} are due to Zr-O and P-O₄ asymmetric stretching which are characteristics of ZrP (Horsley *et al.* 1974). The positions of vibration modes of all types of M-O bonds are strongly influenced by interaction of silicotungstic with the polymer and zirconium phosphate. The band of W-O_b-W (O_b-bridged oxygen and O_t-terminal oxygen) has a blue shift from 779 to around 795 cm^{-1} and W-O_t bond of SWA in the hybrid is red shifted from 972 to 969 cm^{-1} . This is due to the columbic interaction between the

hydroxyl groups of the poly(vinyl alcohol) and silicotungstic acid. The observed main bands are assigned and tabulated for hybrid membranes in Table 3.1.

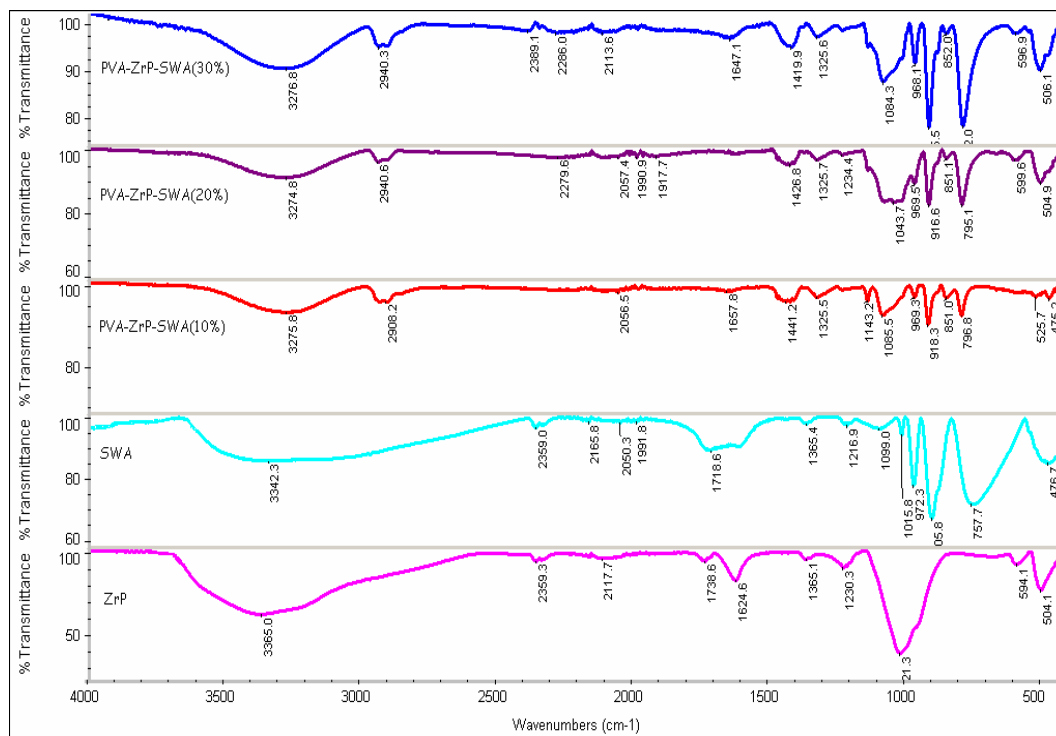


Fig. 3.1 FT-IR spectra of hybrid membranes and its components for comparison.

Table 3.1 Assignments of main absorption bands for hybrid membranes and its components.

Hybrid membranes		α -ZrP		SWA		PVA	
Vibration frequency (cm ⁻¹)	Bond Assignment	Vibration frequency (cm ⁻¹)	Bond Assignment	Vibration frequency (cm ⁻¹)	Bond Assignment	Vibration frequency (cm ⁻¹)	Bond Assignment
506	$\nu_{as}(\text{Zr-O})$	504	$\nu_{as}(\text{Zr-O})$	779	$\nu(\text{W-O}_b\text{-W})$	1420	$\nu(\text{CH}_3)$
600	$\delta_{out}(\text{POH})$	594	$\delta_{out}(\text{POH})$	926	$\nu(\text{Si-O})$	2900	$\nu(\text{CH}_2)$
795	$\nu(\text{W-O}_b\text{-W})$	1021	$\nu_{as}(\text{PO}_4)$	972	$\nu_{as}(\text{W-O}_t)$	3260	$\nu(\text{OH})$
917	W-O_t	1624	$\delta_{as}(\text{OH})$				
969	$\nu_{as}(\text{W=O}_t)$	2117	$\nu(\text{POH})$				
1080	$\nu_{as}(\text{PO}_4)$	2359	$\nu(\text{POH})$				
1440	$\nu(\text{CH}_3)$	3365	$\nu_{as}(\text{OH})$				

3.3.2 X-ray diffraction analysis

Fig. 3.2 shows the XRD profiles obtained for hybrid membranes. X-ray diffractograms were made to gain information on the structural changes induced by the presence α -ZrP and SWA in PVA. For comparison the XRD patterns for the pristine PVA and α -ZrP are also given. The peak found at $2\theta = 20^\circ$ corresponds to the (101) plane of PVA in all hybrid membranes (Shao *et al.* 2003). Broad peaks of the α -ZrP powder indicate that α -ZrP is in the amorphous state. No diffraction peaks characteristic of SWA appears in the spectra containing 10, 20 and 30 % of SWA. This is because the SWA is not crystallized on the polymer matrix and the hybrid behaves as X-ray amorphous. Broad peaks also indicate the conformation of complete homogeneity and compatibility among the components of the membrane.

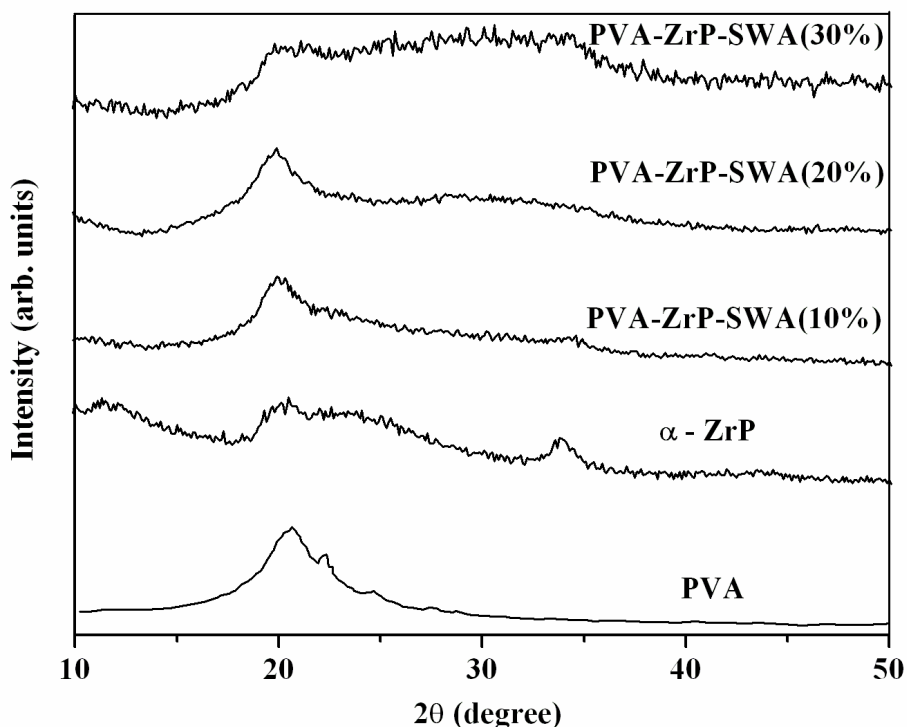


Fig. 3.2 Cu K_α XRD patterns of hybrid membranes and its components for comparison.

3.3.3 Thermal analysis

In Fig. 3.3, the traces of thermogravimetric analysis (TGA) of the hybrid membranes are shown in the temperature range from 50 °C to 800 °C. The TGA curves of the hybrid membranes reveal three main weight loss regions. The first weight loss was occurring at around 100 °C, due to loss of absorbed water molecules. The second weight loss in the temperature region 190–300 °C is due to decomposition of poly(vinyl alcohol) (Hassan and Peppas, 2000). The third weight loss is due to decomposition of silicotungstic acid to respective metal oxides (Hodnett and J. B. Moffat, 1984).

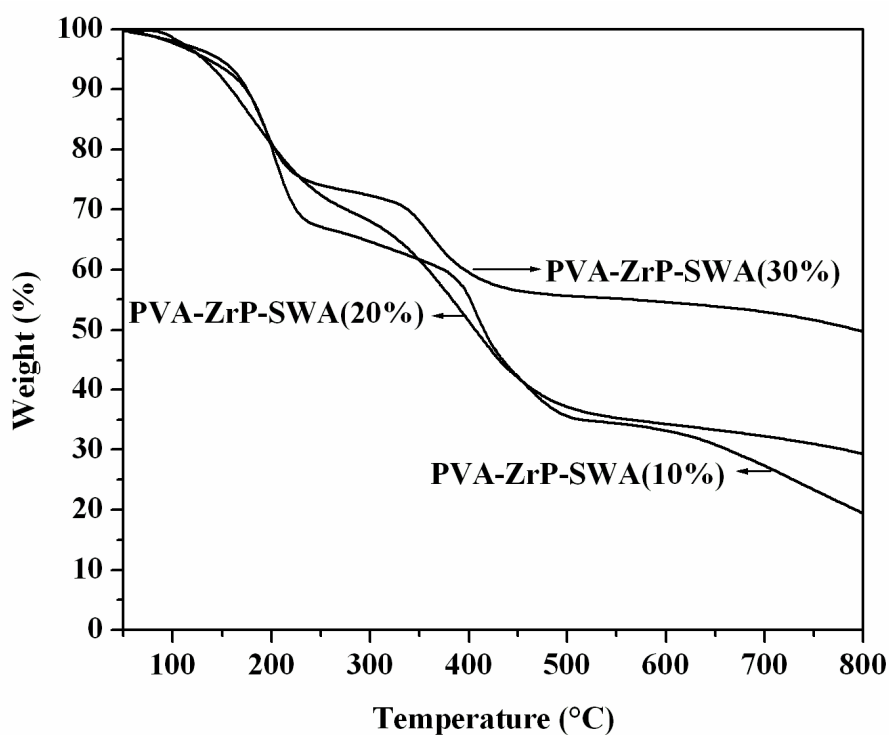


Fig. 3.3 TGA traces of hybrid membranes in a temperature range from 50 to 800 °C.

The differential scanning calorimetry, DSC thermograms of the hybrid membranes are presented in Fig. 3.4 PVA is a partially crystalline polymer exhibiting both the glass

transition temperature, T_g (characteristic of amorphous phase) and melting isotherm, T_m (characteristic of crystalline phase). For pure PVA, the glass transition temperature is around 90 °C and melting temperature is around 216 °C (Hassan and Peppas, 2000). T_g of hybrid membranes are observed around 125 °C which is higher than that of pure PVA. The increased T_g due to the presence of α -ZrP indicates an increase in the thermal stability of the hybrid membranes. The reason for this raise in thermal stability of hybrid membranes is probably due to the formation of hydrogen bonds or the condensation reaction between the residual –OH on the α -ZrP and the –OH on PVA.

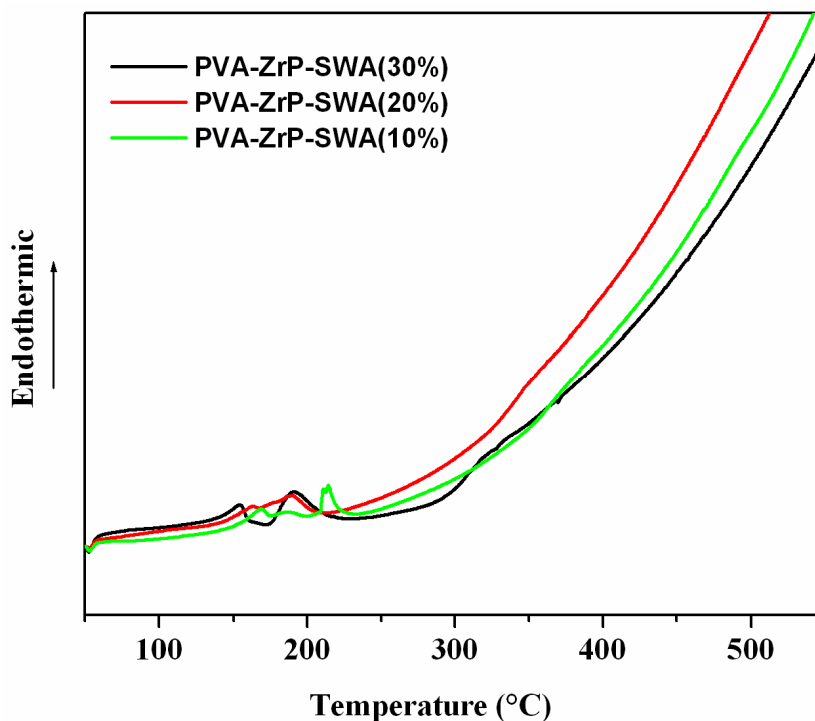


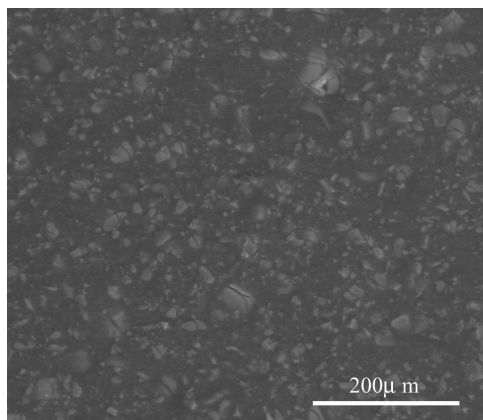
Fig. 3.4 DSC thermograms of hybrid membranes with different contents of silicotungstic acid.

With an increasing SWA content, T_g of the hybrid membranes decreases. This can be attributed to softening of the complexation due to the plasticizing effect of SWA on

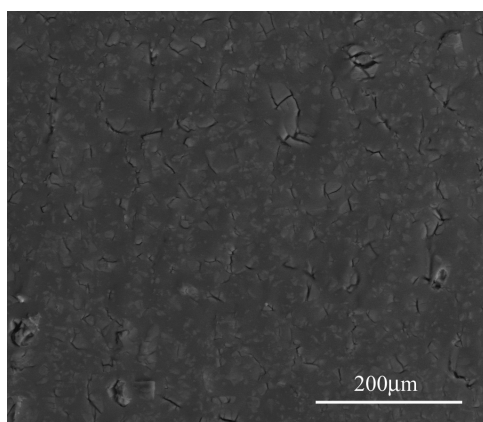
the polymer structure, which is beneficial for the facile proton transport in the membrane. The second endothermic peak corresponds to the melting of the crystalline phases of hybrid membranes. For pure PVA, the endothermic peak at 220 °C is associated with the melting point of the polymer (Hassan and Peppas, 2000). The melting temperature, T_m , was taken as the point of maximum for the transition, whereas the heat of fusion, ΔH_f , which increases with the crystallinity of the polymer, was calculated as the integrated area of the transition peak. The melting point is reduced to 210 °C, 191 °C and 189 °C for 10 %, 20 % and 30 % SWA containing hybrid membranes respectively; the heat of fusion, ΔH_f , is around 109, 73 and 45 J g⁻¹ respectively. The interaction between the polymer and inorganic components breaks the preformed crystals to render the polymer in the amorphous phase to some extent, which favors the improvement of conductivity. The broad endothermic peak until around 225 °C can also be attributed to the dehydration of crystalline water.

3.3.4 Scanning electron microscopic analysis

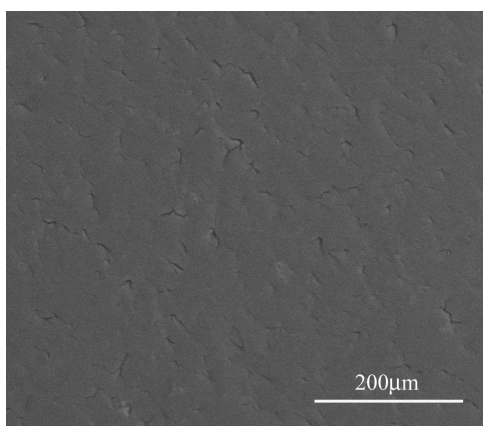
Surface morphology of the dried membrane was investigated using SEM analysis. Fig. 3.5 shows the scanning electron micrographs of 10, 20 and 30 wt % SWA acid substituted hybrid membranes. The distribution of inorganic particles is relatively uniform in the organic matrix. These membranes are compact with low degree of porosity. In the case membranes with 30 wt % of SWA, no phase separation was observed, suggesting that the synthesized films were homogeneous in nature and hence formed dense membrane.



PVA-ZrP-SWA(10%)



PVA-ZrP-SWA(20%)



PVA-ZrP-SWA(30%)

Fig. 3.5 Scanning electron micrographs of PVA-ZrP-SWA hybrid membranes.

3.3.5 Water uptake, swelling and ion exchange capacity (IEC)

The presence of water in the membrane greatly influences the transport properties of the membrane. The water uptake and ion exchange capacity (IEC) play important roles in membrane conductivity. Proton conductivity of the membrane will increase with increasing water uptake and IEC because of the increase in the mobility of ions. The data on water uptake, extent of swelling and IEC for the PVA-ZrP-SWA hybrid membranes are given in Table 3.2. At room temperature, all three factors such as the water absorption, extent of swelling and IEC are increased with an increase in the content of SWA in the hybrid membranes of 250 μm thickness. The increase in water uptake capacity and the swelling is due to the hygroscopic nature of the SWA in the hybrid membrane.

Table 3.2 Water uptake, swelling and IEC values for PVA-ZrP-SWA hybrid membranes of different composition with a thickness of 250 μm .

Membrane	Water uptake (%)	Swelling (%)	IEC(meq g ⁻¹)
PVA-ZrP-SWA(10%)	204	90	0.902
PVA-ZrP-SWA(20%)	388	170	0.958
PVA-ZrP-SWA(30%)	482	230	1.07

3.3.6 Test for SWA leaching

The heteropoly acid stability in aqueous medium of the hybrid membranes was determined by placing membrane samples in water and at different time intervals the water was analyzed for the presence of SWA using UV-visible spectroscopy. For SWA in water an absorption band at 261 nm is observed due to the oxygen to tungsten ($\text{O}_d \rightarrow \text{W}$) charge transfer (Varga *et al.* 1970). Fig. 3.6 shows the UV-visible spectra of the solution immersed with hybrid membrane containing 30 wt % loading

of SWA, at different time intervals. After 3 h of immersion a small band at 261 nm is observed indicating the leaching of SWA in to the water. After 10 h of immersion the intensity of the absorption band increased indicating further leaching of SWA. Whereas, after 10 h of immersion there is no considerable increase in absorption intensity indicating no further leaching of SWA from the hybrid membrane.

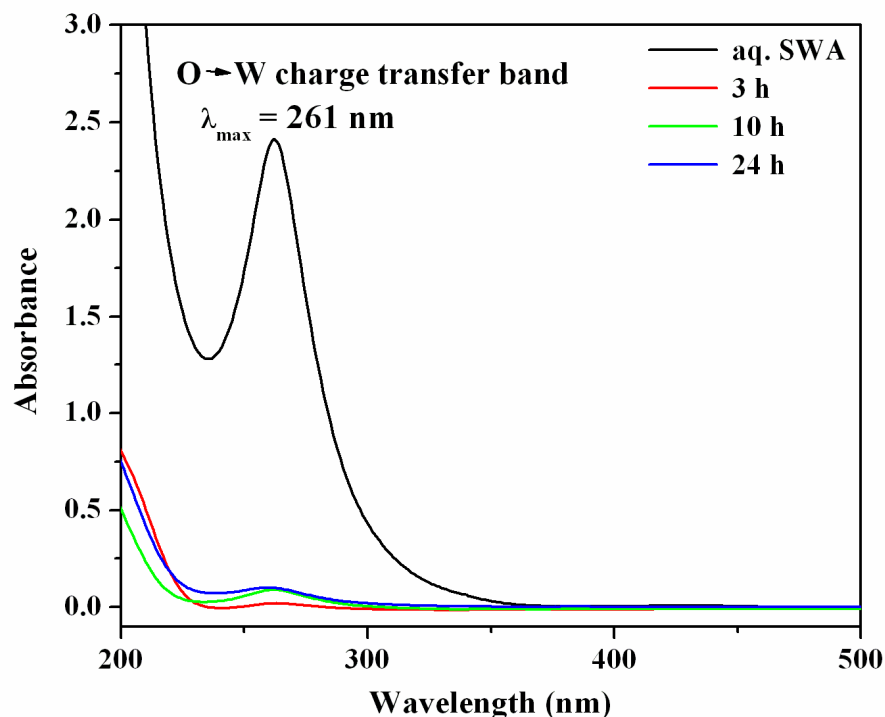


Fig. 3.6 UV-visible spectra of pure SWA in water and for the water immersed with PVA-ZrP-SWA(30%) hybrid membrane at different time intervals.

3.3.7 Proton conductivity study

The temperature dependence of the conductivity of the PVA-ZrP-SWA hybrid membranes with different wt % of SWA is shown in Fig. 3.7. At 60 % of relative humidity, the protonic conductivity of the hybrid membranes was in the range of 10^{-3} S cm⁻¹. The proton conductivity of these hybrid membranes increased with an increasing SWA content. This trend is the same as that observed for water uptake and

IEC. Conductivity increased with temperature and it attains maximum at 60 °C and remains constant up to 80 °C. For the hybrid membrane containing 30 % SWA exhibited conductivity value of $10^{-2} \text{ S cm}^{-1}$ in the temperature range of 60 °C to 80 °C. After 80 °C, conductivity drops due to the evaporation of adsorbed water. Though there is a decrease in conductivity at temperatures above 80 °C, the order of magnitude remains the same. For comparison, the corresponding data for Nafion[®] 115 measured at 100 % relative humidity is included in Fig. 3.7.

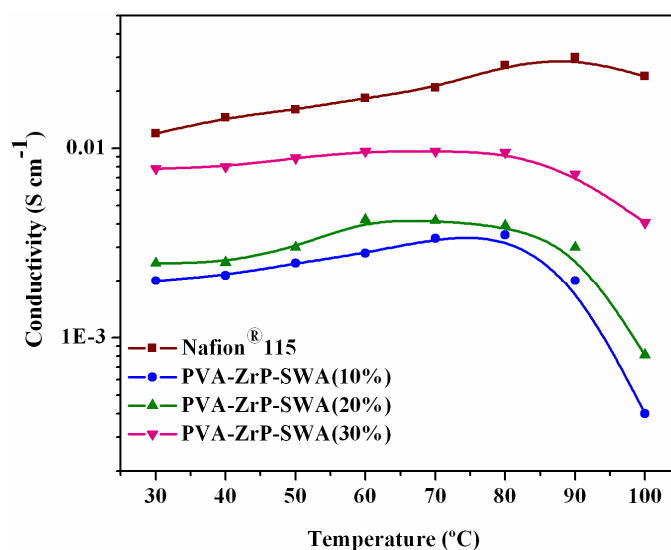


Fig. 3.7 Proton conductivity at 60 % RH as a function of temperature for PVA-ZrP-SWA(10%), PVA-ZrP-SWA(20%), PVA-ZrP-SWA(30%) and Nafion[®] 115 (at 100 % RH).

In the fabricated hybrid membranes, ZrP and SWA are the active proton conducting moieties. The proton conductivity of the individual components of the hybrid membrane is tabulated and compared to the fully fabricated hybrid membranes (Table 3.3). All the three components contribute to proton conductivity. That is, in the fabricated hybrid membranes by combining both organic component PVA and inorganic components ZrP and SWA, the conductivity of the system has been significantly improved. The activation energy (E_a) for conduction in the fabricated

membranes is also affected by forming the hybrid. The E_a , decreased compared to its components (Table 3.3). For membranes containing 10, 20 and 30 wt % of SWA, the E_a values are found to be 6 kJ mol⁻¹, 4.8 kJ mol⁻¹ and 3 kJ mol⁻¹ respectively. This observed trend is attributed to the increase in water content with increase in amounts of SWA in the hybrid membranes.

Table 3.3 Proton conductivity (σ) and activation energy (E_a) for hybrid membranes and its components.

Proton conductor	Proton conductivity (S cm ⁻¹)	Conditions	Activation energy (kJ mol ⁻¹)	Reference
α -Zr(HPO ₄) ₂ .H ₂ O	10 ⁻⁵ - 10 ⁻⁶	20 °C, 90 % RH	48.2	Alberti and Casciola, 1992
H ₄ SiW ₁₂ O ₄₀ . nH ₂ O	10 ⁻²	25 °C, 97 % RH	38.5	Kreuer et al. 1988
PVA	10 ⁻⁶	39 °C	-	Agrawal and Awadhia, 2004
PVA-ZrP-SWA(10%)	3 x 10 ⁻³	60 °C, 60 % RH	6	From the present investigation
PVA-ZrP-SWA(20%)	4 x 10 ⁻³	60 °C, 60 % RH	4.8	
PVA-ZrP-SWA(30%)	1 x 10 ⁻²	60 °C, 60 % RH	3	

3.3.8 Methanol crossover study

Concentration of crossed over methanol with respect to time was plotted for all hybrid membranes and it is compared with that of Nafion[®] 115 in Fig. 3.8. Initially for all hybrid membranes, the concentration of crossed over methanol increased with time and after 90 minutes it reached a steady value. There is no appreciable increase in crossover up to 180 minutes. In the case of Nafion[®] 115, the concentration of crossed

over methanol increased linearly with time. Compared to Nafion[®] 115, methanol crossover was reduced by a factor of two for 10 wt % SWA hybrid membrane. As SWA percentage increased in the formulations, the methanol crossover decreased tremendously. In the case of 30 wt % SWA substituted hybrid membrane, methanol crossover was a magnitude less than that of Nafion[®] 115. Reduced crossover of methanol in hybrid membranes is due to the hydrophilic nature of the fabricated membrane which is capable of retaining methanol. Whereas, in the case of Nafion[®] 115 the hydrophobic nature of the polymer allows methanol crossover to a greater extent. As shown in Fig. 3.9 the methanol permeability for all the hybrid membranes was less compared to that of Nafion[®] 115. It has to be stated that compared to Nafion[®] 115, PVA-ZrP-SWA hybrid membranes show strong resistance to methanol permeability at the expense of proton conductivity. This study clearly indicates that methanol crossover can significantly be reduced using PVA-ZrP-SWA hybrid membrane in DMFC.

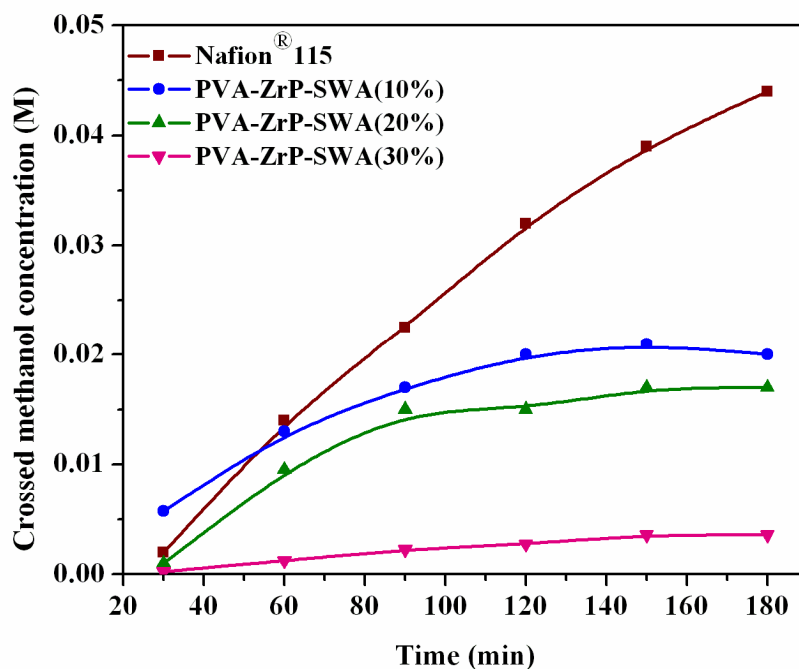


Fig. 3.8 Concentration of crossed over methanol as a function of crossover time.

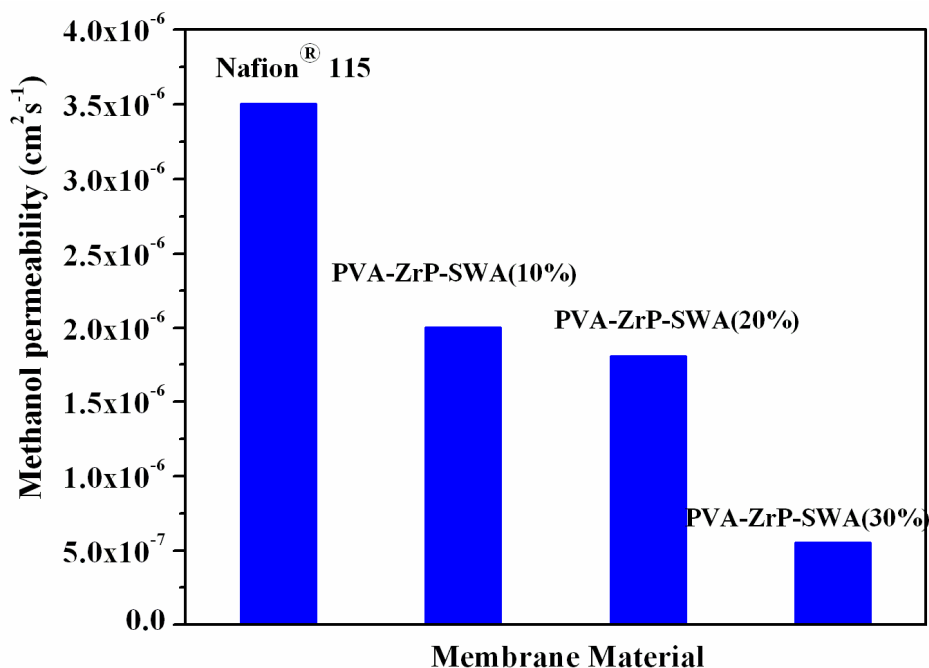


Fig. 3.9 Methanol permeability of hybrid membranes compared with that of Nafion® 115.

3.4 CONCLUSIONS

A new class of hybrid membranes with poly(vinyl alcohol) as an organic matrix and zirconium phosphate and silicotungstic acid as inorganic components were prepared by a simple, sol-gel route. FT-IR and XRD studies confirm the formation of hybrid membranes from their individual organic and inorganic moieties. Thermal analyses such as TGA and DSC reveal the thermal stability of these hybrid membranes with various compositions. UV-visible spectroscopic analysis of water in which the membrane materials were soaked for different time periods confirms the stability of SWA moiety in the hybrid matrix. SEM study reveals the homogeneous and uniform distribution of components in the entire matrix. The fabricated membranes were characterized in order to examine their key properties which are relevant for DMFC applications such as water uptake, swelling, IEC, proton conductivity and for

methanol crossover abilities. It has been found that water uptake, IEC and proton conductivity properties of these membranes increased with silicotungstic acid content in them. These hybrid membranes exhibited reduced methanol crossover compared to the commercial Nafion[®]115 membrane. Though they exhibit slightly lower proton conductivity it appears that they are promising alternate materials for DMFC applications due to the reduced methanol crossover characteristics.

CHAPTER 4

FABRICATION AND PROPERTIES OF HYBRID MEMBRANES BASED ON SALTS OF HETEROPOLY ACID, α -ZIRCONIUM PHOSPHATE AND POLY(VINYL ALCOHOL)

1. INTRODUCTION

The main aim of this piece of research is to evaluate inorganic solid state proton conducting systems and to acquire an improved fundamental understanding of a class of inorganic proton conductors (heteropoly acids [HPA] and their salts) that exhibit high proton conductivity at elevated temperatures (well above 100 °C) and to apply that understanding to direct methanol fuel cell membrane technology. The HPA exhibit proton conductivity among the highest measured in the solid state, more than an order of magnitude higher than Nafion[®]. The ultimate goal is to develop HPA-based materials that can be combined with polymers to fabricate thin films as membrane materials for use in DMFC. HPAs are strong Bronsted acids as well as solid electrolytes (Misono, 1987). For example, hydrated silicotungstic acid ($\text{H}_4\text{SiW}_{12}\text{O}_{40} \cdot 28\text{H}_2\text{O}$) has an ionic conductivity of $2 \times 10^{-2} \text{ S cm}^{-1}$ at room temperature (Nakamura *et al.* 1979; Nakamura *et al.* 1981; Kreuer, 1988). However, solid HPAs cannot be employed as electrolyte in fuel cells due to their high solubility in polar solvents (Nakamura *et al.* 1979; Staiti *et al.* 1997). Consequently, a major research objective is to fix the HPAs in stable structure by forming composites (Staiti, 2001; Tazi and Savadogo, 2000; Zaidi *et al.* 2000; Lin *et al.* 2005; Ponce *et al.* 2003) in which they can maintain their high proton conductivity. Through our preceding piece of investigation, (Chapter 3) we could only mitigate the solubility of heteropoly acid but not fully stabilize them in a hybrid matrix (Fig. 3.6). Therefore, as our next step in this direction, we adopt yet another route in limiting the solubility and leaching of

HPAs by ion exchanging the protons of HPA with larger cations like Cs^+ , NH_4^+ , Rb^+ and Tl^+ . This aspect has been dealt in detail by Ramani *et al.* (2005). In this present work we employ both these approaches simultaneously by forming hybrids with poly(vinyl alcohol), zirconium phosphate and cesium salt of silicotungstic acid. Water insoluble zirconium phosphate further helps in stabilizing heteropoly acid through columbic interactions (Yong-II. and Masayuki 2001).

The conductivity of salts of silicotungstic acid was previously studied by Vakulenko *et al.* (2000). The high protonic conductivity is due to mobile proton that is present as an admixture in the crystalline structure of synthesized salt (Ukshe *et al.* 1989) or due to the presence of crystalline water. The nature of the cation has a great influence on the final properties of the salts of Keggin heteropoly acid. The salts containing small cations, such as Na^+ , are soluble in water or in other polar solvents whereas the salts with large cations, such as Cs^+ , are insoluble in water (Parent and Moffat, 1998). Their low solubility is attributed to the low solvation energy of the large cations. The work on a poly(vinyl alcohol) (PVA) and zirconium phosphate based hybrid membrane with cesium salts of silicotungstic acid as the active component is described.

4.2 EXPERIMENTAL

4.2.1 Preparation of salts of silicotungstic acid

Salts of silicotungstic acid were synthesized at room temperature by neutralization of acid solution with cesium carbonate. Attempts were made to control the number of proton substitution by controlling the stoichiometry of the added cesium carbonate solution. The crystals were dried at room temperature and kept in air atmosphere under constant-humidity conditions, until a constant mass was attained. The Cs/W

atomic ratio composition determined by using X-ray fluorescence (XRF) analysis, agreed with that calculated from the stoichiometric amount of reagents added to prepare Cs salt of silicotungstic acid (Table 4.1).

Table 4.1. Cesium content in salts of silicotungstic acid.

	Cesium content	
	$\text{Cs}_1\text{H}_3\text{SiW}_{12}\text{O}_{40}$	$\text{Cs}_2\text{H}_2\text{SiW}_{12}\text{O}_{40}$
Calculated	1	2
XRF analysis	1	1.9

4.2.2 Fabrication of PVA-ZrP-CsSWA hybrid membranes

A 10 % solution of PVA in water was made under constant stirring at 70 °C and to that zirconium phosphate (10 wt %) and cesium salt of silicotungstic acid (30 wt %) was added and the resultant mixture was refluxed at 70 °C for 8h, to obtain a clear viscous solution. The resulting viscous solution was gelated for 2 days and casted with the desired thickness upon a clean glass plate and dried at room temperature to obtain a film.

4.3 MEMBRANE CHARACTERIZATION

4.3.1. Fourier transform infrared spectroscopic analysis

The FT-IR spectra of PVA-ZrP- Cs_1SWA and PVA-ZrP- Cs_2SWA membranes obtained are shown in Fig. 4.1. The spectrum of a typical membrane reveals the characteristic bands of PVA, α -ZrP and salt of SWA. The FT-IR spectrum of hybrid membranes showed bands at 981, 917, 876 and 790 cm^{-1} , which agree with those reported in literature (Deltcheff *et al.* 1976; Okuhara *et al.* 1996) for silicotungstic

acid. The same characteristic bands are seen in the hybrid membrane containing salts of silicotungstic acid.

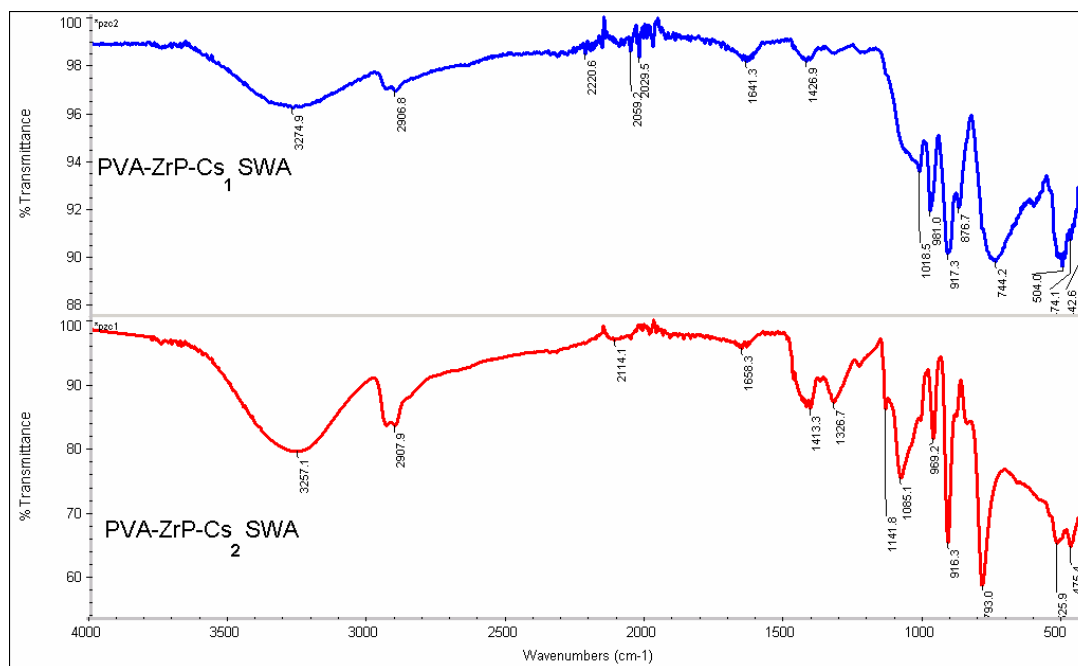


Fig. 4.1 FT-IR spectra of PVA-ZrP-Cs₁SWA and PVA-ZrP-Cs₂SWA hybrid membranes.

The band at 981 cm^{-1} corresponds to the stretching of the $\text{W}=\text{O}_t$ terminal bond and the band at 917 cm^{-1} corresponds to the stretching of Si-O bond which is red shifted from 926 cm^{-1} , this is due to the columbic interaction between the hydroxyl groups of the poly(vinyl alcohol) donor and the salt of silicotungstic acid in the hybrid membrane. The bands at 876 and 793 cm^{-1} corresponds to the $\text{W}-\text{O}_b-\text{W}$ (O_b -bridged oxygen and O_t -terminal oxygen) connecting two $[\text{W}_3\text{O}_{13}]$ units by corner sharing and by edge sharing respectively. The later has blue shifted from 779 cm^{-1} to 793 cm^{-1} which again represents the columbic interaction. The bands at 3260 cm^{-1} and 2907 cm^{-1} represents O-H stretching and $-\text{CH}_2$ stretching; the band around 1420 cm^{-1} is for $-\text{CH}_3$ bending which are characteristic of PVA. The bands around 510 cm^{-1} and 1050 cm^{-1} are due to Zr-O and $\text{P}-\text{O}_4$ symmetric stretching and that around 916 cm^{-1} is due to P-OH

asymmetric stretching which are characteristics of ZrP (Horsley *et al.* 1974). The main bands are assigned and tabulated separately for PVA–ZrP–Cs₁SWA and PVA–ZrP–Cs₂SWA hybrid membranes in Table 4.2.

Table 4.2 Assignments of main absorption bands for PVA-ZrP-Cs₁SWA and PVA-ZrP-Cs₂SWA hybrid membranes.

Vibration frequency (cm ⁻¹)		Bond Assignment
PVA-ZrP-Cs ₁ SWA	PVA-ZrP-Cs ₂ SWA	
981	969	W=O _t stretching
917	916	Si-O stretching
876	-	corner sharing W-O _b -W
744	793	edge sharing W-O _b -W
3274	3257	O–H stretching
2906	2907	–CH ₂ stretching
1426	1413	–CH ₃ bending
504	525	Zr-O symmetric stretching
1018	1085	P-O ₄ symmetric stretching

4.3.2 X-ray diffraction analysis

X-ray diffractograms of PVA–ZrP–Cs₁SWA and PVA–ZrP–Cs₂SWA hybrid membranes are shown in Fig. 4.2. All the indexed peaks are due to Cs salt of silicotungtic acid and are indexed according to the JCPDS card no 51-0416. The broad hump in the 2θ range 20 to 35 is due to the presence of PVA and zirconium phosphate.

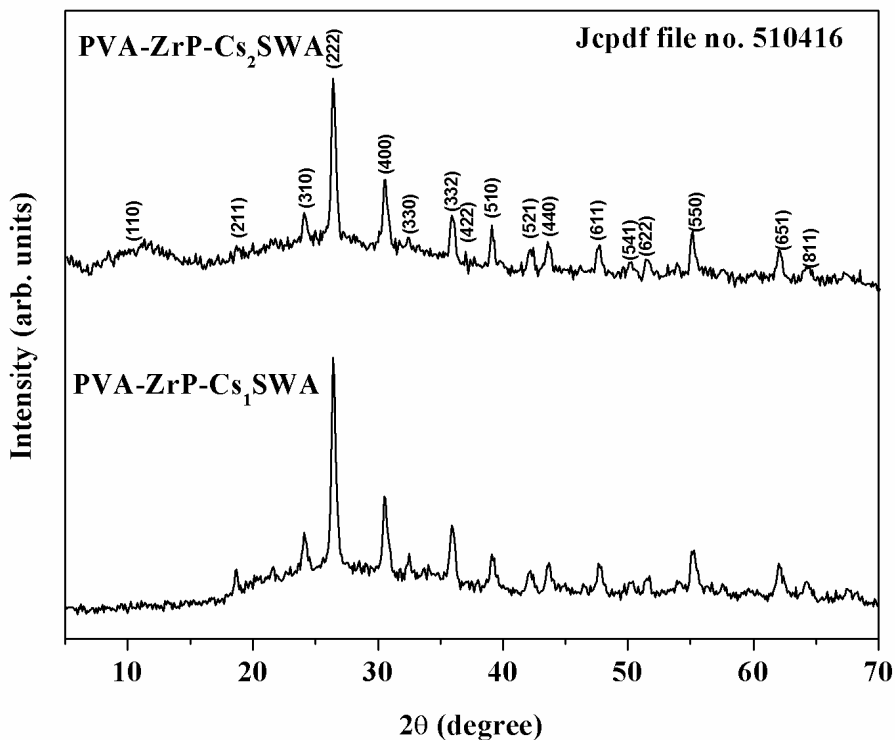


Fig. 4.2 Cu K α XRD patterns of PVA-ZrP-Cs₁SWA and PVA-ZrP-Cs₂SWA hybrid membranes.

4.3.3 Thermal analysis

Fig. 4.3 shows the traces of thermogravimetric analysis of the hybrid membranes in the temperature range from 50 °C to 800 °C. Three thermal degradation stages are seen, the first weight loss occurred at temperatures around 100 °C, which is associated with the loss of absorbed water molecules and a major second weight loss is due to decomposition of poly(vinyl alcohol) in the temperature region 200 – 300 °C and the loss of crystalline water from silicotungstic acid (Hassan and Peppas, 2000). The third major weight loss is due to decomposition of salt of silicotungstic acid to respective metal oxides (Hodnett and J. B. Moffat, 1984) combined with the loss associated with the phase transition of ZrP to nonlayered pyrophosphate (ZrP₂O₇) phase (Costantino *et al.* 1997).

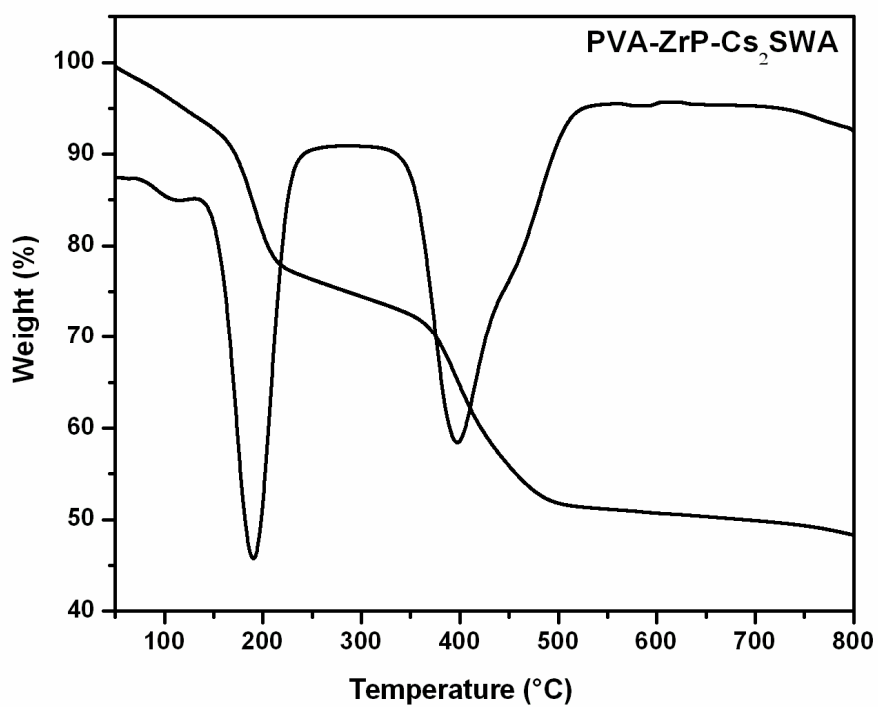
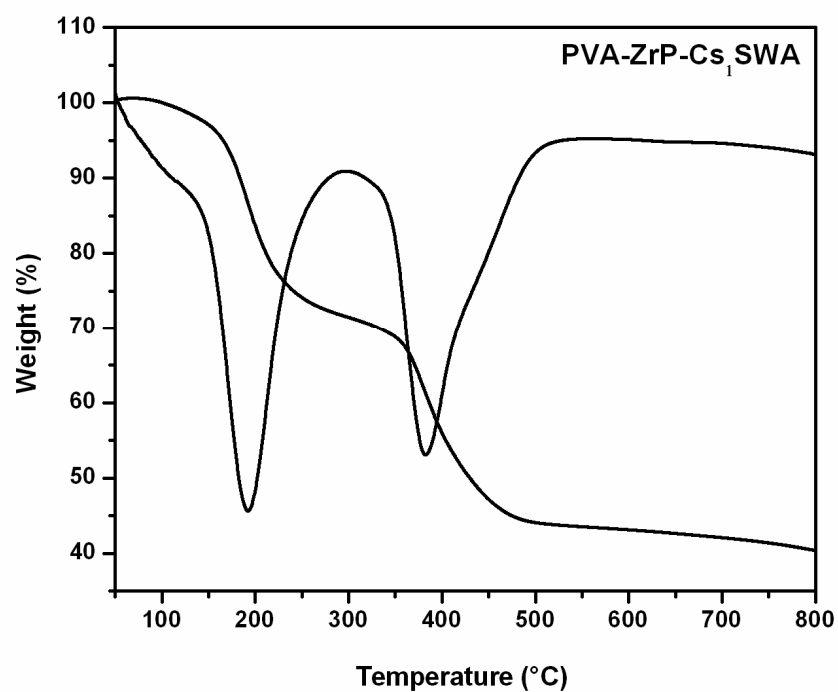
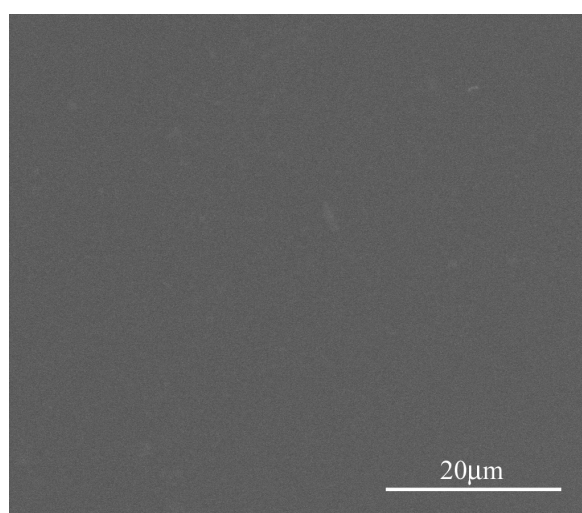


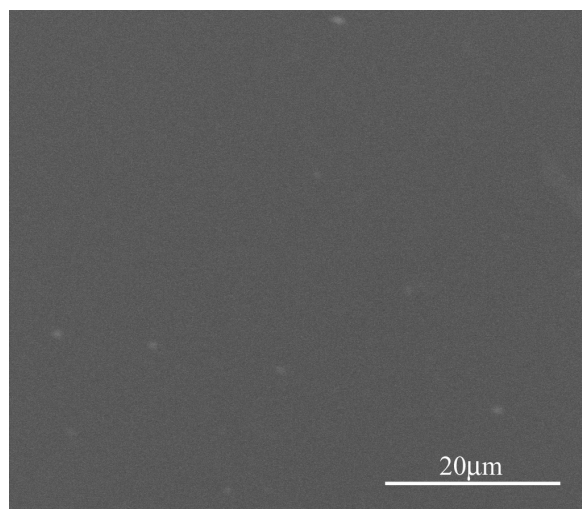
Fig. 4.3 TGA analysis of PVA-ZrP-Cs₁SWA and PVA-ZrP-Cs₂SWA hybrid membranes in a temperature range from 50 to 800 °C.

4.3.4 Scanning electron microscopy analysis

Surface morphology of the dried membrane was investigated by using SEM. Fig. 4.4 shows the scanning electron micrographs of PVA-ZrP-Cs₁SWA and PVA-ZrP-Cs₂SWA hybrid membranes. The distribution of inorganic particles is relatively uniform in the organic matrix. Membranes exhibited a compact morphology with no phase separation suggesting that the synthesized films were homogeneous in nature and hence formed dense membrane.



PVA-ZrP-Cs₁SWA



PVA-ZrP-Cs₂SWA

Fig. 4.4 Scanning electron micrographs of hybrid membranes.

4.3.5 Water uptake, swelling and ion exchange capacity (IEC)

Water uptake and ion exchange capacity (IEC) of the membrane plays an important role in determining the proton conductivity. This is because the presence of water greatly influences the transport properties of the membrane. With increase in water uptake and IEC, proton conductivity increases due to increase in the mobility of ions in the water phase. The data on water uptake, swelling and IEC for the membranes are given in Table 4.3. At room temperature the water absorption and swelling decrease with increase in cesium content for membranes of 180 μm thickness.

Table 4.3 Water uptake, swelling and IEC values for PVA-ZrP-Cs₁SWA and PVA-ZrP-Cs₂SWA hybrid membranes with a 180 μm thickness compared with that of Nafion[®] 115.

Membrane	Water uptake (%)	Swelling (%)	IEC (meq g ⁻¹)
PVA-ZrP-Cs ₁ SWA	260	100	3.2
PVA-ZrP-Cs ₂ SWA	140	85	3
Nafion [®] 115	22	12	0.9

4.3.6 Proton conductivity study

Fig. 4.5 shows temperature dependence of the membrane conductivity. At 50 % of relative humidity, the protonic conductivity of the hybrid membranes was in the range of 10^{-3} to 10^{-2} S cm⁻¹. The proton conductivity increased with increasing substitution of proton with cesium. The charge carriers in the acidic salt of silicotungstic acid are increasing leading to increased proton conductivity in PVA-ZrP-Cs₂SWA compared to PVA-ZrP-Cs₁SWA hybrid membrane. The activation energy of conductivity depends on salt structure, energy being much lower for the salts of high symmetry (Cs₂) than for those of low symmetry (monosubstituted Cs salt) (Vakulenko *et al.* 2000). Proton conductivity is steadily increasing with temperature for both the

hybrid membranes and for comparison the corresponding data for Nafion[®] 115 measured at 100 % relative humidity is included in Fig. 4.5.

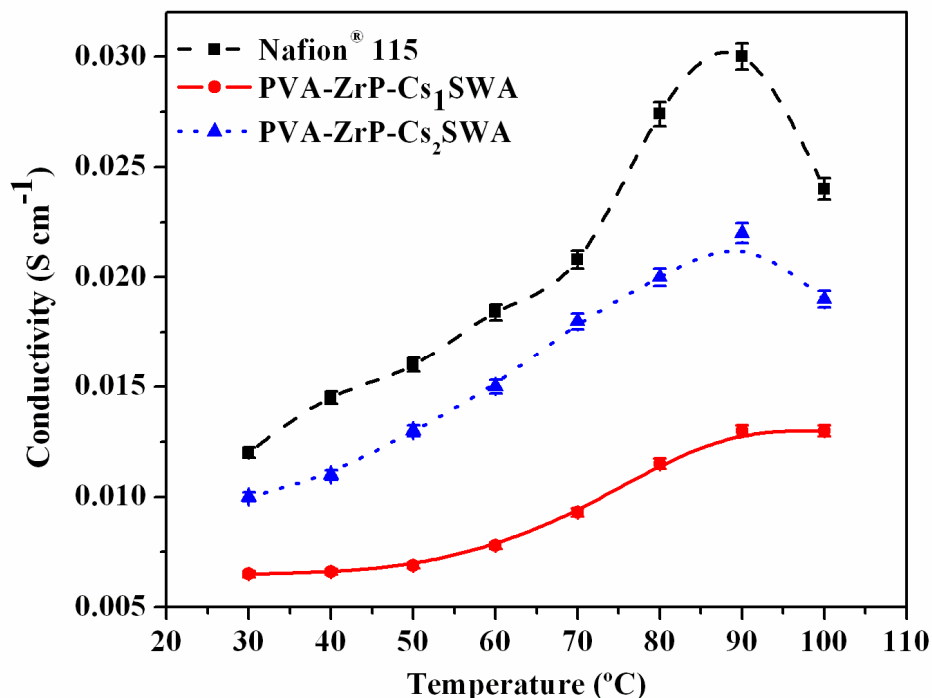


Fig. 4.5 Proton conductivity at 50 % RH as a function of temperature for PVA-ZrP-Cs₁SWA and PVA-ZrP-Cs₂SWA membranes compared with that of Nafion[®] 115 at 100 % RH.

4.3.7 Methanol crossover study

The concentration of crossed methanol as a function of crossover time is determined for PVA-ZrP-Cs₁SWA and PVA-ZrP-Cs₂SWA hybrid membranes and it is compared to that for Nafion[®] 115 in Fig. 4.6. For a duration of 180 min, the methanol crossed over in hybrid membranes is 33 % less compared to Nafion[®] 115. In the case of hybrid membranes, there is an exponential increase in crossover whereas in the case of Nafion[®] 115 it is linear with respect to crossover time. Among the two hybrid membranes, PVA-ZrP-Cs₂SWA shows lesser crossover to methanol. As shown in Fig. 4.7 the methanol permeability for hybrid membranes was less compared to Nafion[®] 115. Compared to Nafion[®] 115 and other related membranes, hybrid

membranes containing cesium salt of SWA show resistance to methanol permeability with appreciable proton conductivity as shown in Table 4.4.

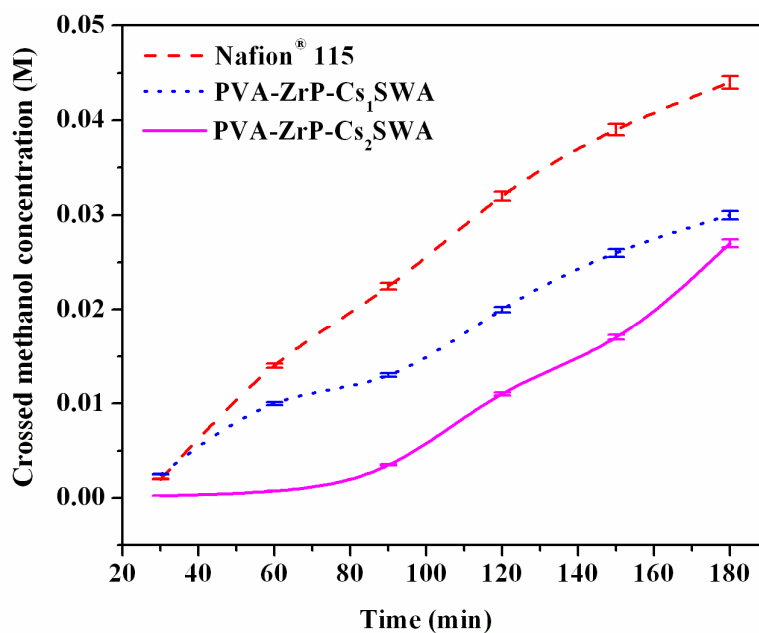


Fig. 4.6 Concentration of crossed methanol as a function of crossover time.

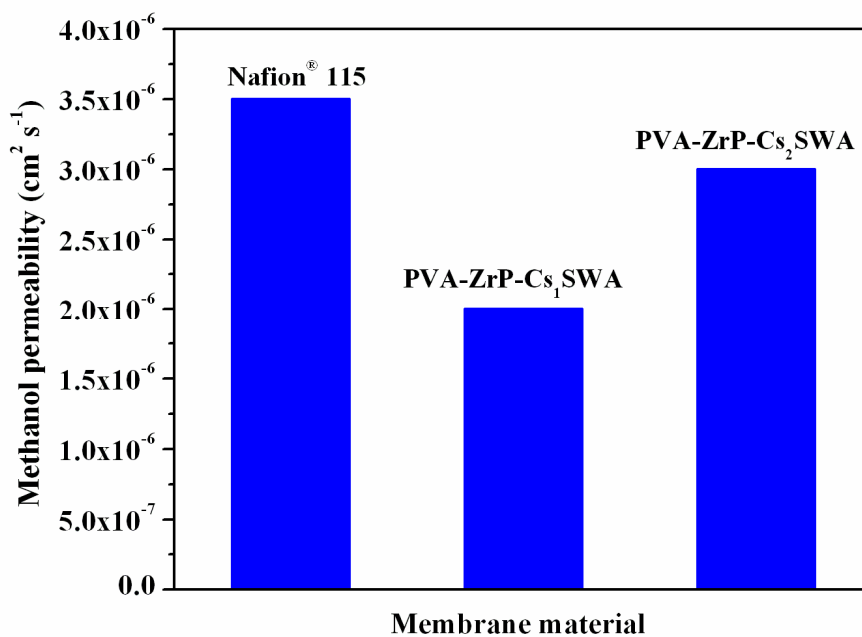


Fig. 4.7 Methanol permeability of PVA-ZrP-Cs₁SWA and PVA-ZrP-Cs₂SWA hybrid membranes compared with that of Nafion® 115.

Table 4.4 Comparison of conductivity and permeability of various membranes.

Membrane	Relative humidity (%)	Temperature (°C)	Conductivity (S cm ⁻¹)	Permeability (cm ² s ⁻¹)	References
PVA/ZrP/Cs ₁ SWA	50	100	0.013	2 x 10 ⁻⁶	a
PVA/ZrP/Cs ₂ SWA	50	100	0.02	3 x 10 ⁻⁶	a
Nafion [®] 115	100	90	0.03	3.5 x 10 ⁻⁶	a
Nafion [®] 115/Cs ⁺ , NH ₄ ⁺ , Rb ⁺ and Tl ⁺ modified PTA	35	120	0.016	-	Ramani <i>et al.</i> 2005.
SPEK/ZP/ZrO ₂ (70/20/10 wt %)	100	70	2.3 x 10 ⁻³	-	Ruffmann <i>et al.</i> 2003
PVA/PWA/SiO ₂	-	-	0.004-0.017	10 ⁻⁷ to 10 ⁻⁸	Xu <i>et al.</i> 2004
PEG/SiO ₂ /SWA	100	80	0.01	10 ⁻⁵ to 10 ⁻⁶	Vernon <i>et al.</i> 2005
PEG/SiO ₂ /PWA	-	-	10 ⁻⁵ to 10 ⁻³	10 ⁻⁶ to 10 ⁻⁷	Lin <i>et al.</i> 2005
PVA/SiO ₂ /SWA	100	100	4.13 x 10 ⁻³	-	Shanmugam <i>et al.</i> 2006
SPEEK/PWA	100	100	1.7 x 10 ⁻²	-	Zaidi <i>et al.</i> 2000

a - Obtained from our measurements

4.3.8 Full cell testing

4.3.8.1 Membrane electrode assembly (MEA) fabrication

Electrocatalysts used were unsupported Pt–Ru black (1:1 atomic ratio, Alfa Aesar) and Pt black (Alfa Aesar) in the anode and cathode, respectively. The catalyst slurry containing catalyst, water, isopropyl alcohol (IPA) and Nafion[®] solution (1100 EW, Du Pont) as binder was sprayed on teflonized carbon cloth (E-Tek). Electrodes of area of 2 × 3 cm² with 6 mg cm⁻² of catalyst loading were fabricated and placed on

either side of the membrane. The membrane electrode assembly (Fig. 4.8) was sandwiched between the two transparent polyacrylic plates constituting the cell fixture by means of eight bolts (Fig. 4.9). Single cell performance was measured by using a passive air-breathing DMFC with a 4 M methanol solution. Methanol was diffused into the anode catalyst layer from the built-in reservoir of 4.5 ml capacity, while oxygen, from the surrounding air, was diffused into the cathode catalyst layer through the opening of the cathode fixture. The single cell performance experiments were carried out at room temperature (25 °C) and at atmospheric pressure. Cell voltage versus current density response was measured galvanostatically by incrementally increasing the current from open circuit and measuring the cell voltage.

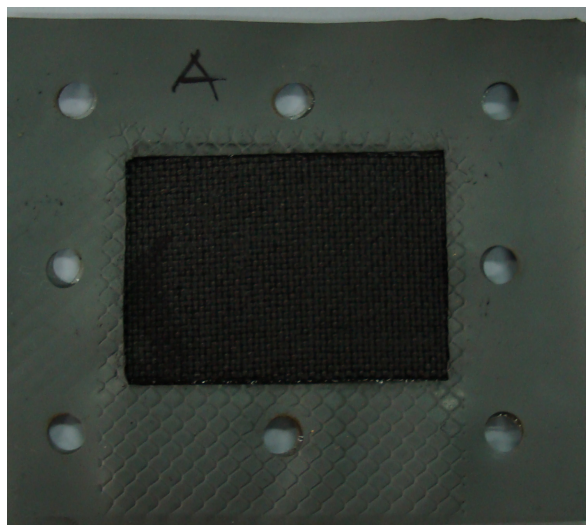


Fig. 4.8 Photograph of a fabricated membrane electrode assembly.

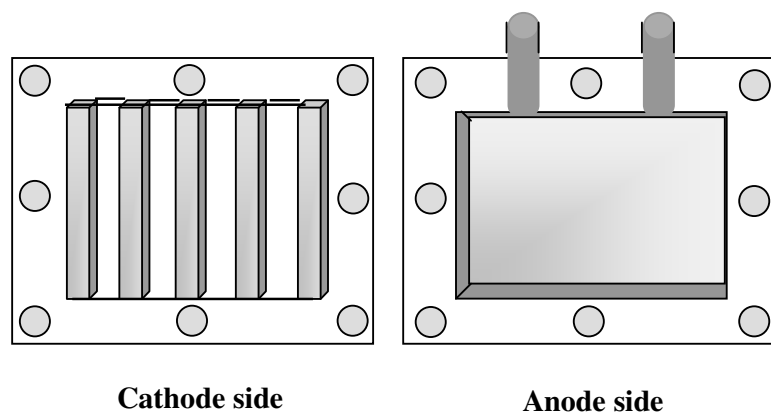


Fig. 4.9 Schematic view of cathode cell fixture and anode cell fixture with built in fuel reservoir.

4.3.8.2 Single cell performance in DMFC

Fig. 4.10 shows the single cell performance of DMFC with PVA–ZrP–Cs₁SWA and PVA–ZrP–Cs₂SWA hybrid membranes as proton conducting electrolyte. For comparison, the single cell performance of Nafion[®] 115 as proton conducting electrolyte under similar condition is also shown. The polarization and power density curves are obtained under unoptimized conditions by a home made passive cell. Cell with PVA–ZrP–Cs₂SWA hybrid membrane delivers a maximum power density of 6 mW cm⁻² which is comparable to that of Nafion[®] 115 (5.4 mW cm⁻²). The cell with PVA–ZrP–Cs₁SWA hybrid membrane exhibited lower performance (2.1 mW cm⁻²) in full cell mode in comparison to PVA–ZrP–Cs₂SWA hybrid membrane and Nafion[®] 115. The open circuit voltage (OCV) for the cell with PVA–ZrP–Cs₂SWA hybrid membrane is 0.652 V and that for PVA–ZrP–Cs₁SWA hybrid membrane is 0.619 V. The increase in OCV compared to Nafion[®] 115 (0.610 V) indicated reduced methanol crossover to the cathode side. The results suggest that these membranes may be suitable for application in DMFC.

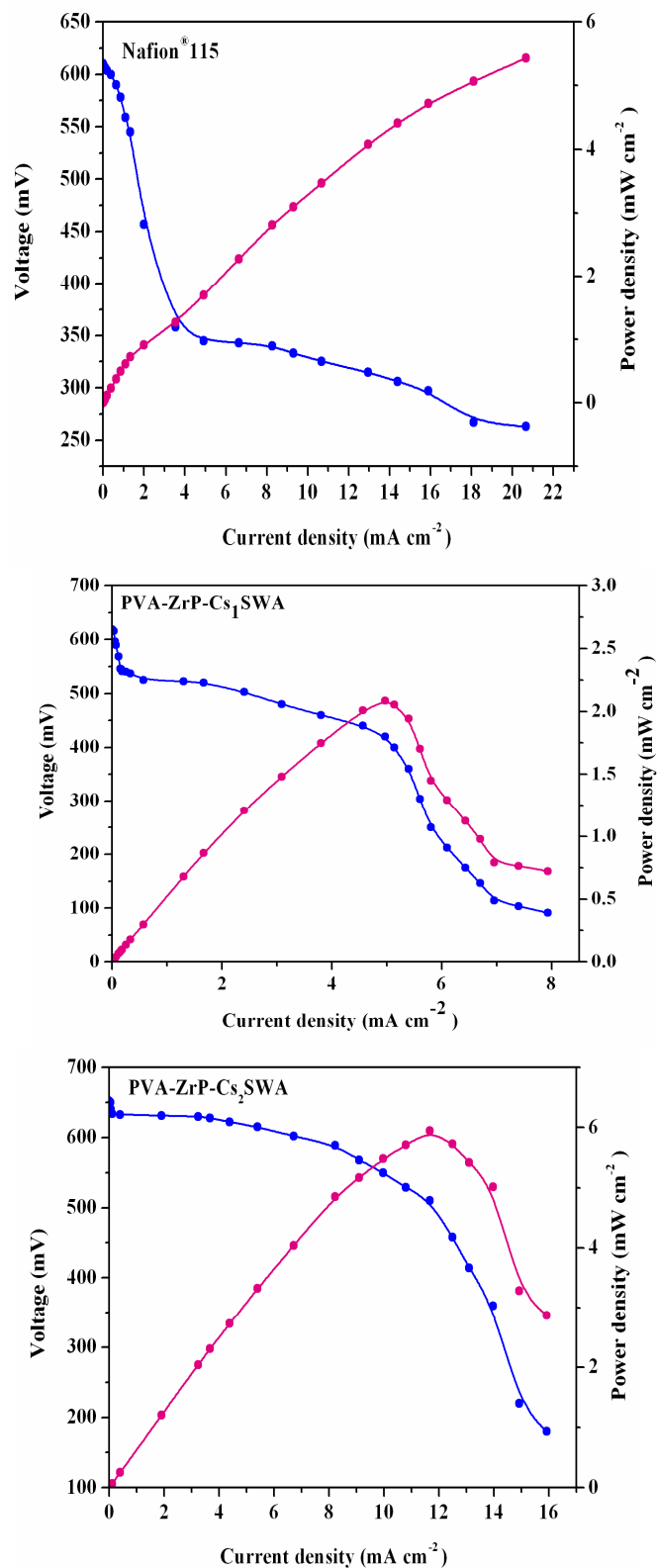


Fig. 4.10 Polarization and power density curves for passive DMFC cell with Nafion® 115, PVA-ZrP-Cs₁SWA and PVA-ZrP-Cs₂SWA hybrid membranes as proton conducting electrolyte at 25 °C and at atmospheric pressure.

4.4 CONCLUSIONS

Though a number of reports are available in literature on stabilizing the HPA in membrane matrix, a combined approach of composite formation with salts of HPA is investigated in this study for the first time. Hybrid membranes based on cesium salt of heteropoly acid, zirconium phosphate and poly(vinyl alcohol) were fabricated and characterized for its applicability in DMFC. The vibration spectroscopy, diffraction studies and thermal analysis provided information on the structure and stability of these hybrid membranes. Water uptake and swelling of the fabricated membranes decreased with increase in cesium content in their composition. At 50 % of relative humidity, the protonic conductivity of the hybrid membranes was in the range of 10^{-3} to 10^{-2} S cm⁻¹. Also, these hybrid membranes exhibited decreased methanol crossover with that of Nafion[®] 115. A maximum power density of 6 mW cm⁻² was obtained with PVA–ZrP–Cs₂SWA hybrid membrane. The open circuit voltage (OCV) for the cell with PVA–ZrP–Cs₂SWA hybrid membrane is 0.652 V and that for PVA–ZrP–Cs₁SWA hybrid membrane is 0.619 V which is higher compared to the cell with Nafion[®] 115 (0.610 V) indicating reduced methanol crossover. The performance of the hybrid membranes in passive cell mode appears promising for DMFC applications.

CHAPTER 5

CESIUM SALTS OF HETEROPOLY ACID EMBEDDED POLY(VINYL ALCOHOL) (PVA) - POLYACRYLAMIDE (PAM) - ORGANIC INORGANIC HYBRIDS AS POSSIBLE ELECTROLYTE FOR DMFC APPLICATION

5.1 INTRODUCTION

Among various hydrophilic polymers, poly(vinyl alcohol) (PVA) exhibits desired characteristics like enhanced chemical stability and it acts as an excellent methanol barrier (Pivovar *et al.* 1999) in addition to its film forming capacity which is essential for an ion-exchange membrane. Since 1986 (Polak *et al.* 1986), a number of research groups have investigated poly(vinyl alcohol) based proton conducting membranes (Xu *et al.* 2004; Qiao *et al.* 2005; Lin *et al.* 2007; Anis 2008). PVA membranes incorporated with heteropoly acids by forming composites are swelling too strongly to be used, the lesson learnt from our previous study (Chapter 3 and Chapter 4). Water uptake and swelling are of key issues of consideration for proton-conducting polymer electrolyte membranes. Extreme swelling causes a loss of the dimensional stability, while low water uptake reduces proton conductivity because of low water absorption capability of the membranes. Hence, PVA membranes with appropriate swelling properties along with good proton conductivities are needed for use in fuel cells (Xu *et al.* 2004). Increase in water content in the membranes beyond optimum levels would result in loss of dimensional stability and cause an increase in methanol permeability. Polymer swelling can be reduced by blending, cross-linking or copolymerizing with other suitable polymers, while an increase in proton conductivity can be achieved by forming hybrids by incorporating proton conductors like heteropoly acids (Xu *et al.* 2004; Vernon *et al.* 2005; Lin *et al.* 2005; Ponce *et al.*

2003; Bello *et al.* 2008). However, a major limiting factor to employ heteropoly acids as membrane material for fuel cell application is its extreme solubility in aqueous medium. This difficulty can be surmounted by forming hybrids with cesium salts of heteropoly acids (Ramani *et al.* 2004).

In the present investigation, the formulation and fabrication of a new class of hybrid membranes containing cesium salt of different heteropoly acids such as phosphomolybdic acid (PMA), phosphotungstic acid (PWA) and silicotungstic acid (SWA) incorporated into the poly(vinyl alcohol) (PVA)-polyacrylamide (PAM) blend are reported. It is for the first time PVA-PAM polymer matrix has been proposed and chosen by us in order to formulate hybrid membrane material with salts of heteropoly acid. A simple fabrication route was adopted in the preparation of these hybrid materials. These membranes are characterized through various physico-chemical techniques, morphological studies and permeability experiments. The suitability of these membranes for direct methanol fuel cell application has been explored by carefully investigating various required key characteristics of the membrane such as proton conductivity, water uptake and ion-exchange property. The membranes exhibited desired properties for DMFC application such as low methanol crossover, optimum swelling with desired proton conductivity, excellent additive and oxidative stability with an additional advantage of cost effectiveness compared to the state of the art commercial Nafion[®] membranes.

5.2 EXPERIMENTAL

5.2.1 Preparation of salts of heteropoly acids

Cesium salts of various heteropoly acids such as phosphomolybdic acid (PMA), phosphotungstic acid (PWA) and silicotungstic acid (SWA) were synthesized at room

temperature by the neutralization of respective acid solution with appropriate amount of 0.1 M cesium carbonate solution. Attempts were made to control the number of protons substituted as two ($\text{Cs}_2\text{HPMo}_{12}\text{O}_{40} \cdot x\text{H}_2\text{O}$ (PMA), $\text{Cs}_2\text{HPW}_{12}\text{O}_{40} \cdot x\text{H}_2\text{O}$ (PWA), $\text{Cs}_2\text{H}_2\text{SiW}_{12}\text{O}_{40} \cdot x\text{H}_2\text{O}$ (SWA)) by controlling the stoichiometry of the added cesium carbonate solution. The crystals were dried at room temperature and kept under constant humidity of air until constant mass was attained.

5.2.2 Fabrication of hybrid membranes

The hybrid membranes were fabricated through a solution-cast method. A 10.0 wt % of PVA (*MW*: 125,000, SRL Chemicals, India) solution in water was prepared under vigorous stirring at 70 °C. To this solution, a mixture of 10.0 wt % of PAM (*MW*: 5,000,000, Otto Kemi, India) dissolved in water and required quantity of one of the cesium salt of heteropoly acids such as phosphomolybdic acid (PMA), phosphotungstic acid (PWA) or silicotungstic acid (SWA) were added and stirred for 6 h, to obtain a homogenous solution. The weight percent of PAM and heteropoly acids in the hybrid membrane was maintained as 10.0 each. The homogeneous solution was spread uniformly on a clean glass plate and leveled perfectly. Water was removed slowly by keeping the glass plate at room temperature and the dried membrane was detached from the glass plate. The obtained dry membrane was immersed into crosslinking bath containing glutaraldehyde (25 wt % glutaraldehyde solution in water, SRL), acetone and hydrochloric acid for 30 min at room temperature (75 % (v/v) aqueous–acetone mixture containing 2 ml of Glu and 2 ml of conc. HCl). The membrane was removed from the crosslinking bath, washed repeatedly with deionized water and dried at ambient temperature. During the chemical treatment (cross-linking), –OH of PVA and the –CHO of glutaraldehyde

(Glu) in the membrane is cross-linked by an acid catalyzed reaction. The resultant moiety can function as the hydrophobic methanol barrier unit to provide the hybrid matrices with desired morphological stability (Kang *et al.* 2002). In addition, the cross-linking prevents the solubility of respective polymers in solvent.

5.3 MEMBRANE CHARACTERIZATION

A new class of inorganic-organic hybrid membranes were made through blending of poly(vinyl alcohol) (PVA) - polyacrylamide (PAM) followed by cross-linking with glutaraldehyde (Glu). Cesium salt of different heteropoly acids such as phosphomolybdic acid (PMA), phosphotungstic acid (PWA) and silicotungstic acid (SWA) were incorporated into the polymer network to form corresponding hybrid membrane materials namely PVA-PAM-CsPMA-Glu, PVA-PAM-CsPWA-Glu and PVA-PAM-CsSWA-Glu respectively as described in the experimental section. They were subjected to extensive physico-chemical characterization studies.

5.3.1 Fourier transformed infrared (FT-IR) spectral studies

Fig. 5.1 shows the Fourier transformed infrared (FT-IR) spectra of various hybrid membranes and their constituent materials. As can be seen, the broad band observed around 3600 cm^{-1} for all three materials is attributed to the O-H stretching band of hydrogen-bonded alcohol. The band appeared at 1169 cm^{-1} has been ascribed to the (C-O) stretching and the bands present at 1396 cm^{-1} was due to the C-O-H bending of the PVA molecule. The spectra exhibit a C-H alkyl stretching band at 2970 cm^{-1} and C-H alkyl bending band at 1458 cm^{-1} for $-\text{CH}_2$ and $-\text{CH}_3$ bonds respectively. The bands at 1746 and 2877 cm^{-1} indicate the aldehyde groups of glutaraldehyde that is crosslinked to PVA. A weak band at 1671 cm^{-1} and a band at 1640 cm^{-1} are assigned to the $-\text{C}=\text{O}$ stretching and N-H bending of acrylamide unit in the hybrid polymer.

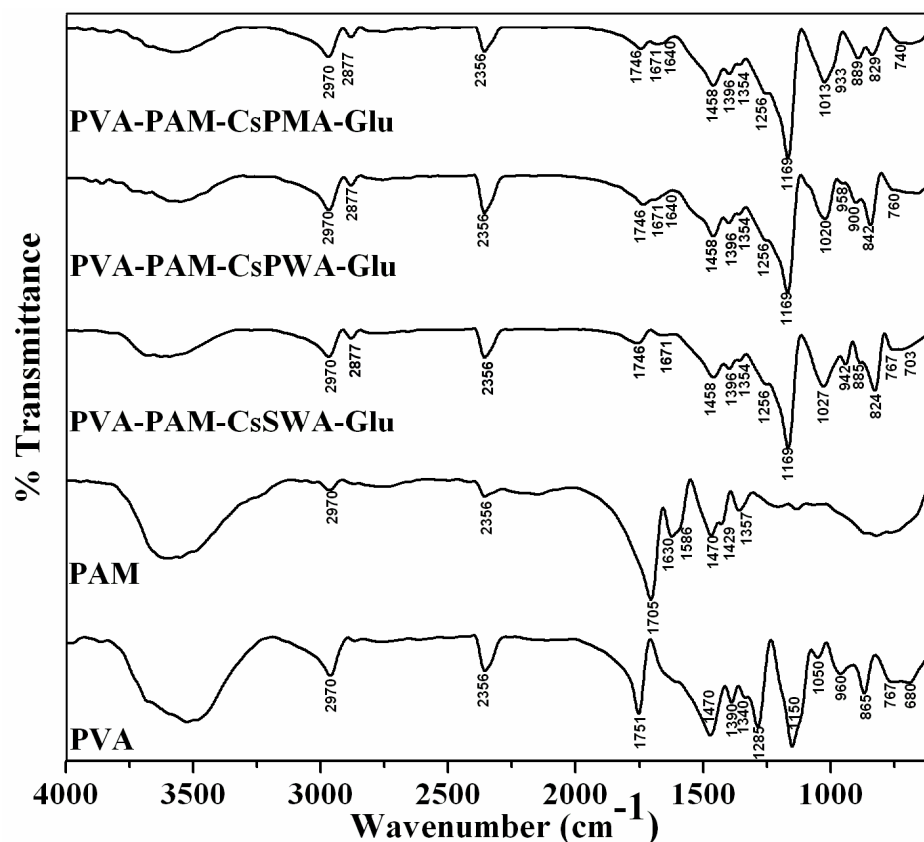


Fig. 5.1 FT-IR spectra of hybrid membrane materials: Cross-linked PVA-PAM blends by glutaraldehyde with cesium salts of different heteropoly acid along with pristine PAM and PVA.

The bands of Keggin ion can be observed between 1100 and 700 cm^{-1} (Deltcheff *et al.* 1976). The strong absorption band at $\sim 1020\text{ cm}^{-1}$ in the hybrid membranes can be assigned to the asymmetric stretching vibration of the central P-O_4 tetrahedron. The band at $\sim 890\text{ cm}^{-1}$ is due to the stretching of $\text{M-O}_c\text{-M}$ bridges between corner sharing MO_6 octahedra and that around $\sim 825\text{ cm}^{-1}$ is due to the stretching of $\text{M-O}_e\text{-M}$ bridges between edge sharing octahedra. The presence of these bands confirmed the existence of the heteropoly acid with Keggin geometry has been preserved in the hybrid membrane. The positions of vibration modes of all types of metal-oxygen (M-O) bonds are strongly influenced by interaction of heteropoly acid with the polymer. The W-O_t bond of SWA and PWA in the hybrid (PVA-PAM-CsSWA-Glu, PVA-PAM-CsPWA-Glu) is red shifted from 980 to 942 and 958 cm^{-1} respectively. The

stretching of $M-O_c-M$ bond with corner sharing oxygen of PMA, PWA and SWA in the hybrid have been blue shifted from 870 to 900 cm^{-1} , 890 to 900 cm^{-1} and 878 to 884 cm^{-1} respectively. This was due to the columbic interaction between the hydroxyl groups of the PVA and heteropoly acid. The main bands are assigned and tabulated separately for the fabricated hybrid membranes in Table 5.1.

Table 5.1. Assignments of main absorption bands of fabricated hybrid membranes.

Vibration frequency (cm^{-1})			Bond assignment
PVA-PAM-CsPMA-Glu	PVA-PAM-CsPWA-Glu	PVA-PAM-CsSWA-Glu	
830	840	825	$M-O_c-M$ stretching
900	900	885	$M-O_c-M$ stretching
-	958	942	$M-O_t$ stretching
1027			X-O stretching
1169			C-O stretching
1256			C-O-C ether link
1396			C-O-H bending
1458			$-CH_2$ bending
1640			N-H bending
1671			Amide $C=O$ stretching
1746			Aldehyde $C=O$ stretching
2970			$-CH_2$ stretching
3600			$-OH$ stretching

5.3.2 X-ray diffraction (XRD) analysis

In Fig. 5.2 the X-ray diffraction (XRD) profiles of the hybrid membranes incorporated with different heteropoly acids are shown. For a comparison, the XRD patterns of PVA and PAM are also given. The peak found at $2\theta = 20^\circ$ corresponds to the (101) plane of PVA in all hybrid membranes (Koji *et al.* 1999). The broad diffraction pattern of PAM indicates the amorphous nature of the polymer. No diffraction peaks characteristic of cesium salt of SWA appears in the hybrid membrane containing 10 % of SWA. This might be due to the finely dispersed SWA in the polymer matrix and the hybrid behaves as X-ray amorphous. Peaks characteristic of cesium salt of PMA and PWA appear in the hybrid membranes containing respective salts of heteropoly acids. A broad peak in all hybrid membranes indicates the conformation of complete homogeneity and compatibility among the components of the membrane.

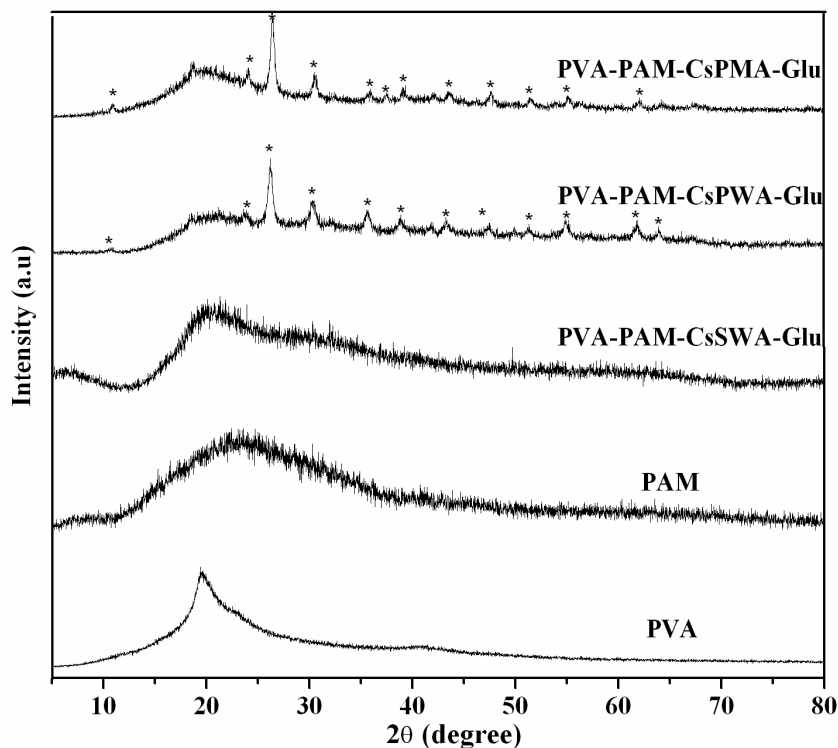


Fig. 5.2 XRD patterns of the PVA-PAM hybrid membranes with different heteropoly acids.

5.3.3 Thermogravimetric (TGA) studies

In Fig. 5.3, the traces of thermogravimetric analysis (TGA) of the hybrid membranes have been shown in the temperature range from 40 °C to 800 °C. The TGA curves of the hybrid membranes reveal four main weight loss regions. The first weight loss has been found in the region 100-200 °C, and this has been attributed to the loss of absorbed water molecules. The second weight loss observed in the temperature region 200-425 °C was due to the degradation of PVA (Hassan and Peppas, 2000) and PAM combined with the loss of crystalline water from heteropoly acid. It is a complex decomposition process with thermal degradation of the ester and ether linkages formed during the process of crosslinking with gluteraldehyde. In addition, ammonia and water may be evolved partly from the polyacrylonitrile structure formed during the PAM decomposition and partly from the remaining PAM at about 400 °C (Tutas *et al.* 1987). The third weight loss found around 425-500 °C was ascribed to the cleavage of C-C backbone of PVA and PAM polymer membrane leading to its carbonation. The fourth weight loss at 550 °C was due to the decomposition of the salt of heteropoly acid to respective metal oxides (Fournier *et al.* 1992). The three hybrid materials exhibit similar thermal behavior showing that they have similar structural characteristics and are stable up to 200 °C.

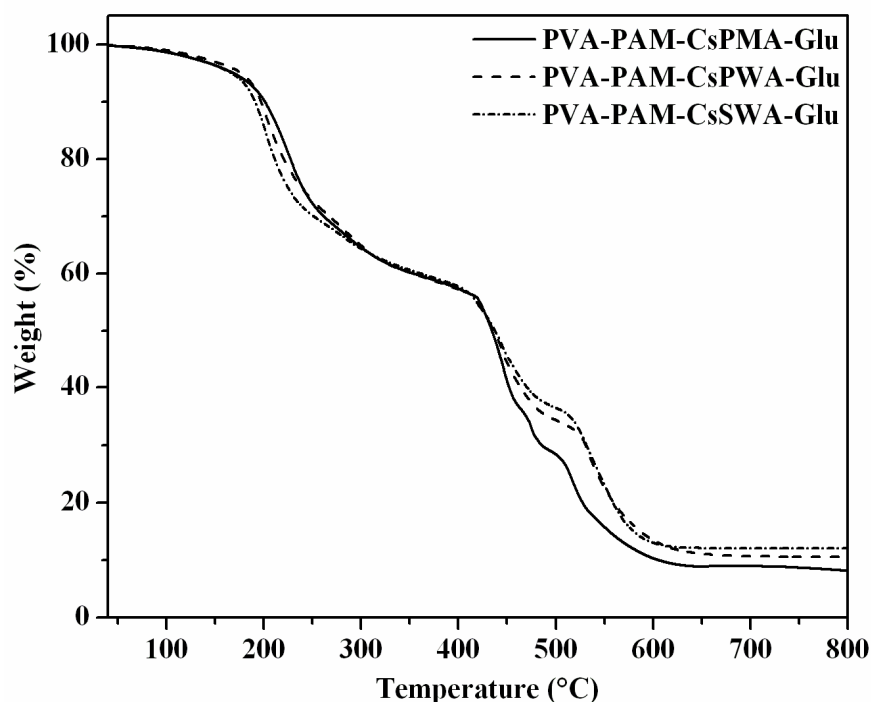


Fig. 5.3 Thermogravimetric analysis (TGA) traces of hybrid membranes in the temperature region 40 and 800 °C.

5.3.4 Scanning electron microscopy interfaced with EDXA

The surface morphological characteristics of all three hybrid membranes in their dry state were examined by using a scanning electron microscopy (SEM). The scanning electron micrographs along with corresponding energy-dispersive X-ray analysis (EDXA) traces are shown in Fig. 5.4. It can be seen from the micrographs that in all cases, heteropoly acid particulates are finely dispersed in the polymer matrix. It appears that the distribution of inorganic particles is relatively uniform in the organic matrix. The average particle size of the heteropoly acid was around 50 nm. Further, the presence of each of the heteropoly acid particles in the polymer matrix was elucidated from the corresponding peaks in the respective energy-dispersive X-ray analysis (EDXA) spectrographs.

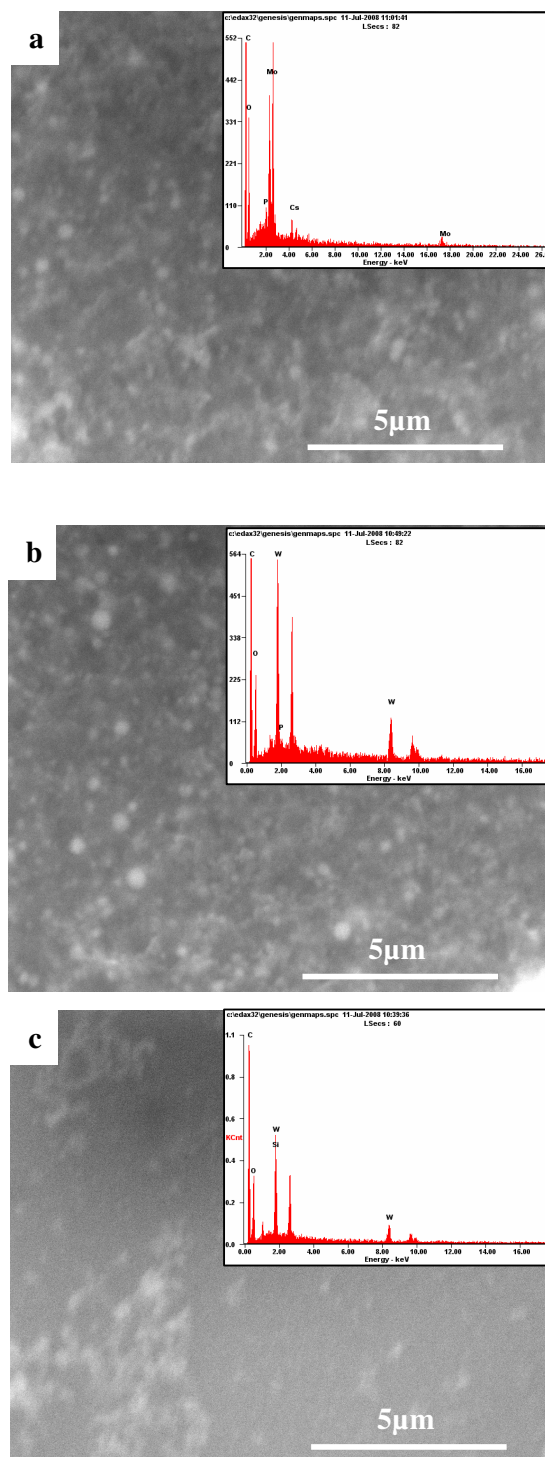


Fig. 5.4 Scanning electron micrographs (SEM) of the surfaces of hybrid membranes incorporated with different heteropoly acids. (a) PVA-PAM-CsPMA-Glu (b) PVA-PAM-CsPWA-Glu (c) PVA-PAM-CsSWA-Glu. The insert spectra represent the corresponding energy-dispersive X-ray analysis (EDXA) spectroscopy traces.

5.3.5 Water uptake, swelling and ion-exchange capacity (IEC)

After the physico-chemical characterization and morphological studies of the fabricated hybrid membranes and their constituents using spectroscopic, thermometric and surface analytical techniques, the newly prepared all three hybrid materials were examined for their suitability to function as a membrane material for direct methanol fuel cells. In this direction, the required key properties such as water uptake, swelling behavior and ion-exchange capacity (IEC) of these materials were tested. The presence of water in the membrane greatly influences the transport properties of these membranes. The water uptake and ion exchange capacity (IEC) play important roles in influencing conductivity characteristics of the membranes. In Table 5.2, the data obtained from water uptake, swelling and ion exchange capacity studies of these materials are given. As can be seen, the extent of water uptake of PMA containing hybrid membrane was found to be higher (66 %) compared to other hybrid membranes with PWA (50 %) or SWA (48 %). The water uptake capacity of these studied hybrid membranes are two to three fold higher compared to Nafion[®] 115 membranes. At room temperature (RT), the swelling extents of all the fabricated hybrid membranes were found to be nearly four to six folds lesser compared to the commercial Nafion[®] 115 membrane, while maintaining higher water uptake due to the presence of hydrophilic property of the heteropoly acid materials. A drastic decrease in the swelling extent of the fabricated PVA based hybrid membrane was attributed appreciably due to the interpenetrating network that has been formed in presence of PAM and Glu. Ion exchange capacities of the hybrid membranes were slightly lower compared to the commercial Nafion[®] 115 polymer electrolyte membrane and this is due to their inherent chemical compositions. Among the fabricated hybrid membranes,

cesium salt of PMA acid exhibited higher IEC compared to cesium salt of PWA and SWA acid containing hybrid membranes and thus affecting the proton conductivity.

Table 5.2 Water uptake, swelling and ion-exchange capacity (IEC) values for different hybrid membranes compared with that of Nafion[®] 115.

Membrane	Thickness (μm)	Water uptake (%)	Swelling (%)	IEC (meq g^{-1})
Nafion [®] 115	125	22	12.0	0.90
PVA-PAM-CsPMA-Glu	250 ± 20	66	2.6	0.73
PVA-PAM-CsPWA-Glu	250 ± 20	50	2.0	0.67
PVA-PAM-CsSWA-Glu	250 ± 20	48	1.9	0.65

5.3.6 Oxidative stability

Oxidative stability of the membrane material is of great concern, since under fuel cell operating conditions, the degradation of the polymer electrolyte is caused by the attack of HO• and HOO• radicals (Hübner and Roduner, 1999). These radicals are formed due to incomplete reduction of diffused oxygen at the anode. Hence, the oxidative stability of hybrid membranes was evaluated at room temperature in Fenton's reagent to simulate the fuel cell operating conditions. Fig. 5.5 shows the results of oxidative stability of prepared hybrid membranes soaked in Fenton's reagent at room temperature. Oxidative stability test carried out at room temperature indicates that all three fabricated hybrid membrane materials exhibited appreciable stability. Initially there was a steep increment in membrane weight and attained a stable value and remained unchanged until 100 h. After 100 h, the weight of all these

three membranes decreased. Hence the durability time of the hybrid membranes can be defined as the lasting time till the raising weight achieves a peak value (Fu *et al.* 2008) and in these cases it is 100 h. For comparison pure PVA and PVA-PAM blends without heteropoly acid with different blend density were also studied. In an hour pure PVA membrane is completely dissolved at room temperature under oxidative treatment. PVA-PAM blends without heteropoly acid were stable until 2 h at room temperature, but they steadily loose their mechanical strength within that time. The improvement in oxidative stability of the hybrid membrane compared to its constituting components is due to its dense structure which restricts the diffusion of the radicals in to the membrane.

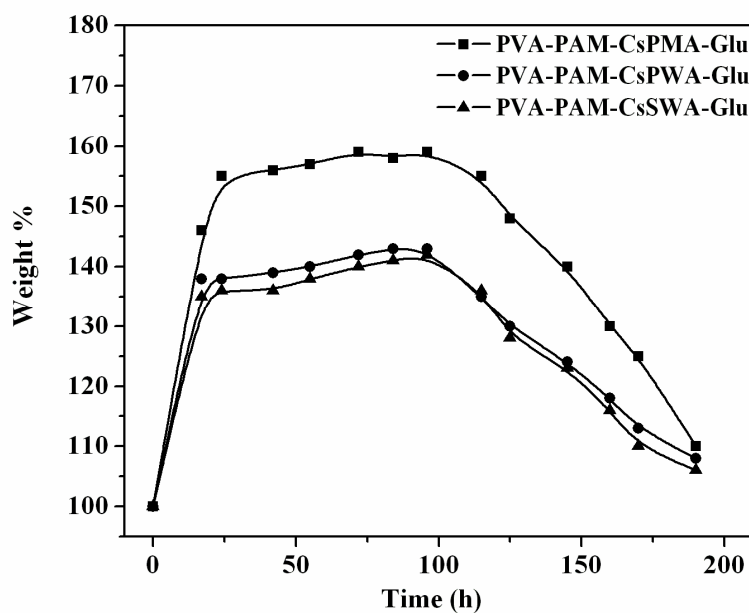


Fig. 5.5 Oxidative stabilities of fabricated membranes immersed in Fenton's reagent at room temperature at various time intervals.

5.3.7 Additive stability

A critical problem associated with the hybrid polymer electrolyte membranes is leaching of the inorganic additive from the polymer matrix which might lead to the performance loss and/or system operational failures in a real fuel cell mode. Hence, in order to establish the stability of these membrane materials in the present study, morphological characteristics of these membranes were tested at different time intervals for duration of five days by immersing the membranes in water using FT-IR technique. Fig. 6a-6c show the FT-IR spectra of hybrid membranes containing various salts of heteropoly acid. Characteristic bands of Keggin ion was observed between 1100 and 700 cm^{-1} . All the spectra confirm the presence of primary Keggin structure establishing the presence of salts of heteropoly acid in the hybrid membrane even after immersing them in water continually for several days. Initially there was a decrease in absorption intensity from 18 h to 73 h of immersion. After 73 h the decrease becomes negligible. This shows that the salts of heteropolyacid present on the surface is washed out at the initial stage due to vigorous stirring conditions. Whereas the salts of heteropolyacids present well inside the three dimensional network of the polymer matrix is quite stable. These spectra remained similar even after 125 h of immersion representing a negligible amount of loss in salts of heteropoly acid due to vigorous stirring conditions. These results ascertain the stability of Cs salts of heteropoly acids in the PVA-PAM matrix.

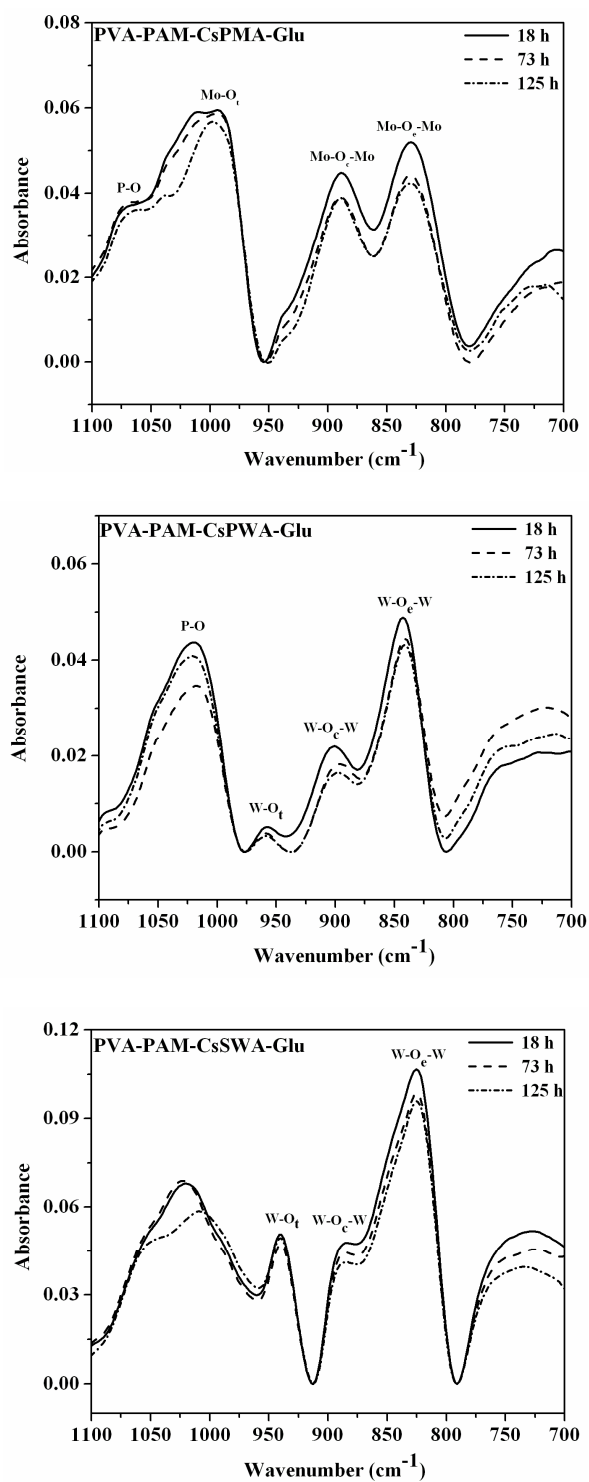


Fig. 5.6 FT-IR spectra of hybrid membranes (a) PVA-PAM-CsPMA-Glu (b) PVA-PAM-CsPWA-Glu (c) PVA-PAM-CsSWA-Glu placed in water for different durations.

5.3.8 Proton conductivity study

Fig. 5.7 shows the proton conductivity characteristics of the fabricated hybrid membranes measured at varying the temperatures ranging from 30 to 90 °C. Among the hybrid membranes studied, cesium salt of PMA substituted hybrid membranes exhibited higher proton conductivity compared to cesium salts of PWA and SWA substituted systems. In particular, PVA-PAM-CsPMA-Glu membrane exhibited the highest proton conductivity in the range of 10^{-2} S cm⁻¹ at 50 % RH. For comparison the proton conductivity of commercial Nafion[®] 115 polymer electrolyte membrane measured at 100 % RH is shown. The presence of salt of heteropoly acid as well as highly acidic N-H proton of polyacrylamide with hydrogen bonded interpenetrating network of the polymer matrix leads to a facile proton transport through the membrane under low humidity conditions. The order of proton conductivities of the hybrid membranes is in accordance with the water uptake ability and IEC of the materials (Table 5.1). Proton conductivity of the fabricated hybrid membranes was lesser compared to the state of the art Nafion[®] 115 membrane. Perfluorosulphonate proton exchange membranes such as Nafion[®] membrane materials enjoy the status of premium proton conductivity among all membrane materials due to their inherent chemical composition.

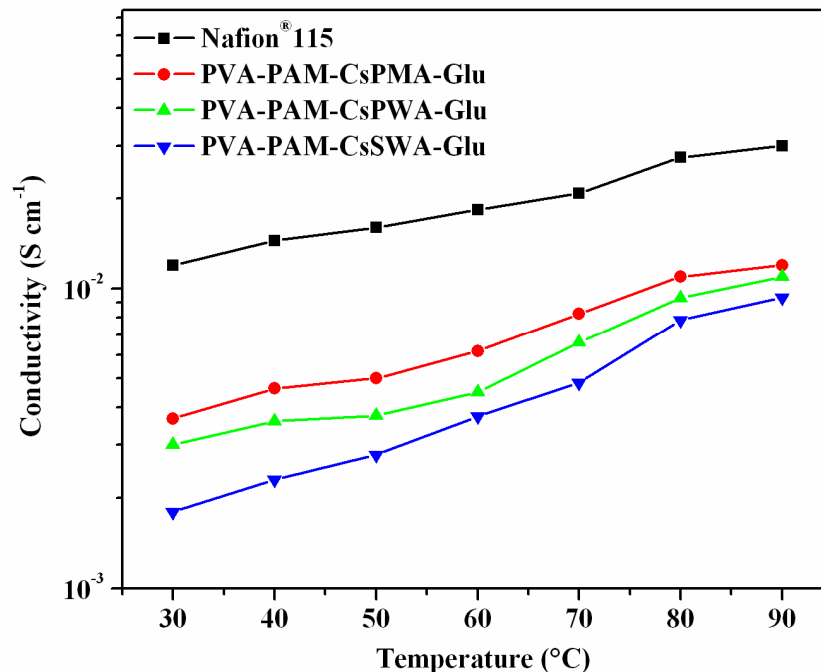


Fig. 5.7 Proton conductivities of the fabricated hybrid membranes and Nafion® 115 membrane at different temperatures.

5.3.9 Methanol crossover study

The concentration of permeated methanol through the hybrid membrane materials such as PVA-PAM-CsPMA-Glu, PVA-PAM-CsPWA-Glu and PVA-PAM-CsSWA-Glu as a function of crossover time has been measured by employing cyclic voltammetric technique and by using a two compartment cell which was divided by housing corresponding membrane material. The results of methanol crossover studies are presented in Fig. 5.8. The rate of crossed over methanol appeared to vary with the variation in incorporated heteropoly acid material in the polymer matrix. Hybrid membrane containing silicotungstic acid, SWA as an active component exhibited lower rate of methanol crossover compared to other heteropoly acid materials such as phosphotungstic acid, PWA or phosphomolybdic acid, PMA containing hybrid membranes. The concentration of crossed methanol through PVA-PAM-CsSWA-Glu hybrid membranes after 180 min was three fold lesser than with that of PVA-PAM-

CsPWA-Glu and four times lower than with that of PVA-PAM-CsPMA-Glu system. Methanol permeability of the respective membranes was determined from the slope of the plots representing the crossed methanol concentration versus time (Fig. 5.8). Fig. 5.9 shows the quantitative representation of methanol permeability of the hybrid membranes and the results were compared with that of commercial Nafion[®] 115 membrane. Methanol permeability is an order of magnitude lesser for the fabricated hybrid membranes compared to Nafion[®] 115. This may be due to the dense interpenetrating network that was formed due to the blending of PVA with PAM followed by crosslinking with glutaraldehyde.

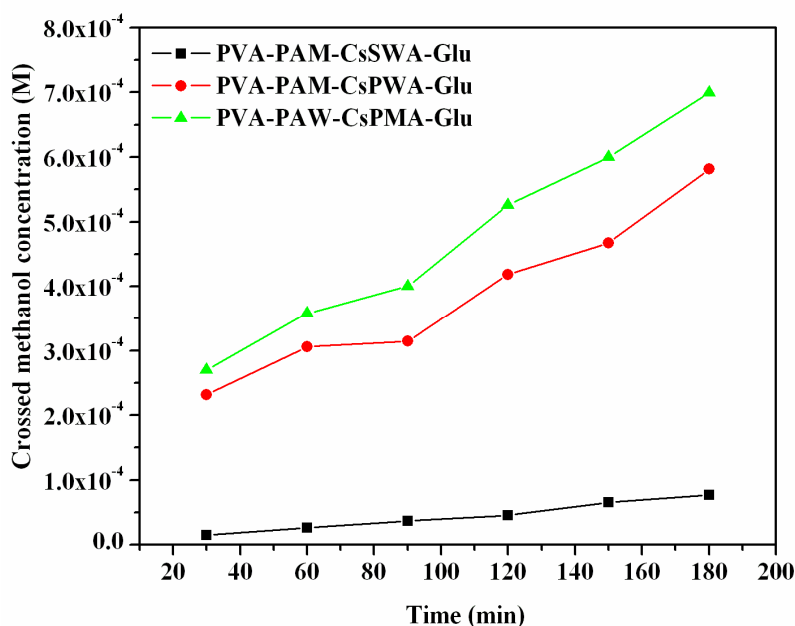


Fig. 5.8. Concentration of crossed over methanol as a function of crossover time.

The increasing order of methanol permeabilities of the membrane materials can be given as: PVA-PAM-CsSWA-Glu < PVA-PAM-CsPWA-Glu < PVA-PAM-CsPMA-Glu << Nafion[®] 115 (Fig. 5.9). The reduced methanol permeation in the hybrid membranes compared with Nafion[®] 115 is considered as an attractive desirable characteristic for the scientists and engineers working with the DMFC field and this property can be attributed to the methanol absorption ability of the heteropoly acids that were incorporated into the polymer matrix of PVA-PAM blend. We rationalize

our observations and findings based on the following concepts. Heteropoly acids possess a unique conceptual character called ‘Pseudoliquid phase behavior’ in which polar molecules like methanol can be readily absorbed into the solid matrix (Misono, 1987). Hence the fabricated heteropoly acid containing hybrid membranes exhibit the capacity to retain methanol without letting it to pass by. The number of methanol molecules adsorbed per anion is approximated to integral number of protons in the heteropoly molecule (Okuhara *et al.* 1989; Bielanski *et al.* 1999; Małecka *et al.* 1999). The order of methanol adsorption per Keggin unit was reported to be as follows: $\text{SiW}_{12}\text{O}_{40}^{4-} > \text{PW}_{12}\text{O}_{40}^{3-} > \text{PMo}_{12}\text{O}_{40}^{3-}$ (Okuhara *et al.* 1989; Małecka *et al.* 1999; Bielański *et al.* 2005; Rykova *et al.* 2003; Antonucci *et al.* 2006) which has been clearly reflected in our results on permeability studies. Compared to Nafion[®] 115 membrane, other commercial membranes as well as related hybrid membranes, the fabricated hybrid membranes with the formulations under this study exhibited excellent tolerance to methanol permeability with appreciable proton conductivity as can be seen from the data presented in Table 5.3.

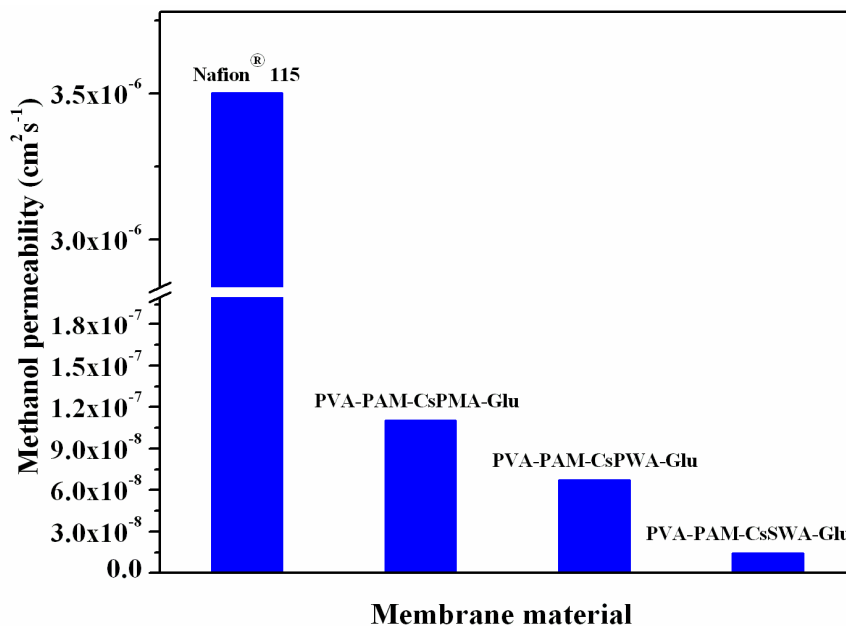


Fig. 5.9 Methanol permeability of fabricated hybrid membranes compared with that of Nafion[®] 115.

Table 5.3 Comparison of proton conductivity and permeability for various membranes (Extension of Table 4.4).

Membrane materials	RH (%)	Temperature (°C)	Conductivity (S cm ⁻¹)	Permeability (cm ² s ⁻¹)	References
PVA-PAM-CsSWA-Glu	50	RT	1.8×10^{-3}	1.38×10^{-8}	Present work
PVA-PAM-CsPWA-Glu	50	RT	3×10^{-3}	6.7×10^{-8}	
PVA-PAM-CsPMA-Glu	50	RT	3.7×10^{-3}	1.1×10^{-7}	
PVA-ZrP-SWA	60	60	10^{-2}	6×10^{-7}	Chapter 3
PVA-ZrP-Cs ₁ SWA	50	100	0.013	2×10^{-6}	Chapter 4
PVA-ZrP-Cs ₂ SWA	50	100	0.02	3×10^{-6}	Chapter 4
PVA/PWA/SiO ₂	-	-	0.004-0.017	10^{-7} to 10^{-8}	Xu <i>et al.</i> 2004
PVACO/PMA	-	30-100	10^{-3}	10^{-6}	Anis <i>et al.</i> 2008
PEG/SiO ₂ /SWA	100	80	0.01	10^{-5} to 10^{-6}	Vernon <i>et al.</i> 2005
PEG/SiO ₂ /PWA	-	-	10^{-5} to 10^{-3}	10^{-6} to 10^{-7}	Lin <i>et al.</i> 2005
SPEEK/PWA	100	100	1.7×10^{-2}	-	Ponce <i>et al.</i> 2003
SPEEK/TPA/MCM-41	-	20	2.75×10^{-3}	10^{-8}	Bello <i>et al.</i> 2008
Nafion® 115	100	90	0.03	3.5×10^{-6}	Present work
CRA-08 ^a	-	60	45×10^{-3}	0.58×10^{-6}	Antonucci <i>et al.</i> 2006 ; Amara and Kerdjoudj, 2003
IonClad® R1010 ^b	-	60	146×10^{-3}	0.6×10^{-6}	Scott <i>et al.</i> 2000 ; Tricoli <i>et al.</i> 2000
SPEEK (SD=87 %)	-	60	13×10^{-3}	17.5×10^{-7}	Li <i>et al.</i> 2003; Silva <i>et al.</i> 2006; Fu <i>et al.</i> 2007

^a Polyethylene-Tetra-fluoroethylene with sulphonyls in divinyl benzene matrix

^b Tetra-fluoroethylene with poly(styrene sulfonic acid)

5.4 CONCLUSIONS

In conclusion, the formation of poly(vinyl alcohol) based hybrid membranes with key properties desired for DMFC applications such as low methanol crossover, low swelling, good oxidation stability and with appreciable proton conductivity in the range of $10^{-2} \text{ S cm}^{-1}$ at 50 % RH has been formulated, fabricated and demonstrated. These hybrid membranes were fabricated through blending of poly(vinyl alcohol) (PVA) - polyacrylamide (PAM) followed by cross-linking with glutaraldehyde (Glu). Cesium salts of different heteropoly acids such as phosphomolybdic acid (PMA), phosphotungstic acid (PWA) and silicotungstic acid (SWA) were incorporated into the polymer network to form corresponding hybrid membrane materials namely PVA-PAM-CsPMA-Glu, PVA-PAM-CsPWA-Glu and PVA-PAM-CsSWA-Glu respectively.

The interpenetrating network formed by the blending of PVA with PAM leads to an order of decrease in methanol crossover and swelling compared to state of the art Nafion[®] 115 membrane employed for DMFC applications. The hybrid membrane containing cesium salt of SWA exhibited very low methanol permeability ($1.4 \times 10^{-8} \text{ cm}^2 \text{ s}^{-1}$) compared to other membranes containing cesium salt of heteropoly acids such as PMA and PWA. The difference in methanol permeability between the fabricated hybrid membranes containing different cesium salt of heteropoly acids is found to be governed by the adsorption ability of the respective heteropoly acids. The enhanced ion exchange capacity and reasonable water uptake characteristics endowed the studied hybrid membrane materials with appreciable proton conductivity. Morphological evidence from scanning electron microscopy interfaced with energy dispersive X-ray analysis showed an even distribution of salts of heteropoly acid

throughout the polymer matrix. These results unequivocally substantiate the potential capacities of PVA-PAM based hybrid membranes with cesium salts of heteropoly acid as an electrolyte material for DMFC applications due to their reduced methanol crossover property, which is considered as a major drawback with the expensive fluorine based commercial Nafion[®] 115 membranes.

CHAPTER 6

DEVELOPMENT OF HYBRID MEMBRANE MATERIALS WITH CESIUM SALTS OF VARIOUS HETEROPOLY ACIDS IN POLY(VINYL ALCOHOL) (PVA) - POLYACRYLONITRILE (PAN) MATRIX FOR DMFC APPLICATION

6.1 INTRODUCTION

Poly(vinyl alcohol) is a semi-crystalline polymer possessing excellent chemical stability, flexibility, easy processability toward film formation, hydrophilicity, selectivity for water over alcohols (Pivovar *et al.* 1999) in addition to other desirable characteristics such that they are non-toxic, and cost effective polymer. These characteristics of PVA are highly desired for their employment as polymer electrolyte in fuel cells. However, the general problems with the PVA based membrane are their poor proton conductivity, and excessive swelling, the later may cause poor mechanical stability. Thus, the challenging task on hand is to reduce the swelling of PVA membranes and to increase their proton conductivity by suitably modifying them without the loss of other desirable characteristics associated with PVA for fuel cell application. In literature, different strategies like blending, cross-linking PVA with Nafion[®] (Shao *et al.* 2002; DeLuca and Elabd, 2006), sulfonated poly(ether ether ketone) (Yang, 2008), poly(styrene sulfonic acid) (Sahu *et al.* 2008), para toluene sulfonic acid (Kumar *et al.* 2009), poly(2-acrylamido-2-methyl-1-propanesulfonic acid) (Qiao *et al.* 2005), *p*-sulfonate phenolic resin (Wu *et al.* 2006), poly(styrene sulfonic acid-co-maleic acid) (Lin *et al.* 2007), sulfo succinic acid (Kim *et al.* 2004), poly(acrylic acid) (Yang *et al.* 2008), chitosan (Jiang *et al.* 2008) and doping with H₃PO₂ (Vargas *et al.* 1999) or H₃PO₄ (Gupta and Singh, 1996) and phosphotungstic acid, PWA (Li *et al.* 2003) were explored. Though incorporating

acids like phosphoric acid significantly increases the proton conductivity of the PVA (Gupta and Singh, 1996) a quick leaching of the doped acids from the polymer matrix especially when in contact with liquid fuels, often results in the decay of proton conductivity (Zhai *et al.* 2007).

In general, the sulfonate or carboxylate, containing PEMs reveal that proton conductivity and methanol permeability is directly influenced by the changes in ion content, water content, temperature or morphology (Elabd *et al.* 2003; Elabd *et al.* 2004; Zawodzinski *et al.* 1991; Zawodzinski *et al.* 1993; Ding *et al.* 2002). In other words, sulfonic acid or carboxylic acid containing polymers are not appropriate candidates in reducing PVA swelling and according to DeLuca and Elabd (2006), they are not suitable for the DMFC application.

Therefore, in order to tailor PVA membrane with optimum water uptake and negligible swelling, blending with N-containing polymer such as PAN or PAM (Reported in Chapter 5) would be a promising approach. In addition, the proton conductivity of PVA membranes can be improved through the formation of hybrids by incorporating proton conductors like heteropoly acids (Li *et al.* 2003; Xu *et al.* 2004). Among various N-containing polymers, polyacrylonitrile (PAN) exhibits good mechanical properties and the composite membranes investigated with PAN exhibited low methanol crossover due to the very low permeability of water and methanol through PAN. For example, blending of sulfonated poly(ether ether ketone) (sPEEK) and polyacrylonitrile (PAN) followed by heating under nitrogen atmosphere at 380 °C reported to significantly reduce the swelling in hot water and resulted in less methanol permeability of the membranes (Wang *et al.* 2007). Carter *et al.* (2002) reported to obtain several advantages like improved mechanical

properties, easier fabrication of membrane electrode assembly (MEA) and a low methanol crossover by the addition of PAN into sulfonated poly[bis(3-methylphenoxy)polyphosphazene].

In the present investigation, the formulation and fabrication of a set of new class of hybrid membranes containing cesium salt of different heteropoly acids such as phosphomolybdic acid (PMA), phosphotungstic acid (PWA) and silicotungstic acid (SWA) into the poly(vinyl alcohol) (PVA)-polyacrylonitrile (PAN) blend are reported. It is for the first time, PVA-PAN polymer matrix has been chosen to formulate composite membrane material with salts of heteropoly acid. A simple fabrication route has been adopted to prepare these composite materials. These membranes are characterized through various physico-chemical techniques, morphological studies and permeability experiments. The suitability of these membranes for direct methanol fuel cell application has been explored by carefully investigating various required key characteristics of the membrane such as proton conductivity, water uptake and ion-exchange property. All of them exhibited desired properties for direct methanol fuel cell application such as low methanol crossover, optimum swelling with desired proton conductivity, excellent additive and oxidative stability with an additional advantage of cost effectiveness compared to present commercial Nafion[®] membranes.

6.2 EXPERIMENTAL

6.2.1 Fabrication of hybrid membranes

The membranes were fabricated by adopting a solution-cast method. A 4.0 wt % of PVA (SRL Chemicals, India) solution was prepared in *N,N*-dimethyl formamide (DMF) medium under vigorous stirring at 70 °C. To this solution, a mixture of 10.0 wt % of PAN (synthesized as reported in Braun *et al.* 2001) dissolved in DMF and required quantity of one of the cesium salt of heteropoly acids such as

phosphomolybdic acid (PMA), phosphotungstic acid (PWA) or silicotungstic acid (SWA) were added and stirred for 2 h, to obtain a homogenous solution. The weight percent of PAN and heteropoly acids in the hybrid membrane was maintained as 10.0 in each case. The homogeneous solution was spread uniformly on a clean glass plate and leveled perfectly. DMF was evaporated by keeping the glass plate in a reduced atmosphere for 2–3 days at 40 °C. The obtained dry membrane was immersed into the cross-linking bath containing glutaraldehyde (25 wt % glutaraldehyde solution in water, SRL), acetone and hydrochloric acid for 30 min at room temperature (75 % (v/v) aqueous–acetone mixture containing 2 ml of Glu and 2 ml of conc. HCl). The cross-linking time has been optimized for the required concentration of Glu by measuring the water uptake at different time intervals during the process of cross-linking. Table 6.1 shows the data on the extents of water uptake at different duration of cross-linking. Below 30 min of cross-linking time, the membrane exhibited low dimensional stability and beyond 60 min of cross-linking time, the membrane became hard and brittle. At 30 min of cross-linking period, the hybrid membrane exhibited higher water uptake compared to 60 min of cross-linking time. Hence, for further studies, 30 min is chosen as an optimum time limit for cross-linking while using 2 ml of 25 % aqueous Glu. After the completion of cross-linking, the membrane was removed from the cross-linking bath, washed repeatedly with deionized water and dried at ambient temperature.

Table 6.1 Water uptake at different cross-linking time for PVA-PAN-CsPMA-Glu hybrid membrane.

Time of crosslinking	Water uptake (%)
5 min	Soften
10 min	Soften
30 min	46
1 h	38
2 h	17 (Hard and brittle)
3 h	17 (Hard and brittle)

During the immersion of the hybrid membrane in to the cross-linking bath, the cross-linking agent (glutaraldehyde, Glu) activated by the catalyst (HCl) can diffuse in to the membrane by means of swelling and reacts with the –OH groups of PVA (Yeom and Lee, 1996). The cross-linking process of PVA by Glu proceeds via the formation of acetal or ether linkage as shown in structure I of Fig. 6.1 and structure II is formed by the monofunctional reaction of Glu. The formation of these structures is well documented in literature (Immelman *et al.* 1993; Lindemann, 1971).

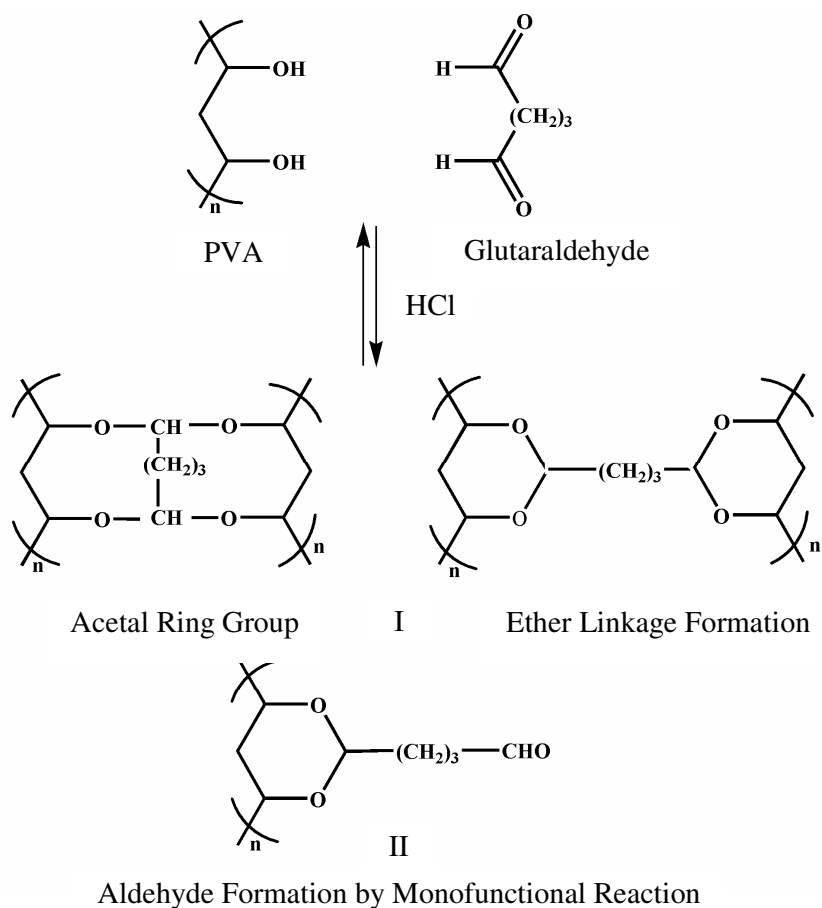


Fig. 6.1 The process of cross-linking of hydroxyl group of PVA with Glu.

6.3 MEMBRANE CHARACTERIZATION

The hybrid membranes made with poly(vinyl alcohol) (PVA)-polyacrylonitrile (PAN) polymer blend by incorporating cesium salt of different heteropoly acids such as phosphomolybdic acid (PMA), phosphotungstic acid (PWA) or silicotungstic acid (SWA) as described in the experimental section were subjected to extensive characterization using various physico-chemical techniques.

6.3.1 Fourier transformed infrared (FT-IR) spectral studies

Figure 6.2 shows the Fourier transformed infrared (FT-IR) spectra of various hybrid membrane materials prepared for this study. As can be seen, the broad band at 3580 cm^{-1} in all three materials is attributed to the O–H stretching band for hydrogen-bonded alcohol. The bands at 1165 cm^{-1} were ascribed to the (C–O) stretching and the bands appeared at 1390 cm^{-1} was attributed to the C–O–H bending of the PVA. The spectra exhibited a C–H alkyl stretching band at 2970 cm^{-1} and C–H alkyl bending band at 1460 cm^{-1} for $-\text{CH}_2$ and $-\text{CH}_3$ bonds respectively. The bands at 1740 and 2875 cm^{-1} indicate that the aldehyde groups of glutaraldehyde which is cross-linked to PVA. A weak band at 2245 cm^{-1} and a band at 1250 cm^{-1} are assigned to the $-\text{C}\equiv\text{N}$ stretching and C–N stretching of acrylonitrile unit in the hybrid polymer. The bands of Keggin ion can be observed between 1100 and 700 cm^{-1} (Deltcheff *et al.* 1976). The strong absorption band at $\sim 1027\text{ cm}^{-1}$ in the hybrid membranes can be assigned to the asymmetric stretching vibration of the central P-O_4 tetrahedron. The band at 890 cm^{-1} is due to the stretching of W–O–W bridges between corner sharing WO_6 octahedra and that around 825 cm^{-1} is due to the stretching of W–O–W bridges between edge sharing octahedra. The presence of these bands confirmed the existence and preservation of the heteropoly acid with Keggin geometry in the hybrid membrane. The positions of vibration modes of all types of metal-oxygen (M–O) bonds are strongly influenced by the interaction of heteropoly acid with the polymer. The W–O_t bond of SWA and PWA in the hybrid (Fig. 6.2b and 6.2c) is red shifted from 980 to 945 and 910 cm^{-1} respectively. The stretching of M–O–M bond with corner sharing oxygen of PMA, PWA and SWA in the hybrid has been red shifted from 864 to 840 cm^{-1} , 890 to 850 cm^{-1} and 878 to 825 cm^{-1} respectively. This was

due to the columbic interaction between the hydroxyl groups of the PVA and heteropoly acid.

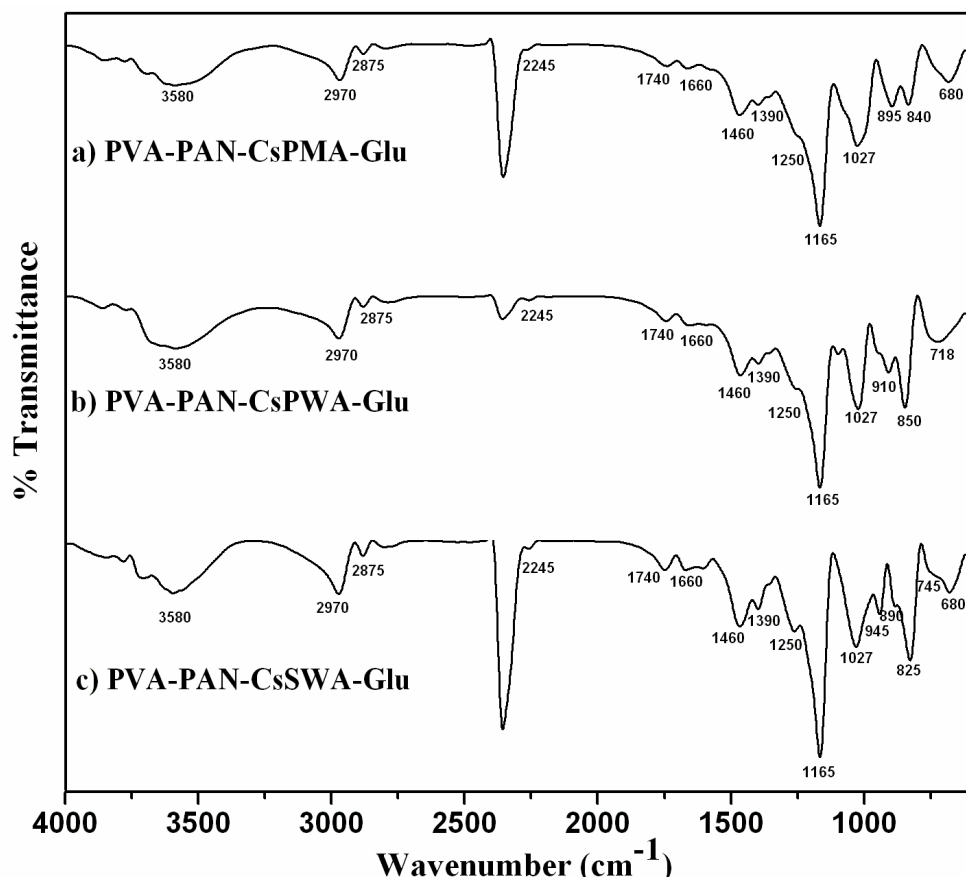


Fig. 6.2 FT-IR spectra of hybrid membrane materials: Cross-linked PVA-PAN blends by glutaraldehyde with cesium salts of different heteropoly acid (a) phosphomolybdic acid (PMA) (b) phosphotungstic acid (PWA) or (c) silicotungstic acid (SWA).

6.3.2 X-ray diffraction (XRD) analysis

In Fig. 6.3, the X-ray diffraction (XRD) profiles of the hybrid membranes incorporated with different heteropoly acids are shown. For a comparison, the XRD patterns of PVA and PAN are also given. The peak found at $2\theta = 20^\circ$ corresponds to the (101) plane of PVA in all hybrid membranes (Koji *et al.* 1999). PAN is a ladder polymer with a peak at $2\theta = 17^\circ$ and a small amount of amorphous portion can be seen

around $2\theta = 21^\circ$. Peaks characteristic of cesium salt of PMA and PWA appear in the hybrid membranes containing respective salts of heteropoly acids (indicated with *). No diffraction peaks characteristic of cesium salt of SWA appears in the hybrid membrane containing 10 % of SWA. This might be due to the finely dispersed SWA in the polymer matrix and the hybrid behaves as X-ray amorphous. A broad peak in all hybrid membranes indicates the complete homogeneity and compatibility among the components of the membrane.

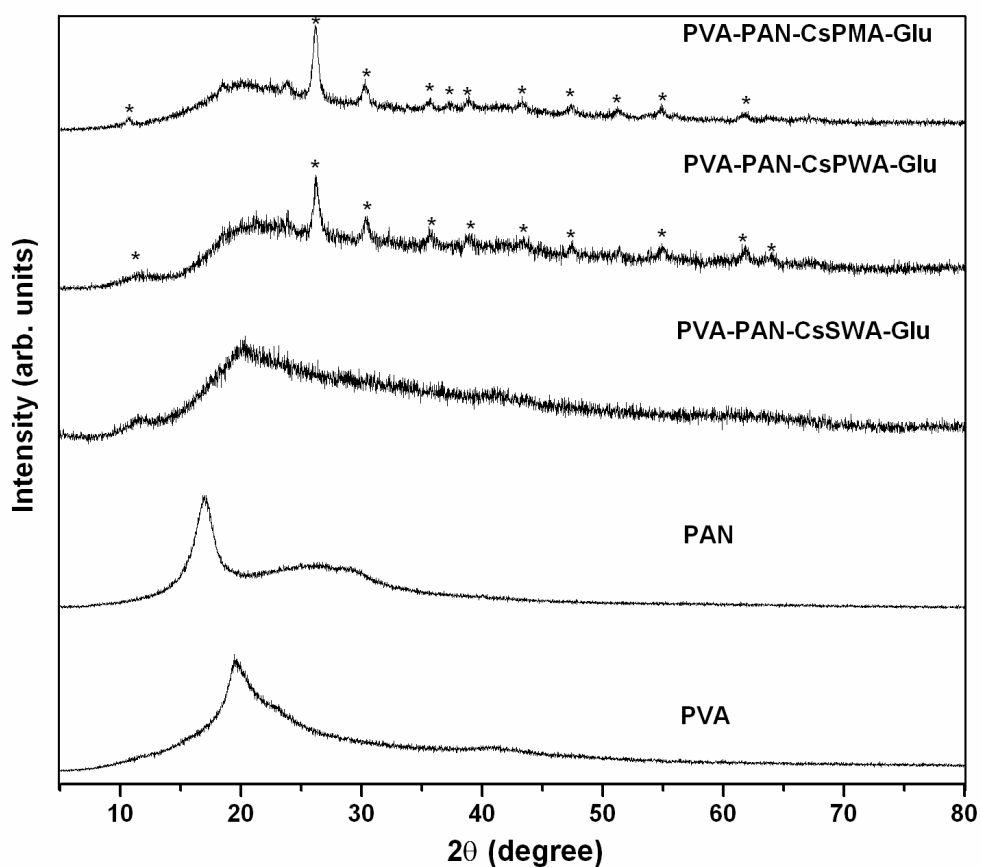


Fig. 6.3 XRD patterns of the PVA-PAN hybrid membranes with different heteropoly acids and pristine PVA and PAN.

6.3.3 Thermogravimetric (TGA) studies

In Fig. 6.4, the traces of thermogravimetric analysis (TGA) of the hybrid membranes have been shown in the temperature range from 40 °C to 800 °C. The TGA curves of the hybrid membranes reveal four main weight loss regions. The first weight loss has been found in the region 100-200 °C, and this has been attributed to the loss of absorbed water molecules. The second weight loss observed in the temperature region 200-425 °C was due to the degradation of PVA combined with the loss of crystalline water from heteropoly acid and oxidative ‘stabilization’ of PAN (David and Ismail, 2003). The third weight loss found around 425-500 °C was ascribed to the cleavage of C-C backbone of PVA polymer membrane leading to its carbonation (Hassan and Peppas, 2000). The fourth weight loss at 550 °C was due to the thermal transformations of PAN to form ladder-like structure combined with the decomposition of the salt of heteropoly acid to respective metal oxides (Fournier *et al.* 1992). The three hybrid materials exhibited similar thermal behavior showing that they have similar structural characteristics and are stable up to 200 °C.

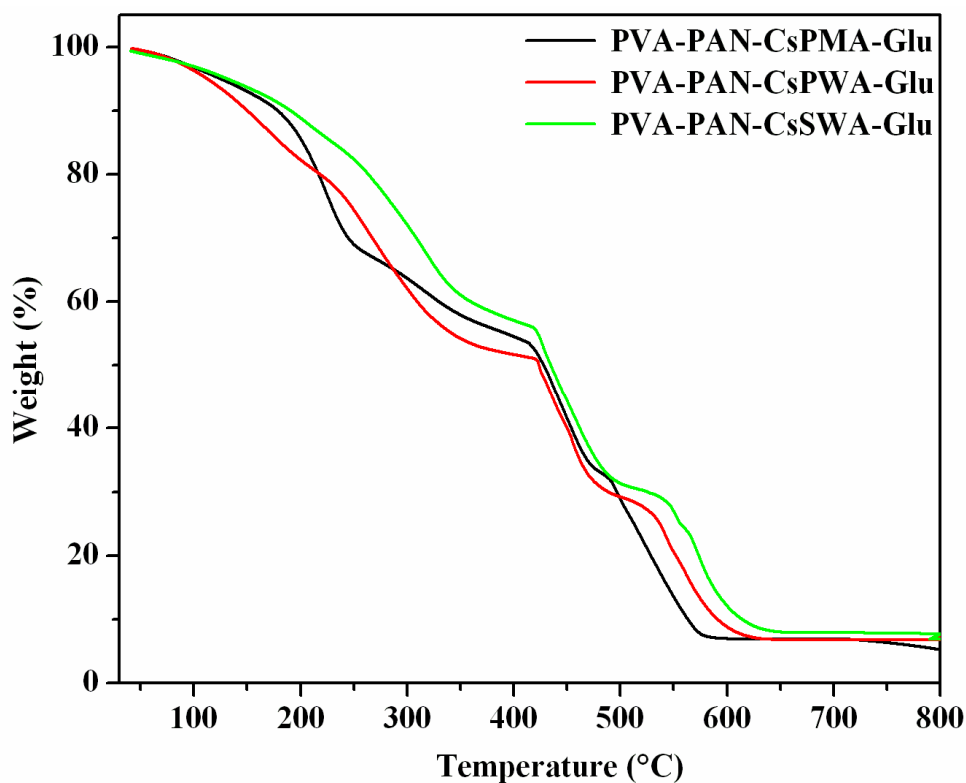


Fig. 6.4 Traces of thermogravimetric analysis (TGA) for hybrid membranes in the temperature region 40 and 800 °C.

6.3.4 Scanning electron microscopy interfaced with EDXA

The surface morphological characteristics of all three hybrid membranes in their dry state were examined by using a scanning electron microscopy (SEM) and the micrographs are shown in Fig. 6.5. It can be seen that the heteropoly acids particles are finely dispersed in the polymer matrix. It appears that the distribution of inorganic particles is relatively uniform in the organic matrix. The average particle size of the heteropoly acid was around 50 nm. Further, the presence of the heteropoly acid particles was confirmed by using energy-dispersive X-ray analysis (EDXA) spectroscopy.

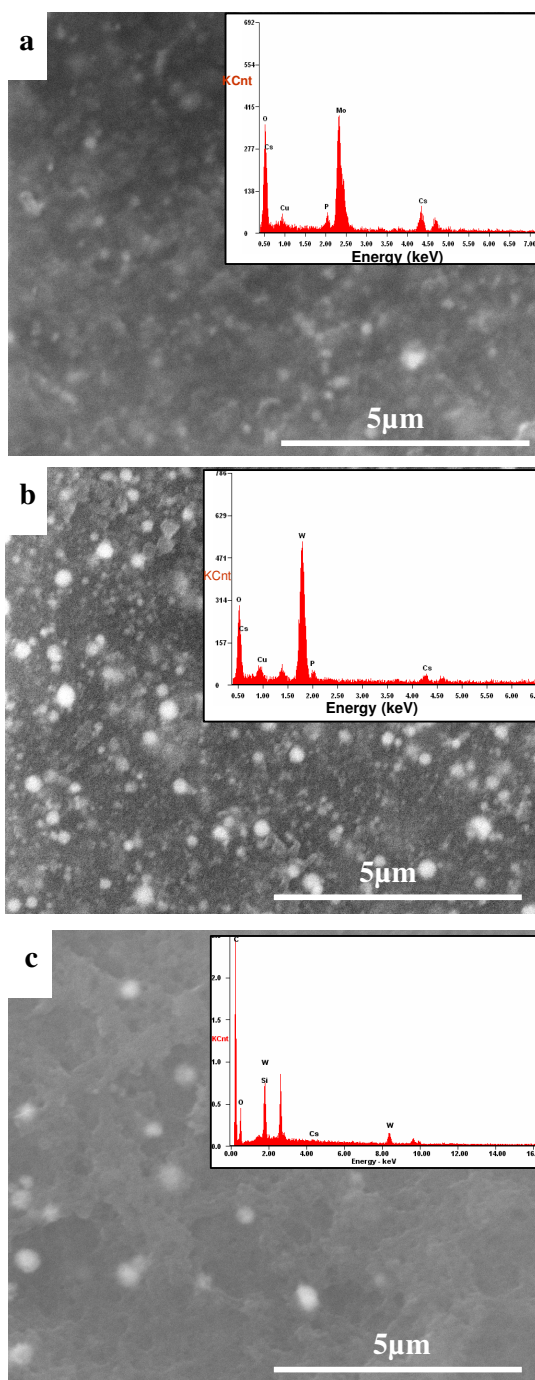


Fig. 6.5 Scanning electron micrographs (SEM) of the surfaces of hybrid membranes incorporated with different heteropoly acids. (a) PVA-PAN-CsPMA-Glu (b) PVA-PAN-CsPWA-Glu (c) PVA-PAN-CsSWA-Glu. The insert spectra represent the corresponding energy-dispersive X-ray analysis (EDXA) spectroscopy traces confirming the presence of finely dispersed heteropoly acids.

6.3.5 Water uptake, swelling and ion-exchange capacity (IEC)

After the physico-chemical characterization and morphological studies of the prepared three hybrid materials, they were examined for their suitability to function as a membrane material for direct methanol fuel cells. In this direction, the required key properties such as water uptake, swelling behavior and ion-exchange capacity (IEC) of these materials were tested. The presence of water in the membrane greatly influences the transport and other diffusive properties of the membrane. The water uptake and ion exchange capacity (IEC) play important roles in influencing conductivity property of the membranes. In Table 6.2, the data obtained from water uptake, swelling and ion exchange capacity studies of these materials are given. The extent of water uptake of PMA containing hybrid membrane was found to be higher compared to other hybrid membranes with PWA or SWA. At the room temperature (RT), the extents of swelling of all the fabricated hybrid membranes were found to be less compared to the commercial Nafion[®] 115 membrane, while they maintained higher water uptake due to the presence of hydrophilic property of the heteropoly acid materials. The extent of swelling characteristic of the fabricated PVA based hybrid membrane was decreased appreciably due to the interpenetrating network that was formed in presence of PAN and glutaraldehyde. Ion exchange capacity of the hybrid membranes was less compared to that of the commercial Nafion[®] 115 polymer electrolyte membrane due to their inherent chemical compositions.

Table 6.2 Water uptake, swelling and ion-exchange capacity (IEC) values for different hybrid membranes.

Membrane	Thickness (μm)	Water uptake (%)	Swelling (%)	IEC (meq g^{-1})
Nafion [®] 115	125	22	12	0.9
PVA-PAN-CsPMA-Glu	300 ± 20	46	4	0.61
PVA-PAN-CsPWA-Glu	300 ± 20	34	3.6	0.7
PVA-PAN-CsSWA-Glu	300 ± 20	30	2.4	0.74

6.3.6 Oxidative stability

Under fuel cell operating conditions, the degradation of the polymer electrolyte is caused by $\text{HO}\bullet$ and $\text{HOO}\bullet$ radicals (Hübner and Roduner, 1999). These radicals are formed due to the incomplete reduction of diffused oxygen at the anode. Hence, the oxidative stability of hybrid membranes was evaluated at room temperature in Fenton's reagent in order to simulate the fuel cell operating conditions. For comparison, pure PVA and PVA-PAN blends without heteropoly acid with different blend density were also studied. In an hour, pure PVA membrane is completely dissolved at room temperature under oxidative treatment. PVA-PAN blends without heteropoly acid were stable until 2h at room temperature, but they then loose their mechanical strength within that time. Figure 6.6 shows the results of oxidative stability of prepared membranes soaked in Fenton's reagent at room temperature.

Oxidative stability test carried out at room temperature indicates that all three fabricated hybrid membrane materials exhibited improved stability. Initially, there was a steep increment in membrane weight and it attained a stable value and remained unchanged until 150 h. After 150 h, the weight of all these three membranes started

decreasing to different extents. Hence the durability time of the hybrid membranes can be defined as the lasting time till the raising weight achieves a peak value (Fu *et al.* 2008) and in these cases it is 150 h. It has to be mentioned that even after 250 h these membranes were mechanically stable. The improvement in oxidative stability of the hybrid membrane compared to its constituting components is due to its dense structure which restricts the diffusion of the radicals in to the membrane.

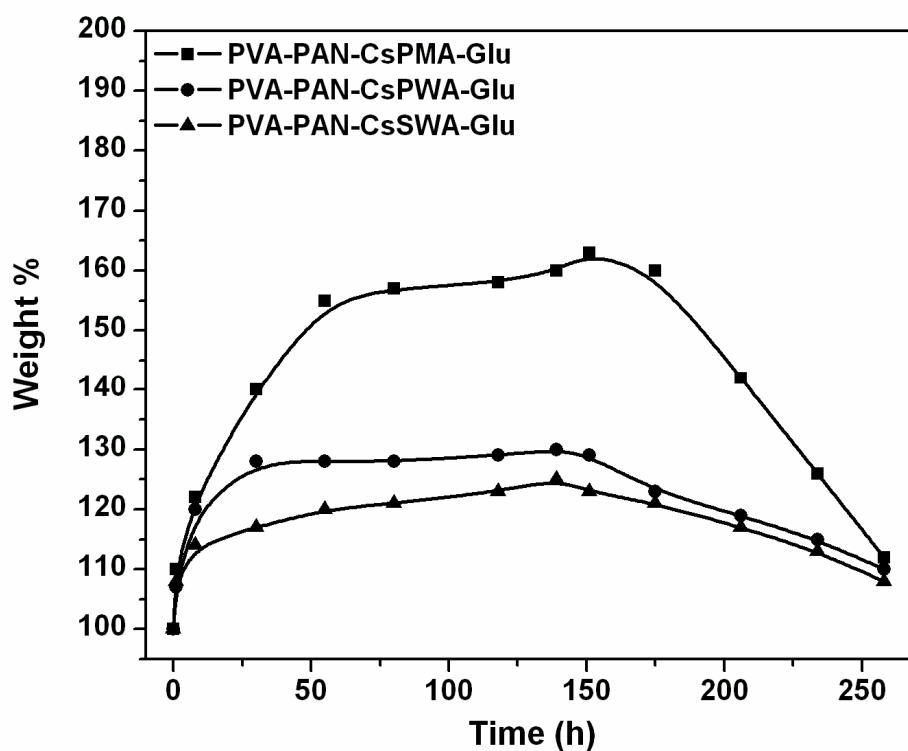


Fig. 6.6 Oxidative stability of fabricated membranes immersed in Fenton's reagent at room temperature at various time intervals.

6.3.7 Additive stability

A common, critical problem associated with the hybrid polymer electrolyte membranes is leaching out of the inorganic additive from the polymer matrix which might lead to the performance loss and/or system operational failures in a real fuel cell mode. Hence, in order to establish the stability features of these membrane materials, morphological characteristics of these membranes were tested at different time intervals for the duration of five days by immersing the membranes in water using FT-IR technique. Figures 6.7(a-c) show the FT-IR spectra of hybrid membranes containing various salts of heteropoly acid. Characteristic bands of Keggin ion was observed between 1100 and 700 cm^{-1} . All the spectra confirm the presence of primary Keggin structure establishing the presence of salts of heteropoly acid in the hybrid membrane even after immersing them in water continually for several days. These spectra remained similar even after 136 h with slight decrease in absorption intensity representing a negligible amount of loss of salts of heteropoly acid and this might be due to vigorous stirring conditions. These results help one to ascertain the stability of Cs salts of heteropoly acids in the PVA-PAN matrix.

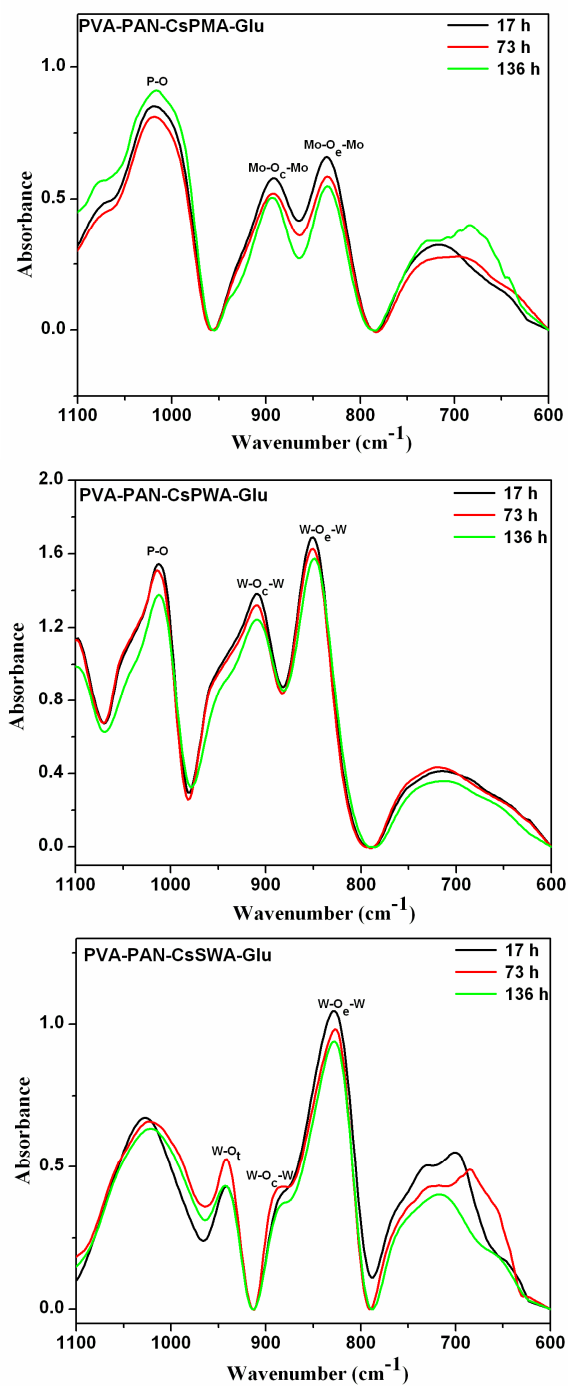


Fig. 6.7 FT-IR spectra of hybrid membranes (a) PVA-PAN-CsPMA-Glu (b) PVA-PAN-CsPWA-Glu (c) PVA-PAN-CsSWA-Glu placed in water at different time intervals.

6.3.8 Proton conductivity study

Figure 6.8 shows the proton conductivity of the fabricated hybrid membranes measured at varying temperatures ranging from 30 to 80 °C. Among the hybrid membranes studied, cesium salt of PMA substituted hybrid membranes exhibited higher conductivity compared to cesium salts of PWA and SWA substituted systems. In particular, PVA-PAN-CsPMA-Glu membrane exhibited the highest proton conductivity in the range of 10^{-1} S cm⁻¹ at 50 % RH surpassing the state of the art Nafion[®] 115 measured at 100 % RH. The order of proton conductivities of the hybrid membranes is in accordance with the water uptake ability of the materials (Table 6.2).

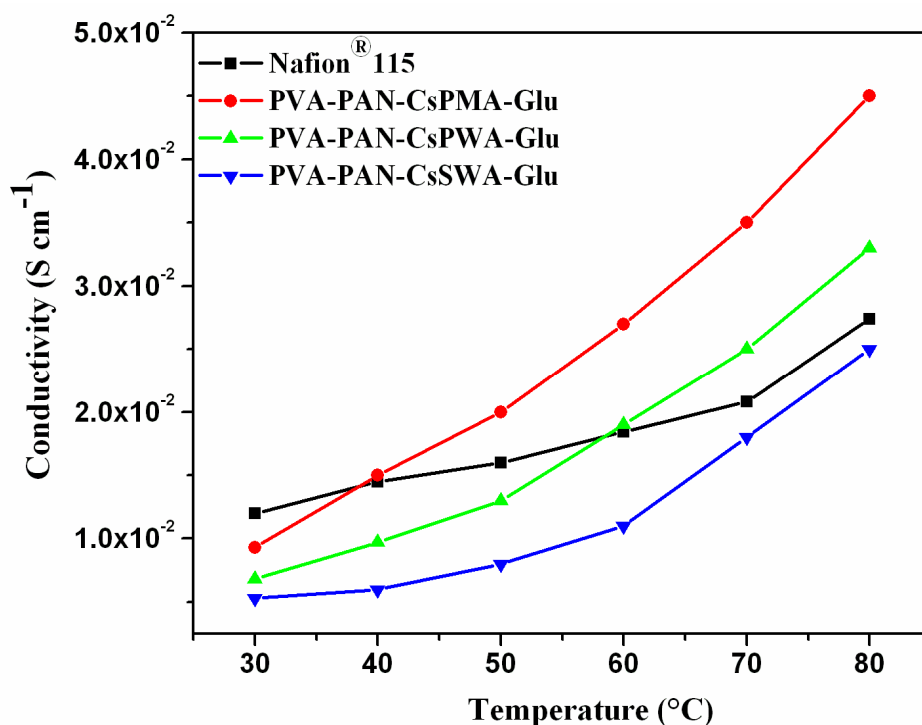


Fig. 6.8 Proton conductivities of the fabricated hybrid membranes and Nafion[®] 115 membrane at different temperatures.

6.3.9 Methanol crossover study

The concentration of permeated methanol through the hybrid membrane materials such as PVA-PAN-CsPMA-Glu, PVA-PAN-CsPWA-Glu and PVA-PAN-CsSWA-Glu as a function of crossover time has been measured by employing cyclic voltammetric technique and by using a two compartment cell which was divided by housing the corresponding membrane test material. The results of methanol cross over studies are presented in Fig. 6.9. The rate of crossed over methanol appeared to vary with the variation in incorporated heteropoly acid material in the hybrid membranes. Hybrid membrane containing silicotungstic acid, SWA as an active component exhibited lower rate of methanol crossover compared to heteropoly acid materials such as phosphotungstic acid, PWA or phosphomolybdic acid, PMA containing hybrid membranes. The concentration of crossed methanol in PVA-PAN-CsSWA-Glu hybrid membranes after 180 min was two fold lesser than that of PVA-PAN-CsPWA-Glu and three times lower than that of PVA-PAN-CsPMA-Glu system. Methanol permeability of the respective membranes was determined from the slope of the plots representing the crossed methanol concentration versus time (Fig. 6.9). Figure 6.10 shows the quantitative representation of methanol permeability capacities of the hybrid membranes and the results were compared with that of commercial Nafion[®] 115 membrane. Methanol permeability is an order of magnitude less for the fabricated hybrid membranes compared to Nafion[®] 115. This may be due to the dense interpenetrating network that was formed due to the blending of PVA with PAN followed by cross-linking with glutaraldehyde.

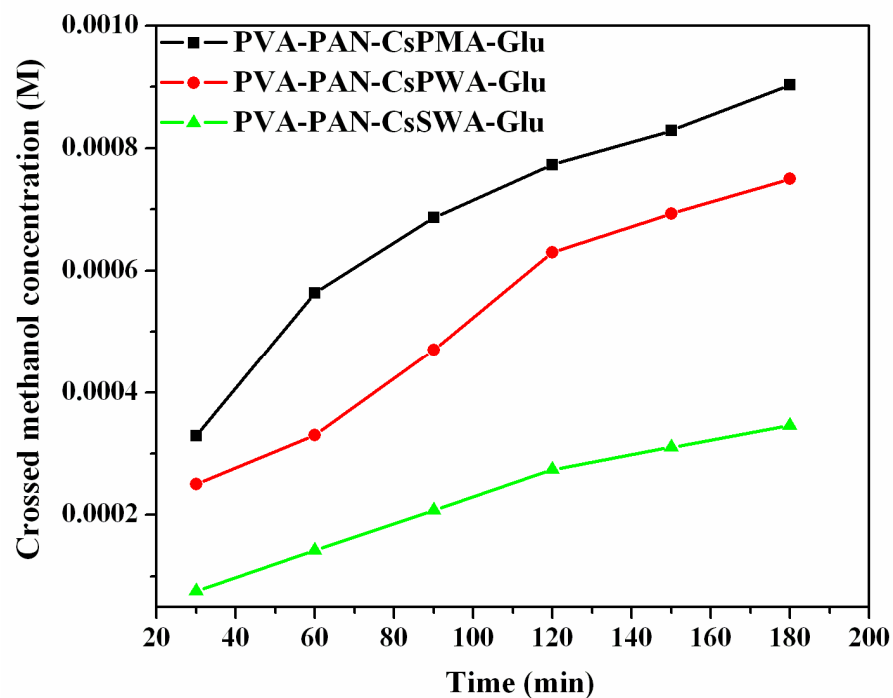


Fig. 6.9 Concentration of crossed over methanol as a function of crossover time.

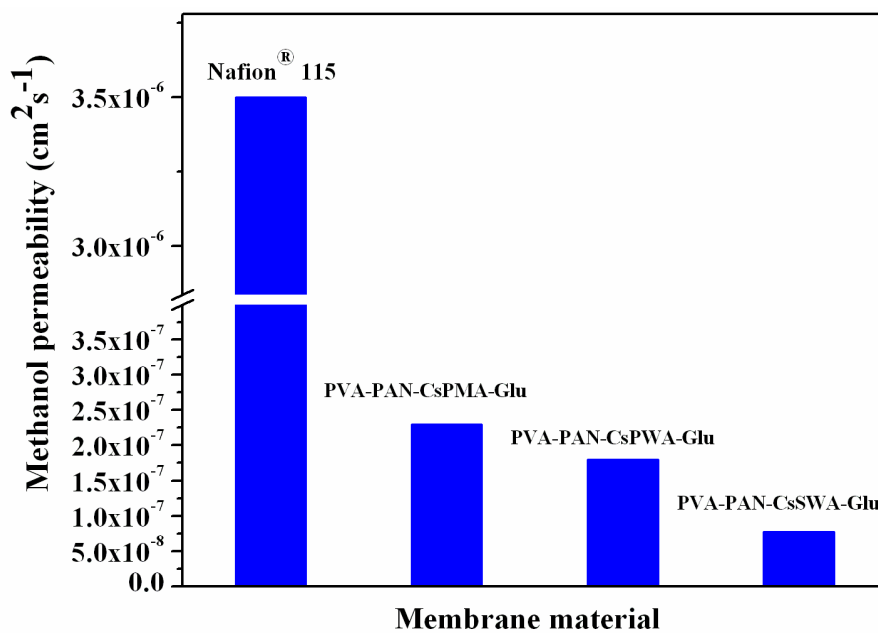


Fig. 6.10 Methanol permeability of fabricated hybrid membranes compared with that of Nafion® 115.

The increasing order of methanol permeability characteristic of the membrane materials can be given as: PVA-PAN-CsSWA-Glu < PVA-PAN-CsPWA-Glu < PVA-PAN-CsPMA-Glu << Nafion[®] 115 (Fig. 6.10). The reduced methanol permeation in the hybrid membranes compared to Nafion[®] 115 membrane is considered as an attractive characteristics for their employment in DMFC applications and this property can be attributed to the methanol absorption ability of the heteropoly acids that were incorporated into the polymer matrix of PVA-PAN blend. Heteropoly acids possess a unique conceptual character called 'Pseudoliquid phase behavior' in which the polar molecules like methanol can be readily absorbed into the solid matrix (Misono, 1987). Hence the fabricated heteropoly acid containing hybrid membranes exhibit the capacity to retain methanol without letting it to pass by. The methanol permeability values of the membrane materials were consistent with those of acid strengths of the corresponding materials that were reflected in IEC measurements (Table 6.2). As reported in literature (Okuhara *et al.* 1989; Misono *et al.* 1982; Shikata *et al.* 1995), the acid strength governs the amount of methanol adsorbed on to the heteropoly acid. The number of methanol molecules adsorbed per anion is approximated to integral number of protons in the heteropoly molecule (Okuhara *et al.* 1989; Bielanski *et al.* 1999; Małecka *et al.* 1999). The order of methanol adsorption per Keggin unit was reported to be as follows: $\text{SiW}_{12}\text{O}_{40}^{4-} > \text{PW}_{12}\text{O}_{40}^{3-} > \text{PMo}_{12}\text{O}_{40}^{3-}$ (Okuhara *et al.* 1989; Małecka *et al.* 1999; Bielański *et al.* 2005; Rykova *et al.* 2003; Antonucci *et al.* 2006) which has been clearly reflected in the results presented on permeability studies showing the same trend. Compared to Nafion[®] 115 membrane, other commercial membranes as well as related hybrid membranes, the fabricated hybrid membranes in this study exhibit excellent tolerance to methanol permeability

with appreciable proton conductivity as can be seen from the values given in Table 6.3.

Table 6.3 Comparison of proton conductivity and methanol permeability values for various membranes (Extension of Table 5.3).

Membrane Materials	RH (%)	Temperature (°C)	Conductivity (S cm ⁻¹)	Permeability (cm ² s ⁻¹)	References
PVA-PAN-CsSWA-Glu	50	RT	5.3×10^{-3}	7.8×10^{-8}	Obtained from our studies
PVA-PAN-CsPWA-Glu	50	RT	6.8×10^{-3}	1.8×10^{-7}	Obtained from our studies
PVA-PAN-CsPMA-Glu	50	RT	9.3×10^{-3}	2.3×10^{-7}	Obtained from our studies
PVA-ZrP-SWA	60	60	10^{-2}	6×10^{-7}	Chapter 3
PVA-ZrP-Cs ₁ SWA	50	100	0.013	2×10^{-6}	Chapter 4
PVA-ZrP-Cs ₂ SWA	50	100	0.02	3×10^{-6}	Chapter 4
Nafion [®] 115	100	90	0.03	3.5×10^{-6}	Obtained from our studies
CRA-08 ^a	-	60	45×10^{-3}	0.58×10^{-6}	Antonucci <i>et al.</i> 2006 ; Amara and Kerdjoudj, 2003
IonClad [®] R1010 ^b	-	60	146×10^{-3}	0.6×10^{-6}	Scott <i>et al.</i> 2000 ; Tricoli <i>et al.</i> 2000
SPEEK (SD=87 %)	-	60	13×10^{-3}	17.5×10^{-7}	Li <i>et al.</i> 2003; Silva <i>et al.</i> 2006; Fu <i>et al.</i> 2007
PVA/PWA/SiO ₂	-	-	0.004-0.017	10^{-7} to 10^{-8}	Xu <i>et al.</i> 2004
PEG/SiO ₂ /SWA	100	80	0.01	10^{-5} to 10^{-6}	Vernon <i>et al.</i> 2005
PEG/SiO ₂ /PWA	-	-	10^{-5} to 10^{-3}	10^{-6} to 10^{-7}	Lin <i>et al.</i> 2005
SPEEK/PWA	100	100	1.7×10^{-2}	-	Ponce <i>et al.</i> 2003

^a - Polyethylene-Tetra-fluoroethylene with sulphonyls in divinyl benzene matrix

^b - Tetra-fluoroethylene with poly(styrene sulfonic acid)

6.4. CONCLUSIONS

This piece of research involves the preparation of poly(vinyl alcohol) based hybrid membranes with key properties desired for DMFC applications such as low methanol crossover, appreciable low swelling and with comparable proton conductivity (10^{-1} to $10^{-3} \text{ S cm}^{-1}$ at 50 % RH) compared to state of the art polymer electrolyte membranes. Hybrid polymer electrolyte membranes were fabricated through blending of poly(vinyl alcohol) (PVA) - polyacrylonitrile (PAN) and by cross-linking with glutaraldehyde (Glu). Cesium salt of different heteropoly acids such as phosphomolybdic acid (PMA), phosphotungstic acid (PWA) and silicotungstic acid (SWA) were incorporated into the polymer network to form hybrid membrane materials namely PVA-PAN-CsPMA-Glu, PVA-PAN-CsPWA-Glu and PVA-PAN-CsSWA-Glu respectively. The interpenetrating network formed by the blending of PVA with PAN lead to an order of decrease in methanol crossover compared to the state of the art Nafion[®] 115 membrane employed for DMFC applications. The hybrid membrane containing cesium salt of SWA exhibited very low methanol permeability ($7.8 \times 10^{-8} \text{ cm}^2 \text{ s}^{-1}$) compared to other membranes containing cesium salt of heteropoly acids such as PMA and PWA. The difference in methanol permeability between the fabricated hybrid membranes containing different cesium salt of heteropoly acids is found to be governed by the methanol adsorption ability of the respective heteropoly acids. The fabricated hybrid membranes have the potential advantage to act as an electrolyte membrane for direct methanol fuel cell (DMFC) applications due to their lower methanol permeability property which is a major difficulty encountered with Nafion[®] membrane in DMFCs.

CHAPTER 7

EFFECT OF BLEND DENSITY ON THE PROPERTIES OF POLY(VINYL ALCOHOL) (PVA) - POLYACRYLONITRILE (PAN) MATRIX WITH CESIUM SALTS OF HETEROPOLY ACIDS INVESTIGATED AS ELECTROLYTES FOR DMFC APPLICATION

7.1 INTRODUCTION

Despite several favorable characteristics of poly(vinyl alcohol) (PVA) to act as a suitable membrane material for fuel cell application (section 6.1), membranes made of pure PVA are found to be quite fragile, especially in the dry state. In addition, due to strong hydrophilic characteristics, PVA membranes are readily swollen by aqueous solutions, and can even be dissolved in aqueous solutions at elevated temperatures. Membrane swelling becomes a critical issue of concern in fuel cell application as it can cause low dimensional stability, diffusion of reactants and destroy the adhesion between the electrode and the membrane. However, PVA can be crosslinked (Qiao *et al.* 2005; Lin *et al.* 2007), co-polymerized (Anis *et al.* 2008), or blended (Swier *et al.* 2005; Smitha *et al.* 2005; Chang *et al.* 2007; Sahu *et al.* 2008) to produce a range of new materials with improved properties.

Blending and cross-linking has shown to be an effective approach to suppress excessive swelling of membranes and often accompanied with a reduction in the permeation flux. Membrane blending and cross-linking will also help to improve the physical properties of the membrane like thermal and mechanical stabilities. Physical and chemical properties of the resultant blend are considered to have the potential features of combining the characteristics of each blend component. From our previous study, blending PVA and PAN followed by cross-linking with

gluteraldehyde (Glu) showed to be an alternate strategy to improve dimensional stability and to reduce methanol crossover property (Chapter 6). This is due to the interaction between the polymers leading to an interpenetrating network. This interaction stabilizes the incorporated cesium salt of heteropoly acid and improves the compatibility of the components of the hybrid.

In the present study, a set of hybrid membranes with different blend ratio of PVA to PAN weight percent were fabricated and their properties were examined for their possible employment in direct methanol fuel cell application. Cesium salt of different heteropoly acids such as phosphomolybdic acid (PMA), phosphotungstic acid (PWA) and silicotungstic acid (SWA) were incorporated into the polymer network as proton conducting additives to form hybrid membrane materials. The objective of this piece of research is to systematically examine the effect of blend density on the membrane performance including water uptake, methanol uptake, swelling, proton conductivity and methanol permeability. The physiochemical properties such as chemical interactions between the hybrid components, structure morphology and thermal stability were investigated.

7.2 EXPERIMENTAL

7.2.1 Fabrication of hybrid membranes

The hybrid membranes were fabricated by following the procedure as described in section 6.2.1. Different blend densities of the polymer matrix were prepared by changing the weight percent of PVA (90, 80 & 70 wt %) and PAN (10, 20 & 30 wt %) to form hybrid membranes namely, PVA(90-70)-PAN(10-30)-CsPMA-Glu, PVA(90-70)-PAN(10-30)-CsPWA-Glu and PVA(90-70)-PAN(10-30)-CsSWA-Glu respectively. The weight percent of phosphomolybdic acid (PMA), phosphotungstic acid (PWA) or silicotungstic acid (SWA) in the hybrid membrane was maintained as

10.0 in each case. The obtained dry membranes were cross-linked with glutaraldehyde for 30 min at room temperature.

7.3 MEMBRANE CHARACTERIZATION

The hybrid membranes made with poly(vinyl alcohol) (PVA)-polyacrylonitrile (PAN) polymer with different blend density by incorporating cesium salt of different heteropoly acids such as phosphomolybdic acid (PMA), phosphotungstic acid (PWA) or silicotungstic acid (SWA) as described in the experimental section was subjected to extensive characterization using various physico-chemical techniques such as FT-IR, XRD, TGA and SEM-EDXA.

7.3.1 Fourier transformed infrared (FT-IR) spectral studies

Figure 7.1(a-c), shows the Fourier transformed infrared (FT-IR) spectra of various hybrid membrane materials with different heteropoly acids and with different blend density. For comparison the FT-IR spectra for individual components considered under this study are also presented Fig. 7.1d. As can be seen, the broad band at 3580 cm^{-1} observed in all hybrid membranes is attributed to the O–H stretching band for hydrogen-bonded alcohol. There is no appreciable difference in the FT-IR spectra of the hybrid membrane materials obtained through varying blend density. The band at 2245 cm^{-1} corresponding to $\text{C}\equiv\text{N}$ stretching of PAN has small intensity in the hybrid membrane. Also, C–N stretching observed at 1250 cm^{-1} is overlapped with C–O stretching of PVA. Hence the variation in PVA to PAN weight percent in the hybrid matrix is not observed in the respective FT-IR spectra. The characteristic bands of PVA, PAN and cesium salts of different heteropoly acids were observed for the hybrid membranes with different blend density (Figure 7.1(a-c)). The main bands are assigned and tabulated separately for the fabricated hybrid membranes in Table 7.1.

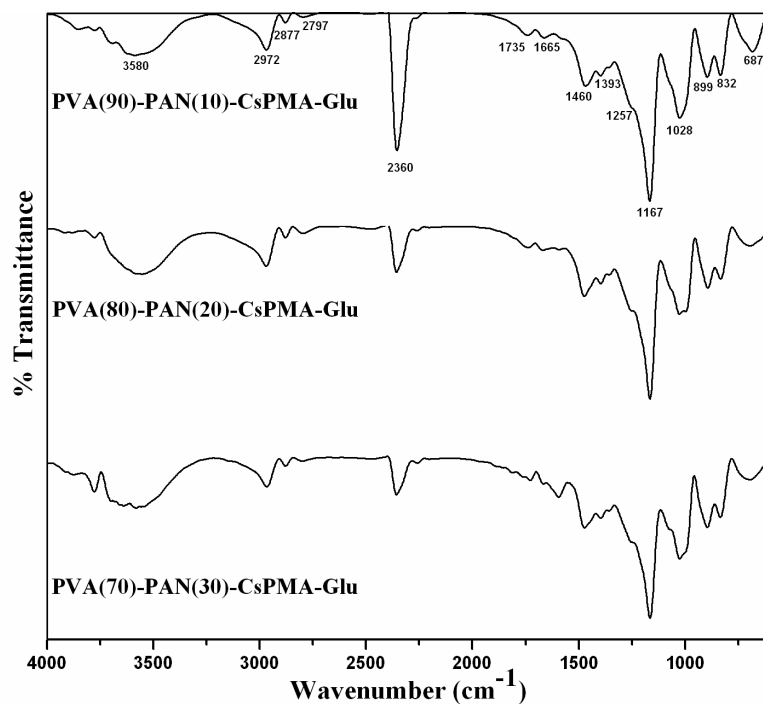


Fig. 7.1a FT-IR spectra of hybrid membranes fabricated with different blend density: Cross-linked PVA-PAN blends by glutaraldehyde with cesium salt of phosphomolybdic acid (PMA).

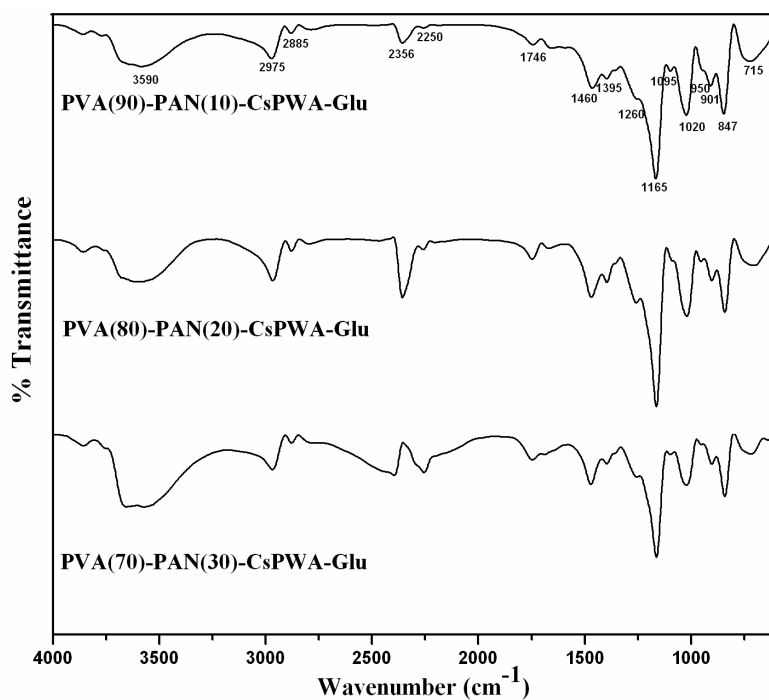


Fig. 7.1b FT-IR spectra of hybrid membranes fabricated with different blend density: Cross-linked PVA-PAN blends by glutaraldehyde with cesium salt of phosphotungstic acid (PWA).

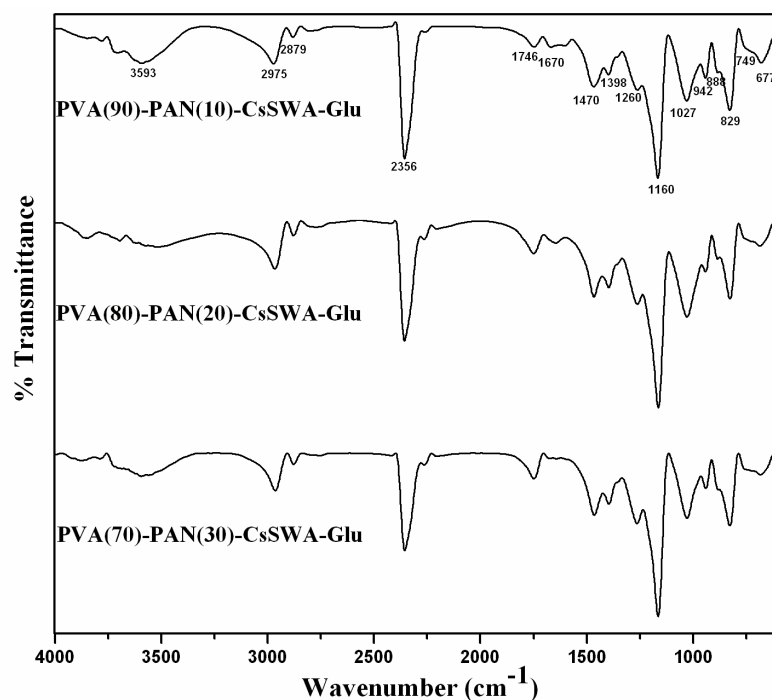


Fig. 7.1c FT-IR spectra of hybrid membranes fabricated with different blend density: Cross-linked PVA-PAN blends by glutaraldehyde with cesium salt of silicotungstic acid (SWA).

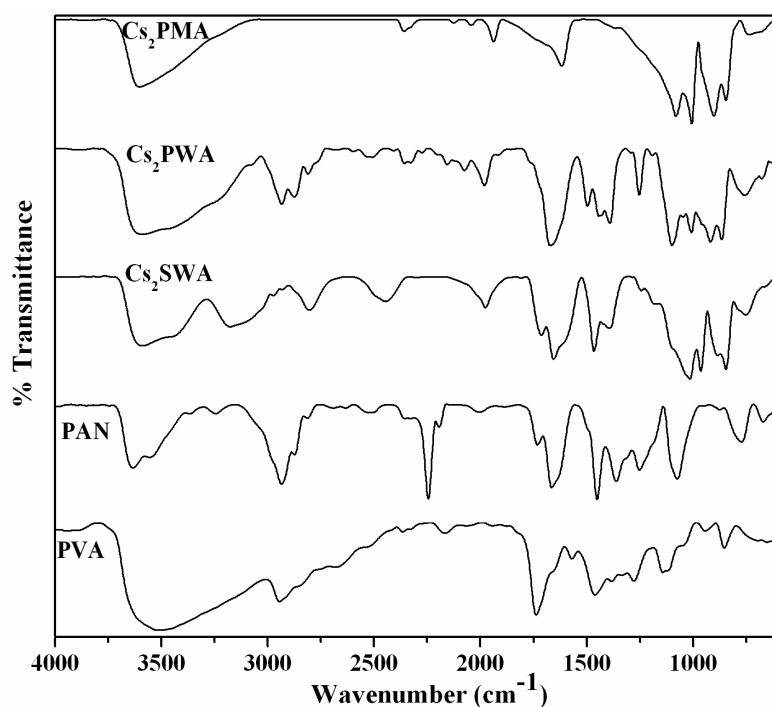


Fig. 7.1d FT-IR spectra of the individual components constituting the hybrid membranes.

Table 7.1 Assignments of main absorption bands of fabricated hybrid membranes fabricated with different blend density.

Vibration frequency (cm ⁻¹)			Bond assignment
PVA-PAN-CsPMA-Glu	PVA-PAN-CsPWA-Glu	PVA-PAN-CsSWA-Glu	
687	-	677	C-H bending
-	715	-	CH ₂ rocking
832	847	829	M-O _e -M stretching
899	901	888	M-O _e -M stretching
-	950	942	M-O _t stretching
1027			X-O stretching
1165			C-O stretching
1250			C-N stretching
1390			C-O-H bending
1460			-CH ₂ bending
1660			N-H bending
1740			Aldehyde C=O stretching
2245			-C≡N stretching
2875			-CH ₃ stretching
2970			-CH ₂ stretching
3580			-OH stretching

7.3.2 X-ray diffraction (XRD) analysis

X-ray diffraction (XRD) profiles of hybrid membranes incorporated with different heteropoly acids and with different blend densities are presented in Fig. 7.2(a-c). For comparison, the XRD patterns of PVA, PAN and respective salts of heteropoly acid are also given. The peak found at $2\theta = 20^\circ$ corresponds to the (1 0 1) plane of

PVA in all hybrid membranes (Koji *et al.* 1999). PAN is a ladder polymer with a peak at $2\theta = 17^\circ$ and a small amount of amorphous portion can be seen around $2\theta = 21^\circ$. The XRD profiles of both PVA and PAN represent the semi-crystalline nature. Peaks characteristic of cesium salt of PMA and PWA appear in the hybrid membranes containing respective salts of heteropoly acids and with different blend density. No diffraction peaks characteristic of cesium salt of SWA appears in the hybrid membranes containing of SWA. This might be due to the higher coordination of SWA than other HPAs leading to a fine dispersion in the polymer matrix compared to PMA and PWA and the hybrid behaves as X-ray amorphous. After the hybrid formation, the crystallinity of host polymers decreased as the polymer chains undergo local segmental motion (Kumar *et al.* 2009). The interaction between polymers and with that of salts of heteropoly acids lead to chain re-organization and thus facilitating free ionic mobility.

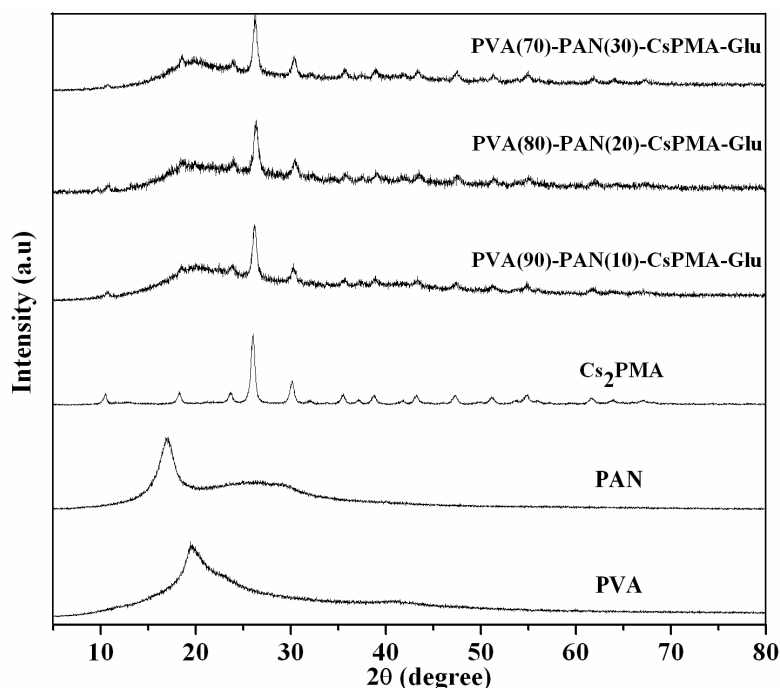


Fig. 7.2a XRD patterns of the PVA-PAN hybrid membranes of different blend density with cesium salt of phosphomolybdic acid (PMA) and its components.

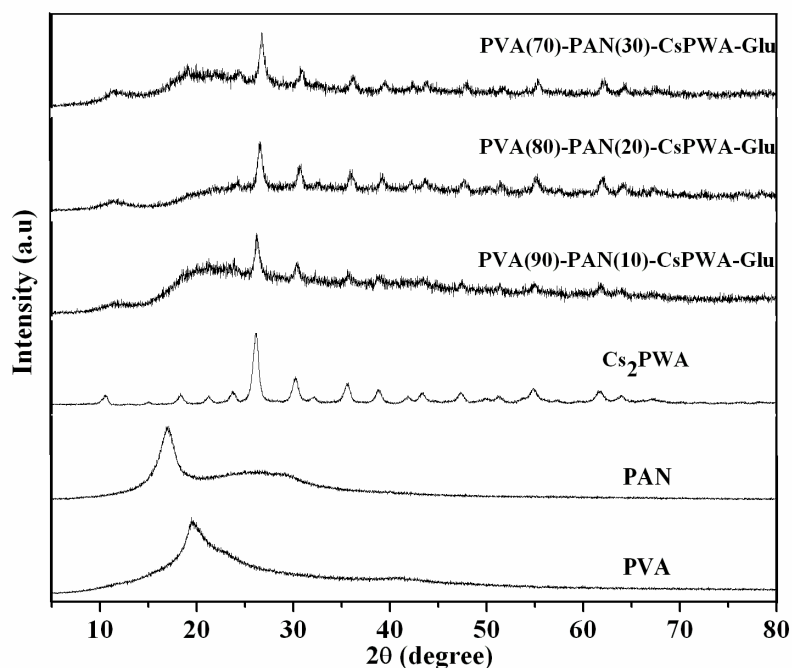


Fig. 7.2b XRD patterns of the PVA-PAN hybrid membranes of different blend density with cesium salt of phosphotungstic acid (PWA) and its components.

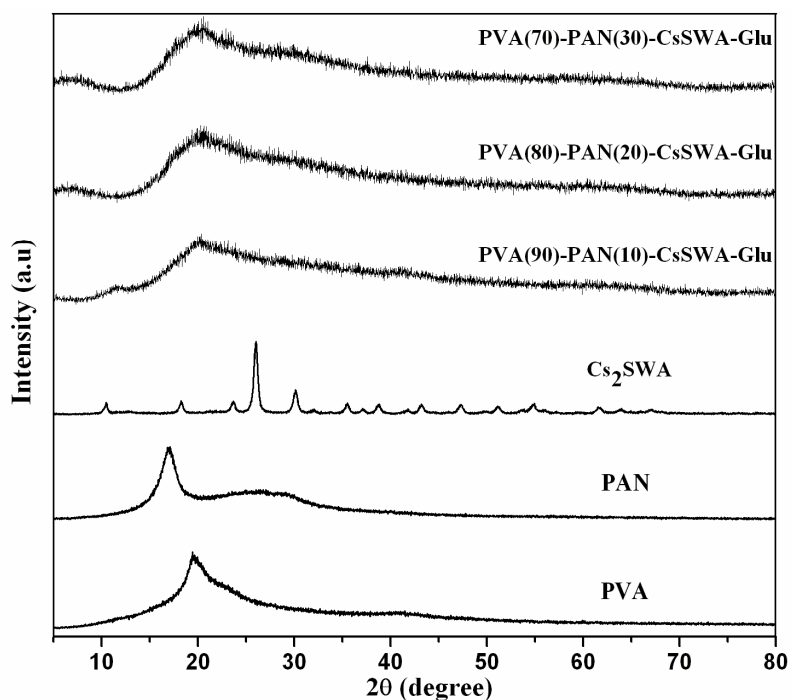


Fig. 7.2c XRD patterns of the PVA-PAN hybrid membranes of different blend density with cesium salt of silicotungstic acid (SWA) and its components.

7.3.3 Thermogravimetric (TGA) studies

The thermal stability of the hybrid membranes with different blend density was studied by using thermogravimetric analysis. In Fig. 7.3(a-c), the traces of thermogravimetric analysis (TGA) of the hybrid membranes have been shown in the temperature range from 40 °C to 800 °C. The TGA curves of the hybrid membranes reveal four main weight loss regions as described in section 6.3.3. The first weight loss observed in the region 100-200 °C was not affected by the change in blend density that has been attributed to the loss of absorbed water molecules. Further degradation steps are influenced by the change in blend density. The weight loss due to the degradation of polymer matrix starts at 200 °C, and proved independent of blend density. With increase in blend density, the polymer matrix is stabilized and complete oxidation of the polymer matrix occurred at higher temperatures. The influence of blend density is observed in the temperature between 200 °C –700 °C corresponding to second, third and fourth weight loss regions. All the hybrid materials irrespective of different blend density and components exhibit similar thermal behavior showing that they all have similar structural characteristics and are stable up to 200 °C.

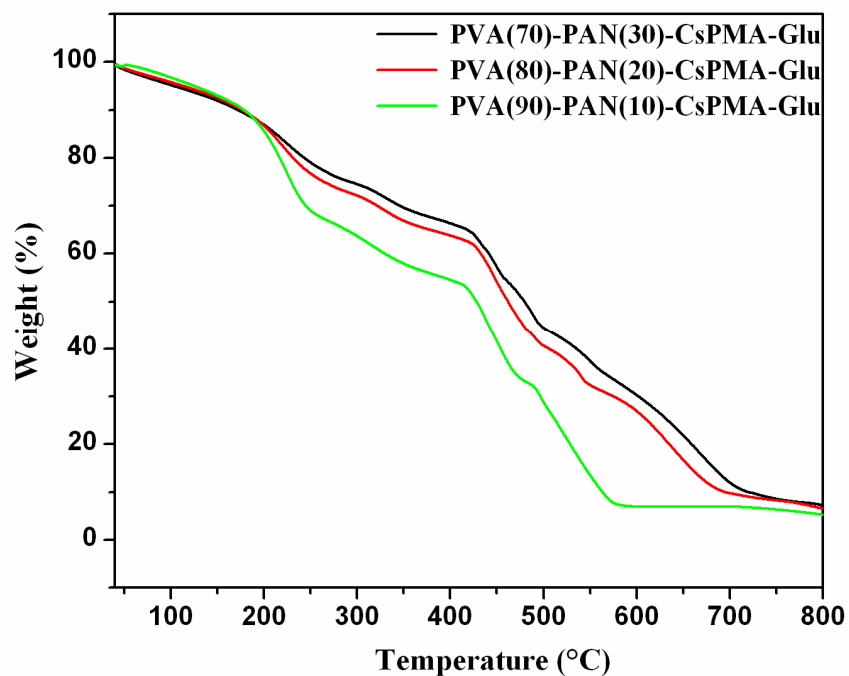


Fig. 7.3a Thermogravimetric analysis (TGA) traces of (a) PVA-PAN-CsPMA-Glu with different blend density in the temperature region 40 to 800 °C.

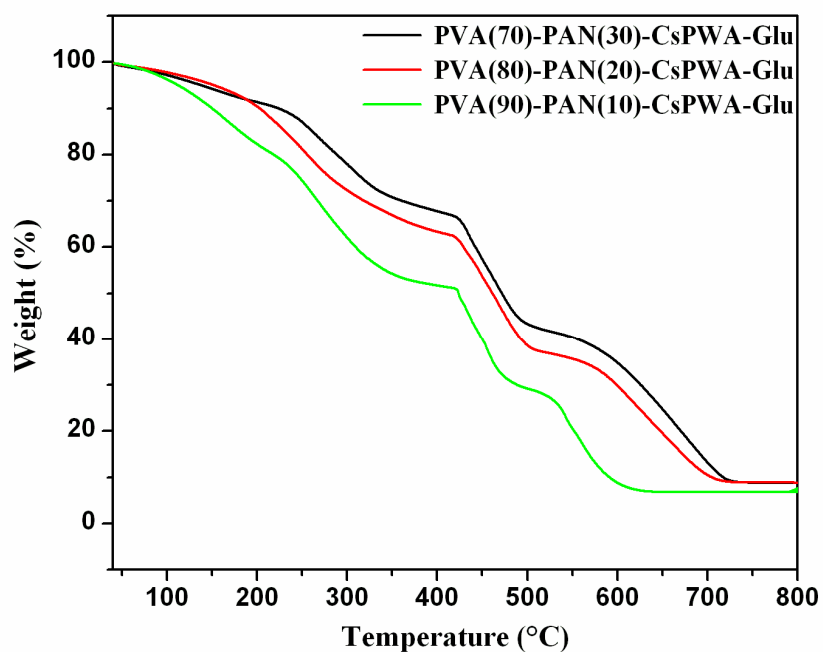


Fig. 7.3b Thermogravimetric analysis (TGA) traces of (a) PVA-PAN-CsPWA-Glu with different blend density in the temperature region 40 to 800 °C.

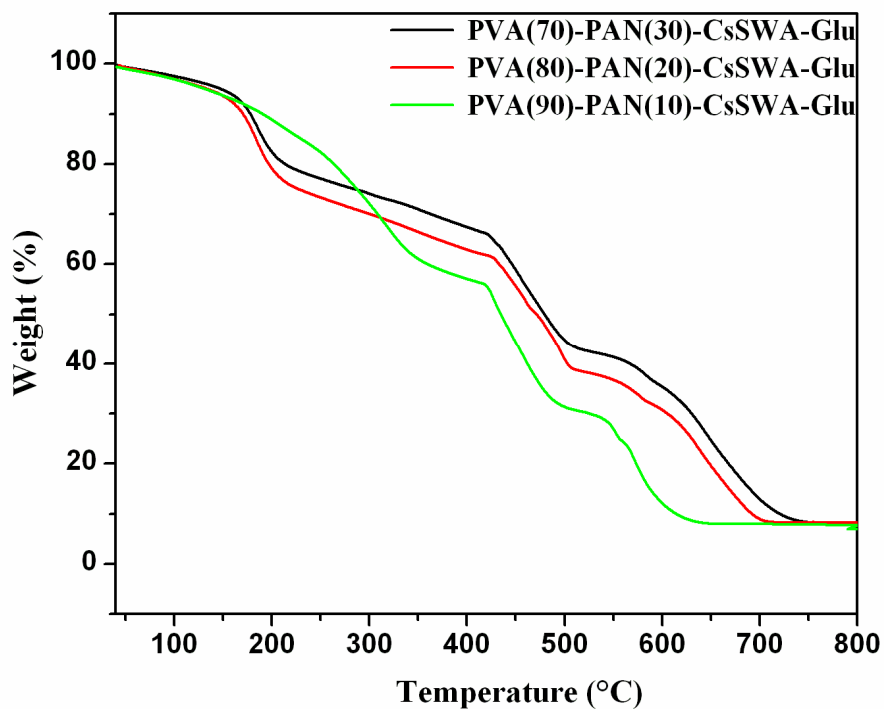


Fig. 7.3c Thermogravimetric analysis (TGA) traces of (a) PVA-PAN-CsSWA-Glu with different blend density in the temperature region 40 to 800 °C.

7.3.4 Scanning electron microscopy interfaced with EDXA

The surface morphological characteristics of the hybrid membranes with different blend density, in their dry state were examined by using a scanning electron microscopy (SEM) and the micrographs are shown in Fig. 7.4(a-c). The cesium salts of different heteropoly acids are distributed throughout the blended polymer matrix. Increase in the blend density leads to improved interaction of heteropoly acid into the polymer matrix, resulting in fine dispersion. The average particle size of the heteropoly acid was around 50 nm and the presence of respective heteropoly acid was confirmed by using energy-dispersive X-ray analysis (EDXA) spectroscopy.

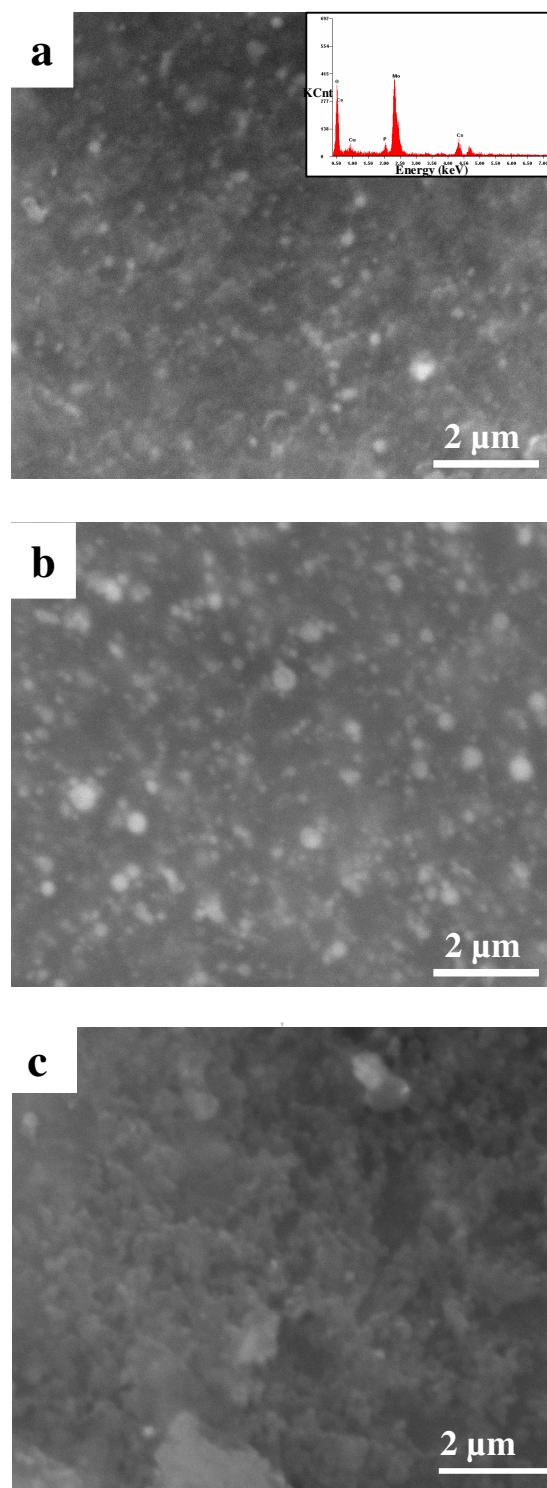


Fig. 7.4a Scanning electron micrographs (SEM) of the surfaces of the PVA-PAN hybrid membranes made of different blend density with cesium salt of phosphomolybdic acid (PMA). The insert spectra represent the corresponding energy-dispersive X-ray analysis (EDXA) traces confirming the presence of phosphomolybdic acid (PMA).

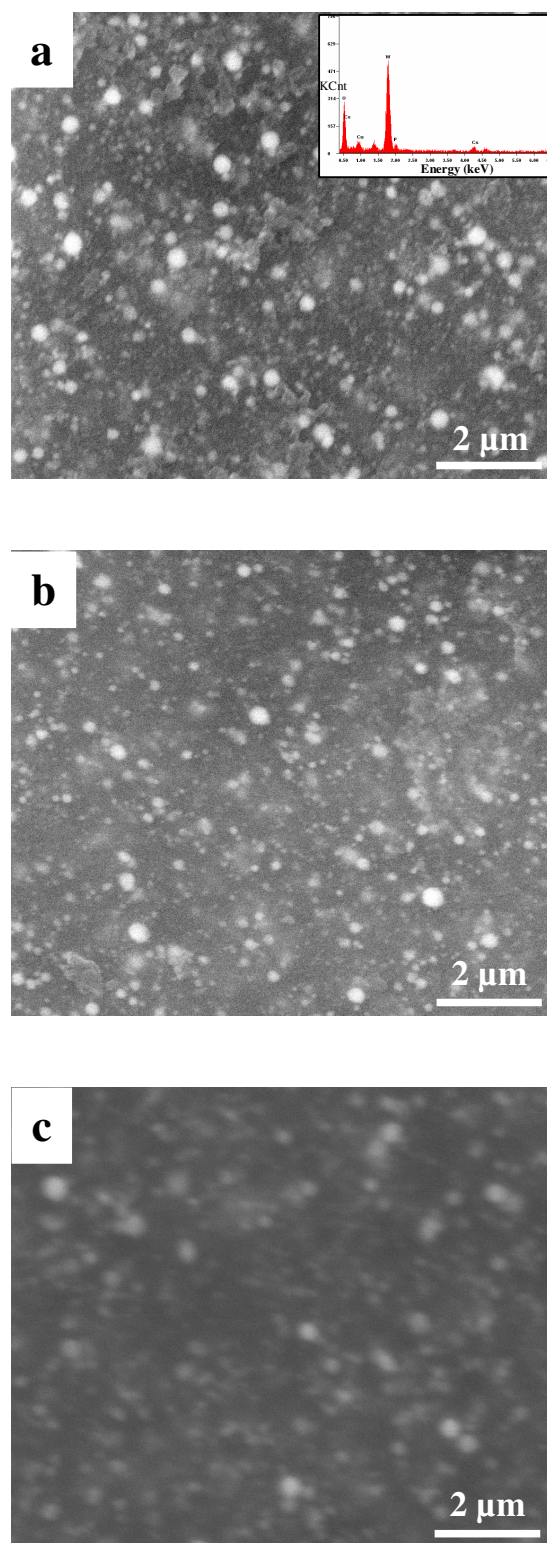


Fig. 7.4b Scanning electron micrographs (SEM) of the surfaces of the PVA-PAN hybrid membranes made of different blend density with cesium salt of phosphotungstic acid (PWA). The insert spectra represent the corresponding energy-dispersive X-ray analysis (EDXA) traces confirming the presence of phosphotungstic acid (PWA).

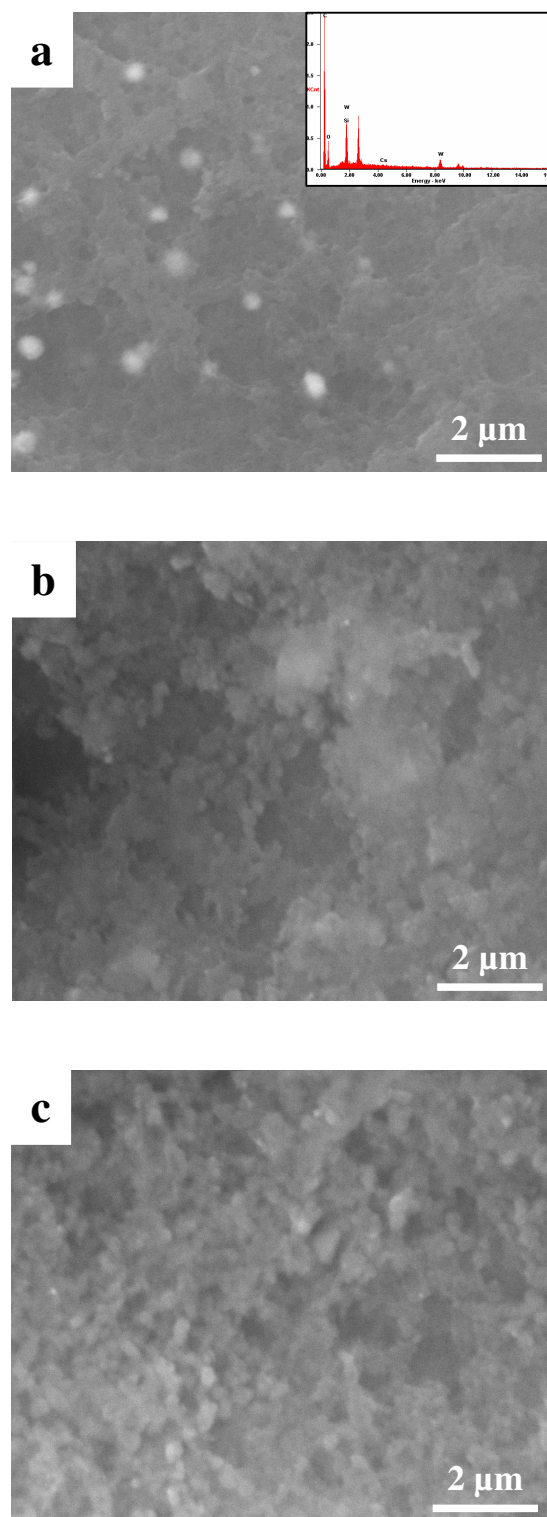


Fig. 7.4c Scanning electron micrographs (SEM) of the surfaces of the PVA-PAN hybrid membranes made of different blend density with cesium salt of silicotungstic acid (SWA). The insert spectra represent the corresponding energy-dispersive X-ray analysis (EDXA) traces confirming the presence of silicotungstic acid (SWA).

7.3.5 Water uptake, methanol uptake, swelling and ion-exchange capacity (IEC)

The prepared hybrid materials were examined for their suitability to function as membrane materials for direct methanol fuel cells. In this direction, the required key properties such as water uptake, methanol uptake, swelling behavior and ion-exchange capacity (IEC) of these materials were tested. An optimum amount of water in the polymer matrix is required to maintain the proton conductivity. Excessive water uptake will lead to low dimensional and mechanical stability and high methanol permeability. Maintaining optimum water uptake is crucial to ensure superior proton conductivity and simultaneously to eliminate stability issues.

In Table 7.2, the data obtained from water/methanol uptake, swelling and ion exchange capacity studies of the hybrid membranes with different blend density are given. Water uptake, swelling and ion exchange capacity were affected by the blend density of the polymer matrix (Table 7.2). An increase in blend density of the polymer matrix decreases the swelling, water uptake and ion exchange capacity. With increase in blend density, the size of the free volume could be restricted resulting in the lower swelling and water uptake.

The extent of methanol uptake of the fabricated membranes was measured and tabulated (Table 7.2). The hybrid membranes exhibited lower methanol uptake compared to Nafion[®] 115. Both water uptake and methanol uptake decreased with increase in polymer density. The water uptake of the hybrid membranes was much higher compared to methanol uptake indicating preferential water absorption over methanol.

Table 7.2 Water uptake, methanol uptake, swelling and ion-exchange capacity (IEC) values for different hybrid membranes compared with that of Nafion® 115.

Membrane	Water uptake (%)	Methanol uptake (%)	Swelling (%)	IEC (meq g ⁻¹)
Nafion® 115	22	80	12	0.9
PVA(90)-PAN(10)-CsPMA-Glu	46	5.7	4	0.61
PVA(80)-PAN(20)-CsPMA-Glu	30	4.2	2.4	0.59
PVA(70)-PAN(30)-CsPMA-Glu	21	2.2	2	0.55
PVA(90)-PAN(10)-CsPWA-Glu	34	6.5	3.6	0.7
PVA(80)-PAN(20)-CsPWA-Glu	27	4.9	2.2	0.65
PVA(70)-PAN(30)-CsPWA-Glu	18	3	1.7	0.62
PVA(90)-PAN(10)-CsSWA-Glu	30	8	2.4	0.74
PVA(80)-PAN(20)-CsSWA-Glu	25	6.5	2	0.7
PVA(70)-PAN(30)-CsSWA-Glu	16	4.6	1.3	0.7

7.3.6 Oxidative stability

For hybrid membranes treated at 70 °C in Fenton's reagent (Fig. 7.5a), the membrane weight initially increased and then decreased, which is similar to the results obtained by Chen *et al.* (2006). When the membrane is soaked into the oxidative solution, there exists two effects: one is swelling of the membrane, which leads to increase in wet membrane weight and the other is oxidative degradation of the polymer matrix due to the permeation of H₂O₂ leading to decrease in wet membrane weight. The two effects act simultaneously on the membrane matrix. Initially the rate of swelling predominates and hence we obtain a peak value Fig. 7.5a.

Hybrid membranes with PVA(80)-PAN(20) and PVA(90)-PAN(10) blend density were stable until 8 h and later it loses its mechanical strength and becomes fragile. Whereas, for hybrid membranes with PVA(70)-PAN(30) blend density exhibited improved oxidative stability compared to PVA(80)-PAN(20) and PVA(90)-PAN(10)

irrespective of incorporated heteropoly acid. The stability study of the membranes was conducted for the duration of 10 h. They were stable up to 10 h of immersion time. The hybrid membranes exhibited excellent stability over its components like, pure PVA and PVA-PAN blend without heteropoly acid and with different blend density. Individual components are stable only for an hour in Fenton's reagent. Since the stability measurement was carried out at a quite rigorous condition (70 °C) the membrane got softened at an early stage of 8 h.

Oxidative stability test carried out at room temperature (under mild condition) indicates that all three fabricated hybrid membrane materials exhibited significantly high stability (Fig. 7.5b). Initially there was a steep increment in membrane weight and attained a stable value and remained unchanged until 120 h. With an increase in blend density, the oxidative stability increased. Until 120 h of oxidative stability study for hybrid membranes with PVA(70)-PAN(30) blend density, no stable value has been reached. The membrane weight percent for hybrid membranes with PVA(70)-PAN(30) blend density is continuously increasing and the membranes showed no softening even after 120 h of immersion. This observation is found to be similar for all hybrid membranes with different salts of heteropoly acid. The improvement in oxidative stability of the fabricated hybrid membrane with different blend density is due to its dense structure which restricts the diffusion of the radicals in to the membrane.

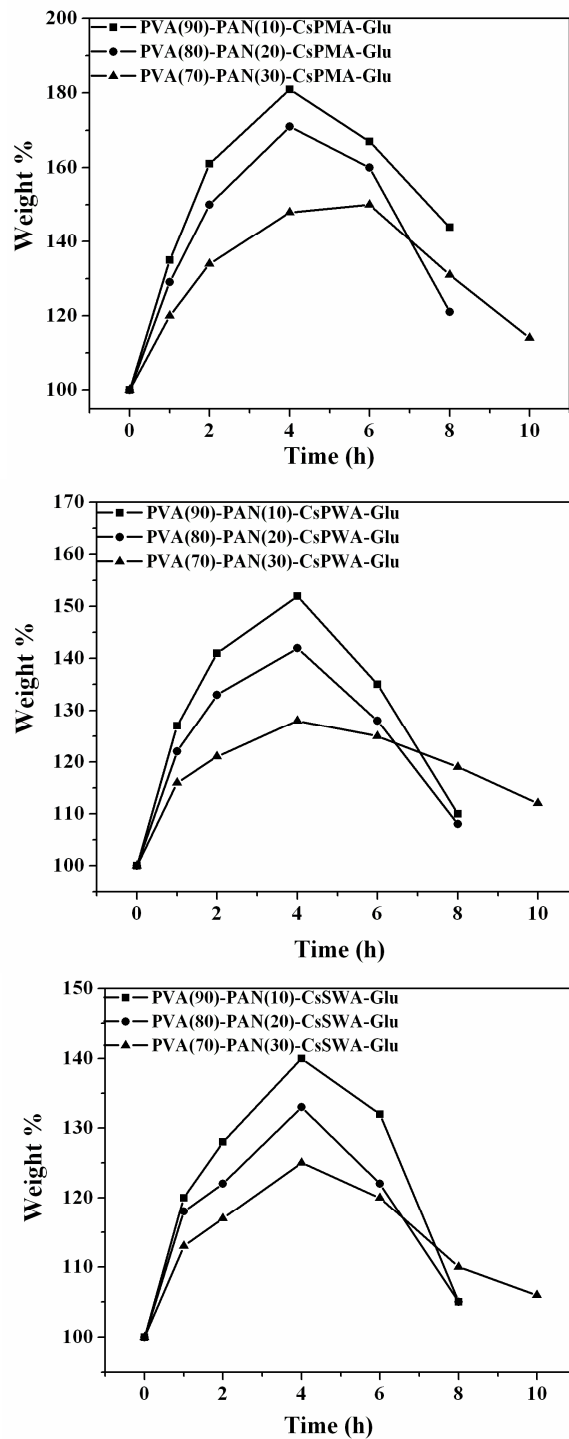


Fig. 7.5a Oxidative stability of fabricated membranes with different blend density immersed in Fenton's reagent at 70 °C for various time intervals (a) PVA-PAN-CsPMA-Glu (b) PVA-PAN-CsPWA-Glu (c) PVA-PAN-CsSWA-Glu.

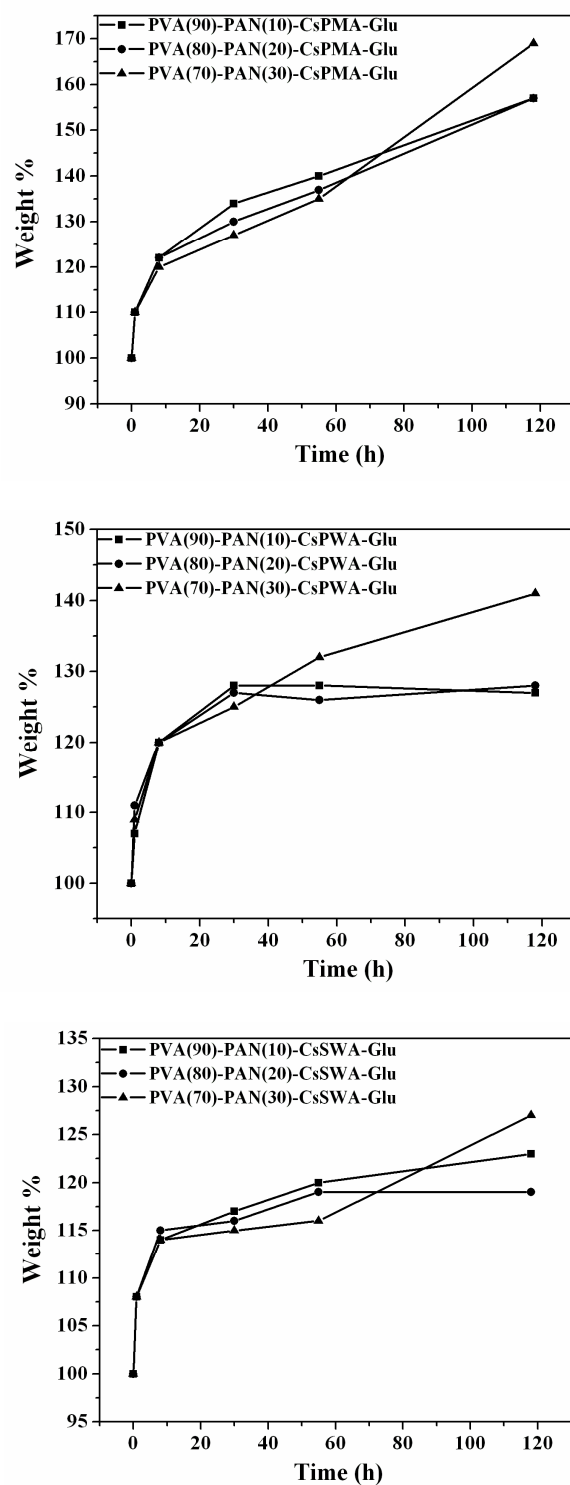


Fig. 7.5b Oxidative stability of fabricated membranes with different blend density immersed in Fenton's reagent at room temperature for various time intervals (a) PVA-PAN-CsPMA-Glu (b) PVA-PAN-CsPWA-Glu (c) PVA-PAN-CsSWA-Glu.

7.3.7 Additive stability

In order to establish the additive stability in the fabricated hybrid membranes, morphological characteristics of these membranes were tested at different time intervals for duration of five days by immersing the membranes in water using FT-IR technique. Figures 7.6a-7.6c show the FT-IR spectra of hybrid membranes with different blend density containing various salts of heteropoly acid. Characteristic bands of Keggin ion was observed between 1100 and 700 cm^{-1} . All the spectra confirm the existence of primary Keggin structure establishing the presence of salts of heteropoly acid in the hybrid membrane even after immersing them in water continually for several days. These spectra remained similar even after 136 h with slight decrease in absorption intensity representing a negligible amount of loss in salts of heteropoly acid due to vigorous stirring conditions. In addition, the increase in blend density of the polymer matrix further retards the leaching of heteropoly acid moiety. At a blend density of PVA-PAN (70-30) weight percent, there was no leaching of the inorganic additive even after 136 h of soaking (Fig. 7.6(a-c)). These results help us to ascertain the stability of Cs salts of heteropoly acids in the PVA-PAN matrix.

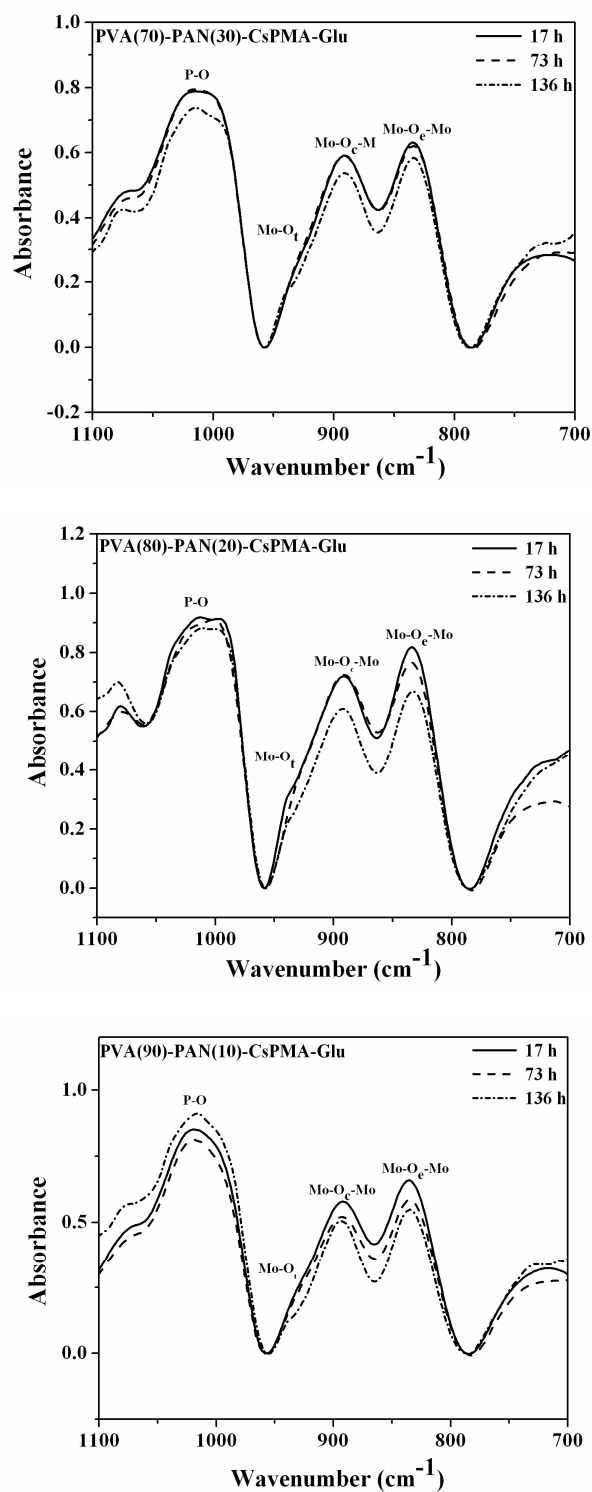


Fig. 7.6a FT-IR spectra of PVA-PAN-CsPMA-Glu membrane with different blend density placed in water for different time intervals.

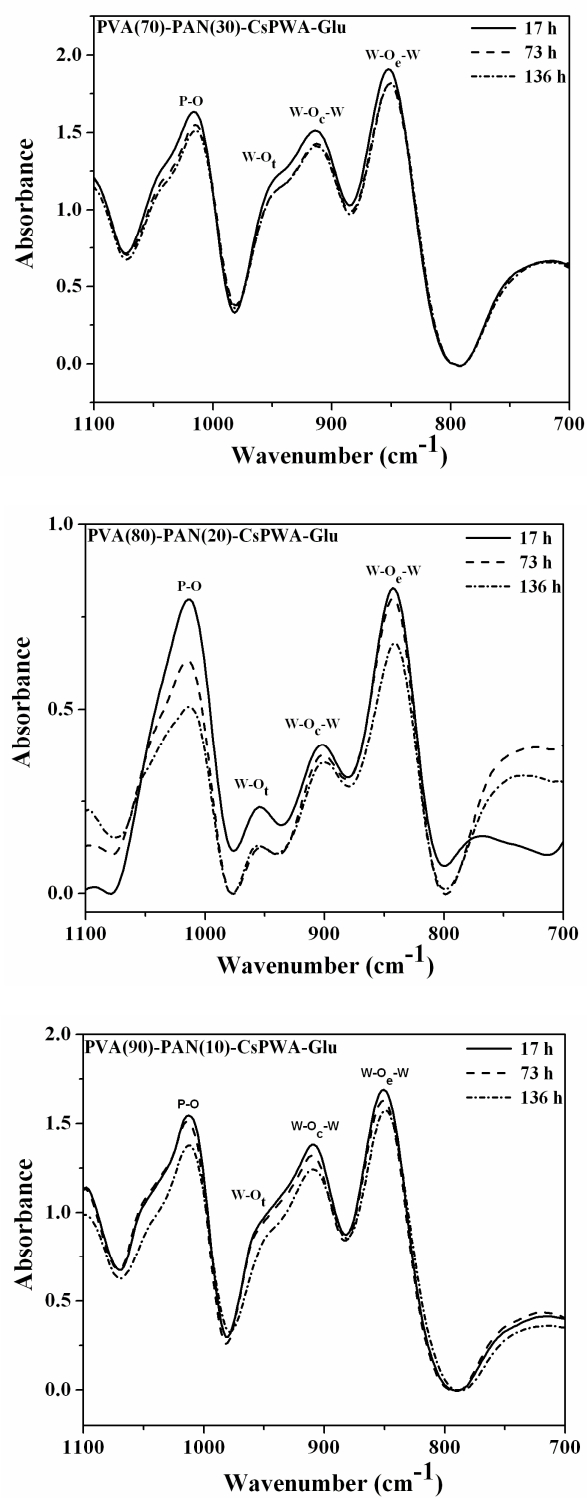


Fig. 7.6b FT-IR spectra of PVA-PAN-CsPWA-Glu membrane with different blend density placed in water for different time intervals.

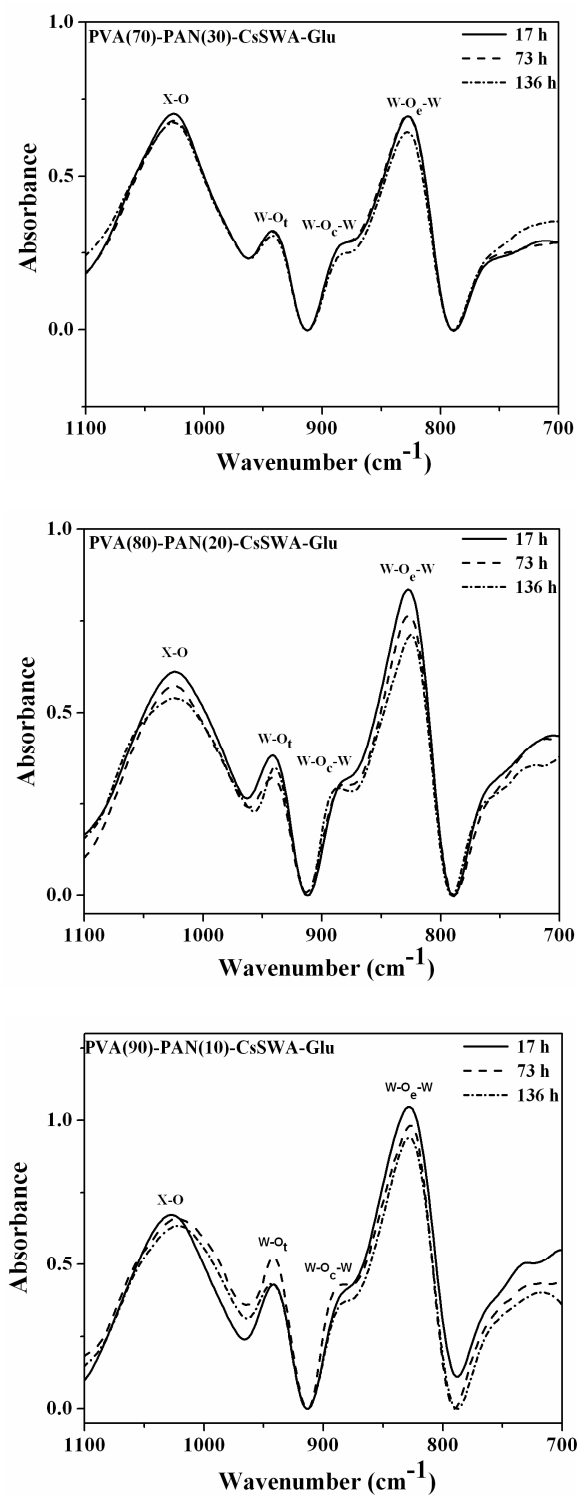


Fig. 7.6c FT-IR spectra of PVA-PAN-CsSWA-Glu membrane with different blend density placed in water for different time intervals.

7.3.8 Proton conductivity study

Fig. 7.7 shows the proton conductivity of the fabricated hybrid membranes measured at 50 % relative humidity at varying temperatures from 30 to 80 °C. For comparison, the corresponding data for Nafion[®] 115 measured at 100 % relative humidity is included. The conductivity of Nafion[®] 115 as well as hybrid membranes increases from 30 to 80 °C. At 50 % of relative humidity, the protonic conductivity of the hybrid membranes was in the range of 10^{-3} to 10^{-1} S cm⁻¹. Among the hybrid membranes studied, cesium salt of PMA substituted hybrid membranes exhibited higher conductivity compared to cesium salts of PWA and SWA substituted systems. This same trend in proton conductivity was also observed for hybrid membranes with polyacrylamide (PAM) as blending polymer (see Fig. 5.7. in Section 5.3.8). In particular, PVA(90)-PAN(10)-CsPMA-Glu membrane exhibited the highest proton conductivity in the range of 10^{-1} S cm⁻¹ at 50 % RH surpassing the state of the art Nafion[®] 115 measured at 100 % RH irrespective of polymer blend density.

The proton conductivity depends on the water uptake than on the IEC implying the effect of the water channels or clusters formed in the polymer matrix for facilitating proton transport inside the hybrid matrix. The proton conductivity of the hybrid membranes increases with increasing water content. The amount of water absorbed and hydrophilic domains of variable sizes contribute for proton conduction (Zawodzinski *et al.* 1993; James *et al.* 2000). Cesium salt of PMA containing hybrid membrane exhibits increase in water uptake than cesium salts of PWA and SWA containing hybrid membranes and it is reflected the trend observed in the proton conductivity results.

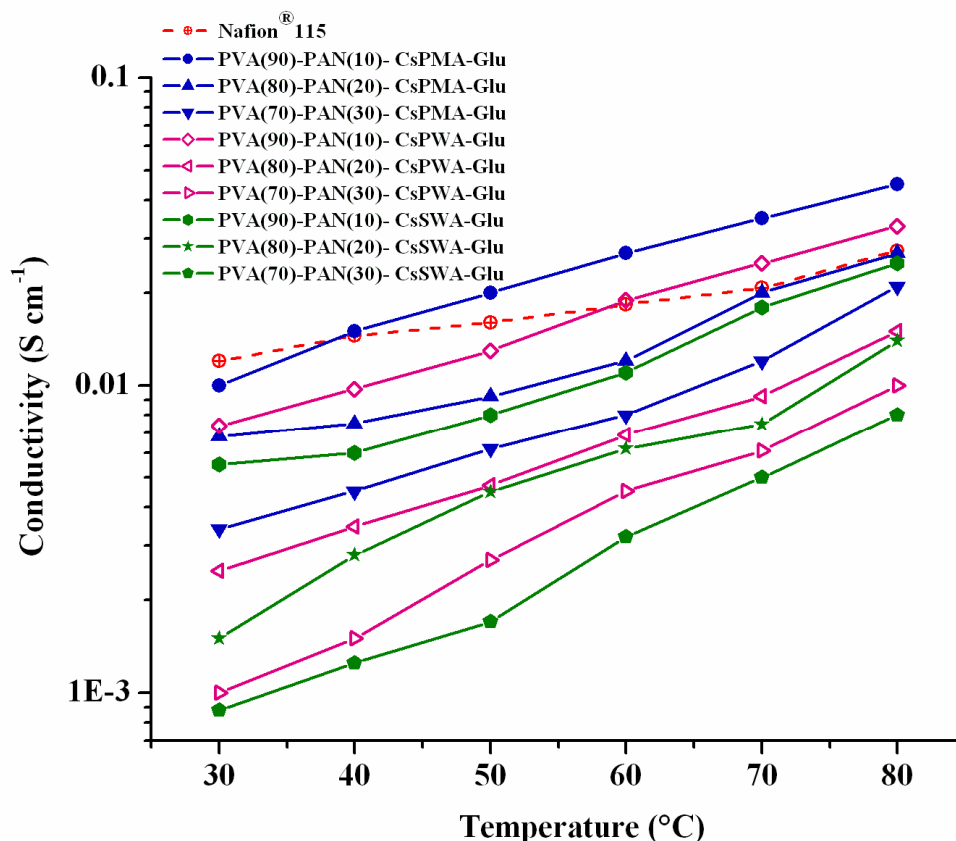


Fig. 7.7 Temperature dependence conductivity of hybrid membranes with different blend density.

The superior proton conductivity attained in cesium salt of PMA containing system can be attributed to the more ionic nature of the Mo-O_t (t-terminal) bond than W-O_t bonds. This ionic character imparts protonic character to the hydrogen on these sites. Since the W-O bond is more covalent, the protons are not free as in case with Mo-O system. In addition, the presence of cesium ions makes the system more polarizable. The charge on the heteropoly anion is spread and the size of the anion ($\text{PMo}_{12}\text{O}_{40}^{3-} < \text{PW}_{12}\text{O}_{40}^{3-}$) is yet another factor. It is not the net charge on the M-O terminal bond alone that contributes for proton conductivity.

The proton conductivity is also affected by the blend density of the polymer matrix. Increase in blend density of the polymer matrix decreases the proton conductivity.

With increase in blend density, the proton mobility and the size of the free volume could be restricted resulting in low proton conductivity.

All the fabricated hybrid membranes exhibited positive temperature–conductivity dependencies obeying Arrhenius type behavior. The activation energy of proton conduction, that can be derived from the slope of $\log \sigma$ versus $1/T$ plots for all the hybrid membranes is between 25–40 kJ mol⁻¹, attributing proton transfer through the Grotthus mechanism (Colomban and Novak, 1992).

7.3.9 Methanol crossover study

The results of methanol crossover studies are presented in Fig. 7.8(a-c). The rate of crossed over methanol appeared to vary with the variation in incorporated heteropoly acid and with blend density. Hybrid membrane containing SWA as an active component exhibited lower rate of methanol crossover compared to heteropoly acid materials such as PWA or PMA containing hybrid membranes.

Methanol permeability of the respective membranes was determined from the slope of the plots representing the crossed methanol concentration versus time (Fig. 7.9). Methanol permeability is an order of magnitude lesser for the fabricated hybrid membranes compared to Nafion[®] 115. This may be due to the dense interpenetrating network that was formed due to the blending of PVA with PAN followed by cross-linking with glutaraldehyde.

The increasing order of methanol permeabilities of the membrane materials with different heteropoly acids can be given as: PVA-PAN-CsSWA-Glu < PVA-PAN-CsPWA-Glu < PVA-PAN-CsPMA-Glu << Nafion[®] 115 (Fig. 7.9). The reduced methanol permeation in the hybrid membranes compared with Nafion[®] 115 can be

attributed to the methanol absorption ability of the heteropoly acids (Pseudoliquid phase behavior) that were incorporated into the polymer matrix of PVA-PAN blend. Hence, the fabricated heteropoly acid containing hybrid membranes exhibit the capacity to retain polar molecules like methanol without letting it to pass by. The methanol permeability values of the membrane materials were consistent with those of acid strengths of the corresponding materials that were reflected in IEC measurements (Table 7.2). As reported in literature (Okuhara *et al.* 1989; Misono *et al.* 1982; Shikata *et al.* 1995), the acid strength governs the amount of methanol adsorbed on heteropoly acid. The number of methanol molecules adsorbed per anion is approximated to integral number of protons in the heteropoly molecule (Okuhara *et al.* 1989; Bielanski *et al.* 1999; Małecka *et al.* 1999). The order of methanol adsorption per Keggin unit was reported to be as follows: $\text{SiW}_{12}\text{O}_{40}^{4-} > \text{PW}_{12}\text{O}_{40}^{3-} > \text{PMo}_{12}\text{O}_{40}^{3-}$ (Okuhara *et al.* 1989; Małecka *et al.* 1999; Bielański *et al.* 2005; Rykova *et al.* 2003; Antonucci *et al.* 2006) which has been clearly reflected in the results on permeability studies.

Methanol permeability is also affected by the blend density. With increase in PAN content, the permeability decreases due to the reduction of free volume. The low methanol permeability can also be related to the lower methanol uptake of the hybrid membranes (Table 7.2) compared to Nafion[®] 115.

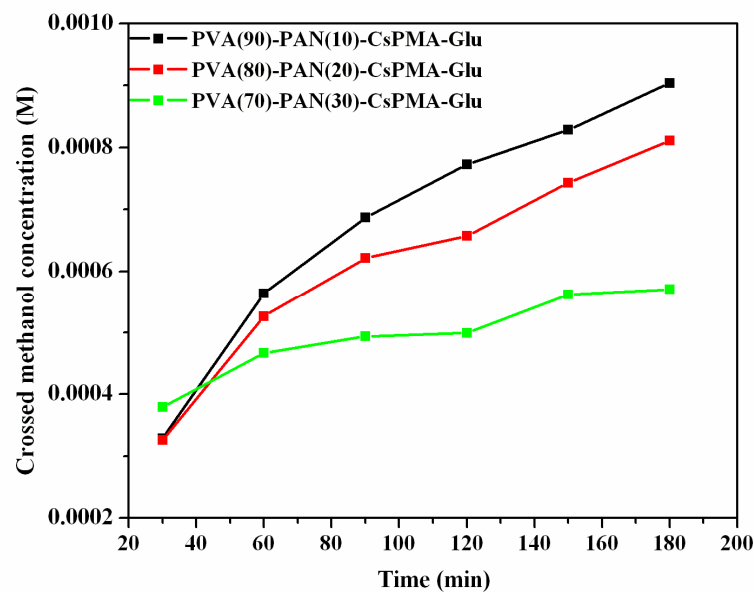


Fig. 7.8a Concentration of crossed over methanol as a function of crossover time for PVA-PAN-CsPMA-Glu hybrid membrane with different blend density.

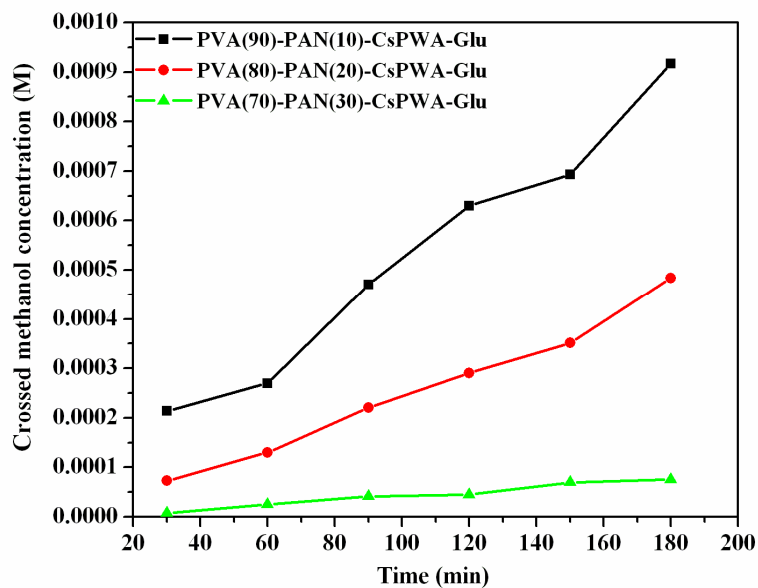


Fig. 7.8b Concentration of crossed over methanol as a function of crossover time for PVA-PAN-CsPWA-Glu hybrid membrane with different blend density.

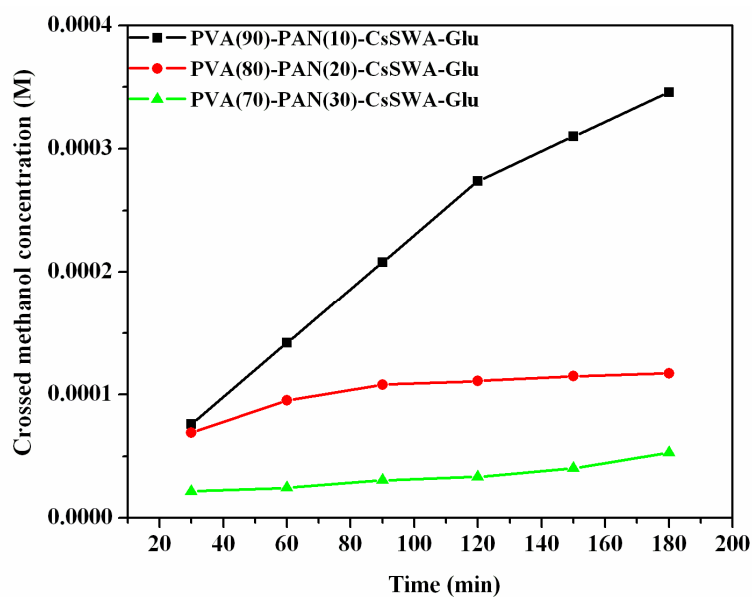


Fig. 7.8c Concentration of crossed over methanol as a function of crossover time for PVA-PAN-CsSWA-Glu hybrid membrane with different blend density.

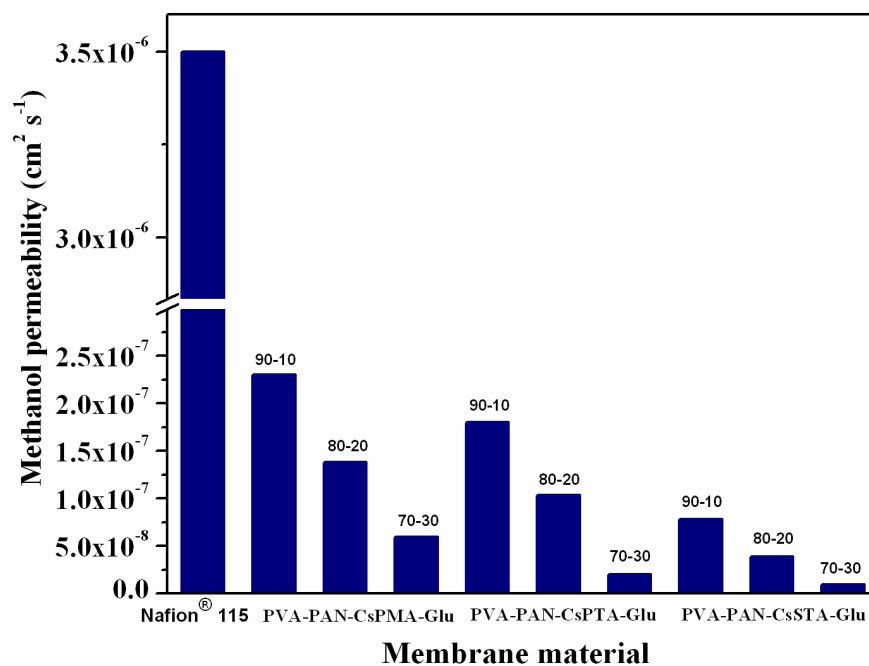


Fig. 7.9 Methanol permeability of hybrid membranes with different blend density compared with that of Nafion® 115.

7.3.10 Selectivity

The ratio of the conductance and the methanol crossover of the membrane is a useful parameter to describe membrane performance in the DMFC. Higher the selectivity (proton conductivity/methanol permeability) values, better the membrane performance. Selectivity of the Nafion[®] 115 and the fabricated hybrid membranes at room temperature are presented in Fig. 7.10. All the hybrid membranes outperformed Nafion[®] 115. The high selectivity of the hybrid membranes is attributed to the dense interpenetrating network that is formed, leading to low methanol permeability.

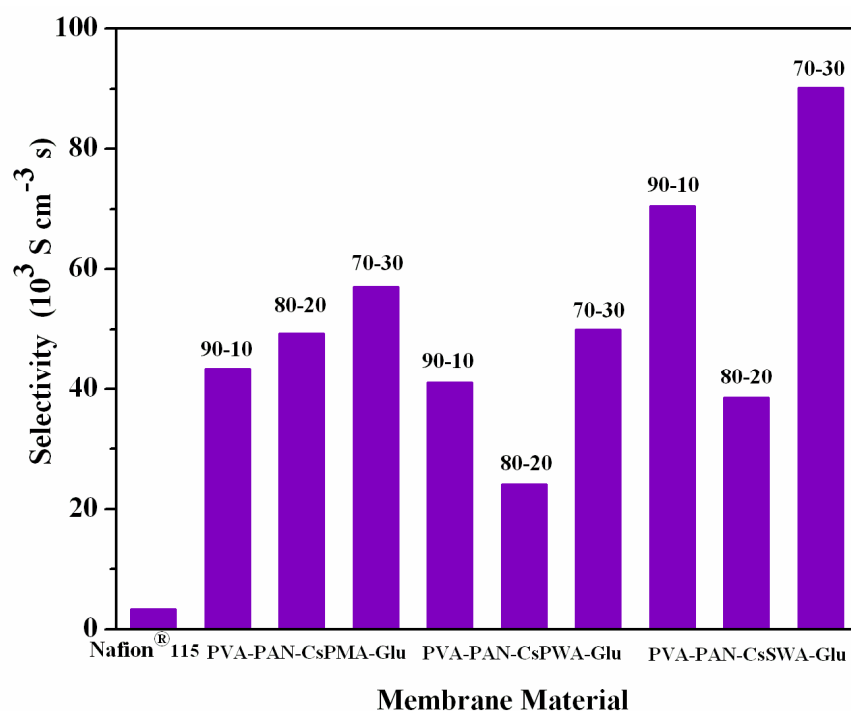


Fig. 7.10. Selectivity of hybrid membranes compared with that of Nafion[®] 115.

7.4 CONCLUSIONS

A series of hybrid membranes has been formulated by blending poly(vinyl alcohol) (PVA) and polyacrylonitrile (PAN) followed by cross-linking with glutaraldehyde. Cesium salt of different heteropoly acids such as phosphomolybdic acid (PMA), phosphotungstic acid (PWA) and silicotungstic acid (SWA) were incorporated into the polymer network to form organic-inorganic hybrid membranes. The effects of blend density on water uptake, swelling, proton conductivity and methanol crossover were discussed. The interpenetrating network formed by the blending of PVA with PAN leads to an order of decrease in methanol crossover compared to state of the art Nafion[®] 115 membrane. With increase in blend density, the free volume of the hybrid membranes is restricted leading to low swelling and methanol crossover. The difference in methanol permeability between the fabricated hybrid membranes containing different cesium salt of heteropoly acids is found to be governed by the adsorption ability of the respective heteropoly acids. The proton conductivity of the hybrid membranes were in the range of 10^{-3} to 10^{-1} S cm⁻¹ measured at varying temperatures ranging from 30 to 80 °C and 50 % RH. In particular, PVA(90)-PAN(10)-CsPMA-Glu membrane exhibited the highest proton conductivity in the range of 10^{-1} S cm⁻¹ at 50 % RH surpassing the state of the art Nafion[®] 115 measured at 100 % RH. The high selectivity (proton conductivity/methanol permeability) of the hybrid membranes is attributed to the dense interpenetrating network that is formed leading to low methanol permeability. The methanol crossover of the hybrids with different blend density decreased at the expense of proton conductivity of the material. Nevertheless, the proton conductivity of the hybrid membranes was comparable to that of Nafion[®] 115, whereas methanol resistance of the former membranes was lowered by orders of magnitude than that of the latter. These results

have proved the potential of the hybrid materials under this study for their employment as polymer electrolyte membranes for DMFCs application. Thus the last three chapters reflect the stepwise improvement achieved in the fabricated membranes, though the nature of studies carried out are quite similar in all the three cases.

CHAPTER 8

SUMMARY AND CONCLUSIONS

Direct methanol fuel cells (DMFCs) are attractive power sources for portable and stationary applications. One of the challenges for commercializing DMFC technology is to develop less expensive, non-fluorine based membrane material, with no or limited crossover of methanol through the membrane (a process that decreases the performance of cathode and leads to fuel loss). In order to alleviate the problems associated with the state of the art Du pont product Nafion[®], such as environmentally unfriendly fluorine based production, methanol crossover and low dimensional stability at high temperatures and low humidified operations of a fuel cell, spurt of research activities are focused to develop an alternate membrane possessing appreciable proton conductivity, low swelling and low diffusion for methanol by a simple and environmentally benign fabrication method.

As Nafion[®] holds the utmost electronegative environment possible in a chemical system, it is nearly impossible to design a membrane that will have better ionic conductivity compared to Nafion[®]. Realizing this limitation, it was considered worthwhile to design a membrane which may possess ionic conductivity less than that of Nafion[®], but should have at least one property (for fuel cell applications) better than that of Nafion[®]. Since the fuel crossover from anode to the cathode drastically reduces the performance in a DMFC, it was considered that the membrane development must mainly focus on this aspect of fuel crossover. In this direction, organic-inorganic hybrid membranes with poly(vinyl alcohol) (PVA) as organic matrix and heteropoly acids (HPA) as proton conducting moiety were investigated in the present work and documented in this thesis.

The summary and conclusions drawn from this study are as follows:

- Hybrid membranes with poly(vinyl alcohol) (PVA) as an organic matrix and zirconium phosphate (ZrP) and silicotungstic acid (SWA) as inorganic components were prepared by a sol-gel route. The fabricated membranes were characterized using spectroscopic, thermometric and morphological techniques and in addition, to examine their key properties which are relevant for DMFC applications such as water uptake, swelling, ion exchange capacity (IEC), proton conductivity and the extent of methanol crossover. It has been found that water uptake, IEC and proton conductivity properties of these membranes increased with silicotungstic acid content in them. These hybrid membranes exhibited reduced methanol crossover compared to the commercial Nafion[®] 115 membrane. The solubility of SWA is mitigated by forming hybrid with ZrP and PVA.
- Though a number of reports are available in literature on stabilizing the HPA in membrane matrix, a combined approach of composite formation with salts of HPA is investigated in this study for the first time. Hybrid membranes based on cesium salt of heteropoly acid, zirconium phosphate and poly(vinyl alcohol) were fabricated and characterized for its applicability in DMFC. At 50 % of relative humidity, the protonic conductivity of the hybrid membranes was in the range of 10^{-3} to 10^{-2} S cm⁻¹. Also, these hybrid membranes exhibited decreased methanol crossover compared to Nafion[®] 115. A maximum power density of 6 mW cm⁻² was obtained with PVA-ZrP-Cs₂SWA hybrid membrane. The open circuit voltage (OCV) for the cell with PVA-ZrP-Cs₂SWA hybrid membrane is 0.652 V and that for PVA-ZrP-

Cs₁SWA hybrid membrane is 0.619 V which is higher compared to the cell with Nafion[®] 115 (0.610 V) indicating reduced methanol crossover. The performance of the hybrid membranes in passive cell mode appears promising for DMFC applications.

- PVA membranes incorporated with heteropoly acids by forming composites are swelling too strongly to be used. In order to improve the dimensional stability of PVA based membranes, blending of poly(vinyl alcohol) (PVA) - polyacrylamide (PAM) followed by cross-linking with glutaraldehyde (Glu) was investigated. Cesium salts of different heteropoly acids such as phosphomolybdic acid (PMA), phosphotungstic acid (PWA) and silicotungstic acid (SWA) were incorporated into the polymer network to form corresponding hybrid membrane materials. The interpenetrating network formed by the blending of PVA with PAM leads to an order of decrease in methanol crossover and swelling compared to state of the art Nafion[®] 115 membrane employed for DMFC applications. The hybrid membrane containing cesium salt of SWA exhibited very low methanol permeability ($1.4 \times 10^{-8} \text{ cm}^2 \text{ s}^{-1}$) compared to other membranes containing cesium salt of heteropoly acids such as PMA and PWA. The difference in methanol permeability between the fabricated hybrid membranes containing different cesium salt of heteropoly acids is found to be governed by the adsorption ability of the respective heteropoly acids. The studied hybrid membranes are endowed with the enhanced ion exchange capacity, reasonable water uptake characteristics and appreciable proton conductivity.

- Polyacrylonitrile (PAN) is chosen as a blending agent to improve the dimensional stability of PVA membrane. The hybrid membranes were fabricated through a solution-cast method. Cesium salt of different heteropoly acids such as phosphomolybdic acid (PMA), phosphotungstic acid (PWA) and silicotungstic acid (SWA) were incorporated into the polymer network to form hybrid membrane materials. The interpenetrating network formed by the blending of PVA with PAN leads to an order of decrease in methanol crossover compared to the state of the art Nafion[®] 115 membrane employed for DMFC applications. The hybrid membrane containing cesium salt of SWA exhibited very low methanol permeability ($7.8 \times 10^{-8} \text{ cm}^2 \text{ s}^{-1}$) compared to other membranes containing cesium salt of heteropoly acids such as PMA and PWA. Among the hybrid membranes studied, cesium salt of PMA substituted hybrid membranes exhibited higher conductivity in the range of $10^{-1} \text{ S cm}^{-1}$ at 50 % RH surpassing the state of the art Nafion[®] 115 measured at 100 % RH. The order of proton conductivities of the hybrid membranes is in accordance with the water uptake ability of the materials.
- As an extension of the above studies, the effects of blend density on water uptake, swelling, proton conductivity and methanol crossover were investigated. A series of hybrid membranes has been formulated by blending poly(vinyl alcohol) (PVA) and polyacrylonitrile (PAN) followed by cross-linking with glutaraldehyde. With increase in blend density, the free volume of the hybrid membranes is restricted leading to low swelling and methanol crossover. The difference in methanol permeability between the fabricated hybrid membranes containing different cesium salt of heteropoly acids is found to be governed by the adsorption ability of the respective heteropoly

acids. The proton conductivity of the hybrid membranes were in the range of 10^{-3} to 10^{-1} S cm⁻¹ measured at varying temperatures ranging from 30 to 80 °C and 50 % RH. Increase in blend density of the polymer matrix decreases the proton conductivity. With increase in blend density, the proton mobility and the size of the free volume could be restricted resulting in low proton conductivity. The high selectivity (proton conductivity/methanol permeability) of the hybrid membranes is attributed to the dense interpenetrating network that is formed leading to low methanol permeability. The methanol crossover of the hybrids with different blend density decreased at the expense of proton conductivity of the material. Nevertheless, the proton conductivity of the hybrid membranes was comparable to that of Nafion[®] 115, whereas methanol resistance of the former membranes was lowered by orders of magnitude than that of the latter.

These results have proved the potential advantage of the newly fabricated hybrid materials to act as an electrolyte membrane for direct methanol fuel cell (DMFC) applications due to their lower methanol permeability property which is a major challenge encountered with Nafion[®] membrane in DMFCs.

FUTURE PROPOSITION

- The chemical interactions between the components of the PVA blend and the change in performance between PVA-PAM and PVA-PAN blended systems have to be critically analyzed. Molecular modeling investigation on the possible role of blending agent will shine light on proton transport mechanism in such complicated systems.

- The compatibility of the fabricated hybrid membranes with electrodes and subsequent studies in a full cell mode are required.

REFERENCES

1. **Adams, B.A. and E.L. Holmes** (1936) Synthetic resins and their use. *Fr. Patent*, 796,796.
2. **Agmon, N.** (1995) The Grotthuss mechanism. *Chem. Phys. Lett.*, **244**, 456-462.
3. **Agrawal, S.L. and A. Awadhia** (2004) DSC and conductivity studies on PVA based proton conducting gel electrolytes. *Bull. Mater. Sci.*, **27**, 523-527.
4. **Ahmad, M.I., S.M.J. Zaidi and S.U. Rahman** (2006) Proton conductivity and characterization of novel composite membranes for medium-temperature fuel cells. *Desalination*, **193**, 387-397.
5. **Albert, G. and M. Casciola** *Layer hydrates*, pp 238. In: P. Colomban (eds.) *Proton Conductors*, Cambridge University Press, New York, 1992.
6. **Alberti G. and M. Casciola** (2003) Composite membranes for medium-temperature PEM fuel cells. *Annu. Rev. Mater. Res.*, **33**, 129-154.
7. **Alberti, G., M. Casciola, U. Constantino and R. Vivani** (1996) Layered and pillared metal (IV) phosphates and phosphonates. *Adv. Mater.*, **8**, 291-303.
8. **Alberti, G., M. Casciola, U. Costantino, A. Peraio and E. Montoneri** (1992) Protonic conductivity of layered zirconium phosphonates containing $-\text{SO}_3\text{H}$ groups. I. Preparation and characterization of a mixed zirconium phosphonate of composition $\text{Zr}(\text{O}_3\text{PR})_{0.73}(\text{O}_3\text{PR}')_{1.27} \cdot n\text{H}_2\text{O}$, with $\text{R} = -\text{C}_6\text{H}_4-\text{SO}_3\text{H}$ and $\text{R}' = -\text{CH}_2-\text{OH}$. *Solid State Ionics*, **50**, 315-322.
9. **Amara, M. and H. Kerdjoudj** (2003) Modification of cation-exchange membrane properties by electro-adsorption of polyethyleneimine. *Desalination*, **155**, 79-87.
10. **Angran, W., B.A.O Yongzhong, W. Zhixue and H. Zhiming** (2008) Synthesis and characterization of proton-conducting polymer electrolytes based on acrylonitrile-styrene sulfonic acid copolymer/layered double hydroxides nanocomposites. *Chin. J. Chem. Eng.*, **16**, 938-943.
11. **Anis, A, A.K. Banthia and S. Bandyopadhyay** (2008) Synthesis and characterization of polyvinyl alcohol copolymer/phosphomolybdic acid-based crosslinked composite polymer electrolyte membranes. *J. Power Sources*, **179**, 69-80.
12. **Antonucci, P.L., A.S. Arico, P. Creti, E. Ramunni and V. Antonucci** (1999) Investigation of a direct methanol fuel cell based on a composite Nafion-silica electrolyte for high temperature operation. *Solid State Ionics*, **125**, 431-437.

13. **Antonucci, V., A.S. Aricò, V. Baglio, J. Brunea, I. Buder, N. Cabello, M. Hogarth, R. Martin and S. Nunes** (2006) Membranes for portable direct alcohol fuel cells. *Desalination*, **200**, 653-655.
14. **Apichatachutapan, W., R.B. Moore and K.A. Mauritz** (1996) Asymmetric [Nafion®]/[Zirconium Oxide] hybrid membranes via in-situ sol-gel chemistry. *J. Appl. Polym. Sci.*, **62**, 417-426.
15. **Appleby, A.J. and F.R. Foulkes** *Fuel cell handbook*. Van Nostrand Reinhold, New York, 1989.
16. **Arico, A.S., S. Srinivasan and V. Antonucci** (2001) DMFCs: From fundamental aspects to technology development. *Fuel Cells*, **1**, 133-161.
17. **Atkins, J.R., C.R. Sides, S.E. Creager, J.L. Harris, W.T. Pennington, B.H. Thomas and D.D. DesMarteau** (2003) Effect of equivalent weight on water sorption, PTFE-like crystallinity, and ionic conductivity in Bis[(Perfluoroalkyl)Sulfonyl] imide perfluorinated ionomers. *J. New Mat. Electrochem. Syst.*, **6**, 9–15.
18. **Babir, F. and T. Gomez** (1996) Efficiency and economics of proton exchange membrane (PEM) fuel cell. *Int. J. Hydrogen Energy*, **21**, 891-901.
19. **Bae, B., B.-H. Chun, H.-Y. Ha, I.-H. Oh and D. Kim** (2002) Preparation and characterization of plasma treated PP composite electrolyte membranes. *J. Membr. Sci.*, **202**, 245-252.
20. **Baglio, V., A.D. Blasi, A.S. Aricò, V. Antonucci, P.L. Antonucci, F. Nannetti and V. Tricoli** (2005) Investigation of the electrochemical behaviour in DMFCs of chabazite and clinoptilolite-based composite membranes. *Electrochim. Acta*, **50**, 5181-5188.
21. **Baglio, V., A.S. Aricò, V. Antonucci, I. Nicotera, C. Oliviero, L. Coppola and P.L. Antonucci**, (2006) An NMR spectroscopic study of water and methanol transport properties in DMFC composite membranes: Influence on the electrochemical behaviour. *J. Power Sources*, **163**, 52-55.
22. **Bahar, B., A.R. Hobson, J.A. Kolde and D. Zuckerbrod** (1996) Ultra-thin integral composite membrane. *US. Patent*, 5,547,551.
23. **Bailly, C., D.J. Williams, F.E. Karasz and W.J. MacKnight** (1987) The sodium salts of sulfonated poly(aryl ether-ether-ketone)(PEEK): Preparation and Characterization. *Polymer*, **28**, 1009-1016.
24. **Baradie, B., J.P. Dodelet and P. Guay** (1998) Hybrid Nafion®-inorganic membrane with potential applications for polymer electrolyte fuel cells. *J. Electroanal. Chem.*, **489**, 209–214.
25. **Basura, V.I., P.D. Beattie and S. Holdcroft** (1999) Temperature and pressure dependence of O₂ reduction at Pt|Nafion® 117 and Pt|BAM® 407 interfaces. *J. Electroanal. Chem.*, **468**, 180–192.

26. **Bauer, F. and M.W. Porada** (2004) Microstructural characterization of Zr-phosphate–Nafion[®] membranes for direct methanol fuel cell (DMFC) applications. *J. Membr.Sci.*, **233**, 141-149.
27. **Bauer, F. and M.W. Porada** (2005) Characterisation of zirconium and titanium phosphates and direct methanol fuel cell (DMFC) performance of functionally graded Nafion(R) composite membranes prepared out of them *J. Power Sources*, **145**, 101–107.
28. **Bello, M., S.M. Javaid Zaidi and S.U. Rahman** (2008) Proton and methanol transport behavior of SPEEK/TPA/MCM-41 composite membranes for fuel cell application. *J. Membr. Sci.*, **322**, 218-224.
29. **Berzelius J.** (1826) Beitrag zur näheren kenntniss des molybdäns. *Pogg. Ann. Phys. Chem.*, **6**, 369-392.
30. **Bielański, A., A. Lubańska, A. Micek-Ilnicka and J. Poźniczek** (2005) Polyoxometalates as the catalysts for tertiary ethers MTBE and ETBE synthesis. *Coord. Chem. Rev.*, **249**, 2222-2231.
31. **Bielanski, A., J. Datka, B. Gil, A.M-Lubanska and A.M-Ilnicka** (1999) Sorption of methanol on tungstosilicic acid. *Phys. Chem. Chem. Phys.*, **1**, 2355-2360.
32. **Bockris, J.O'M. and S. Srinivasan** *Fuel Cells: Their Electrochemistry*, McGraw-Hill, New York, 1969.
33. **Bouchet, R and Siebert E.** (1999) Proton conduction in acid doped polybenzimidazole. *Solid State Ionics*, **118**, 287-299.
34. **Bouchet, R., S. Miller, M. Deulot and J.L. Sonquet** (2001) A thermodynamic approach to proton conductivity in acid-doped polybenzimidazole. *Solid State Ionics*, **145**, 69-78.
35. **Bozkurt, A., M. Ise, K.D. Kreuer, W.H. Meyer and G. Wegner** (1999) Proton-conducting polymer electrolytes based on phosphoric acid. *Solid State Ionics*, **125**, 225-233.
36. **Braun, D., H. Cherdron and H. Ritter**, *Polymer Synthesis: Theory and Practice: Fundamentals, Methods, Experiments*, Springer, 2001.
37. **Büchi, F.N., B. Gupta, O. Haas and G.G. Scherer** (1995) Study of radiation-grafted FEP-G-polystyrene membranes as polymer electrolytes in fuel cells. *Electrochim. Acta*, **40**, 345-353.
38. **Bumsuk, J., K. Bokyung and M.Y. Jung** (2004) Transport of methanol and protons through partially sulfonated polymer blend membranes for direct methanol fuel cell. *J. Membr. Sci.*, **245**, 61-69.
39. **Byun, S.C., Y.J. Jeong, J.W. Park, S.D. Kim, H.Y. Ha and W.J. Kim** (2006) Effect of solvent and crystal size on the selectivity of ZSM-5/Nafion

composite membranes fabricated by solution-casting method. *Solid State Ionics*, **177**, 3233-3243.

40. **Cai, H., K. Shao, S.Zhong, C. Zhao, G. Zhang, X. Li and H. Na** (2007) Properties of composite membranes based on sulfonated poly(ether ether ketone)s (SPEEK)/phenoxy resin (PHR) for direct methanol fuel cells usages. *J. Membr. Sci.*, **297**, 162–173.
41. **Carter, R., R. Wycisk, H. Yoo and P.N. Pintauro** (2002) Blended polyphosphazene/ polyacrylonitrile membranes for direct methanol fuel cells. *Electrochem. Solid-State Lett.*, **5**, A195–A197.
42. **Casciola, M. and U, Constantino** (1986) Relative humidity influence on proton conduction of hydrated pellicular zirconium phosphate in hydrogen form. *Solid State Ionics*, **20**, 69-73.
43. **Casciola, M., G. Alberti, A. Ciarletta, A. Cruccolini, P. Piaggio and M. Pica** (2005) Nanocomposite membranes made of zirconium phosphate sulfophenylene phosphonate dispersed in polyvinylidene fluoride: Preparation and proton conductivity. *Solid State Ionics*, **176**, 2985-2989.
44. **Casciola, M., G. Alberti, M. Sganappa and R. Narducci** (2006) On the decay of Nafion proton conductivity at high temperature and relative humidity. *J. Power Sources*, **162**,141-145.
45. **Chang H.Y. and C.W. Lin** (2003) Proton conducting membranes based on PEG/SiO₂ nanocomposites for direct methanol fuel cells. *J. Membr. Sci.*, **218**, 295-306.
46. **Chang, B.-J., D.J. Kim, J.H. Kim, S-B. Lee and H.J. Joo** (2008) Sulfonated poly(fluorene-co-sulfone)ether membranes containing perfluorocyclobutane groups for fuel cell applications. *J. Membr. Sci.*, **325**, 989–996.
47. **Chang, J.H., J.H. Park, G.G. Park, C.S. Kim and O.O. Park** (2003) Proton-conducting composite membrane derived from sulfonated hydrocarbon and inorganic materials. *J. Power Sources*, **124**, 18-25.
48. **Chen, C-Y., J.I.G-Rodriguez, M.C. Duke, R.F.D. Costa, A.L. Dicks and J.C.D. Costa** (2007) Nafion/polyaniline/silica composite membranes for direct methanol fuel cell application. *J. Power Sources*, **166**, 324-330.
49. **Chen, L-C., T.L. Yu, H-L. Lin and S-H. Yeh** (2008) Nafion/PTFE and zirconium phosphate modified Nafion/PTFE composite membranes for direct methanol fuel cells. *J. Membr. Sci.*, **307**, 10-20.
50. **Chen, Y.L., Y.Z. Meng and A.S. Hay** (2005) Direct synthesis of sulfonated poly(phthalazinoneether) for proton exchange membrane via N–C coupling reaction. *Polymer*, **46**, 1125–1132.
51. **Choa, E.K., J-S. Parka, S-H. Park, Y-W. Choi, T-H. Yang, Y-G. Yoon, C-S. Kim,W-Y. Lee and S-B. Park** (2008) A study on the preferable preparation

method of SPEEK/BPO₄ composite membranes via an in situ sol–gel process. *J. Membr. Sci.*, **318**, 355–362.

52. **Choi, W.C., J.D. Kim and S.I. Woo** (2001) Modification of proton conducting membrane for reducing methanol crossover in a direct-methanol fuel cell. *J. Power Sources*, **96**, 411–414.
53. **Colicchio, I., F. Wen, H. Keul, U. Simon and M. Moeller** (2009) Sulfonated poly(ether ether ketone)–silica membranes doped with phosphotungstic acid. Morphology and proton conductivity. *J. Membr. Sci.*, **326**, 45–57.
54. **Costamagna, P. and S. Srinivasan** (2001) Quantum jumps in the PEMFC science and technology from the 1960s to the year 2000: Part I. Fundamental scientific aspects. *J. Power Sources*, **102**, 242–252.
55. **Costantino, U., R. Vivani, V. Zima and E. Cernoskova** (1997) Thermoanalytical study, phase transitions, and dimensional changes of α -Zr(HPO₄)₂·H₂O large crystals. *J. Solid State Chem.*, **132**, 17–23.
56. **Croce, F., J. Hassoun, C. Tizzani and B. Scrosati** (2006) Nanoporous composite, low cost, protonic membranes for direct methanol fuel cells. *Electrochem. Commun.*, **8**, 1125–1131.
57. **Cui, Z., N. Li, X. Zhou, C. Liu, J. Liao, S. Zhang and W. Xing** (2007) Surface-modified Nafion[®] membrane by casting proton-conducting polyelectrolyte complexes for direct methanol fuel cells. *J. Power Sources*, **173**, 162–165.
58. **Cui, Z., W. Xing, C. Liu, J. Liao and H. Zhang** (2008) Chitosan/heteropolyacid composite membranes for direct methanol fuel cell. *J. Power Sources*, **188**, 24–29.
59. **Curtin, D.E., R.D. Lousenberg, T.J. Henry, P.C. Tangeman and M.E. Tisack** (2004) Advanced materials for improved PEMFC performance and life. *J. Power Sources*, **131**, 41–48.
60. **D'Alelio, G.** (1944) Ion exchanger. *US Patent*, 2,366,007.
61. **David FCC**, (2004) David FCC launches Sterion membranes. *Fuel Cells Bull.*, **2004**, 2.
62. **David, L.I.B. and A.F. Ismail** (2003) Influence of the thermostabilization process and soak time during pyrolysis process on the polyacrylonitrile carbon membranes for O₂/N₂ separation. *J. Membr. Sci.*, **213**, 285–291.
63. **Deb, P.C., L.D. Rajputy, V.R. Hande, S. Sasane and A. Kumar** (2007) Modification of sulfonated poly(ether ether ketone) with phenolic resin. *Polym. Adv. Technol.*, **18**, 419–426.
64. **Deltcheff, C.R., R. Thouvenot and R. Franck** (1976) Spectras i.r. et Raman d'hétéropolyanions α - XM₁₂O₄₀ⁿ⁻ de structure de type Keggin (X = B^{III}, Si^{IV}, Ge^{IV}, P^V, As^V et M = W^{VI} et Mo^{VI}). *Spectrochim. Acta A*, **32**, 587–597.

65. **DeLuca, N.W. and Y.A. Elabd** (2006) Nafion[®]/poly(vinyl alcohol) blends: Effect of composition and annealing temperature on transport properties. *J. Membr. Sci.*, **282**, 217–224.
66. **Dimitrova, P., K.A. Friedrich, B. Vogt and U. Stimming** (2002) Transport properties of ionomer composite membranes for direct methanol fuel cells. *J. Electroanal. Chem.*, **532**, 75-83.
67. **Dimitrova, P.G., B. Baradie, D. Foscallo, C. Poinsignon and J.Y. Sanchez** (2001) Ionomeric membranes for proton exchange membrane fuel cell (PEMFC): sulfonated polysulfone associated with phosphatoantimonic acid. *J. Membr. Sci.*, **185**, 59-71.
68. **Ding, J., C. Chuy and S. Holdcroft** (2002) Enhanced conductivity in morphologically controlled proton exchange membranes: synthesis of macromonomers by SFRP and their incorporation into graft polymers. *Macromolecules*, **35**, 1348–1355.
69. **Donoso, P., W. Gorecki, C. Berthier, F. Defendini, C. Poinsignon and M.B. Armand** (1988) NMR, conductivity and neutron scattering investigation of ionic dynamics in the anhydrous polymer protonic conductor PEO(H₃PO₄)_x. *Solid State Ionics*, **28-30**, 969-974.
70. **Doyle, M. and G. Rajendran** *Hand Book of Fuel-Cell Fundamentals, Technology and Applications*, pp.351. In W. Vielstich, A. Lamm, and H.A. Gasteiger, (eds.) John Wiley & Sons Ltd., London, 2003.
71. **Duvdevani, T., M. Philosoph, M. Rakhman, D. Golodnitsky and E. Peled** (2006) Novel composite proton-exchange membrane based on silica-anchored sulfonic acid (SASA). *J. Power Sources*, **161**, 1069-1075.
72. **Elabd Y.A., Napadensky E., J.M. Sloan, D.M. Crawford and C.W. Walker** (2003) Triblock copolymer ionomer membranes. Part I: methanol and proton transport. *J. Membr. Sci.*, **217**, 227–242.
73. **Elabd, Y.A., F.L. Beyer and C.W. Walker** (2004) Triblock copolymer ionomer membranes. Part II: structure characterization and its effects on transport properties and direct methanol fuel cell performance. *J. Membr. Sci.*, **231**, 181–188.
74. **Elamathi, S., G. Nithyakalyani, D. Sangeetha and S. Ravichandran** (2008) Preparation and evaluation of ionomeric membranes based on sulfonated-poly (styrene_isobutylene_styrene) membranes for proton exchange membrane fuel cells (PEMFC). *Ionics*, **14**, 377–385.
75. **England, W.A., M.G. Cross, A. Hamnett, P.J. Wiseman and J.B. Goodenough** (1980) Fast proton conduction in inorganic ion-exchange compounds. *Solid State Ionics*, **1**, 231-249.
76. **Feng, F., Z. Yang, D.H. Coutinho, J.P. Ferraris and Jr., K.J. Balkus** (2005) Synthesis of proton conducting tungstosilicate mesoporous materials and polymer composite membranes. *Micropor. Mesopor. Mater.*, **81**, 217-234.

77. **Fontanella, J.J., M.C. Wintergill, J.U.S. Wainright, R.F. Savinell and M. Litt** (1998) High pressure electrical conductivity studies of acid doped polybenzimidazole. *Electrochim. Acta*, **43** 1289-1294.
78. **Fournier, M., C.F- Jantou, C. Rabia, G. Hervé and S. Launay** (1992) Polyoxometalates catalyst materials: X-ray thermal stability study of phosphorus-containing heteropolyacids $H_{3+x}PM_{12-x}V_xO_{40} \cdot 13-14H_2O$ (M= Mo,W; $x=0-1$). *J. Mater. Chem.*, **2**, 971-978.
79. **Fu, R-Q., J-J. Woo, S-J. Seo, J-S. Lee and S-H. Moon** (2008) Covalent organic/inorganic hybrid proton-conductive membrane with semi-interpenetrating polymer network: Preparation and characterizations. *J. Power Sources*, **179**, 458-466.
80. **Fu, T., C. Zhao, S. Zhong, G. Zhang, K. Shao, H. Zhang, J. Wang and H. Na** (2007) SPEEK/epoxy resin composite membranes *in situ* polymerization for direct methanol fuel cell usages. *J. Power Sources*, **165**, 708-716.
81. **Gao, Y., G.P. Robertson, M.D. Guiver, G.Wang, X. Jian, S.D. Mikhailenko, X. Li and S. Kaliaguine** (2006) Sulfonated copoly(phthalazinone ether ketone nitrile)s as proton exchange membrane materials. *J. Membr. Sci.*, **278**, 26-34.
82. **Gaowen, Z. and Z. Zhentao** (2005) Organic/inorganic composite membranes for application in DMFC. *J. Membr. Sci.*, **261**, 107-113.
83. **Gebel, G.** (2000) Structural evolution of water swollen perfluorosulfonated ionomers from dry membrane to solution. *Polymer*, **41**, 5829-5838.
84. **Genies, C., R. Mercier, B. Sillion, N. Cornet, G. Gebel and M. Pineri** (2001) Soluble sulfonated naphthalenic polyimides as materials for proton exchange membranes. *Polymer*, **42**, 359-373.
85. **Ghassemi, H., J.E. McGrath and T.A. Zawodzinski** (2006) Structure-property-performance relationships of sulfonated poly(arylene ether sulfone)s as a polymer electrolyte for fuel cell applications. *Polymer*, **47**, 4132-4139.
86. **Gierke, T. D., G.E. Munn and F. C. Wilson** (1981) The morphology in Nafion perfluorinated membrane products, as determined by wide- and small-angle X-ray studies. *J. Polymr. Sci., Part B: Polym. Phys.*, **19**, 1687-1704.
87. **Gil, M., X.L. Ji, X.F. Li, H. Na, J.E. Hampsey and Y.F. Lu** (2004) Direct synthesis of sulfonated aromatic poly(ether ether ketone) proton exchange membranes for fuel cell applications. *J. Membr. Sci.*, **234**, 75-81.
88. **Gillespie, R.J. and E. A. Robinson** *In Nonaqueous Solvent Systems*, pp. 117-210. In T.C. Waddington (eds.) Academic Press, New York, 1965.
89. **Giordano, N., P. Staiti, S. Hocevar and A. S. Arico** (1996) High performance fuel cell based on phosphotungstic acid as proton conducting electrolyte. *Electrochim. Acta*, **41**, 397-403.

90. **Glipa, X., M.E. Haddad, D.J. Jones and J. Rozie`re** (1997) Synthesis and characterisation of sulfonated polybenzimidazole: a highly conducting proton exchange polymer. *Solid State Ionics*, **97**, 323-331.
91. **Gosalawit, R., S. Chirachanchai, H. Manuspiya and E. Traversa** (2006) Krytox-Silica-Nafion[®] composite membrane: A hybrid system for maintaining proton conductivity in a wide range of operating temperatures. *Catal. Today*, **118**, 259-265.
92. **Grondin, J., D. Rodriguez and J.C. Lassegues** (1995) Proton conducting polymer electrolyte-The Nylon 6-10/H₃PO₄ blends. *Solid State Ionics*, **77**, 70-75.
93. **Gubler L, D. Kramer, J. Belack, Ö. Ünsal, T.J. Schmidt and G.G. Scherer** (2007) Celtec_V – A polybenzimidazole-based membrane for the direct methanol fuel cell. *J Electrochem Soc.*, **154**, B981-B987.
94. **Gupta P.N. and K.P. Singh** (1996) Characterization of H₃PO₄ based PVA complex system. *Solid State Ionics*, **86-88**, 319-323.
95. **Gupta, B., F.N. Buechi, G.G. Scherer and A. Chapiro** (1994) Development of radiation grafted FEP-g-polystyrene membranes. Some structure-property correlations. *Polym. Adv.Technol.*, **5**, 493-498.
96. **Hassan, C.M. and N.A. Peppas** (2000) Structure and applications of poly(vinyl alcohol) hydrogels produced by conventional cross-linking or by freezing/thawing methods. *Adv. Polym. Sci.*, **153**, 37-65.
97. **Haufe, S. and U. Stimming** (2001) Proton conducting membranes based on electrolyte filled microporous matrices. *J. Membr. Sci.*, **185**, 95-103.
98. **He, R.H., Q.F Li, G. Xiao and N.J. Bjerrum** (2003) Proton conductivity of phosphoric acid doped polybenzimidazole and its composites with inorganic proton conductors. *J Membr. Sci.*, **226**, 169-184.
99. **Hickner, M.A., H. Ghassemi, Y.S. Kim, B.R. Einsla and J.E. McGrath** (2004) Alternative polymer systems for proton exchange membranes (PEMs). *Chem. Rev.*, **104**, 4587-4612.
100. **Hill, M.L., Y.S. Kim, B.R. Einsla and J.E. McGrath** (2006) Zirconium hydrogen phosphate/disulfonated poly(arylene ether sulfone) copolymer composite membranes for proton exchange membrane fuel cells. *J. Membr. Sci.*, **283**, 102-108.
101. **Ho, W.S. and K.K. Sirkar** *Membrane Handbook*. Van Nostrand Reinhold, NewYork, 1992.
102. **Hodnett B.K. and J. B. Moffat** (1984) Application of temperature-programmed desorption to the study of heteropoly compounds: Desorption of water and pyridine. *J. Catal.*, **88**, 253-263.

103. **Hogarth, W.H.J., J.C.D. da Costa and G.Q.(Max) Lu** (2005) Solid acid membranes for high temperature (>C) proton exchange membrane fuel cells. *J. Power Sources*, **142**, 223-237.
104. **Honga, Y.T., C.H. Lee, H.S. Park, K.A. Min, H.J. Kim, S.Y. Nam and Y.M. Lee** (2008) Improvement of electrochemical performances of sulfonated poly(arylene ether sulfone) *via* incorporation of sulfonated poly(arylene ether benzimidazole). *J. Power Sources*, **175**, 724–731.
105. **Honma, I., H. Nakajima, O. Nishikawa, T. Sugimoto and S. Nomura** (2003) Organic/inorganic nano-composites for high temperature proton conducting polymer electrolytes. *Solid State Ionics*, **162**, 237-245.
106. **Honma, I., S. Hirakawa, K. Yamada and J.M. Bae** (1999) Synthesis of organic/inorganic nanocomposites protonic conducting membrane through sol-gel processes. *Solid State Ionics*, **118**, 29-36.
107. **Hoogers, G.** *Fuel Cell Technology Handbook*. CRC Press, 2002.
108. **Horsley, S.E., D.V. Nowell and D.T. Stewart** (1974) The infrared and Raman spectra of α -zirconium phosphate. *Spectrochimica Acta*, **30A**, 535-541.
109. **Hsu, W.Y. and T.D. Gierke** (1982) Elastic theory for ionic clustering in perfluorinated ionomers. *Macromolecules*, **15**, 101-105.
110. **Huang, L-N., L.-C. Chen, T.L. Yu and H-L. Lin** (2006) Nafion/PTFE/silicate composite membranes for direct methanol fuel cells. *J. Power Sources*, **161**, 1096-1105.
111. **Hübner, G. and E. Roduner** (1999) EPR investigation of HO radical initiated degradation reactions of sulfonated aromatics as model compounds for fuel cell proton conducting membranes. *J. Mater. Chem.*, **9**, 409-418.
112. **Immelman, E., R.D. Sanderson, E.P. Jacobs and A.J.V. Reenen** (1993) Poly (vinyl alcohol) gel sublayers for reverse osmosis membranes. I. Insolubilization by acid-catalyzed dehydration. *J. Appl. Polym. Sci.* **50**, 1013-1034.
113. **Jang, M.Y. and Y. Yamazaki** (2005) Preparation and characterization of composite membranes composed of zirconium tricarboxybutylphosphonate and polybenzimidazole for intermediate temperature operation. *J. Power Sources*, **139**, 2-8.
114. **Jiang, R., H.R. Kunz and J.M. Fenton** (2006) Influence of temperature and relative humidity on performance and CO tolerance of PEM fuel cells with Nafion®–Teflon®–Zr(HPO₄)₂ higher temperature composite membranes. *Electrochim. Acta*, **51**, 5596-5605.
115. **Jiang, Z., X. Zheng, H. Wu and F. Pan** (2008) Proton conducting membranes prepared by incorporation of organophosphorus acids into alcohol barrier polymers for direct methanol fuel cells. *J. Power Sources*, **185**, 85–94.

116. **Jin, X., M.T. Bishop, T.S. Ellis and F.E. Karasz** (1985) A sulphonated poly(aryl ether ketone). *Br. Polymer J.*, **17**, 4-10.
117. **Jones, D.J. and Roziere, J.** (2001) Recent advances in the functionalisation of polybenzimidazole and polyetherketone for fuel cell applications. *J. Membr. Sci.*, **185**, 41-58.
118. **Jorissen, L., V. Gogel, J. Kerres and J. Garche** (2002) New membranes for direct methanol fuel cells. *J. Power Sources*, **105**, 267-273.
119. **Jung, D.H., Y-B. Myoung, S-Y. Cho, D.R. Shin and D.H. Peck** (2001) A performance evaluation of direct methanol fuel cell using impregnated tetraethyl-orthosilicate in cross-linked polymer membrane. *Int. J. Hydrogen Energy*, **26**, 1263-1269.
120. **Jung, E.H., U.H. Jung, T.H. Yang, D.H. Peak, D.H. Jung and S.H. Kim** (2007) Methanol crossover through PtRu/Nafion composite membrane for a direct methanol fuel cell. *Int. J. Hydrogen Energy*, **32**, 903-907.
121. **Jung, H-Y. and J-K. Park** (2007) Blend membranes based on sulfonated poly(ether ether ketone) and poly(vinylidene fluoride) for high performance direct methanol fuel cell. *Electrochim. Acta*, **52**, 7464-7468.
122. **Kaliaguine, S., S.D. Mikhailenko, K.P. Wang, P. Xing, G. Robertson and M. Guiver** (2003) Properties of SPEEK based PEMs for fuel cell application. *Catal. Today*, **82**, 213-222.
123. **Kang, M.-S., Y.-J. Choi and S.-H. Moon** (2002) Water-swollen cation-exchange membranes prepared using poly(vinyl alcohol) (PVA)/poly(styrene sulfonic acid-co-maleic acid) (PSSA-MA). *J. Membr. Sci.*, **207**, 157-170.
124. **Karthikeyan C.S., S.P. Nunes, L.A.S.A. Prado, M.L. Ponce, H. Silva, B. Ruffmann and K. Schulte** (2000) Polymer nanocomposite membranes for DMFC application. *Prog. Polym. Sci.*, **25**, 1463-1502.
125. **Karthikeyan C.S., S.P. Nunes, L.A.S.A. Prado, M.L. Ponce, H. Silva, B. Ruffmann and K. Schulte** (2005) Polymer nanocomposite membranes for DMFC application, *J. Membr. Sci.*, **254**, 139-146.
126. **Katsoulis, D.E.** (1998) A survey of applications of polyoxometalates. *Chem. Rev.*, **98**, 359-388.
127. **Kerres, D., W. Cui and S. Reichle** (1996) New sulfonated engineering polymers via the metalation route. I. Sulfonated poly(ethersulfone) PSU Udel® via metalation-sulfination-oxidation. *J. Polym. Sci. A*, **34**, 2421-2438.
128. **Kerres, J., W. Zhang, A. Ullrich, C.-M. Tang, M. Hein, V. Gogel, T. Frey and L. Jorissen** (2002) Synthesis and characterization of polyaryl blend membranes having different composition, different covalent and/or ionic cross-linking density, and their application to DMFC. *Desalination*, **147**, 173-178.

129. **Kerres, J.A.** (2001) Development of ionomer membranes for fuel cells. *J. Membr. Sci.*, **185**, 3–27.
130. **Kerres, J.A.** (2005) Blended and cross-linked ionomer membranes for application in membrane fuel cells. *Fuel Cells*, **5**, 230-247.
131. **Kim H.K.** and **H. Chang** (2007) Organic/inorganic hybrid membranes for direct methanol fuel cells. *J. Membr. Sci.*, **288**, 188–194.
132. **Kim, D.S., G.P. Robertson, M.D. Guiver** and **Y.M. Lee** (2006) Synthesis of highly fluorinated poly(arylene ether) copolymers for proton exchange membrane materials, *J. Membr. Sci.*, **281**, 111–120.
133. **Kim, D.S., H.B. Park, J.W. Rhim** and **Y.M. Lee** (2004) Preparation and characterization of crosslinked PVA/SiO₂ hybrid membranes containing sulfonic acid groups for direct methanol fuel cell applications. *J. Membr. Sci.*, **240**, 37-47.
134. **Kim, D.S., I.C. Park, H.I. Cho, D.H. Kim, G.Y. Moon, H.K. Lee** and **J.W. Rhim** (2009) Effect of organo clay content on proton conductivity and methanol transport through crosslinked PVA hybrid membrane for direct methanol fuel cell. *J. Ind. Eng. Chem.*, **15**, 265-269.
135. **Kim, D.S., K.H. Shin, H.B. Park, Y.S. Chung, S.Y. Nam** and **Y.M. Lee** (2006) Synthesis and characterization of sulfonated poly(arylene ether sulfone) copolymers containing carboxyl groups for direct methanol fuel cells. *J. Membr. Sci.*, **278**, 428–436.
136. **Kim, H-J., Y-G. Shul** and **H. Han** (2006) Sulfonic-functionalized heteropolyacid–silica nanoparticles for high temperature operation of a direct methanol fuel cell. *J. Power Sources*, **158**, 137-142.
137. **Kim, T.K., M. Kang, Y.S. Choi, H.K. Kim, W. Lee, H. Chang** and **D. Seung** (2007) Preparation of Nafion-sulfonated clay nanocomposite membrane for direct methanol fuel cells via a film coating process. *J. Power Sources*, **165**, 1-8.
138. **Kim, Y., J.S. Lee, C.H. Rhee, H.K. Kim** and **H. Chang** (2006) Montmorillonite functionalized with perfluorinated sulfonic acid for proton-conducting organic–inorganic composite membranes. *J. Power Sources*, **162**, 180-185.
139. **Kim, Y.C., J.Y. Jeong, J.Y. Hwang, S.D. Kim, S.C. Yi** and **W.J. Kim** (2008) Incorporation of heteropoly acid, tungstophosphoric acid within MCM-41 via impregnation and direct synthesis methods for the fabrication of composite membrane of DMFC. *J. Membr. Sci.*, **325**, 252–261.
140. **Kim, Y.S., B. Einsla, M. Sankir, W. Harrison** and **B.S. Pivovar** (2006) Structure–property–performance relationships of sulfonated poly(arylene ether sulfone)s as a polymer electrolyte for fuel cell applications. *Polymer*, **47**, 4026–4035.

141. **Kim, Y.S., F. Wang, M.Hickner, T.A. Zawodzinski and J.E. McGrath** (2003) Fabrication and characterization of heteropolyacid ($\text{H}_3\text{PW}_{12}\text{O}_{40}$)/directly polymerized sulfonated poly(arylene ether sulfone) copolymer composite membranes for higher temperature fuel cell applications. *J. Membr. Sci.*, **212**, 263-282.
142. **Kim, Y.S., M.A. Hickner, L. Dong, B.S. Pivovar and J.E. McGrath** (2004) Sulfonated poly(arylene ether sulfone) copolymer proton exchange membranes: composition and morphology effects on the methanol permeability. *J. Membr. Sci.*, **243**, 317-326.
143. **Kim, Y.T., M.K. Song, K.H. Kim, S.B. Park, S.K. Min and H.W. Rhee** (2004) Nafion/ZrSPP hybrid membrane for high temperature operation of PEMFCs. *Electrochim. Acta*, **50**, 645-648.
144. **Kim, Y-T., K-H. Kim, M-K. Song and H-W. Rhee** (2006) Nafion/ZrSPP composite membrane for high temperature operation of proton exchange membrane fuel cells. *Curr. Appl. Phys.*, **6**, 612-615.
145. **Koji, N., Y. Tomonori, I. Kenji and S. Fumio** (1999) Properties and structure of poly(vinyl alcohol)/silica composites. *J. Appl. Polym. Sci.*, **74**, 133-138.
146. **Kreuer K.D.** (2001) On the development of proton conducting polymer membranes for hydrogen and methanol fuel cells. *J. Membr. Sci.*, **185**, 29–39.
147. **Kreuer, K.-D.** (1988) Fast proton transport in solids. *J. Mol. Struct.*, **177**, 265-276.
148. **Kreuer, K.D. M. Hampele, K. Dolde and A. Rabenau** (1988) Proton transport in some heteropolyacidhydrates a single crystal PFG-NMR and conductivity study. *Solid State Ionics*, **28–30**, 589-593.
149. **Kreuer, K.D., A. Fuchs, M. Ise, M. Spaeth and J. Maier** (1998) Imidazole and pyrazole-based proton conducting polymers and liquids. *Electrochim. Acta*, **43** 1281-1288.
150. **Kreuer, K.D., A. Rabenau and W. Weppner** (1982) Vehicle Mechanism. A New Model for the Interpretation of the Conductivity of Fast Proton Conductors. *Angew. Chem. Int. Ed. Engl.*, **21**, 208-209.
151. **Krishnan, P., J-S. Park and C-S. Kim** (2006) Preparation of proton-conducting sulfonated poly(ether ether ketone)/boron phosphate composite membranes by an in situ sol–gel process. *J. Membr. Sci.*, **279**, 220-229.
152. **Krishnan, P., J-S. Park, T-H. Yang, WY. Lee and C-S. Kim** (2006) Sulfonated poly(ether ether ketone)-based composite membrane for polymer electrolyte membrane fuel cells. *J. Power Sources*, **163**, 2-8.
153. **Kumar, B. and J.P. Fellner** (2003) Polymer-ceramic composite protonic conductors. *J. Power Sources*, **123**, 132–136.

154. **Kumar, G.G., P. Uthirakumar, K. S. Nahma and R.N. Elizabeth** (2009) Fabrication and electro chemical properties of poly vinyl alcohol/para toluene sulfonic acid membranes for the applications of DMFC. *Solid State Ionics*, **180**, 282–287.
155. **Kumar, G.G., D. N. Lee, P. Kim, K.S. Nahma and R.N. Elizabeth** (2008) Characterization of PVdF-HFP/Nafion/AlO[OH]_n composite membranes for direct methanol fuel cell (DMFC). *Eur Polymer J.*, **44**, 2225–2230.
156. **Küver, A. and K.P-Kamloth** (1998) Comparative study of methanol crossover across electropolymerized and commercial proton exchange membrane electrolytes for the acid direct methanol fuel cell. *Electrochim. Acta*, **43**, 2527–2535.
157. **Kwak, S-H., T-H. Yang, C-S. Kim and K.H. Yoon** (2004) Polymer composite membrane incorporated with a hygroscopic material for high-temperature PEMFC. *Electrochim. Acta*, **50**, 653-657.
158. **Lafitte, B. and P. Jannasch** *On the prospects for phosphonated polymers as proton exchange fuel cell membranes*, pp.119–185. In T.S. Zhao, K.D. Kreuer, T. Van Nguyen (eds.) *Advances in Fuel Cells*, Elsevier, 2007.
159. **Larminie, J. and A. Dicks** *Fuel cell systems explained*. John Wiley and Sons Inc., England, 2000.
160. **Lasségues, J.C.** *Mixed Inorganic-organic Systems: the Acid/Polymer Blends*, pp. 311-328. In: Colomban Ph. ed. *Proton Conductors, Solids, Membranes and Gels – Materials and Devices*, Cambridge Univ. Press, 1992.
161. **Lee, C.H., K.A. Min, H.B. Park, Y. T. Hong, B. O. Jung and Y.M. Lee** (2007) Sulfonated poly(arylene ether sulfone)–silica nanocomposite membrane for direct methanol fuel cell (DMFC). *J. Membr. Sci.*, **303**, 258–266.
162. **Lee, H-K, J-I Kim, J-H Park and T-H. Lee** (2004) A study on self-humidifying PEMFC using Pt–ZrP–Nafion composite membrane. *Electrochim. Acta*, **50**, 761-768.
163. **Lee, J. and C.S. Marvel** (1984) Polyaromatic ether-ketone sulfonamides prepared from polydiphenyl ether-ketones by chlorosulfonation and treatment with secondary amines. *J. Polym. Sci. Polym.* **22**, 295-301.
164. **Lee, J.K., W. Li and A. Manthiram** (2009) Poly(arylene ether sulfone)s containing pendant sulfonic acid groups as membrane materials for direct methanol fuel cells, *J. Membr. Sci.*, **330**, 73-79.
165. **Lee, K. and J.D. Nam** (2006) Optimum ionic conductivity and diffusion coefficient of ion-exchange membranes at high methanol feed concentrations in a direct methanol fuel cell. *J. Power Sources*, **157**, 201-206.
166. **Lee, W., A. Shibasaki, K. Saito, K. Sugita, K. Okvyama and T. Sugo** (1996) Proton Transport Through Polyethylene-Tetrafluoroethylene-

Copolymer-Based Membrane Containing Sulfonic Acid Group Prepared by RIGP. *J. Electrochem. Soc.*, **143**, 2795-2799.

167. **Li L., L. Xu and Y. Wang** (2003) Novel proton conducting composite membranes for direct methanol fuel cell. *Mater. Lett.*, **57**, 1406–1410.
168. **Li, C., G. Sun, S. Ren, J. Liu, Q. Wang, Z. Wu, H. Sun and W. Jin** (2006) Casting Nafion–sulfonated organosilica nano-composite membranes used in direct methanol fuel cells. *J. Membr. Sci.*, **272**, 50-57.
169. **Li, L. and Y. Wang** (2006) Proton conducting composite membranes from sulfonated polyethersulfone Cardo and phosphotungstic acid for fuel cell application. *J. Power Sources*, **162**, 541-546.
170. **Li, L., J. Zhang and Y. Wang** (2003) Sulfonated poly(ether ether ketone) membranes for direct methanol fuel cell. *J. Membr. Sci.*, **226**, 159–167.
171. **Li, L., J. Zhang and Y. Wang** (2003) Sulfonated polyether ether ketone membranes cured with different methods for direct methanol fuel cells. *J. Mater. Sci. Lett.*, **22**, 1595-1597.
172. **Li, Q., J.O. Jensen, R.F. Savinell and N.J. Bjerrum** (2009) High temperature proton exchange membranes based on polybenzimidazoles for fuel cells. *Prog. Polym. Sci.*, **43**, 449-477.
173. **Li, Q., R. He, J.O. Jensen and N. J. Bjerrum** (2003) Approaches and recent development of polymer electrolyte membranes for fuel cells operating above 100 °C. *Chem. Mater.*, **15**, 4896-4915.
174. **Li, S., Z. Zhou, M. Liu, W. Li, J. Ukai, K. Hase and M. Nakanishi** (2006) Synthesis and properties of imidazole-grafted hybridinorganic–organic polymer membranes. *Electrochim. Acta*, **51**, 1351-1358.
175. **Li, Y., F. Wang, J. Yang, D. Liu, A. Roy, S. Case, J. Lesko and J.E. McGrath** (2006) Synthesis and characterization of controlled molecular weight disulfonated poly(arylene ether sulfone) copolymers and their applications to proton exchange membranes. *Polymer*, **47**, 4210–4217.
176. **Liang, Z.X., T.S. Zhao and J. Prabhuram** (2006) Diphenylsilicate-incorporated Nafion[®] membranes for reduction of methanol crossover in direct methanol fuel cells. *J. Membr. Sci.*, **283**, 219-224.
177. **Lin, C.W., R. Thangamuthu and C.J. Yang** (2005) Proton-conducting membranes with high selectivity from phosphotungstic acid-doped poly(vinyl alcohol) for DMFC applications. *J. Membr. Sci.*, **253**, 23-31.
178. **Lin, C.W., R. Thangamuthu and P.H. Chang** (2005) PWA-doped PEG/SiO₂ proton-conducting hybrid membranes for fuel cell applications. *J. Membr. Sci.*, **254**, 197-205.
179. **Lin, C.W., Y.F. Huang and A.M. Kannan** (2007) Cross-linked poly(vinyl alcohol) and poly(styrene sulfonic acid-co-maleic anhydride)-based semi-

interpenetrating network as proton-conducting membranes for direct methanol fuel cells. *J. Power Sources*, **171**, 340-347.

180. **Lin, W.F., J.T. Wang and R.F. Savinell** (1997) On-line FTIR spectroscopic investigations of methanol oxidation in a direct methanol fuel cell. *J. Electrochem. Soc.*, **144** 1917-1922.
181. **Lin, Y-F., C-Y. Yen, C-C.M. Ma, S-H. Liao, C-H. Hung and Y-H. Hsiao** (2007) Preparation and properties of high performance nanocomposite proton exchange membrane for fuel cell. *J. Power Sources*, **165**, 692-700.
182. **Lindemann, M.K.** (1971) Vinyl alcohol polymers. *Encycl. Polym. Sci. Technol.*, **14**, 208-239.
183. **Ling, J. and O. Savadogo** (2004) Comparison of methanol crossover among four types of nafion membranes. *J. Electrochem. Soc.* **151**, A1604- A1610.
184. **Litt, M.H., R. Ameri, Y. Wang, R. Savinell and J. Wainwright** (1999) Polybenzimidazoles/phosphoric acid solid polymer electrolytes: Mechanical and Electrical properties. *Mater Res Soc Symp Proc.*, **548**, 313-323.
185. **Liu, B., Y.S. Kim, W. Hu, G. P. Robertson, B.S. Pivovar and M.D. Guiver** (2008) Homopolymer-like sulfonated phenyl- and diphenyl-poly(arylene ether ketone)s for fuel cell applications. *J. Power Sources*, **185**, 899-903.
186. **Liu, J.G., T.S. Zhao, Z.X. Liang and R. Chen** (2006) Effect of membrane thickness on the performance and efficiency of passive direct methanol fuel cells. *J. Power Sources*, **153**, 61-67.
187. **Liu, W., K. Ruth and G. Rusch** (2001) Membrane Durability in PEM Fuel Cells. *J. New Mater. Electrochem. Syst.*, **4**, 227-232.
188. **Livingston, D.I., P.M. Kamath and R.S. Corley** (1956) Poly- α,β,β -trifluorostyrene. *J. Polym. Sci.*, **20**, 485-490.
189. **Lobato, J., P. Cañizares, M.A. Rodrigo, J.J. Linares and A.F-Fragua** (2006) Application of Sterion[®] membrane as a polymer electrolyte for DMFCs. *Chemical Engineering Sci.*, **61**, 4773-4782.
190. **Lufrano, F., V. Baglio, P. Staiti, A.S. Arico and V. Antonucci** (2008) Polymer electrolytes based on sulfonated polysulfone for direct methanol fuel cells. *J. Power Sources*, **179**, 34-41.
191. **Lufrano, F., V. Baglio, P. Staiti, A.S. Arico and V. Antonucci** (2006) Development and characterization of sulfonated polysulfone membranes for direct methanol fuel cells. *Desalination*, **199**, 283-285.
192. **Ma, Y.L, J.S Wainright, M.H Litt and R.F Savinell** (2004) Conductivity of PBI membranes for high-temperature polymer electrolyte fuel cells. *J Electrochem Soc.*, **151**, A8-A16.

193. **Magnet, H.J.R. in: C. Berger (Ed.), *Handbook of Fuel Cell Technology*, Prentice-Hall, Englewood Cliffs, NJ, USA, 1968.**
194. **Małacka, A., J. Poźniczek, A. Micek-Ilnicka and A. Bielan'ski (1999)** Gas phase synthesis of MTBE on dodecatungstosilicic acid as the catalyst. *J. Mol. Catal. A Chem.*, **138**, 67-81.
195. **Manea, C. and M. Mulder (2002)** Characterization of polymer blends of polyethersulfone/sulfonated polysulfone and polyethersulfone/sulfonated polyetheretherketone for direct methanol fuel cell applications. *J. Membr. Sci.*, **206**, 443-453.
196. **Martinelli, A., A. Matic, P. Jacobsson, L. Börjesson, M.A. Navarra, A. Farnicola, S. Panero and B. Scrosati (2006)** Structural analysis of PVA-based proton conducting membranes. *Solid State Ionics*, **177**, 2431-2435.
197. **Martinelli, A., A. Matic, P. Jacobsson, L. Börjesson, M.A. Navarra, D. Munaò, S. Panero and B. Scrosati (2007)** A study on the state of PVA in PVDF-based proton conducting membranes by Raman spectroscopy. *Solid State Ionics*, **178**, 527-531.
198. **Martinelli, A., M.A. Navarra, A. Matic, S. Panero, P. Jacobsson, L. Börjesson and B. Scrosati (2005)** Structure and functionality of PVdF/PAN based, composite proton conducting membranes. *Electrochim. Acta*, **50**, 3992-3997.
199. **Matsuda, A., N. Nakamoto, K. Tadanaga, T. Minami and M. Tatsumisago (2006)** Operation of PEFC using composite sheets composed of phosphosilicate gels and thermally stable organic polymers. *Solid State Ionics*, **177**, 2437-2441.
200. **Mauritz, K.A. (1998)** Organic-inorganic hybrid materials: perfluorinated ionomers as sol-gel polymerization templates for inorganic alkoxides. *Mater. Sci. Eng.*, **C6**, 121-133.
201. **Mecheri, B., A. D'Epifanio, E. Traversa and S. Licoccia (2007)** Sulfonated polyether ether ketone and hydrated tin oxide proton conducting composites for direct methanol fuel cell applications. *J. Power Sources*, **169**, 247-252.
202. **Mikhailenko, S.D., S.M. Zaidi and S. Kaliaguine (2000)** Electrical properties of sulfonated polyether ether ketone/polyetherimide blend membranes doped with inorganic acids. *J. Polym. Sci. Pol. Phys.*, **38**, 1386-1395.
203. **Misono, M. (1987)** Heterogeneous catalysis by heteropoly compounds of molybdenum and tungsten. *Catal. Rev.-Sci. Eng.*, **29**, 269-321.
204. **Misono, M., N. Mizuno, K. Katamura, A. Kasai, Y. Konishi, K. Sakata, T. Okuhara and Y. Yoneda (1982)** Catalysis by heteropoly compounds. III. The structure and properties of 12-heteropolyacids of molybdenum and tungsten ($H_3PMo_{12-x}W_xO_{40}$) and their salts pertinent to heterogeneous catalysis. *Bull. Chem. Soc. Jpn.*, **55**, 400-406.

205. **Miyatake, K. and A.S. Hay** (2001) Synthesis and properties of poly(arylene ether)s bearing sulfonic acid groups on pendant phenyl rings. *J. Polym. Sci. Part A: Polym. Chem.*, **39**, 3211–3217.
206. **Nakajima H. and I. Honma** (2002) Proton-conducting hybrid solid electrolytes for intermediate temperature fuel cells. *Solid State Ionics*, **148**, 607-610.
207. **Nakamura, O., I. Ogino and T. Kodama** (1981) Temperature and humidity ranges of some hydrates of high-proton-conductive dodecamolybdophosphoric acid and dodecatungstophosphoric acid crystals under an atmosphere of hydrogen or either oxygen or air. *Solid State Ionics*, **3-4**, 347-351.
208. **Nakamura, O., T. Kodama, I. Ogino and Y. Miyake** (1979) High-conductivity solid proton conductors: dodecamolybdophosphoric acid and dodecatungstophosphoric acid crystals. *Chem. Lett. Chem. Soc. Jpn.*, **8**, 17-18.
209. **Neburchilov, V., J. Martin, H. Wang and J. Zhang** (2007) A review of polymer electrolyte membranes for direct methanol fuel cells. *J. Power Sources*, **169**, 221–238.
210. **Nguyen, T.V. and N. Vanderborgh** (1998) The rate of isothermal hydration of perfluorosulfonic acid membranes. *J. Membr. Sci.*, **143**, 235-248.
211. **Nolte, R., K. Ledjeff, M. Bauer and R. Mülhaupt** (1993) Partially sulfonated poly(arylene ether sulfone) - A versatile proton conducting membrane material for modern energy conversion technologies. *J. Membr. Sci.*, **83**, 211-220.
212. **Norddin M.N.A.M., A.F. Ismail, D. Rana, T. Matsuura, A. Mustafa and A.T-Mohammadi** (2008) Characterization and performance of proton exchange membranes for direct methanol fuel cell: Blending of sulfonated poly(ether ether ketone) with charged surface modifying macromolecule. *J. Membr. Sci.*, **323**, 404–413.
213. **Noshay, A. and J.E. McGrath** *Block Copolymers: Overview and Critical Survey*, Academic Press, New York, 1977.
214. **Nouel, K.M. and P.S. Fedkiw** (1998) Nafion[®]-based composite polymer electrolyte membranes. *Electrochim. Acta*, **43**, 2381-2387.
215. **Nunes, S.P., B. Ruffmann, E. Rikowski, S. Vetter and K. Richau** (2002) Inorganic modification of proton conductive polymer membranes for direct methanol fuel cells. *J. Membr. Sci.*, **203**, 215-225.
216. **Okuhara, T., N. Mizuno and M. Misono** (1996) Catalytic chemistry of heteropoly compounds. *Adv. Catal.*, **41**, 113-252.
217. **Okuhara, T., S. Tatematsu, K.Y. Lee and M. Misono** (1989) Catalysis by heteropoly compounds. XII. Absorption properties of 12-tungstophosphoric acid and its salts. *Bull. Chem. Soc. Jpn.*, **62**, 717-723.

218. **Othman, M.H.D., A.F. Ismail and A. Mustafa** (2007) Proton conducting composite membrane from sulfonated poly (ether ether ketone) and boron orthophosphate for direct methanol fuel cell application. *J. Membr. Sci.*, **299**, 156–165.
219. **Panero, S., P. Fiorenza, M.A. Navarra, J. Romanowska and B. Scrosati** (2005) Silica-added, hybrid poly(vinyl alcohol) membranes for fuel cell application. *J. Electrochem. Soc.*, **152**, A2400-A2405.
220. **Parent, M.A. and J.B. Moffat** (1998) Cation/anion effects on the acidic strengths of the stoichiometric and nonstoichiometric microporous thallium (I) salts of 12-tungstophosphoric, 12-tungstosilicic, and 12-molybdophosphoric acids from the isomerization of 1-butene. *J. Catal.*, **177**, 335-342.
221. **Park H.B., H.S. Shin, Y.M. Lee and J.W. Rhim** (2005) Annealing effect of sulfonated polysulfone ionomer membranes on proton conductivity and methanol transport. *J. Membr. Sci.*, **247**, 103–110.
222. **Park Y-S. and Y. Yamazaki** (2005) Low methanol permeable and high proton-conducting Nafion/calcium phosphate composite membrane for DMFC. *Solid State Ionics*, **176**, 1079-1089.
223. **Park Y-S. and Y. Yamazaki** (2006) Low water/methanol permeable Nafion/CHP organic–inorganic composite membrane with high crystallinity. *Eur. Polymer J.*, **42**, 375-387.
224. **Park, Y-il. and M. Nagai** (2001) Proton exchange nanocomposite membranes based on 3-glycidoxypropyltrimethoxysilane, silicotungstic acid and α -zirconium phosphate hydrate. *Solid State Ionics*, **145**, 149-160.
225. **Penner, R.M. and C.R. Martin** (1985) Ion transporting composite membranes. I. Nafion[®]-impregnated Gore-Tex. *J. Electrochem. Soc.*, **132**, 514–515.
226. **Pivovar B.S, Y.X Wang and E.L Cussler** (1999) Pervaporation membranes in direct methanol fuel cells. *J Membr Sci.*, **154**, 155-162.
227. **Polak, A.J, S.P-Weeks and A.J. Beuhler** (1986) Applications of novel proton-conducting polymers to hydrogen sensing. *Sensors and Actuators*, **9**, 1-7.
228. **Połtarzewski, Z., W. Wieczorek, J. Przyłuski and V. Antonucci** (1999) Novel proton conducting composite electrolytes for application in methanol fuel cells. *Solid State Ionics*, **119**, 301-304.
229. **Ponce, M.L., L. Prado, B. Ruffmann, K. Richau, R. Mohr and S.P. Nunes** (2003) Reduction of methanol permeability in polyetherketone–heteropolyacid membranes. *J. Membr. Sci.*, **217**, 5-15.
230. **Ponce, M.L., L.A.S. de A. Prado, V. Silva and S.P. Nunes** (2004) Membranes for direct methanol fuel cell based on modified heteropolyacids. *Desalination*, **162**, 383-391.

231. **Qiao, J., T. Hamaya and T. Okada** (2005) Chemically modified poly(vinylalcohol)-poly (2-acrylamido -2-methyl-1-propanesulfonic acid) as a novel proton-conducting fuel cell membrane. *Chem. Mater.*, **17**, 2413-2421.
232. **Qiao, J., T. Hamaya and T. Okada** (2005) New highly proton conductive polymer membranes poly(vinyl alcohol)-2-acrylamido-2-methyl-1-propanesulfonic acid (PVA-PAMPS). *J. Mater. Chem.*, **15**, 4414-4423.
233. **Qinfeng, L., H.A. Hjirker and N.J. Bjerrum** (2001) Phosphoric acid doped polybenzimidazole membranes. *J. Appl. Electrochem.*, **31**, 773-779.
234. **Ramani, V., H.R. Kunz and J.M. Fenton** (2004) Investigation of Nafion[®]/HPA composite membranes for high temperature/low relative humidity PEMFC operation. *J. Membr. Sci.*, **232**, 31-44.
235. **Ramani, V., H.R. Kunz and J.M. Fenton** (2005) Stabilized heteropolyacid/Nafion[®] composite membranes for elevated temperature/low relative humidity PEFC operation. *Electrochim. Acta*, **50**, 1181-1187.
236. **Ramani, V., H.R. Kunz and J.M. Fenton** (2006) Metal dioxide supported heteropolyacid/Nafion[®] composite membranes for elevated temperature/low relative humidity PEFC operation. *J. Membr. Sci.*, **279**, 506-512.
237. **Ramani, V., HR. Kunz and J.M. Fenton** (2004) Investigation of Nafion[®]/HPA composite membranes for high temperature/low relative humidity PEMFC operation. *J. Membr. Sci.*, **232**, 31-44.
238. **Rao, N., T.P. Andersen and P. Ge** (1994) Tin mordenite membranes for direct methanol fuel cells. *Solid State Ionics*, **72**, 334-337.
239. **Regina, A., E. Fontananova, E. Drioli, M. Casciola, M. Sganappa and F. Trotta** (2006) Preparation and characterization of sulfonated PEEK-WC membranes for fuel cell applications: A comparison between polymeric and composite membranes. *J. Power Sources*, **160**, 139-147.
240. **Reichman, S., T. Duvdevani, A. Aharon, M. Philosoph, D. Golodnitsky and E. Peled** (2006) A novel PTFE-based proton-conductive membrane. *J. Power Sources*, **153**, 228-233.
241. **Ren, S., C. Li, X. Zhao, Z.Wu, S.Wang, G. Sun, Q. Xin and X. Yang** (2005) Surface modification of sulfonated poly (ether ether ketone) membranes using Nafion solution for direct methanol fuel cells. *J. Membr. Sci.*, **247**, 59-63.
242. **Ren, S., G. Sun, C. Li, Z. Liang, Z. Wu, W. Jin, X. Qin and X. Yang** (2006) Organic silica/Nafion[®] composite membrane for direct methanol fuel cells. *Fuel Cells Bull.*, **2006**, 12-16.
243. **Rhee, C.H., Y. Kim, J.S. Lee, H.K. Kim and H. Chang** (2006) Synthesis and characterization of silicotungstic acid based organic-inorganic nanocomposite membrane. *J. Power Sources*, **159**, 1015-1024.

244. **Rikukawa, M. and K. Sanui** (2000) Proton conducting polymer electrolyte membranes based on hydrocarbon polymers. *Prog. Polym. Sci.*, **25** 1463–1502.
245. **Rikukawa, M., D. Inagaki, K. Kaneko, Y. Takeoka, I. Ito, Y. Kanzaki and K. Sanui** (2005) Proton conductivity of smart membranes based on hydrocarbon polymers having phosphoric acid groups. *J. Mol. Struct.* **739**, 153-161.
246. **Robertson, G.P., S.D. Mikhailenko, K. Wang, P. Xing, M.D. Guiver and S. Kaliaguine** (2003) Casting solvent interactions with sulfonated poly(ether ether ketone) during proton exchange membrane fabrication. *J. Membr. Sci.*, **219**, 113-121.
247. **Romero P.G., J.A. Asensio and S. Borrós** (2005) Hybrid proton-conducting membranes for polymer electrolyte fuel cells: Phosphomolybdic acid doped poly(2,5-benzimidazole)—(ABPBI-H₃PMo₁₂O₄₀). *Electrochim. Acta*, **50**, 4715-4720.
248. **Rozière, J. and D.J. Jones** (2003) Non-fluorinated polymer materials for proton exchange membrane fuel cells. *Annu. Rev. Mater. Res.*, **33**, 503-555.
249. **Roziere, J., D.J. Jones, M. Marrony, X. Glipa and B. Mula** (2001) On the doping of sulfonated polybenzimidazole with strong bases. *Solid State Ionics*, **145** 61-68.
250. **Ruffmann, B., H. Silva, B. Schulte and S.P. Nunes** (2003) Organic/inorganic composite membranes for application in DMFC. *Solid State Ionics*, **162-163**, 269-275.
251. **Rykova, A.I., T.M. Burkat and V.N. Pak** (2003) Hydrate and alcoholate forms of phosphomolybdic heteropolyacid and their formation under conditions of isothermal sorption of water, methanol, and ethanol vapors. *Russ. J. Gen. Chem.*, **73**, 697-700.
252. **Saarinen, V., T. Kallio, M. Paronen, P. Tikkanen, E. Rauhala and K. Kontturi** (2005) New ETFE-based membrane for direct methanol fuel cell. *Electrochim. Acta*, **50** 3453-3460.
253. **Saccà, A., A. Carbone, E. Passalacqua, A. D'Epifanio, S. Licoccia, E. Traversa, E. Sala, F. Traini and R. Ornelas** (2005) Nafion–TiO₂ hybrid membranes for medium temperature polymer electrolyte fuel cells (PEFCs). *J. Power Sources*, **152**, 16-21.
254. **Saccà, A., I. Gatto, A. Carbone, R. Pedicini and E. Passalacqua** (2006) ZrO₂–Nafion composite membranes for polymer electrolyte fuel cells (PEFCs) at intermediate temperature. *J. Power Sources*, **163**, 47-51.
255. **Sadrabadi M.M.H., S.H. Emami and H. Moaddel** (2008) Preparation and characterization of nanocomposite membranes made of poly (2,6-dimethyl-1,4-phenylene oxide) and montmorillonite for direct methanol fuel cells. *J. Power Sources*, **183**, 551-556.

256. **Sahu, A.K., G. Selvarani, S.D. Bhat, S. Pitchumani, P. Sridhar, A.K. Shukla, N. Narayanan, A. Banerjee and N. Chandrakumar** (2008) Effect of varying poly(styrene sulfonic acid) content in poly(vinyl alcohol)-poly(styrene sulfonic acid) blend membrane and its ramification in hydrogen-oxygen polymer electrolyte fuel cells. *J. Membr. Sci.*, **319**, 298-305.
257. **Samms S.R, S. Wasmus and R.F. Savinell** (1996) Thermal stability of proton conducting acid doped polybenzimidazole in simulated fuel cell environments. *J Electrochem. Soc.*, **143**, 1225-1232.
258. **Sancho, T., J. Lemus, M. Urbiztondo, J. Soler and M.P. Pina** (2008) Zeolites and zeotype materials as efficient barriers for methanol cross-over in DMFCs. *Micropor. Mesopor. Mat.*, **115**, 206–213.
259. **Sauk, J., J. Byun and H. Kim** (2005) Composite Nafion/polyphenylene oxide (PPO) membranes with phosphomolybdic acid (PMA) for direct methanol fuel cells. *J. Power Sources*, **143** 136-141.
260. **Savado, O.** (1998) Emerging membranes for electrochemical systems: (I) solid polymer electrolyte membranes for fuel cell systems. *J. New Mater. Electrochem. Syst.*, **1**, 47-66.
261. **Savado, O.** (2004) Emerging membranes for electrochemical systems: Part II. High temperature composite membranes for polymer electrolyte fuel cell (PEFC) applications. *J. Power Sources*, **127**, 135–161.
262. **Savinell R.F and M.H. Litt** (1996) Proton conducting polymers used as membranes. (Case Western Reserve University), *US patent*, 5,525,436.
263. **Savinell, R., E. Yeager, D. Tryk, U. Landau, J. Wainright, D. Weng, K. Lux, M. Litt and C. Rogers** (1994) A polymer electrolyte for operation at temperatures up to 200°C. *J. Electrochem. Soc.*, **141**, L46-L48.
264. **Schechter, A. and R.F. Savinell** (2002) Imidazole and 1-methyl imidazole in phosphoric acid doped polybenzimidazole, electrolyte for fuel cells. *Solid State Ionics*, **147**, 181-187.
265. **Schultz, T., S. Zhou and K. Sundmacher** (2001) Current status of and recent developments in the direct methanol fuel cell. *Chem. Eng. Technol.*, **24**, 1223-1233.
266. **Schuster, M., W.H. Meyer, G. Wegner, H.G. Herz, M. Ise, M. Schuster, K.D. Kreuer and J. Maier** (2001) Proton mobility in oligomer-bound proton solvents: imidazole immobilization via flexible spacers. *Solid State Ionics*, **145**, 85-92.
267. **Scott, K., W. M. Taama and P. Argyropoulos** (2000) Performance of the direct methanol fuel cell with radiation-grafted polymer membranes. *J. Membr. Sci.*, **171**, 119-130.

268. **Sen, U., S.U. Celik, A. Ata and A. Bozkurt** (2008) Anhydrous proton conducting membranes for PEM fuel cells based on Nafion/Azole composites. *Int. J. Hydrogen Energy*, **33**, 2808–2815.
269. **Shahi V.K.** (2007) Highly charged proton-exchange membrane: Sulfonated poly(ether sulfone)-silica polyelectrolyte composite membranes for fuel cells. *Solid State Ionics*, **177**, 3395–3404.
270. **Shang, X., X. Li, M. Xiao and Y. Meng** (2006) Synthesis and characterization of sulfonated fluorene-containing poly(arylene ether ketone) for high temperature proton exchange membrane. *Polymer*, **47**, 3807–3813.
271. **Shanmugam, S., B. Viswanathan and T.K. Varadarajan** (2006) Synthesis and characterization of silicotungstic acid based organic–inorganic nanocomposite membrane. *J. Membr. Sci.*, **275** 105-109.
272. **Shao, C. I., H.Y. Kim, J. Gong, B. Ding, D.R. Lee and S.J. Park** (2003) Fiber mats of PVA/silica hybrid via electrospinning. *Mater. Lett.*, **57**, 1579-1584.
273. **Shao, P.L., K.A. Mauritz and R.B. Moore** (1995) {Perfluorosulfonate ionomer}/[Mixed inorganic oxide] nanohybrids via polymer-in situ sol-gel chemistry. *Chem. Mater.*, **7**, 192-200.
274. **Shao, Z.-G., H. Xu, M. Li and I.-M. Hsing** (2006) Hybrid Nafion–inorganic oxides membrane doped with heteropolyacids for high temperature operation of proton exchange membrane fuel cell. *Solid State Ionics*, **177**, 779-785.
275. **Shao, Z.-G., X. Wang and I.-M. Hsing** (2002) Composite Nafion/polyvinyl alcohol membranes for the direct methanol fuel cell. *J. Membr. Sci.*, **210**, 147–153.
276. **Shen, M., S. Roy, J.W. Kuhlmann, K. Scott, K. Lovell and J.A. Horsfall** (2005) Grafted polymer electrolyte membrane for direct methanol fuel cells. *J. Membr. Sci.*, **251**, 121–130.
277. **Shen, Y., X. Qiu, J. Shen, J. Xi and W. Zhu** (2006) PVDF-g-PSSA and Al₂O₃ composite proton exchange membranes. *J. Power Sources*, **161**, 54-60.
278. **Shikata, S., T. Okuhara and M. Misono** (1995) Catalysis by hetropoly compounds. Part XXVI I. Gas phase synthesis of methyl tert-butyl ether over heteropolyacids. *J. Mol. Catal. A Chem.*, **100**, 49-49.
279. **Shim, J., H.Y. Ha, H.S.A. Hong and I.H. Oh** (2002) Characteristics of the Nafion ionomer-impregnated composite membrane for polymer electrolyte fuel cells. *J. Power Sources*, **109**, 412-417.
280. **Silva, V.S., B. Ruffmann, H. Silva, V.B. Silva, A. Mendes, L.M. Madeira and S. Nunes** (2006) Zirconium oxide hybrid membranes for direct methanol fuel cells—Evaluation of transport properties. *J. Membr. Sci.*, **284**, 137-144.

281. **Silva, V.S., B. Ruffmann, S. Vetter, A. Mendes, L.M. Madeira and S.P. Nunes** (2005) Characterization and application of composite membranes in DMFC. *Catal. Today*, **104**, 205-212.
282. **Simon, W.E. and D.L. Nored** (1987) Manned spacecraft electrical power systems. *Proc. IEEE.*, **75**, 277-307.
283. **Slade, S., S.A. Campbell, T.R. Ralph and F.C. Walsh** (2002) Ionic conductivity of an extruded Nafion 1100 EW series of membranes. *J. Electrochem. Soc.*, **149**, A1556–A1564.
284. **Smitha, B., S. Sridhar and A.A. Khan** (2005) Solid polymer electrolyte membranes for fuel cell applications-a review. *J. Membr. Sci.*, **259**, 10–26
285. **Søgaard, S.R., Q. Huan, P. Lund, A. Donnadio, M. Casciola and E.M. Skou** (2007) Preparation and analysis of new proton conducting membranes for fuel cells. *Solid State Ionics*, **178**, 493-500.
286. **Son, D-H., R.K. Sharma, Y-G. Shul and H. Kim** (2007) Preparation of Pt/zeolite–Nafion composite membranes for self-humidifying polymer electrolyte fuel cells. *J. Power Sources*, **165**, 733-738.
287. **Song, M.-K., S-B. Park, Y-T. Kim, K-H. Kim, S-K. Min and H-W. Rhee** (2004) Characterization of polymer-layered silicate nanocomposite membranes for direct methanol fuel cells. *Electrochim. Acta*, **50**, 639–643.
288. **Springer, T.E. and S. Gottesfeld** (1993) Water uptake by and transport through Nation[®] 117 membranes. *J. Electrochem. Soc.*, **140**, 1041-1047.
289. **Staiti, P.** (2001) Proton conductive membranes constituted of silicotungstic acid anchored to silica-polybenzimidazole matrices. *J. New Mater. Electrochem. Syst.*, **4**, 181-186.
290. **Staiti, P. and M. Minutoli** (2001) Influence of composition and acid treatment on proton conduction of composite polybenzimidazole membranes. *J. Power Sources*, **94**, 9-13.
291. **Staiti, P., A.S. Aricò, V. Baglio, F. Lufrano, E. Passalacqua and V. Antonucci** (2001) Hybrid Nafion–silica membranes doped with heteropolyacids for application in direct methanol fuel cells, *Solid State Ionics*, **145**, 101-107.
292. **Staiti, P., M. Minutoli and S. Hocevar** (2000) Membranes based on phosphotungstic acid and polybenzimidazole for fuel cell application. *J. Power Sources*, **90**, 231-235.
293. **Staiti, P., S. Hocevar and N. Giordano** (1997) Fuel cells with H₃PW₁₂O₄₀.29H₂O as solid electrolyte. *Int. J. Hydrogen Energy*, **22**, 809-814.
294. **Steiner, P. and R. Sandor** (1991) Polybenzimidazole prepreg: improved elevated temperature properties with autoclave processability. *High Perform. Polym.*, **3**, 139-150.

295. **Sun, J., L.R. Jordan, M. Forsyth and D.R. MacFarlane** (2001) Acid–Organic base swollen polymer membranes. *Electrochim. Acta*, **46**, 1703–1708.
296. **Surampudi, S., S.R. Narayanan, E. Vamos, H. Frank, G. Halpert, A. LaConti, J. Kosek, G.K.S. Prakash and G.A. Olah** (1994) Advances in direct oxidation methanol fuel cells. *J. Power Sources*, **47**, 377–385.
297. **Tanaka, R., H. Yamamoto, A. Shono, K. Kubo and M. Sakurai** (2000) Proton conducting behavior in non-crosslinked and crosslinked polyethylenimine with excess phosphoric acid. *Electrochim. Acta*, **45**, 1385–1389.
298. **Tay, S., X. Zhang, Z. Liu, L. Hong and S.H. Chan** (2008) Composite Nafion® membrane embedded with hybrid nanofillers for promoting direct methanol fuel cell performance. *J. Membr. Sci.*, **321**, 139–145.
299. **Tazi, B. and O. Savadogo** (2000) Parameters of PEM fuel-cells based on new membranes fabricated from Nafion®, silicotungstic acid and thiophene. *Electrochim. Acta*, **45**, 4329–4339.
300. **Tezuka, T., K. Tadanaga, A. Matsuda, A. Hayashi and M. Tatsumisago** (2005) Utilization of glass papers as a support for proton conducting inorganic–organic hybrid membranes from 3-glycidoxypropyltrimethoxysilane, tetraalkoxysilane and orthophosphoric acid. *Solid State Ionics*, **176**, 3001–3004.
301. **Tricoli, V., N. Carretta and M. Bartolozzi** (2000) A comparative investigation of proton and methanol transport in fluorinated ionomeric membranes. *J. Electrochem. Soc.*, **147**, 1286–1290.
302. **Tripathi, B.P., M. Kumar and V.K. Shahi** (2009) Highly stable proton conducting nanocomposite polymer electrolyte membrane (PEM) prepared by pore modifications: An extremely low methanol permeable PEM. *J. Membr. Sci.*, **327**, 145–154.
303. **Tutas, M., M. Saglam, M. Yuksel and C. Guler** (1987) Investigation of the thermal decomposition kinetics of polyacrylamide using a dynamic TG technique. *thermochim. Acta*, **111**, 121–126.
304. **Ulbricht, M.** (2004) Membrane separations using molecularly imprinted polymers. *J. Chromatogr. B*, **804**, 113–125.
305. **Ukshe E.A., L.S. Leonova and A.I. Korosteleva** (1989) Protonic conduction in heteropoly compounds. *Solid State Ionics*, **36**, 219–223.
306. **Vaivars, G., N.W. Maxakato, T. Mokrani, L. Petrik, J. Klavins, G. Gericke and V. Linkov** (2004) Zirconium phosphate based inorganic direct methanol fuel cell. *Mater. Sci.*, **10**, 162–165.
307. **Vakulenko, A., Y. Dobrovolsky, L. Leonova, A. Karelin, A. Kolesnikova and N. Bukun** (2000) Protonic conductivity of neutral and acidic silicotungstates. *Solid State Ionics*, **136–137**, 285–290.

308. **Varga, G.M., E. Papaconstation and M.T. Pope (1970)** Heteropoly blues. IV. Spectroscopic and magnetic properties of some reduced polytungstates. *Inorg. Chem.*, **9**, 662- 667.
309. **Vargas, M.A., R.A. Vargas and B-E. Mellander (1999)** New proton conducting membranes based on PVAL/H₃PO₂/H₂O. *Electrochimi. Acta*, **44**, 4227-4232.
310. **Verbrugge, M.W. (1989)** Methanol diffusion in perfluorinated ion-exchange membranes. *J. Electrochem. Soc.*, **136**, 417-423.
311. **Vernon, D.R., F. Meng, S.F. Dec, D.L. Williamson, J.A. Turner and A.M. Herring (2005)** Synthesis, characterization, and conductivity measurements of hybrid membranes containing a mono-lacunary heteropolyacid for PEM fuel cell applications. *J. Power Sources*, **139**, 141-151.
312. **Viswanathan, B. and M. Aulice Scibioh** *Fuel cells – Principles and applications*. University Press (India) Private Limited, 2006.
313. **Viswanathan, B. and M. Helen (2007)** Is nafion, the only choice? *Bull. Catal. Soc. India*, **6**, 50-66.
314. **Wainright J.S, J.T Wang, D. Weng, R.F Savinell and M. Litt (1995)** Acid-doped polybenzimidazoles - A new polymer electrolyte. *J Electrochem. Soc.*, **142**, L121-L123.
315. **Wakizoe, M., O.A. Velez and S. Srinivasan (1995)** Analysis of proton exchange membrane fuel cell performance with alternate membranes. *Electrochim. Acta*, **40**, 335-344.
316. **Wang, F., A.H. Michael, S.K. Yu, A. Thomas, Zawodzinski and J.E. McGrath (2002)** Direct polymerization of sulfonated poly(arylene ether sulfone) random (statistical) copolymers: candidates for new proton exchange membranes. *J. Membr. Sci.*, **197**, 231-242.
317. **Wang, F., M. Hickner, Y.S. Kim, T.A. Zawodzinski and J.E. McGrath (2002)** Direct polymerization of sulfonated poly(arylene ether sulfone) random (statistical) copolymers: candidates for new proton exchange membranes. *J. Membr. Sci.*, **197**, 231–242.
318. **Wang, F., T. Chen, J. Xu, T. Liu, H. Jiang, Y. Qi, S. Liu and X. Li (2006)** Synthesis and characterization of poly(arylene ether ketone) (co)polymers containing sulfonate groups. *Polymer*, **47**, 4148–4153.
319. **Wang, J., X. Zheng, H. Wu, B. Zheng, Z. Jiang, X. Hao and B. Wang (2008)** Effect of zeolites on chitosan/zeolite hybrid membranes for direct methanol fuel cell. *J. Power Sources*, **178**, 9–19.
320. **Wang, J., Z. Yue and J. Economy (2007)** Preparation of proton-conducting composite membranes from sulfonated poly(ether ether ketone) and polyacrylonitrile. *J. Membr. Sci.*, **291**, 210–219.

321. **Wang, J.T., R.F. Savinell, J. Wainright, M. Litt and H. Yu** (1996) A H_2/O_2 fuel cell using acid doped polybenzimidazole as polymer electrolyte. *Electrochim. Acta*, **41**, 193-197.
322. **Wang, J.T., S. Wasmus and R.F. Savinell** (1996) Real-time mass spectrometric study of the methanol crossover in a direct methanol fuel cell. *J. Electrochem. Soc.*, **143**, 1233-1239.
323. **Wang, J.T., T. Wasmus, R.F. Savinell and M. Litt** (1996) A direct methanol fuel cell using acid-doped polybenzimidazole as polymer electrolyte. *J. Appl. Electrochem.*, **26**, 751-756.
324. **Wang, L., B.L. Yi, H.M. Zhang and D.M. Xing** (2007) $CS_{2.5}H_{0.5}PWO_{40}/SiO_2$ as addition self-humidifying composite membrane for proton exchange membrane fuel cells. *Electrochim. Acta*, **52**, 5479-5483.
325. **Wang, L., D.M. Xing, Y.H. Liu, Y.H. Cai, Z.-G. Shao, Y.F. Zhai, H.X. Zhong, B.L. Yi and H.M. Zhang** (2006) Pt/SiO₂ catalyst as an addition to Nafion/PTFE self-humidifying composite membrane. *J. Power Sources*, **161**, 61-67.
326. **Wang, L., Y.Z. Meng, S.J. Wang, X.H. Li and M. Xiao** (2005) Synthesis and properties of sulfonated poly(arylene ether) containing tetraphenylmethane moieties for proton-exchange membrane. *J. Polym. Sci. Part A: Polym. Chem.*, **43**, 6411-6418.
327. **Wasmus, S., A. Valeriu, G.D. Mateescu, D.A. Tryk and R.F. Savinell** (1995) Characterization of H₃PO₄-equilibrated Nafion[®] 117 membranes using ¹H and ³¹P NMR spectroscopy. *Solid State Ionics*, **80**, 87-92.
328. **Wasmus, S., B.A. Dauch, H. Moadel, P.L. Rinaldi, M.H. Litt, C. Rogers, A. Valeriu, G.D. Mateescu, D.A. Tryk and R.F. Savinell** (1995) *Proceedings of the 187th Electrochemical Society Meeting Reno*, Ext. Abstract 466, NV, May 21-26.
329. **Watanabe, M.** (1995) Solid polymer electrolyte fuel cell. *US Patent*, 5,472,799.
330. **Watanabe, M., H. Uchida, Y. Seki, M. Emori and P. Stonehart** (1996) Self-humidifying polymer electrolyte membranes for fuel cells. *J. Electrochem. Soc.*, **143**, 3847-3852.
331. **Weeks, S.P, J.J. Zupancic and J.R. Swedo** (1988) Proton conducting interpenetrating polymer networks. *Solid State Ionics*, **31**, 117-125.
332. **Wei, J., C. Stone and A.E. Steck** (1995) Trifluorostyrene and substituted trifluorostyrene copolymeric compositions and ion-exchange membranes formed therefrom. *US Patent*, 5,422,411.
333. **Wei, J., C. Stone and A.E. Steck** (1995) Trifluorostyrene and substituted trifluorostyrene copolymeric compositions and ion-exchange membranes formed therefrom. *Ballard Power Systems*, WO95/08581.

334. **Weng, D., J.S Wainright, U. Landau and R.F Savinell** (1996) Electro-osmotic drag coefficient of water and methanol in polymer electrolytes at elevated temperatures. *J. Electrochem. Soc.*, **143**, 1260-1263.
335. **Wieczorek, W. and J.R. Stevens** (1996) Proton transport in polyacrylamide based hydrogels doped with H_3PO_4 or H_2SO_4 . *Polymer*, **38**, 2057-2065.
336. **Woo, M.H, O. Kwon, S. H. Choi, M. Zi Hong, H-W. Ha and K. Kim** (2006) Zirconium phosphate sulfonated poly (fluorinated arylene ether)s composite membranes for PEMFCs at 100–140 °C. *Electrochim. Acta*, **51**, 6051-6059.
337. **Wu, C-S, F-Y Lin, C-Y Chen and P.P. Chu** (2006) A polyvinyl alcohol/p-sulfonate phenolic resin composite proton conducting membrane. *J. Power Sources*, **160**, 1204–1210.
338. **Wu, H., B. Zheng, X. Zheng, J. Wang, W. Yuan and Z. Jiang** (2007) Surface-modified Y zeolite-filled chitosan membrane for direct methanol fuel cell. *J. Power Sources*, **173**, 842–852.
339. **Xie G. and T. Okada** (1995) Water transport behavior in Nafion-117 membranes. *J. Electrochem Soc.*, **142**, 3057-3062.
340. **Xing, B. and O. Savadogo** (1999) The effect of acid doping on the conductivity of polybenzimidazole (PBI). *J. New. Mater. Electrochem. Syst.*, **2**, 95-101.
341. **Xing, B. and O. Savadogo** (2000) Hydrogen/oxygen polymer electrolyte membrane fuel cells (PEMFCs) based on alkaline-doped polybenzimidazole (PBI). *Electrochem. Commun.*, **2** 697-702.
342. **Xing, D., H. Zhang, L. Wang, Y. Zhai and B. Yi** (2007) Investigation of the Ag-SiO₂/sulfonated poly(biphenyl ether sulfone) composite membranes for fuel cell. *J. Membr. Sci.*, **296**, 9-14.
343. **Xu, W., C. Liu, X. Xue, Y. Su, Y. Lv, W. Xing and T. Lu** (2004) New proton exchange membranes based on poly (vinyl alcohol) for DMFCs. *Solid State Ionics*, **171**, 121-127.
344. **Yang T.** (2008) Preliminary study of SPEEK/PVA blend membranes for DMFC applications. *Int. J. Hydrogen Energy*, **33**, 6772-6779.
345. **Yang, C., P. Costamagna, S. Srinivasan, J. Benziger and A.B. Bocarsly** (2001) Approaches and technical challenges to high temperature operation of proton exchange membrane fuel cells. *J. Power Sources*, **103**, 1–9.
346. **Yang, C., S. Srinivasan, A.S. Aric`o, P. Cret`i and V. Baglio** (2001) Composite Nafion/Zirconium Phosphate Membranes for Direct Methanol Fuel Cell Operation at High Temperature. *Electrochem. Solid-State Lett.*, **4**, A31–A34.

347. **Yang, C-C.** (2007) Synthesis and characterization of the cross-linked PVA/TiO₂ composite polymer membrane for alkaline DMFC. *J. Membr. Sci.*, **288**, 51-60.
348. **Yang, C-C., S-J. Chiu and C-T. Lin** (2008) Electrochemical performance of an air-breathing direct methanol fuel cell using poly(vinyl alcohol)/hydroxyapatite composite polymer membrane. *J. Power Sources*, **177**, 40-49.
349. **Yang, C-C., Y-J. Lee and J.M. Yang** (2009) Direct methanol fuel cell (DMFC) based on PVA/MMT composite polymer membranes. *J. Power Sources*, **188**, 30-37.
350. **Yang, J.M., H.Z. Wang and C.C. Yang** (2008) Modification and characterization of semi-crystalline poly(vinyl alcohol) with interpenetrating poly(acrylic acid) by UV radiation method for alkaline solid polymer electrolytes membrane. *J Membr. Sci.*, **322**, 74-80.
351. **Yang, T.** (2008) Preliminary study of SPEEK/PVA blend membranes for DMFC applications. *Int. J. Hydrogen Energy*, **33**, 6772 – 6779.
352. **Yeom, C-K and K-H Lee** (1996) Pervaporation separation of water-acetic acid mixtures through poly(vinyl alcohol) membranes crosslinked with glutaraldehyde. *J. Membr. Sci.*, **109**, 257-265.
353. **Yong-Il, P. and N. Masayuki** (2001) Proton exchange nanocomposite membranes based on 3-glycidoxypropyltrimethoxysilane, silicotungstic acid and α -zirconium phosphate hydrate. *Solid State Ionics*, **145**, 149-160.
354. **Yoshikawa, M., K. Tsubouchi, M.D. Guiver and G.P. Robertson** (1999) Modified polysulfone membranes. III. Pervaporation separation of benzene-cyclohexane mixtures through carboxylated polysulfone membranes. *J. Appl. Polym. Sci.*, **74**, 407-412.
355. **Yoshitake, M., Y. Kunisa, E. Endoh and E. Yanagisawa** (2005) Solid polymer type fuel cell and production method thereof. *US Patent*, 6,933,071.
356. **Zadowzinski, T.A., J. Davey, J. Valerio and S. Gottesfeld** (1995) The water content dependence of electro-osmotic drag in proton conducting polymer electrolytes. *Electrochim. Acta*, **40**, 297-302.
357. **Zaidi, S.M.J.** (2005) Preparation and characterization of composite membranes using blends of SPEEK/PBI with boron phosphate. *Electrochim. Acta*, **50**, 4771-4777.
358. **Zaidi, S.M.J. and M.I. Ahmad** (2006) Novel SPEEK/heteropolyacids loaded MCM-41 composite membranes for fuel cell applications. *J. Membr. Sci.*, **279**, 548-557.
359. **Zaidi, S.M.J., S.D. Mikhailenko, G.P. Robertson, M.D. Guiver and S. Kaliaguine** (2000) Proton conducting composite membranes from polyether

ether ketone and heteropolyacids for fuel cell applications. *J. Membr. Sci.*, **173**, 17-34.

360. **Zawodzinski, T.A., C. Derouin, S. Radzinski, R.J. Sherman, V.T. Smith, T.E. Springer and S. Gottesfeld** (1993) Water-uptake by and transport through Nafion[®] 117 membranes. *J. Electrochem. Soc.*, **140**, 1041–1047.
361. **Zawodzinski, T.A., M. Neeman, L.O. Sillerud and S. Gottesfeld** (1991) Determination of water diffusion coefficients in perfluorosulfonate ionomeric membranes. *J. Phys. Chem.*, **95**, 6040–6044.
362. **Zeng, R., Y. Wang, S. Wang and P.K. Shen** (2007) Homogeneous synthesis of PFSI/silica composite membranes for PEMFC operating at low humidity. *Electrochim. Acta*, **52**, 3895-3900.
363. **Zhai Y., H. Zhang, Y. Zhang and D. Xing** (2007) A novel H₃PO₄/Nafion–PBI composite membrane for enhanced durability of high temperature PEM fuel cells. *J. Power Sources*, **169**, 259-264.
364. **Zhai, Y., H. Zhang, J. Hu and B. Yi** (2006) Preparation and characterization of sulfated zirconia (SO₄²⁻/ZrO₂)/Nafion composite membranes for PEMFC operation at high temperature/low humidity. *J. Membr. Sci.*, **280**, 148-155.
365. **Zhang, H., X. Fan, J. Zhang and Z. Zhou** (2008) Modification research of sulfonated PEEK membranes used in DMFC. *Solid State Ionics*, **179**, 1409–1412.
366. **Zhang, Y., H. Zhang, X. Zhu, L. Gang, C. Bi and Y. Liang** (2007) Fabrication and characterization of a PTFE-reinforced integral composite membrane for self-humidifying PEMFC. *J. Power Sources*, **165**, 786-792.
367. **Zhao, C., Z. Wang, D. Bi, H. Lin, K. Shao, T. Fu, S. Zhong and H. Na** (2007) Blend membranes based on disulfonated poly(aryl ether ether ketone)s (SPEEK) and poly(amide imide) (PAI) for direct methanol fuel cell usages. *Polymer*, **48**, 3090-3097.
368. **Zhong, S., C. Liu and H. Na** (2009) Preparation and properties of UV irradiation-induced crosslinked sulfonated poly(ether ether ketone) proton exchange membranes. *J. Membr. Sci.*, **326**, 400–407.
369. **Zhong, S., X. Cui, H. Cai, T. Fu, C. Zhao and H. Na** (2007) Crosslinked sulfonated poly(ether ether ketone) proton exchange membranes for direct methanol fuel cell applications. *J. Power Sources*, **164**, 65-72.

LIST OF PUBLICATIONS BASED ON THIS RESEARCH WORK

I REFEREED JOURNALS

1. **Helen, M., B. Viswanathan and S. Srinivasa Murthy** (2006) Fabrication and properties of hybrid membranes based on salts of heteropolyacid, Zirconium Phosphate and Polyvinyl alcohol. *J. Power Source* **163**, 433–439.
2. **Helen, M., B. Viswanathan and S. Srinivasa Murthy** (2007) Synthesis and characterization of hybrid membranes based on α -ZrP and silicotungstic acid. *J. Membr. Sci.*, **292**, 98–105.
3. **Viswanathan B. and M. Helen** (2007) Is nafion[®], the only choice? *Bull. Catal. Soc. India* **6**, 50-66.

II REFEREED ARTICLES/BOOK CHAPTERS

1. **Viswanathan, B., M. Helen and S. Srinivasa Murthy** (2005) Noble metal based anodes for polymer electrolyte membrane fuel cells. Review Book, Editor. Satoshi Kaneco, Japan, *Photo/ Electrochemistry & Photobiology for Environment, Energy & Fuel* 61-104.
2. **Helen, M., B. Viswanathan, L. Himakumar, and S. Srinivasa Murthy** (2006) Strategies for the design of membranes for fuel cells. Review Book, Editor. Satoshi Kaneco, Japan, *Photo/ Electrochemistry & Photobiology for Environment, Energy & Fuel* 1-42.

III NATIONAL/INTERNATIONAL CONFERENCE

1. **Viswanathan B. and M. Helen** (2006) Strategies for the design and fabrication of membranes for fuel cells, *National seminar on challenges in fuel cell Technology: India's perspective*, December 1 & 2, 2006, Indian Institute of Technology Delhi, India.
2. **Helen, M.** (2008) Membrane Catalysis, *Joint Research Fellows Workshop*, 2nd August 2008, Indian Institute of Technology Madras, India.
3. **Helen, M., B. Viswanathan and S. Srinivasa Murthy** (2008) Nanocomposite membranes for DMFC applications' *International conference on functional materials*, November 27-29, 2008, Indian Institute of Technology Madras, India., (**Best Poster Award**).

4. **M. Helen, B. Viswanathan and S. Srinivasa Murthy** (2009)
Polyoxometalate based membranes for possible DMFC applications, *Hybrid Materials 2009, First International Conference on Multifunctional, Hybrid and Nanomaterials*, March 15-19, 2009, Tours, France.